



38th International Conference
on the Applications of the Mössbauer Effect, ICAME
and the International Conference on Hyperfine
Interactions and Their Applications, HYPERFINE

ICAME & HYPERFINE 2025

BOOK OF ABSTRACTS

Gdańsk, 7-12 September 2025

Timetable of ICAME 2025

	Sunday 7/09	Monday 8/09	Tuesday 9/09	Wednesday 10/09	Thursday 11/09	Friday 12/09
08:00 - 08:15		Opening ceremony	K3 M.T. Sougrati	K5 T. Nishida	K7 P. de Souza	K8 H. Kobayashi
08:15 - 08:30						
08:30 - 08:45						
08:45 - 09:00		K1 F.J. Litterst				
09:00 - 09:15			I1 K. Liu	19 T. Zhang	O21 F. Renz MIMOS	I17 H.H. Klaus
09:15 - 09:30			I2 Y. Guo	I10 E. Tabor	I13 M. Roskosz	O35 S. Tsutsui
09:30 - 09:45		K2 W.A. MacFarlane			O22 M. Jakubowska	O36 S. Kubuki
09:45 - 10:00			O2 S. Farid	O15 Y.A. Abdu	O23 M. Wang	O37 E.E. Alp
10:00 - 10:15		coffee break	coffee break	coffee break	coffee break	coffee break
10:15 - 10:30						
10:30 - 10:45		A1 A. Chumakov	K4 Z. Klencsár	I7 D.H. Ryan	I14 B. Kalska-Szostko	Iron Analytics
10:45 - 11:00				O10 S. Kitao	O24 S. Krehula	LynXes WissEL
11:00 - 11:15		A2 J.M. Greneche		O11 R. Masuda	O25 D. Peddis	O38 J.M. Michalik
11:15 - 11:30				O12 Z. Homonnay	O26 S. Slimani	O39 T. Szumiatla
11:30 - 11:45		A3 M. Gracheva		coffee break	coffee break	O40 M. Hayashi
11:45 - 12:00						coffee break
12:00 - 12:15		coffee break		I8 D. Kubániová	I15 X. Li	Closing ceremony
12:15 - 12:30						
12:30 - 12:45		T5 E.E. Alp		O13 V. Schönenmann	O27 P. Adler	
12:45 - 13:00				O14 C. Dong	O28 E.C. Passamani	
13:00 - 13:30						
13:30 - 14:00		LUNCH	LUNCH	LUNCH	LUNCH	LUNCH
14:00 - 14:30						
14:30 - 14:45				14.30-14.45 Conference photo	I16 C. Bartha	
14:45 - 15:00	T1 J. Juraszek		Y2 K. Podgórska		O29 R. Röhlsberger	
15:00 - 15:15		T6 S. Yaroslavtsev	Y3 X. Li		O30 J. Evers	
15:15 - 15:30			Y4 T. Samuel		O31 I. Sergeev	
15:30 - 15:45	T2 S.M. Dubiel		Y5 A. Sławek		O32 N. Nagasawa	
15:45 - 16:00			Y6 M. Hausner		coffee break	
16:00 - 16:15						
16:15 - 16:30		coffee break	coffee break		O33 S. Sadashivaiah	
16:30 - 16:45				Excursion	O34 D. Beszas	
16:45 - 17:00	T3 E. Kuzmann	Commemorative Session J. Stanek, J. Gałązka	I4 K.R. Szymański		O41 M.Y. Hu	
17:00 - 17:15			O7 D. Nagy		O43 J. Zhao	
17:15 - 17:30			O8 A. Stejskal			
17:30 - 17:45	T4 P. Butkiewicz				IBAME meeting 17.30 - 19.00	
17:45 - 18:00						
18:00 - 18:30					Conference Dinner 19:00 - 23:00	
19:00 - 19:30		IBAME meeting 18.00 - 19.30	Common Poster Session 18:30 - 21:00			
19:30 - 20:00	Welcome party 19:00-21:00					
20:30 - 21:00						

Timetable of HYPERFINE 2025

	Sunday 7/09	Monday 8/09	Tuesday 9/09	Wednesday 10/09	Thursday 11/09	Friday 12/09
08:00 - 08:15		Opening ceremony	H11 S.Cottenier			K8 H.Kobayashi
08:15 - 08:30						
08:30 - 08:45		K1 F.J.Litterst		H17 V.Polytimos	HI11 T.E.Lellinger	
08:45 - 09:00			HI2 F.Pratt			HI17 H.H.Klauss
09:00 - 09:15				HI8 S.Go	HI12 T.Schumm	O35 S.Tsutsui
09:15 - 09:30			HO1 T.Prokscha			O36 S.Kubuki
09:30 - 09:45		K2 W.A.MacFarlane	HO2 H.A.Torii	HO11 M.Fukutome	HO18 Y.F.Guo	
09:45 - 10:00			HO3 S.Nishimura	HO12 G.Georgiev	HO19 Y.Hirayama	O37 E.E.Alp
10:00 - 10:15		coffee break	coffee break	coffee break	coffee break	coffee break
10:15 - 10:30						
10:30 - 10:45		A1 A.Chumakov	HI3 W.Higemoto	HI9 M.Mukai	HI13 B.Jasińska	Iron Analytics
10:45 - 11:00						LynXes WissEL
11:00 - 11:15		A2 J.M.Greneche	HI4 H.Ariga-Miwa	HI10 L.Bocklage	HI14 P.Rocha-Rodrigues	O38 J.M.Michalik
11:15 - 11:30						O39 T.Szumiata
11:30 - 11:45		A3 M.Gracheva	HO4 M.Mihara	HO13 J.Suh	HO20 R.P.Moreira	O40 M.Hayashi
11:45 - 12:00		coffee break	coffee break	coffee break	coffee break	coffee break
12:00 - 12:15			HO5 S.Takeshita	HO14 T.T.Dang	HO21 P.A.Sousa	
12:15 - 12:30			HO6 K.Yokoyama	HO15 M.J.Zai	HO22 J.Schell	
12:30 - 12:45		T5 E.E.Alp	HO7 A.D.Pant		HO23 A.Neves Cesario	Closing ceremony
12:45 - 13:00			O42 R.Reddy		HO24 B.Feng	
13:00 - 13:30						
13:30 - 14:00		LUNCH	LUNCH	LUNCH	LUNCH	LUNCH
14:00 - 14:30						
14:30 - 14:45	T1 J.Juraszek			14.30-14.45 Conference photo	HI15 A.Zarzycki	
14:45 - 15:00		T6 S.Yaroslavtsev	HI5 X.Yang			
15:00 - 15:15			HI6 K.Stoychev		HI16 W.Sato	
15:15 - 15:30	T2 S.M.Dubiel	Y1 M.H.Hoock	HO9 Y.Mizoi		HO25 M.Uenomachi	
15:30 - 15:45		O1 M.Sikora SOLARIS	HO10 M.Priyadarsini		HO26 K.Okai	
15:45 - 16:00		coffee break	coffee break		coffee break	
16:00 - 16:15						
16:15 - 16:30						
16:30 - 16:45						
16:45 - 17:00	T3 E.Kuzmann	Commemorative Session J.Stanek, J.Gałązka	IAC meeting 16.30 - 17.30	Excursion		
17:00 - 17:15						
17:15 - 17:30	T4 P.Butkiewicz					
17:30 - 17:45						
17:45 - 18:00						
18:00 - 18:30			Common Poster Session 18.30-21.00			
19:00 - 19:30						
19:30 - 20:00	Welcome party 19:00-21:00				Conference Dinner 19:00 - 23:00	
20:30 - 21:00						

Joint Conferences ICAME & HYPERFINE



BOOK OF ABSTRACTS 2025

Edited by:
Karolina Czarnacka
Jakub Grotel

September 7-12, Gdańsk, Poland

WELCOME MESSAGE

We are honored to welcome you to the joint conferences **ICAME & HYPERFINE 2025**, held in Gdańsk, Poland, between 7th and 12th September 2025. Both meetings, ICAME - 38th International Conference on the Applications of the Mössbauer Effect and HYPERFINE - the International Conference on Hyperfine Interactions and Their Applications, have a long tradition dating back to the 1960s. The conferences have been the main forum for exchanging knowledge and information between scientists studying hyperfine interactions (basic research) and specialists using nuclear methods, particularly Mössbauer spectroscopy, which exploits these interactions (application research). With the development of experimental techniques based on hyperfine interactions and using large research facilities such as as synchrotrons, the need for closer cooperation between both environments arose, leading to HYPERFINE and ICAME's merger. The first combined ICAME and HYPERFINE conferences took place in 2021 in Braşov, Romania.

The years of the pandemic have strongly weakened the direct interaction between scientists, while the organization of hybrid conferences has not met expectations. We are delighted that you decided to attend the ICAME & HYPERFINE 2025 conference in person. The conference is organized by the Polish community of scientists specializing in Mössbauer spectroscopy and hyperfine interactions from different universities and research institutes in Poland.

The conference venue is in Gdańsk, a famous city in northern Poland with almost half a million inhabitants. It is an important cultural, scientific, and economic center that is conveniently connected by air with most European cities. The location by the Baltic Sea guarantees good conditions for work and also for rest. It is a city with over a thousand years of history, whose identity over the centuries has been shaped under the influence of various cultures. Gdańsk is considered a symbolic place of the beginning of the fall of communism in Central Europe, and it is the city of Lech Wałęsa and Solidarity.

The scientific program of the conference covers the traditional topics of the previous ICAME and HYPERFINE events. We warmly welcome all the Mössbauer and Hyperfine community to active participation in the joint ICAME & HYPERFINE 2025!

General Chair Elżbieta Jartych
Chair ICAME Jakub Cieślak
Chair HYPERFINE Marta Marszałek

LOCAL ORGANIZING COMMITTEE

General Chair:	Elżbieta Jartych	Lublin University of Technology
Co-Chair:	Agata Lisińska-Czekaj	Gdańsk University of Technology
Co-Chair:	Dionizy Czekaj	Gdańsk University of Technology
Chair ICAME:	Jakub Cieślak	AGH University of Krakow
Secretary ICAME:	Tomasz Pikula	Lublin University of Technology
Chair HYPERFINE:	Marta Marszałek	Institute of Nuclear Physics Polish Academy of Sciences
Secretary HYPERFINE:	Karolina Siedliska	Lublin University of Technology
Members:		
	Paweł Bartosik	Lublin University of Technology
	Kvetoslava Burda	AGH University of Krakow
	Karolina Czarnacka	Lublin University of Technology
	Przemysław Duda	Warsaw University of Technology
	Katarzyna Dziedzic-Kocurek	Jagiellonian University
	Maria Dziurawicz	University of Silesia
	Agnieszka Grabias	Łukasiewicz Institute of Microelectronics and Photonics
	Jakub Grotel	Lublin University of Technology
	Aneta Hanc-Kuczkowska	University of Silesia
	Rafał Idczak	University of Wrocław
	Beata Kalska-Szostko	University of Białystok
	Mariola Kądziołka-Gaweł	University of Silesia
	Jakub Kisała	Lublin University of Technology
	Kamila Komędera	AGH University of Krakow
	Agnieszka Kulińska	Institute of Nuclear Physics Polish Academy of Sciences
	Agnieszka Łukiewska	Czestochowa University of Technology
	Dariusz Malczewski	University of Silesia
	Nika Spiridis	Jerzy Haber Institute of Catalysis and Surface Chemistry
	Paweł Stoch	AGH University of Krakow
	Zbigniew Surowiec	MCS University in Lublin
	Tadeusz Szumiata	Casimir Pulaski Radom University
	Tomasz Ślęzak	AGH University of Krakow

INTERNATIONAL ADVISORY COMMITTEE OF ICAME

Members of the International Board on the Application of the Mössbauer Effect (IBAME)

INTERNATIONAL ADVISORY COMMITTEE OF HYPERFINE

Members of the International Advisory Committee (IAC) and Executive Committee (EC)

INTERNATIONAL PROGRAM COMMITTEE

ICAME

Esen Ercan Alp	Argonne National Laboratory	USA
César Augusto Barrero Meneses	University of Antioquia	Colombia
Paul Bingham	Sheffield Hallam University	United Kingdom
Stuart Campbell	UNSW Canberra	Australia
Jakub Cieřlak	AGH University of Krakow	Poland
Benilde Costa	University of Coimbra	Portugal
Catherine Frandsen	Technical University of Denmark	Denmark
Yann Garcia	Catholic University of Louvain	Belgium
Jean-Marc Greneche	Le Mans University	France
Ajay Gupta	University of Petroleum and Energy Studies	India
Raphael Hermann	Oak Ridge National Laboratory	USA
Juan Antonio Jaén	University of Panama	Panama
Elżbieta Jartych	Lublin University of Technology	Poland
Ewa Jędryka	Institute of Physics Polish Academy of Sciences	Poland
Stjepko Krehula	Ruder Boskovic Institute	Croatia
Victor Eugen Kuncser	National Institute of Materials Physics	Romania
Erno Kuzmann	Eötvös Loránd University	Hungary
Pierre Emmanuel Lippens	Charles Gerhardt Institute of Montpellier	France
Libor Machala	Palacký University in Olomouc	Czech Republic
Roberto Mantovan	Institute for Microelectronics and Microsystems	Italy
José Francisco Marco	Rocasolano Institute of Physical Chemistry	Spain
Denes Nagy	Wigner Research Centre for Physics	Hungary
Tetsuaki Nishida	Environmental Materials Institute Fukuoka	Japan
Jun Okabayashi	The University of Tokyo	Japan
Gustavo Pasquevich	La Plata National University	Argentina
Edson Caetano Passamani	Federal University of Espírito Santo	Brazil
Marek Przybylski	AGH University of Krakow	Poland

Michael Reissner	Technical University of Vienna	Austria
Ralf Röhlsberger	German Electron Synchrotron DESY	Germany
Rudolf Rüffer	European Synchrotron Radiation Facility Grenoble	France
Volker Schünemann	University of Kaiserslautern-Landau	Germany
Vladimir Sepelak	Karlsruhe Institute of Technology	Germany
Virender K. Sharma	Texas A&M University	USA
Krzysztof Szymański	University of Białystok	Poland
Nikolay Velinov	Institute of Catalysis Bulgarian Academy of Sciences	Bulgaria
Junhu Wang	Dalian Institute of Chemical Physics	China
Tao Zhang	Dalian Institute of Chemical Physics	China

HYPERFINE

Stefaan Cottenier	Ghent University	Belgium
Pierre Dalmas de Reotier	CEA Grenoble	France
Georgi Georgiev	IJCLab	France
Andrzej Golnik	Warsaw University	Poland
Lars Hemmingsen	University of Copenhagen	Denmark
Wayne Hutchison	University of New South Wales	Australia
Agnieszka Kulińska	Institute of Nuclear Physics Polish Academy of Sciences	Poland
Dariusz Malczewski	University of Silesia Katowice	Poland
Marta Marszałek	Institute of Nuclear Physics Polish Academy of Sciences	Poland
Mototsugu Mihara	Osaka University	Japan
Lino Pereira	Catholic University of Louvain	Belgium
Helena Maria Petrilli	Universidade de São Paulo	Brazil
Marek Wójcik	Institute of Physics Polish Academy of Sciences Warsaw	Poland
Matthew Zacate	Northern Kentucky University	USA

SPONSORS & EXHIBITORS

Main sponsor:	Lukasiewicz Institute of Microelectronics and Photonics, Warsaw, Poland
Industrial sponsor:	Iron Analytics, Czech Republic
Zoltan Nemeth	LynXes
Franz Renz	MIMOS
Andrew Dan	WissEL

LOCAL HONORARY COMMITTEE

Katarzyna Brzózka	Casimir Pulaski Radom University
Mieczysław Budzyński	MCS University in Lublin
Jan Chojcan	University of Wrocław
Henryk Drulis	Institute of Low Temperature and Structure Research Wrocław
Stanisław Dubiel	AGH University of Kraków
Jolanta Gałązka-Friedman	Warsaw University of Technology
Michał Kopcewicz	Institute of Electronic Materials Technology Warsaw
Józef Korecki	Jerzy Haber Institute of Catalysis and Surface Chemistry
Krzysztof Królas	Jagiellonian University
Kazimierz Łątka	Jagiellonian University
Antoni Pędziwiatr	Jagiellonian University
Barbara Sawicka	Institute of Nuclear Physics Polish Academy of Sciences Kraków, University of Victoria Canada
Jerzy Sawicki	Jagiellonian University, University of Victoria Canada
Zbigniew M. Stadnik	Jagiellonian University, University of Ottawa Canada
Jan Stanek	Jagiellonian University
Jan Świerczek	Czestochowa University of Technology
Krzysztof Tomala	AGH University of Kraków

PRIZES

The International Board on the Application of the Mössbauer Effect (IBAME) presents two awards for outstanding work involving the Mössbauer effect and its applications:

1. the **IBAME Young Scientist Award** for researchers up to the age of 35, for high-quality contribution to science based on research that involves application of the Mössbauer effect;
2. the **IBAME Science Award** for high quality contribution to science based on research that involves application of the Mössbauer effect over an extended period of at least 20 years.

The following prizes have been awarded at ICAME 2025:

The **IBAME Young Scientist Award** goes to:

Dr. Maria Gracheva, HUN-REN Centre for Energy Research, Hungary.

The **IBAME Science Award** goes to:

Prof. Aleksandr Chumakov, European Synchrotron Radiation Facility, France,

Prof. Jean-Marc Greneche, Le Mans University, France.

TOPICS ICAME

- T01 Magnetism and solid-state physics
- T02 Chemistry
- T03 Nanostructures and thin films
- T04 Materials science and industrial applications
- T05 Biological and medical applications
- T06 Earth sciences, mineralogy, cultural heritage and environmental sciences
- T07 Lattice dynamics and vibrational properties
- T08 Experimental techniques, methodology and coherent phenomena

TOPICS HYPERFINE

- T01 Radioactive ion beams, radioisotope probes and ion-solid interactions
- T02 Nuclear moments, nuclear structure, low temperature nuclear orientation
- T03 Laser spectroscopy, NMR/NQR, perturbed angular distribution/correlation, PALS
- T04 Muon spin rotation/relaxation/resonance and muon-Xray
- T05 Synchrotron radiation, neutron scattering and other complementary techniques
- T06 Materials (metals, insulators, semiconductors, nanomaterials, thin films)
- T07 Theoretical methods for hyperfine field calculations, lattice and defect dynamics
- T08 Applications in biology, chemistry, medicine, engineering, geoscience

Notes

Table of Contents

ICAME Conference Program.....	11
HYPERFINE Conference Program.....	19
Tutorial Lectures	27
Awarded Lectures.....	35
ICAME Keynote Lectures.....	39
ICAME Invited Lectures	49
ICAME Young Session	67
ICAME Oral Contributions.....	75
HYPERFINE Invited Lectures.....	119
HYPERFINE Oral Contributions.....	137
ICAME Posters.....	161
HYPERFINE Posters	237

Please note that all abstracts are listed in alphabetical and numerical order with respect to the presenting author and session topic.

ICAME Conference Program



Day 1. Sunday – September 7, 2025

Room: AMSTERDAM

09:00-18:00	Registration		
TUTORIAL LECTURES			
14:30-15:15	T1	J. Juraszek	⁵⁷ Fe Mössbauer Spectroscopy: Principles, Methodology and Advanced Applications in Material Science
15:15-16:00	T2	S.M. Dubiel	Mössbauer Spectroscopy in Investigation of Harmonically Modulated Spin and Charge Structures
16:00-16:30	Coffee break		
16:30-17:15	T3	E. Kuzmann	History of Industrial Applications of Mössbauer Spectroscopy
17:15-18:00	T4	P. Butkiewicz	Determination of the Components of the Electric Field Gradient Tensor in Mössbauer Spectroscopy Using the Velocity Moments Formalism
19:00-21:00	Welcome party		

Day 2. Monday – September 8, 2025

Rooms: AMSTERDAM + GDAŃSK + KOPENHAGA

08:00-18:00	Registration		
08:00-08:30	Opening ceremony		
KEYNOTE LECTURES			
08:30-09:15	K1	F.J. Litterst	Quantum Spin Liquids: What Can We Learn From Mössbauer Spectroscopy and Muon Spin Rotation/Relaxation?
09:15-10:00	K2	W.A. MacFarlane	Ion-implanted β -NMR as a Probe of Materials
10:00-10:30	Coffee break		
AWARDED LECTURES			
10:30-11:00	A1	A. Chumakov	Forty-five Year Pleasure of Nuclear Resonance Scattering
11:00-11:30	A2	J.M. Greneche	Local Order in Micro- up to Nanostructures Studied by ^{57}Fe Mössbauer Spectrometry
11:30-12:00	A3	M. Gracheva	The Role of Root Exudates in Iron Metabolism of Plants
12:00-12:15	Coffee break		

SYNCHROTRON SESSION			
12:15-13:00	T5	E.E. Alp	Nuclear Resonant Scattering Beamline Capabilities Worldwide
13:00-14:45	Lunch		
14:45-15:30	T6	S. Yaroslavtsev	Synchrotron Applications of Mössbauer Techniques (ID14 ESRF)
15:30-15:45	Y1	M.H. Hock	Nuclear Forward Scattering and Density Functional Theory Studies of Photo- and Catalytically Active Iridium Complexes
15:45-16:00	O1	M. Sikora	Research Opportunities at SOLARIS Synchrotron
16:00-16:30	Coffee break		
16:30-17:30	Commemorative session		
18:00-19:30	IBAME meeting (room GDAŃSK)		

Day 3. Tuesday – September 9, 2025
Rooms: GDAŃSK + KOPENHAGA

08:00-08:45	K3	M.T. Sougrati	Spent LiFePO ₄ Batteries Management: Towards Direct Recycling Strategies
08:45-09:15	I1	K. Liu	Mössbauer Studies on Catalysts for H ₂ Storage Using Dibenzyltoluene
09:15-09:45	I2	Y. Guo	Spectroscopic and Computational Studies of Unique Spin States in Biological Iron-Sulfur Clusters and Their Synthetic Congeners
09:45-10:00	O2	S. Farid	Real-Time Insights into Amorphous NiFeB Catalysts for Water Oxidation: An operando Mössbauer Study
10:00-10:30	Coffee break		
10:30-11:15	K4	Z. Klencsár	Data and Model Description Framework Developed for Laboratory Mössbauer Spectroscopy
11:15-11:30	O3	J.M. Byrne	MinSight: Web-based Fitting for Mössbauer Spectroscopy
11:30-11:45	O4	T. Pikula	PolMoss: A User-friendly Software for ⁵⁷ Fe Mössbauer Spectra Simulation and Fitting
11:45-12:00	Coffee break		

12:00-12:30	I3	S. Stankov	Lattice Dynamics of Ultrathin Films and Nanostructures from in situ Nuclear Inelastic Scattering and ab initio Theory
12:30-12:45	O5	A. Panchwancee	Stabilizing Non-collinear Spin Structures in Thin Flms: A Novel Approach Using Oblique Incidence Deposition for Precise Control and Detection via NFS
12:45-13:00	O6	L. Bocklage	Nuclear GISAXS on Self-assembled Magneto-resistive Multilayer Nanowires
13:00-14:30	Lunch		
YOUNG SESSION			
14:30-14:45	Y2	K. Podgórska	¹⁵¹ Eu Mössbauer Spectroscopy and Magnetic Studies of EuSnP Single Crystals
14:45-15:00	Y3	X. Li	Solvent-Dependent Two-Step Spin Crossover Behavior in 3D Coordination Frameworks
15:00-15:15	Y4	T. Samuel	Preparation and Physico-Chemical Characterization of AISI 304 Stainless Steel Film Deposited by DC Magnetron Sputtering
15:15-15:30	Y5	A. Sławek	Mössbauer Investigations of FeCoNiZn _x System
15:30-15:45	Y6	M. Hausner	Interactions of Gamma Photons with Ensemble of Nuclei Described by Quantum Mechanical Model
16:00-16:30	Coffee break		
16:30-17:00	I4	K.R. Szymański	Velocity Moments and Tensor Properties of Mössbauer Spectra
17:00-17:15	O7	D. Nagy	Remote Control and Alarm Monitoring of Mössbauer Laboratories
17:15-17:30	O8	A. Stejskal	Flexible Intensity Control of Resonantly Scattered Gamma-Rays Using Multi-Frequency Vibrating Resonant Absorber
18:30-21:00	Poster session		

Day 4. Wednesday – September 10, 2025

Room: GDAŃSK

08:00-08:45	K5	T. Nishida	Local Distortion of Highly Conducting Glass and Glass Ceramics
08:45-09:15	I5	M. Saito	Collective Atomic Dynamics in Glass Revealed by Mössbauer Time-Domain Interferometry

09:15-09:30	O9	P. Bruna	Mössbauer Spectroscopy Investigation of Crystallization in (FeCoCrNi)-(B,Si) High-Entropy Metallic Glasses
09:30-10:00	I6	D. Malczewski	Application Of Mössbauer Spectroscopy To Study Metamict Minerals And Their Thermally-Induced Recrystallization Process
10:00-10:30	Coffee break		
10:30-11:00	I7	D.H. Ryan	Exploring Valence and Magnetic Order Using ¹⁵¹ Eu Mössbauer Spectroscopy
11:00-11:15	O10	S. Kitao	Eu-Activated SiAlON Studied by Synchrotron-Radiation-Based ¹⁵¹ Eu Mössbauer Spectroscopy
11:15-11:30	O11	R. Masuda	Synchrotron-radiation-based Mössbauer Spectroscopy for Europium Hydrides under Hydrogen Pressure up to 80 GPa
11:30-11:45	O12	Z. Homonnay	Influence of Eu-doping on the Magnetic Structure of Goethite: A Mössbauer Study
11:45-12:00	Coffee break		
12:00-12:30	I8	D. Kubániová	Mössbauer Spectroscopy of Nanoparticle Suspensions
12:30-12:45	O13	V. Schünemann	Magnetic and Vibrational Properties of a Molecular Fe ₁₈ Dy ₆ Wheel
12:45-13:00	O14	C. Dong	Unraveling the Sodium Storage Mechanism of Atomically Dispersed Sn on Hard Carbon via Mössbauer Spectroscopy
13:00-14:30	Lunch		
14:30-14:45	Conference photo		
15:00	Excursion		

Day 4. Wednesday – September 10, 2025

Room: KOPENHAGA

08:00-08:45	K6	Y. Huang	Mössbauer Spectroscopy: Unlocking the Structural and Mechanistic Insights of Single-Atom Catalysts
08:45-09:15	I9	T. Zhang	Study of Single-Atom Catalysts with in-situ/operando Mössbauer Spectroscopy
09:15-09:45	I10	E. Tabor	Iron-Based Zeolite Heterogeneous Catalysts: Insights into Active Centers and Reaction Pathways through Mössbauer Spectroscopy

09:45-10:00	O15	Y.A. Abdu	Mössbauer Characterization of Low Temperature Iron-based Fischer-Tropsch Catalysts
10:00-10:30	Coffee break		
10:30-11:00	I11	L. Kubičková	Mössbauer Study of Iron Nitrides: Exploring Biomedical and Thermoelectric Applications
11:00-11:15	O16	K. Burda	Hypertension Development May Be Impacted by Gold, Silver, and Titanium Oxide Nanoparticles
11:15-11:30	O17	K. Dziedzic-Kocurek	Exploring the Magnetic Moment of Iron in Oxyhaemoglobin - A Story Still Unfolding
11:30-11:45	O18	M. Kądziołka-Gaweł	Identification of Heme and Non-heme Iron in Foods: Mössbauer Spectroscopy Study
11:45-12:00	Coffee break		
12:00-12:30	I12	J. Okabayashi	Operando Mössbauer Spectroscopy Under Reversible Strain for Magneto-Strictive Materials
12:30-12:45	O19	H.H. Klauss	Quasi-two-dimensional Magnetism and Antiferromagnetic Ground State in $\text{Li}_2\text{FeSiO}_4$
12:45-13:00	O20	K. Komędera	High-entropy Magnetism of Murunskites
13:00-14:30	Lunch		
14:30-14:45	Conference photo		
15:00	Excursion		

Day 5. Thursday – September 11, 2025

Rooms: GDAŃSK + KOPENHAGA

08:00-08:45	K7	P. de Souza	A Global Mössbauer Spectrum for Martian Soil
08:45-09:00	O21	F. Renz	Two-Dimensional Mössbauer Spectroscopy – New Horizons in Molecular Magnetism and Space Exploration
09:00-09:30	I13	M. Roskosz	Use of Nuclear Resonance in Studies of Space Returned Samples from Ryugu and Bennu Asteroids
09:30-09:45	O22	M. Jakubowska	Classification Method of Ordinary Chondrites Based on Mössbauer Spectroscopy - What Can It Tell Us About Meteorites?

09:45-10:00	O23	M. Wang	Aromatic Substituent Effects on the Spin Crossover Properties of [Fe(H ₂ Bpz ₂) ₂ (bipy-R)] Complexes
10:00-10:30	Coffee break		
10:30-11:00	I14	B. Kalska-Szostko	How Do the Synthesis Conditions Influence the Final Properties of Nanoparticles
11:00-11:15	O24	S. Krehula	Mössbauer Spectroscopy Study of Sn-doped α -Fe ₂ O ₃ Nanoparticles
11:15-11:30	O25	D. Peddis	New Insights into the Crystal and Magnetic Structure of Hematite
11:30-11:45	O26	S. Slimani	Magnetic Structure of Hollow Nanoarchitectures
11:45-12:00	Coffee break		
12:00-12:30	I15	X. Li	Interplay between Structural, Electronic, and Magnetic Properties of Iron Oxides at Extreme Conditions
12:30-12:45	O27	P. Adler	Pressure-Induced Electronic and Magnetic Transitions in the Iron(IV) Oxide Sr ₂ FeO ₄
12:45-13:00	O28	E.C. Passamani	Hybrid Iron-based Nanoadsorbents: Morphological, Structural, Magnetic and Hyperfine Properties
13:00-14:30	Lunch		
14:30-15:00	I16	C. Bartha	Complex Structural, Mössbauer Spectroscopy and Magnetic Investigations of Rare-Earth Iron Garnets Obtained by Different Processing Routes
15:00-15:15	O29	R. Röhlberger	A Mobile Mini-beamline for Mössbauer Spectroscopy at the European X-ray Free-Electron Laser
15:15-15:30	O30	J. Evers	Single-shot Mössbauer Spectroscopy at X-ray Free-electron Lasers
15:30-15:45	O31	I. Sergeev	Recent Results and Development at the P01 Beamline, PETRA III, DESY
15:45-16:00	O32	N. Nagasawa	Nuclear Resonant Scattering in Public Beamline of SPring-8
16:00-16:30	Coffee break		
16:30-16:45	O33	S. Sadashivaiah	Ultrafast Control of Coherence in Nuclear Resonant X-rays
16:45-17:00	O34	D. Bessas	Nuclear Resonance Scattering Beamline ID14 at the European Synchrotron Radiation Facility
17:00-17:15	O41	M.Y. Hu	NRXS and Atomic Dynamics Simulations

17:15-17:30	O43	J. Zhao	Application of Nuclear Resonant Scattering at High Pressure and High Temperature at Advanced Photon Source
17:30-19:00	IBAME meeting (room HAMBURG)		
19:00-23:00	Conference dinner		

Day 6. Friday – September 12, 2025

Rooms: AMSTERDAM + GDAŃSK + KOPENHAGA

08:00-08:45	K8	H. Kobayashi	Mössbauer Study of a Critical Charge Mode in a Strange Metal
08:45-09:15	I17	H.H. Klauss	Altermagnetism: A Conceptual Overview and What We Learn with Mössbauer Spectroscopy and Other Local Probes
09:15-09:30	O35	S. Tsutsui	Successive Transitions in Ca ₅ Ir ₃ O ₁₂ Revealed by ¹⁹³ Ir Synchrotron-Radiation-Based Mössbauer Spectroscopy
09:30-09:45	O36	S. Kubuki	Relationships among Structure, Photocatalytic and Electrical Properties of Lanthanide-Substituted Goethite Nanoparticles
09:45-10:00	O37	E.E. Alp	High Throughput Nuclear Resonant Time Domain Interferometry: NR-TDI
10:00-10:30	Coffee break		
10:30-10:40	J. Navařík - Iron Analytics		
10:40-10:50	Z. Nemeth - LynXes		
10:50-11:00	A. Dan - WissEL		
11:00-11:15	O38	J.M. Michalik	Structure, Microstructure, and Hyperfine Interactions in Hf- and Ni-Substituted TiFe Alloy for Hydrogen Storage
11:15-11:30	O39	T. Szumiata	Quality Inspection of 3D Printed Steel Elements, Marine Engine Crankshafts, Wind Turbine Shafts and Nanomagnetic Ferrofluids with Mössbauer Spectrometry
11:30-11:45	O40	M. Hayashi	Effect of Partial Pressures of Oxygen on Oxidation States and Coordination Structures of Iron Ions and on Iron Oxide Activity Coefficients in Silicate Slags
11:45-12:00	Coffee break		
12:00-13:00	Closing ceremony		
13:00-14:30	Lunch		

HYPERFINE Conference Program



Day 1. Sunday – September 7, 2025

Room: AMSTERDAM

09:00-18:00	Registration		
TUTORIAL LECTURES			
14:30-15:15	T1	J. Juraszek	^{57}Fe Mössbauer Spectroscopy: Principles, Methodology and Advanced Applications in Material Science
15:15-16:00	T2	S.M. Dubiel	Mössbauer Spectroscopy in Investigation of Harmonically Modulated Spin and Charge Structures
16:00-16:30	Coffee break		
16:30-17:15	T3	E. Kuzmann	History of Industrial Applications of Mössbauer Spectroscopy
17:15-18:00	T4	P. Butkiewicz	Determination of the Components of the Electric Field Gradient Tensor in Mössbauer Spectroscopy Using the Velocity Moments Formalism
19:00-21:00	Welcome party		

Day 2. Monday – September 8, 2025

Rooms: AMSTERDAM + GDAŃSK + KOPENHAGA

08:00-18:00	Registration		
08:00-08:30	Opening ceremony		
KEYNOTE LECTURES			
08:30-09:15	K1	F.J. Litterst	Quantum Spin Liquids: What Can We Learn From Mössbauer Spectroscopy and Muon Spin Rotation/Relaxation?
09:15-10:00	K2	W.A. MacFarlane	Ion-implanted β -NMR as a Probe of Materials
10:00-10:30	Coffee break		
AWARDED LECTURES			
10:30-11:00	A1	A. Chumakov	Forty-five Year Pleasure of Nuclear Resonance Scattering
11:00-11:30	A2	J.M. Greneche	Local Order in Micro- up to Nanostructures Studied by ^{57}Fe Mössbauer Spectrometry
11:30-12:00	A3	M. Gracheva	The Role of Root Exudates in Iron Metabolism of Plants
12:00-12:15	Coffee break		

SYNCHROTRON SESSION			
12:15-13:00	T5	E.E. Alp	Nuclear Resonant Scattering Beamline Capabilities Worldwide
13:00-14:45	Lunch		
14:45-15:30	T6	S. Yaroslavtsev	Synchrotron Applications of Mössbauer Techniques (ID14 ESRF)
15:30-15:45	Y1	M.H. Hoock	Nuclear Forward Scattering and Density Functional Theory Studies of Photo- and Catalytically Active Iridium Complexes
15:45-16:00	O1	M. Sikora	Research Opportunities at SOLARIS Synchrotron
16:00-16:30	Coffee break		
16:30-17:30	Commemorative session		

Day 3. Tuesday – September 9, 2025

Room: AMSTERDAM

08:00-08:45	HI1	S. Cottenier	Teaching Hyperfine Interactions to the World: From the Good Old Internet to Artificial Intelligence (www.hyperfinecourse.org)
08:45-09:15	HI2	F. Pratt	Measuring Spin Dynamics and Quantum Entanglement in Frustrated Spin Systems using μ SR
09:15-09:30	HO1	T. Prokscha	Muon Spectroscopy at the Swiss Muon Source $S\mu S$
09:30-09:45	HO2	H.A Torii	Hyperfine Spectroscopy of Muonium and Muonic Atoms for Precise Determination of the Muon Magnetic Moment
09:45-10:00	HO3	S. Nishimura	Transient μ SR with High-Field μ SR Spectrometer at J-PARC
10:00-10:30	Coffee break		
10:30-11:00	HI3	W. Higemoto	Quantum Critical Behavior in Heavy Fermion Superconductor Studied by μ SR
11:00-11:30	HI4	H. Ariga-Miwa	μ +SR Investigations of Microporous Aluminosilicates: Probing Interactions with Pd Nanoparticles in Catalysis
11:30-11:45	HO4	M. Mihara	Performance Evaluation of Improved Muon Spin Imaging Device Using Charged Particle Trackers in μ -e Decay Process
11:45-12:00	Coffee break		

12:00-12:15	HO5	S. Takeshita	Hyperfine Field Measurement and Local Structure of Muonic Organic Materials
12:15-12:30	HO6	K. Yokoyama	Muonium as a Probe of Point Defects in Type-Ib Diamond
12:30-12:45	HO7	A.D Pant	Muon Spin Rotation and Relaxation Study in Albumin and Hemoglobin Derivatives
12:45-13:00	O42	V. Raghavendra Reddy	Structural Modifications across Dielectric Maxima in Lead-free BaTiO ₃ -based Relaxors: ¹¹⁹ Sn Hyperfine Interaction Study
13:00-14:30	Lunch		
14:30-15:00	HI5	X. Yang	Recent Studies of Exotic Nuclei Using High-Resolution Laser Spectroscopy
15:00-15:30	HI6	K. Stoychev	Towards High-Precision g-Factor Measurements on Stable and Radioactive Beams with the TDRIV Method
15:30-15:45	HO9	Y. Mizoi	Enhancement of Spin Polarized RI and Muon Beam Imaging via Machine Learning Techniques
15:45-16:00	HO10	M. Priyadarsini	Interface Resolved Magnetism of Metal-Organic (Fe ⁵⁷ / C ₄₂ H ₂₈) Thin Films; Studies under X-ray Standing Waves
16:00-16:30	Coffee break		
16:30-17:30	IAC meeting (room HAMBURG)		
18:30-21:00	Poster session		

Day 4. Wednesday – September 10, 2025

Room: AMSTERDAM

08:30-09:00	HI7	V. Polytimos	Exploring Nuclear Structure in Even-Even Er-W Isotopes in the Framework of IBM-1 with Intrinsic Triaxial Deformation
09:00-09:30	HI8	S. Go	Nuclear Gamma-Ray Polarimetry Based on Multi-Layer Semiconductor Compton Cameras
09:30-09:45	HO11	M. Fukutome	Measurement of Charge Radii in Neutron-Rich Regions Using Charge-Changing Cross Sections
09:45-10:00	HO12	G. Georgiev	Nuclear Moments of Isomeric States around ¹³² Sn
10:00-10:30	Coffee break		
10:30-11:00	HI9	M. Mukai	β-decay Spectroscopy of ¹⁸⁷ Ta and Recent Results at KISS

11:00-11:30	HI10	L. Bocklage	Nuclear Quantum Memory for Hard X Ray Photons
11:30-11:45	HO13	J. Suh	Precision Measurements of the Ground State Hyperfine Splitting of Antihydrogen
11:45-12:00	Coffee break		
12:00-12:15	HO14	T.T. Dang	Local Order-Disorder Phase Transition in Complex Perovskite Relaxor Lead Iron Tungstate $\text{Pb}(\text{Fe}_{2/3}\text{W}_{1/3})\text{O}_3$
12:15-12:30	HO15	M.J. Zai	Critical Temperature and Phonon Evaluation in Hydride Systems Using Computational Methods
13:00-14:30	Lunch		
14:30-14:45	Conference photo		
15:00	Excursion		

Day 5. Thursday – September 11, 2025

Room: AMSTERDAM

08:30-09:00	HI11	T.E. Lellinger	Exploring New Nuclear Magic Numbers with Continuous Beam Collinear Laser Spectroscopy at COLLAPS
09:00-09:30	HI12	T. Schumm	Laser Mössbauer spectroscopy on Thorium-229
09:30-09:45	HO18	Y.F. Guo	High-Resolution and High-Sensitivity Collinear Resonance Ionization Spectroscopy of Rb and Cs Isotopes
09:45-10:00	HO19	Y. Hirayama	Laser Resonant Ionization Spectroscopy at Kiss
10:00-10:30	Coffee break		
10:30-11:00	HI13	B. Jasińska	Positron Annihilation Lifetime Spectroscopy – Assumptions and Applications
11:00-11:30	HI14	P. Rocha-Rodrigues	Local Probing of Structural Phase Transitions in Ferroelectric Layered Perovskite Systems Using PAC Spectroscopy
11:30-11:45	HO20	R.P. Moreira	First Principles and Experimental Local Probe Study of Ge-based Clinopyroxene Series
11:45-12:00	Coffee break		
12:00-12:15	HO21	P.A. Sousa	Phase Transitions and Uniaxial Negative Thermal Expansion in $\text{CsNdNb}_2\text{O}_7$: Combined Local Probe and Diffraction Study

12:15-12:30	HO22	J. Schell	The Solid State Physics Programme at ISOLDE-CERN
12:30-12:45	HO23	A. Neves Cesário	Local Structural Order in Layered Perovskite Solid Solutions
12:45-13:00	HO24	B. Feng	Evaluation of Local Chemical Environment via PAC Spectroscopy Using ¹¹¹ In-Labeled Radiotracers: From Quantification to Cell-Based Validation
13:00-14:30	Lunch		
14:30-15:00	HI15	A. Zarzycki	New Frontiers of Mössbauer Spectroscopy – Phase Transitions of FePd Thin Alloy Films
15:00-15:30	HI16	W. Sato	Enhancement of Electrical Conductivity by Controlling the Chemical States of Impurity In in ZnO
15:30-15:45	HO25	M. Uenomachi	Development of a Novel Nuclear Medicine Imaging Method with Local Microenvironment Sensing Based on Ultrasound- Guided Double-Photon Angular Correlation
15:45-16:00	HO26	K. Okai	Controlling the Isomeric State of Thorium-229 using X-rays
16:00-16:30	Coffee break		
19:00-23:00	Conference dinner		

Day 6. Friday – September 12, 2025

Rooms: AMSTERDAM + GDAŃSK + KOPENHAGA

08:00-08:45	K8	H. Kobayashi	Mössbauer Study of a Critical Charge Mode in a Strange Metal
08:45-09:15	I17	H.H. Klauss	Altermagnetism: A Conceptional Overview and What We Learn with Mössbauer Spectroscopy and Other Local Probes
09:15-09:30	O35	S. Tsutsui	Successive Transitions in Ca ₅ Ir ₃ O ₁₂ Revealed by ¹⁹³ Ir Synchrotron-Radiation-Based Mössbauer Spectroscopy
09:30-09:45	O36	S. Kubuki	Relationships among Structure, Photocatalytic and Electrical Properties of Lanthanide-Substituted Goethite Nanoparticles
09:45-10:00	O37	E.E. Alp	High Throughput Nuclear Resonant Time Domain Interferometry: NR-TDI
10:00-10:30	Coffee break		
10:30-10:40	J. Navařík - Iron Analytics		
10:40-10:50	Z. Nemeth - LynXes		

10:50-11:00	A. Dan - WissEL		
11:00-11:15	O38	J.M. Michalik	Structure, Microstructure, and Hyperfine Interactions in Hf- and Ni-Substituted TiFe Alloy for Hydrogen Storage
11:15-11:30	O39	T. Szumiata	Quality Inspection of 3D Printed Steel Elements, Marine Engine Crankshafts, Wind Turbine Shafts and Nanomagnetic Ferrofluids with Mössbauer Spectrometry
11:30-11:45	O40	M. Hayashi	Effect of Partial Pressures of Oxygen on Oxidation States and Coordination Structures of Iron Ions and on Iron Oxide Activity Coefficients in Silicate Slags
11:45-12:00	Coffee break		
12:00-13:00	Closing ceremony		
13:00-14:30	Lunch		

Notes

Abstracts of Oral Contributions



Tutorial Lectures

TUTORIAL-T08

Nuclear Resonant Scattering Beamline Capabilities Worldwide

Esen Ercan Alp^{1*}

¹Advanced Photon Source, Argonne National Laboratory, USA

*eea@anl.gov

We will present a comprehensive and comparative review of currently available nuclear resonant scattering capabilities at synchrotron sources in the World. Our purpose is to facilitate easier access to these facilities for the worldwide Mössbauer community. Currently, there are 5 different synchrotron sources that offer one or more experimental stations for different isotopes and different techniques of nuclear resonant scattering. The facilities are (in sequence of commissioning) ESRF (Grenoble, France), APS (Argonne, USA), Spring-8 (Hyogo, Japan), PETRA-III (Hamburg, Germany) and HEPS (Beijing, China).

In the last 40 years since the first successful demonstration, the nuclear resonant techniques have proliferated. Currently, the following techniques can be considered distinct enough from each other:

- i) nuclear forward scattering in the time domain,
- ii) nuclear forward scattering in the energy domain,
- iii) nuclear resonant inelastic x-ray scattering,
- iv) nuclear resonant time domain interferometry.

We will present a comprehensive review of accelerator related parameters like bunch structure allocation, type of undulator and upstream optics, and sample environments in terms of temperature, magnetic field, high pressure, and in-situ/in-operando experiments.

TUTORIAL-T08

Determination of the Components of the Electric Field Gradient Tensor in Mössbauer Spectroscopy Using the Velocity Moments Formalism

Paweł Butkiewicz^{1*}, Wojciech Olszewski², Dariusz Satuła², Krzysztof Szymański²

¹Doctoral School Of University of Białystok, University of Białystok, K. Ciolkowskiego 1K, 15–245 Białystok, Poland

²Faculty of Physics, University of Białystok, K. Ciolkowskiego 1L, 15–245 Białystok, Poland

*p.butkiewicz@uwb.edu.pl

The velocity moments formalism reveals the tensorial nature of the Mössbauer spectrum [1]. This approach allows for the separation of electric quadrupole and magnetic dipole interactions within a single-site spectrum. For a single sublattice, the first velocity moment, in the case of using unpolarized radiation, constructed based on the spectral properties, is given by

$$W^1 = \sum_{i=1}^8 v_i a_i,$$

where a_i denotes the intensity of absorption line located on the velocity scale at v_i (the a_i values are normalized so that $\sum_{i=1}^8 a_i = 1$). Concurrently, the first moment of velocity can be expressed as a property of the tensor field associated with the electric field gradient (EFG):

$$W^1 = \delta + \frac{1}{4} \boldsymbol{\gamma} \cdot \vec{\mathbf{U}} \cdot \boldsymbol{\gamma},$$

with δ denoting the isomer shift, $\boldsymbol{\gamma}$ representing the direction of wave vector of source radiation, and $\vec{\mathbf{U}} = \frac{eQc}{2E_\gamma} \vec{\boldsymbol{\phi}}$, where $\vec{\boldsymbol{\phi}}$ symbolizes the EFG, e is value of elementary charge, Q is the nuclear quadrupole moment, E_γ is energy of nuclear transition.

While crystallographic symmetries often prevent the complete determination of electric field gradient components, this method provides additional insights beyond conventional spectral analysis.

In this study, the GaFeO₃ crystal is presented as a case study—the first application of the velocity moments method for extracting its EFG tensor components. Detailed comparisons between experimental results and theoretical predictions [2] underscore both the potential and the limitations of the method, particularly concerning space group symmetry constraints. Furthermore, general expressions will be presented to illustrate the capabilities of EFG determination across various space groups. These insights contribute to a deeper understanding of the interplay between crystallographic environments and electric field gradients, opening new avenues for advancing Mössbauer spectroscopy techniques.

[1] K. Szymański, *Physics Reports* **423** (2006) 295-338.

[2] M. Biernacka et al., *Physical Review B* **108** (2023) 195101.

TUTORIAL-T01

Mössbauer Spectroscopy in Investigation of Harmonically Modulated Spin and Charge Structures

Stanisław M. Dubiel

AGH University of Krakow, Faculty of Physics and Applied Computer Science,
30-059 Kraków, Poland

Stanislaw.Dubiel@fis.agh.edu.pl

Relevance of Mössbauer spectroscopy (MS) in investigation of harmonically modulated electronic structures, i.e., spin-density waves (SDWs) and charge-density waves (CDWs) will be presented and discussed. CDWs exist in 1D and 2D chalcogenides, e.g., TaS₃, NbSe₃, TaS₂, VS₂, and NbSe₂, while SDWs in 3D metals, e.g., Zr, Cr, as well as in 3D compounds like Mn₃Si and UCu₂Si₂ [1]. SDWs are known to exist in metallic chromium, and they were also suggested to occur in iron-pnictides, e.g., [2]. SDWs can co-exist with CDWs.

In the first part of the lecture potential of MS pertinent to SDWs and CDWs will be outlined. In particular, it will be shown that (a) commensurate structures can be distinguished from incommensurate ones, and (b) amplitude and sign of higher-order harmonics, hence shape of SDWs and/or CDWs, can be determined from the Mössbauer spectra [3-5].

In the second part, applications of MS using the effect on ¹¹⁹Sn nuclei (chromium and its alloys) and on ⁵⁷Fe nuclei (Fe-pnictides) will be exemplified and discussed. Particularly, it will be showed that Mössbauer spectra are very sensitive to size of grains, presence of foreign atoms and strain [6-8]. Consequently, to obtain the correct information on virgin properties of SDWs and/or CDWs measurements have to be performed on single-crystalline and strain-free samples. More detailed information can be found elsewhere [9].

- [1] T. Butz (ed.): in Nuclear Spectroscopy on Charge Density Waves Systems, 1992, Kluwer Academic Publ., pp. 7-311.
- [2] M. Li, Y. Zhang, Z.-K. Liu et al., *Nature Communications* **5** (2014) 3711.
- [3] G. Le Caër and S. M. Dubiel, *J. Magn. Magn. Mater.* **92** (1990) 251.
- [4] J. Cieślak and S. M. Dubiel, *Nucl. Instr. Methods in Phys. Res. B* **95** (1995) 131.
- [5] J. Cieślak and S. M. Dubiel, *Nuclear Instr. Methods in Phys. Res. B* **101** (1995) 295.
- [6] S. M. Dubiel and J. Cieślak, *Phys. Rev. B* **51** (1995) 9341.
- [7] S. M. Dubiel, J. Cieślak, F. E. Wagner, *Phys. Rev. B* **53** (1996) 268.
- [8] S. M. Dubiel, *J. Magn. Magn. Mater.* **124** (1992) 31.
- [9] S. M. Dubiel, *Croat. Chem. Acta* **88** (2016) 523.

TUTORIAL-T03

^{57}Fe Mössbauer Spectroscopy: Principles, Methodology and Advanced Applications in Material Science

Juraszek Jean^{1*}

¹Groupe de Physique des Matériaux, Université de Rouen Normandie, Rouen, France

*jean.juraszek@univ-rouen.fr

This tutorial will provide an overview of ^{57}Fe Mössbauer spectroscopy, beginning with the fundamental principles of the Mössbauer effect and the key hyperfine parameters it reveals, such as the isomer shift, quadrupole splitting, and magnetic hyperfine splitting. These phenomena offer highly sensitive insights into the local structural, electronic, and magnetic environments of materials. We will then present the general methodology of Mössbauer spectroscopy, including experimental considerations, data acquisition, and spectral interpretation. Various application examples will illustrate how the technique contributes to the study of phase composition, oxidation states, and magnetic behavior in materials science. A dedicated part of the tutorial will focus on Conversion Electron Mössbauer Spectroscopy (CEMS), a powerful variant particularly suited for surface and thin-film analysis [1,2]. The tutorial will also feature recent case studies from current research, including investigations into the effects of epitaxial strain on the metamagnetic transition in FeRh metallic thin films [3], as well as studies on the antiferromagnetic spin structure in multiferroic BiFeO₃ epitaxial thin films [2,4,5].

- [1] J. Juraszek, O. Zivotsky, H. Chiron et al., *Rev. Sci. Instrum.*, **80** (2009) 043905.
- [2] S. R. Burns, O. Paull, J. Juraszek, et al., *Adv. Mater.* (2020) 2003711.
- [3] C. Bordel, J. Juraszek, D. W. Cooke et al., *Phys. Rev. Letters*, **109** (2012) 117201.
- [4] D. Sando, A. Agbelele, D. Rahmedov et al., *Nature Materials* **12**, (2013) 641.
- [5] D. Sando, F. Appert, O. Paull et al., *Phys. Rev. Materials* **8** (2024) L071401.

TUTORIAL-T04

History of Industrial Applications of Mössbauer Spectroscopy

Ernő Kuzmann

Department of Analytical Chemistry, Institute of Chemistry, Eötvös Loránd University,
Budapest, Hungary

erno.kuzmann@ttk.elte.hu

The first papers related to industrial applications of Mössbauer spectroscopy appeared in the early 1960s. The basic question is: What can be considered as industrial applications of Mössbauer spectroscopy? According to the John Cashion's classification [1] which takes into consideration the viewpoint of the industrial experts: All applications of Mössbauer spectroscopy which can solve directly existing industrial problems or may give information leading to their solution, and performed with natural or current industrial materials which may lead to improvement in processes, or in the materials, or wider uses of the material as well as those assisting the development of new materials or processes of reasonably certain future industrial importance. According to most of the Mössbauer spectroscopists: All applications of Mössbauer spectroscopy which can anyhow related to materials and processes which may potentially be applied in industrial fields (aiming to understand properties, improve and develop materials and processes) and even including those works which future industrial applications are not clear at present. I will give my historical overview according the majority of Mössbauer spectroscopists. My standpoint is: What is science today is industry tomorrow!

In my presentation, I mainly intend to present a historical overview within the individual fields, but in order to emphasize the role of the ISIAME conferences, I will divide the overview into the period before the ISIAME conferences (between 1960 and 1984) and the era starting with the first ISIAME conference (from 1984). Highlighting some examples, I will give more details of the main areas of application before ISIAMEs, and then I will outline how the applications that were received later on, as well as for new areas, were reflected in the history of ISIAMEs.

[1] J. Cashion, *Hyperfine Interactions* **45** (1989) 217.

TUTORIAL-T08

Synchrotron Applications of Mössbauer Techniques (ID14 ESRF)

Sergey Yaroslavtsev

ESRF-The European Synchrotron, Grenoble, France

sergey.yaroslavtsev@esrf.fr

The general advantage of synchrotron techniques is a small beam size, which makes it an indispensable tool to study high pressures, tiny inclusions, and thin films, and it also provides more flexibility for the environment setup. Moreover, synchrotrons have brought several new techniques based on the Mössbauer effect [1]. Synchrotron Mössbauer Source (SMS), Nuclear Forward Scattering (NFS), Nuclear Inelastic Scattering (NIS), Synchrotron Radiation-based Perturbed Angular Correlation spectroscopy (SRPAC), nuclear Bragg diffraction (NBD), nuclear reflectometry (NR), and others are now available at nuclear resonance beamlines. Such beamlines already exist all over the world – at ESRF (France), PETRA-III (Germany), Spring-8 (Japan), APS (USA), and soon at HEPS (China). The first three mentioned techniques are most frequently used, thus, they will be described in more details during tutorial.

SMS provides spectra in the energy domain similar to conventional Mössbauer spectroscopy. Thus, it can be almost directly compared with laboratory data, making this technique easy to understand. SMS has similar integral flux as regular radioactive source, but with much higher area density due to the small beam size. Moreover, beam size could be decreased even more by using focusing Kirkpatrick–Baez mirrors or beryllium lenses. Another advantage of SMS is a zero non-resonant background, which increase the signal-to-noise ratio and makes the fitting of spectra easier in cases when the saturation effect is well pronounced.

NFS is a different take on the same matter. This technique has much higher intensity. Another advantage is that NFS provides emission spectra (in comparison with the absorption spectra of SMS) increasing the signal-to-noise ratio. It allows to measure spectra faster. Moreover, NFS could be utilized with many different isotopes. Thus, NFS could cover more research fields. Spectra are measured in the time-domain creating the main disadvantage of the technique, which is that fitting procedure becomes more complicated, especially if the sample has multiple phases.

NIS is completely different technique, which allows to study isotope selective phonon density of states (DOS). As a result of data analysis, one can extract partial DOS, the force constant, the entropy, the internal energy, the heat capacity, and even more, providing detailed information about vibrations and phonons. Moreover, the Lamb-Mössbauer factor (f_{LM}) can be extracted as a direct result from a single spectrum, while conventional spectroscopy requires multiple measurements at different temperatures.

During the tutorial, the details about possibilities of nuclear resonance beamlines will be given. Examples of synchrotron application in different fields will be presented, including high pressure, operando batteries, and catalysis, focused ion beam (FIB) cuts of samples obtained with well-focused laser heating, and others.

[1] I. Kупenko, X. Li, S.C. Müller, D. Bessas, S. Yaroslavtsev, G. Aprilis, A.I. Chumakov, J.-P. Celse, R. Rüffer, *High Pressure Research* **44** (2024) 310-336.

Notes

Abstracts of Oral Contributions



ICAME Awarded Lectures

ICAME-AWARDED-T08

Forty-five Year Pleasure of Nuclear Resonance Scattering

Aleksandr Chumakov

European Synchrotron Radiation Facility – The European Synchrotron, Grenoble, France

chumakov@esrf.fr

It is generally accepted that engaging in nuclear resonance scattering is a pleasure. However, while the validity of this statement seems unquestionable, this aspect of our work has never been rigorously proven. Moreover, objective reasons for identifying what we do in this way have not been thoroughly analyzed, and, to the best of our knowledge, have possibly never been discussed. Finally, even for those who believe in this statement, the various nuances of pleasure derived from nuclear resonance scattering have neither been classified nor identified.

In this contribution, we aim to fill this gap in understanding our everyday work. Due to the lack of comprehensive statistical data covering the entire nuclear resonance community over the sixty-eight-year history of Mössbauer spectroscopy, we base our analysis on the author's own limited forty-five-year experience. Nevertheless, despite the constrained scope of this research, we expect the conclusions to be sufficiently general and representative.

Within this study, we identify five varieties of pleasure associated with nuclear resonance scattering:

- pleasure in having full control over the research project;
- pleasure derived from quickly moving from an idea to an experiment;
- pleasure in understanding;
- pleasure in being useful to others;
- pleasure in being in good company.

We analyze these aspects of nuclear resonance scattering through examples from the study of the first nuclear resonance multilayer [1], the development of inelastic x-ray scattering with nuclear resonance analysis [2], investigations into the "Boson peak" puzzle in atomic vibrations of glasses [3], advancements in X-ray instrumentation [4], and studies of Dicke's superradiance in an ensemble of nuclei excited by a free electron laser [5]. Finally, we explore the fifth feature, i.e., "pleasure in being in good company," in more detail and broader terms.

- [1] A.I.Chumakov, G.V.Smirnov, A.Q.R.Baron, J.Arthur, D.E.Brown, S.L.Ruby, G.S.Brown, and N.N.Salashchenko, *Phys. Rev. Lett.* **71** (1993) 2489.
- [2] A.I.Chumakov, A.Q.R.Baron, R.Rüffer, H.Grünsteudel, H.F.Grünsteudel, and A.Meyer, *Phys. Rev. Lett.* **76** (1996) 4258.
- [3] A.I.Chumakov, G.Monaco, A.Fontana, A.Bosak, R.P.Hermann, D.Bessas, B.Weinger, W.A.Crichton, M.Krisch, R.Rüffer, G.Baldi, G.Carini Jr., G.Carini, G.D'Angelo, E.Gilioli, G.Tripodo, M.Zanatta, B.Winkler, V.Milman, K.Refson, M.T.Dove, N.Dubrovinskaia, L.Dubrovinsky, R.Keding, and Y.Z.Yue, *Phys. Rev. Lett.* **112** (2014) 025502.
- [4] A.I.Chumakov, Y.Shvyd'ko, I.Sergueev, D.Bessas, and R.Rüffer, *Phys. Rev. Lett.* **123** (2019) 097402.
- [5] A.I.Chumakov, A.Q.R.Baron, I.Sergueev, C.Strohm, O.Leupold, Y.Shvyd'ko, G.V.Smirnov, R.Rüffer, Y.Inubushi, M.Yabashi, K.Tono, T.Kudo, T.Ishikawa, *Nature Physics* **14** (2018) 261.

ICAME-AWARDED-T05

The Role of Root Exudates in Iron Metabolism of Plants

Maria Gracheva^{1,2*}, Zoltán Klencsár¹, Krisztina Kovács²,
Zoltán Homonnay², Ádám Solti²

¹Budapest Neutron Centre, HUN-REN Centre for Energy Research, Budapest, Hungary

²ELTE Eötvös Loránd University, Budapest, Hungary

* maria.gracheva@ek.hun-ren.hu

Plants employ various strategies to solubilize and uptake Fe from the soil, and root exudates, a diverse array of compounds released by plant roots, play a crucial role in iron acquisition, particularly under Fe-deficient conditions. There are several mechanisms to improve iron bioavailability: (a) acidification — pumping of protons and secretion of organic acids, enhancing Fe solubility, (b) chelation — releasing of complexing molecules with varying affinities for Fe, and (c) reduction — releasing of substances that can facilitate the reduction of Fe to the form more readily absorbed by plants [1]. Understanding the complex interactions between root exudates and Fe availability is essential for developing strategies to improve plant growth and nutritional quality in iron-limited soils.

The present work discusses several examples of root exudates, such as organic acids (citric acid) and coumarins (fraxetin), which are believed to be able to chelate and/or to reduce Fe³⁺. Iron speciation in the presence of citric acid varies with the iron-to-citrate molar ratio, and iron photoreduction effects have been studied in comparison to root-associated reduction effects [2, 3]. While citric acid plays a key role in iron complexation, fraxetin and riboflavin do not appear to affect iron speciation under typical biological conditions, contrary to some reports (Fig. 1A). However, iron reduction by fraxetin occurs under highly acidic conditions (pH < 2) as shown at Fig. 1B. In the presence of the root tip in the solution, however, the reduction of iron took place at a broad range of physiological pH values, while addition of fraxetin made the reduction possible even at pH > 7.5. However, Mössbauer analysis and optical microscopy study of the roots showed that the reduced Fe²⁺ species are located only in the tip of the root, while the rest of the root contains iron in ferric form (Fig. 1C).

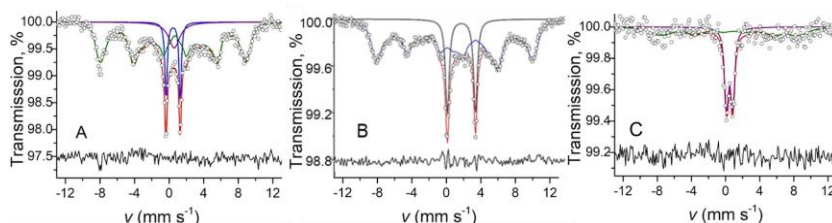


Figure 1. Mössbauer spectra of the frozen solution of ⁵⁷Fe(III)-EDTA (A) and ⁵⁷Fe(III)Cl₃ (B) mixed with fraxetin at 10:1 Fe to fraxetin molar ratio and of the roots of the plants incubated in the ⁵⁷Fe(III)-EDTA solution with fraxetin added (C). The spectra were measured at T = 87 K.

This work was supported by the grant K-146865 of NKFIH, Hungary. Á.S. was supported by the János Bolyai Scholarship of the Hungarian Academy of Sciences (BO-00113-23-8).

[1] Z. Molnár, W. Solomon, L. Mutum, T. Janda, *Plants* **12** (2023) 1945.

[2] M. Gracheva, Z. Homonnay, A. Singh, et al., *Photochem. Photobiol. Sci.* **21** (2022) 983.

[3] M. Gracheva, Z. Klencsár, Z. Homonnay, et al., *Biometals* **37** (2024) 461.

ICAME-AWARDED-T01

Local Order in Micro- up to Nanostructures Studied by ^{57}Fe Mössbauer Spectrometry

Jean-Marc Greneche

Institut des Molécules et Matériaux du Mans, IMMM UMR CNRS 6283,

Le Mans Université, 72085 Le Mans Cedex 9 France

jean-marc.greneche@univ-lemans.fr

Over the past 45 years, I have used Mössbauer spectrometry, essentially ^{57}Fe , to study crystalline and amorphous compounds, molecular structures, nanoparticles, and nanostructured architectures, in oxides, fluorides, and metallic materials alike. Thanks to the instrumental facilities developed in our laboratory, Mössbauer experiments carried out at different temperatures and in the presence of an external magnetic field, combined with specific fitting modelling, make it possible to study carefully the atomic environment of Fe nuclei. Some studies are aimed at improving the composition of certain crystalline compounds, understanding global and local magnetic properties, and understanding the atomic structure in the bulk and on the surface of nanostructures. These studies on artificial, well-reproducible materials prepared according to different chemical or physical processes have been very useful for studying natural materials, opening up a wide range of applications. The presentation will illustrate some relevant studies showing the significant and decisive contribution of Mössbauer spectrometry.

Abstracts of Oral Contributions



ICAME Keynote Lectures

ICAME-KEYNOTE-T02

Mössbauer Spectroscopy: Unlocking the Structural and Mechanistic Insights of Single-Atom Catalysts

Yanqiang Huang

State Key Laboratory of Catalysis, Dalian Institute of Chemical Physics, Chinese Academy of Sciences, Dalian 116023, China

yqhuang@dicp.ac.cn

Single-atom catalysts (SACs), characterized by isolated metal sites with unique coordination environments, have garnered significant attention due to their catalytic mechanisms and potential for a wide range of catalytic reactions. However, characterizing the precise coordination structure of SACs and identifying catalytic centers with similar coordination environments remains a significant challenge. In this report, Mössbauer spectroscopy is presented as a powerful technique for precisely probing the coordination and electronic structure of Mössbauer-active isotopes (such as ^{119}Sn , ^{57}Fe , etc.) in SACs at the atomic level, enabling "quantitative" identification of various SAC catalytic centers. Moreover, *in situ/operando* Mössbauer spectroscopy, along with rapid freeze-quench Mössbauer spectroscopy, provides a robust method to elucidate the dynamic evolution of catalytic center structures, allowing for real-time insight into the true structural configurations and catalytic mechanisms of SACs. Finally, the challenges and opportunities associated with Mössbauer spectroscopy in SAC studies are discussed, emphasizing the need for further development of this technique to fully unlock its potential in catalyst design and mechanistic understanding.

- [1] B. Qiao, A. Wang, X. Yang, L.F. Allard, Z. Jiang, Y. Cui, J. Liu, J. Li, T. Zhang, *Nature Chemistry* **3** (2011) 634.
- [2] X.-F. Yang, A. Wang, B. Qiao, J. Li, J. Liu, T. Zhang, *Accounts of Chemical Research* **46** (2013) 1740.
- [3] A. Wang, J. Li, T. Zhang, *Nature Reviews Chemistry* **2** (2018) 65.
- [4] X. Li, C. Cao, S. Hung, Y. Lu, W. Cai, A. I. Rykov, S. Miao, S. Xi, H. Yang, Z. Hu, J. Wang, J. Zhao, E. E. Alp, W. Xu, T. Chan, H. Chen, Q. Xiong, H. Xiao, Y. Huang, J. Li, T. Zhang, B. Liu, *Chem* **6** (2020) 3440.
- [5] Y. Deng, J. Zhao, S. Wang, R. Chen, J. Ding, H.-J. Tsai, W.-J. Zeng, S.-F. Huang, W. Xu, J. Wang, F. Jaouen, X. Li, Y. Huang, B. Liu, *Journal of the American Chemical Society* **145** (2023) 7242.
- [6] R. Chen, J. Zhao, Y. Li, Y. Cui, Y. Lu, S. Hung, S. Wang, W. Wang, G. Huo, Y. Zhao, W. Liu, J. Wang, H. Xiao, X. Li, Y. Huang, B. Liu, *Journal of the American Chemical Society* **145** (2023) 20683.
- [7] R. Chen, J. Zhao, X. Zhang, Q. Zhao, Y. Li, Y. Cui, M. Zhong, J. Wang, X. Li, Y. Huang, B. Liu, *Journal of the American Chemical Society* **146** (2024) 24368.

ICAME-KEYNOTE-T08

Data and Model Description Framework Developed for Laboratory Mössbauer Spectroscopy

Zoltán Klencsár^{1,2*}, Junhu Wang¹, Rile Ge¹, Duorong Liu¹, Alexandre I. Rykov¹,
Tao Zhang¹

¹Mössbauer Effect Data Center, Dalian Institute of Chemical Physics,
Chinese Academy of Sciences, Dalian, China

²HUN-REN Centre for Energy Research, Budapest, Hungary

*klencsar.zoltan@ek.hun-ren.hu

Sharing of data of scientific research via deposition in data repositories is a standard practice of scientific work performed according to open science principles. The data accumulating in this way has great potential to enhance the scientific research process. However, to realize this potential, deposited scientific data must be sufficiently complete and easy to locate and use in future research. To ensure that deposited data possess these attributes, associated data records must be compiled in a standard format by using a field-specific standard set of metadata. The establishment of a standard metadata set and associated record format, which are widely recognized and accepted in the field of Mössbauer spectroscopy, is essential for the efficient search and utilization of Mössbauer spectroscopy related experimental and theoretical data submitted to scientific data repositories [1].

To enable the creation of such data records in the field of laboratory Mössbauer spectroscopy, a data and model description framework has been worked out by defining the record format and metadata schema that can establish a sufficiently complete description of the measurement conditions and the experimentally obtained Mössbauer spectra along with the associated data treatment and analysis details. Metadata describing experimental circumstances and data treatment procedures commonly encountered in laboratory Mössbauer spectroscopy were defined by considering the requirements of reproducibility and replicability of the associated results. The framework identifies distinct information segments related to various aspects of Mössbauer spectroscopy measurements, and organizes metadata into corresponding metadata groups. To implement this structured metadata schema, a corresponding text file structure has been designed in compliance with XML file syntax guidelines. Both the metadata schema and the associated XML file structure were designed to be suitable to accommodate future extensions. To facilitate the creation of repository records, at the Mössbauer Effect Data Center [2], the development of a web application was initiated to enable the creation of repository records with the proposed content, structure, and format by generating properly structured XML files based on user inputs.

The developed framework will be presented alongside key challenges that need to be addressed to enable the field of Mössbauer spectroscopy to fully benefit from the emerging trend of open data initiatives. Future possibilities that could be achieved through the adoption of the developed framework will also be discussed.

[1] D.L. Nagy, H. Spiering, E. Szilágyi, Towards a metadata standard for laboratory Mössbauer spectroscopy, International Conference on the Applications of the Mössbauer Effect (Brasov, Romania, 2021), *Book of Abstracts ICAME 2021* (eds. S. Greculeasa, C. Locovei, V. Kuncser) p. 99.

[2] Mössbauer Effect Data Center, <https://medc.dicp.ac.cn/>

ICAME-KEYNOTE-T01

Mössbauer Study of a Critical Charge Mode in a Strange Metal

Hisao Kobayashi

¹Graduate School of Science, University of Hyogo, Koto, Hyogo 678-1297, Japan

kobayash@sci.u-hyogo.ac.jp

In intermetallic rare-earth compounds with heavy-fermion characteristics, tuning the ground state via non-thermal parameters is a crucial experimental approach for investigating anomalous phenomena, such as non-Fermi-liquid (strange metallic) states that emerge near a quantum critical point. In these systems, rare-earth ions typically exhibit an almost integer valence, associated with a small characteristic energy scale. In contrast, intermediate-valence rare-earth compounds display a much larger energy scale due to stronger hybridization between the 4f electrons of the rare-earth ions and the conduction electrons.

Synchrotron radiation (SR)-based ¹⁷⁴Yb Mössbauer spectroscopy is a cutting-edge technique for probing the electronic states of Yb ions in a compound [1]. The energy resolution achieved by this method significantly surpasses that of conventional Yb Mössbauer spectroscopies. The valence-fluctuating compound YbAlB₄ crystallizes in two structural forms: α -YbAlB₄ and β -YbAlB₄, both adopting orthorhombic layered structures. α -YbAlB₄ behaves as a heavy fermion compound, exhibiting Fermi-liquid characteristics below T*~8 K, whereas β -YbAlB₄ shows anomalous quantum critical behavior without the need for external tuning [2]. We employed this advanced spectroscopy to explore the relationship between valence fluctuations of Yb ions and the strange metallic properties in β -YbAlB₄ at low temperatures. Our study provides direct evidence of unusually slow charge fluctuations in the strange metallic phase of β -YbAlB₄ [1].

In this presentation, I will demonstrate the application of cutting-edge SR-based Mössbauer spectroscopy to investigate charge dynamics in strange metals under multi-extreme experimental conditions.

[1] H. Kobayashi, et al., *Science* **378** (2023) 908.

[2] Y. Matsumoto, et al., *Science* **331** (2011) 316.

ICAME-KEYNOTE-T01

Quantum Spin Liquids: What Can We Learn From Mössbauer Spectroscopy and Muon Spin Rotation/Relaxation?

F. Jochen Litterst^{1,2*}, Cynthia Contreras Medrano²; Elaheh Sadrollahi^{1,3}, Kim Paul Schmidt¹; Otto Mustonen⁴, Sami Vasala^{2,5}, Elisa Baggio Saitovitch²

¹Technische Universität Braunschweig, 38106 Braunschweig, Germany

²Centro Brasileiro de Pesquisas Físicas, 22290-180 Rio de Janeiro, Brazil

³University of Dresden, 01069 Dresden, Germany

⁴Aalto University, 00076 Espoo, Finland

⁵Helmholtz-Zentrum Dresden-Rossendorf, 01328 Dresden, Germany

*j.litterst@tu-braunschweig.de

Quantum spin liquids are characterized by missing long-range magnetic order and spontaneous symmetry breaking, keeping spins fluctuating fast down to lowest temperatures. In 1973, P.W. Anderson had proposed a scenario describing these properties and related it to resonating valence bond states. This gave impact for wide theoretical and experimental studies. Experimental observations of quantum spin liquid-like behavior have been reported mainly for frustrated quantum antiferromagnets. The nature of quantum spin liquid-like behavior in individual systems is yet still under discussion.

In our contribution, we will give a brief introduction to the physics of different kinds of spin liquids and describe what local probe methods may contribute to its understanding. The specific problems concerning the analysis and interpretation of Mössbauer spectroscopy and Muon Spin Rotation and Relaxation data will be addressed by reviewing data from the literature and discussing recent experiments.

HYPERFINE-KEYNOTE-T01

Ion-implanted β -NMR as a Probe of Materials

W. Andrew MacFarlane^{1, 2, 3}

¹ Department of Chemistry, University of British Columbia, 2036 Main Mall, Vancouver, BC, V6T 1Z1, Canada

² Stewart Blusson Quantum Matter Institute, University of British Columbia, 2355 East Mall, Vancouver, BC, V6T 1Z4, Canada

³ TRIUMF, 4004 Wesbrook Mall, Vancouver, BC, V6T 2A3, Canada

wam@chem.ubc.ca

Beta-detected NMR uses the anisotropic emission of high energy β particles from radioactive beta decay to detect the state of the nuclear spin and thus the nuclear magnetic resonance. To be useful, the radioactive half-life $\tau_{1/2}$ must be $< \sim T_1$, the spin-lattice relaxation time, so the radioisotope must be short-lived with $\tau_{1/2}$ on the scale of seconds or less. Using the on-line isotope separation scheme, like CERN's ISOLDE, the ISAC facility at TRIUMF provides intense keV energy beams of such rare isotopes for research, including to a facility dedicated to β NMR studies of materials. Primarily, this uses the simplest, lightest β NMR nucleus, ^8Li . As with muon spin rotation (μSR), the hyperfine probe is extrinsic and can be implanted into any material. One of the most important capabilities of "ion-implanted" β NMR is the ability to study thin films and to make depth-resolved NMR measurements in solids on the nanometre scale. In this talk, I will review this implementation of β NMR and its capabilities [1, 2] and present examples of its use.

[1] W. MacFarlane, *Zeitschrift für Physikalische Chemie* **236** (2022) 757.

[2] W. MacFarlane, *Solid State Nuclear Magnetic Resonance* **68–69** (2015) 1.

ICAME-KEYNOTE-T04

Local Distortion of Highly Conducting Glass and Glass Ceramics

Tetsuaki Nishida

Environmental Materials Institute, Fukuoka, Japan

tnishida3730@gmail.com

“Glass is liquid with a mask of solid.” Mössbauer spectroscopy is a powerful tool to evaluate the local structure of glass and glass ceramics containing Mössbauer nuclides such as ^{57}Fe , ^{119}Sn , ^{151}Eu , and ^{197}Au . Quadrupole splitting (Δ) of Fe^{III} reflects *local distortion* of FeO_4 , SiO_4 , BO_4 , AlO_4 , GaO_4 , VO_4 units, *etc.*, since they have essentially the same local structure by sharing corner oxygen atoms. Systematic Mössbauer and DTA studies of oxide glasses led to the discovery of a linear relationship, “*Tg- Δ rule*”, between glass transition temperature (T_g), which increased from 180 to 800 °C, and Δ of Fe^{III} , which increased from 0.44 to 1.30 $\text{mm}\cdot\text{s}^{-1}$ [1, 2]. This finding means that macroscopic physical properties could be regulated by the *local distortion* of the network. This experimental rule was supported by the *conformer model* proposed for polymers [3], $T_g = E_h/\text{Scg}$, in which E_h is the excess enthalpy necessary to create free volume fraction for the glass transition, while Scg conformational entropy that is inversely proportional to the number of fragments involved in the cooperative rearrangements.

Conducting potassium iron vanadate glass, $25\text{K}_2\text{O}\cdot 10\text{Fe}_2\text{O}_3\cdot 65\text{V}_2\text{O}_5$, of pseudo-1D chain structure and low DC resistivity (ρ) of 2.3 $\text{k}\Omega\cdot\text{cm}$ was incidentally prepared on the way of heat treatment conducted at around the crystallization temperature (T_c) of 340 °C [4]. Much lower ρ of 25 $\Omega\cdot\text{cm}$ could be achieved in barium iron vanadate glass, $15\text{BaO}\cdot 15\text{Fe}_2\text{O}_3\cdot 70\text{V}_2\text{O}_5$, which had a 3D-network with many pathways available for the conduction [5]. These results are involved with *decreased local distortion* or *structural relaxation* of the network. Introduction of metal oxide with a narrow bandgap could furthermore decrease the ρ values [2, 6-10].

Iron-containing conducting vanadate glass has been successfully applied to electronic materials such as discharge needle of air cleaner, cathode active material of lithium-ion battery (LIB), and bifunctional rare-earth-free catalyst of metal-air battery. At ICAME2025, current topics will be delivered on new cathode active materials of LIB, such as $20\text{Li}_2\text{O}\cdot 10\text{Fe}_2\text{O}_3\cdot 5\text{P}_2\text{O}_5\cdot 3\text{Cr}_2\text{O}_3\cdot 62\text{V}_2\text{O}_5$ glass, which revealed amazing discharge capacities of 295, 265, and 249 $\text{mAh}\cdot\text{g}^{-1}$ at 1st, 50th, and 100th cycles, respectively. They are much superior to the capacity of LiFePO_4 (170 $\text{mAh}\cdot\text{g}^{-1}$), known as the conventional cathode active material.

- [1] T. Nishida H. Ide, Y. Takashima, *Bull. Chem. Soc. Jpn.* **63** (1990) 548.
- [2] T. Nishida, S. Kubuki, N. Oka, *J. Mater. Sci.: Mater. Electron.* **32** (2021) 23655.
- [3] S. Matsuoka, X. Quan, *Macromolecules* **24** (1991) 2770.
- [4] T. Nishida, J. Kubota, Y. Maeda, F. Ichikawa, T. Aomine, *J. Mater. Chem.* **6** (1996) 1889.
- [5] K. Fukuda, A. Ikeda, T. Nishida, *Solid State Phenom.* **90-91** (2003) 215.
- [6] K. Matsuda, S. Kubuki, T. Nishida, *AIP Conf. Proc.* **1622** (2014) 3.
- [7] T. Nishida, S. Kubuki, K. Matsuda, Y. Otsuka, *Croat. Chem. Acta* **88** (2015) 427.
- [8] T. Nishida, Y. Izutsu, M. Fujimura, K. Osouda, Y. Otsuka, S. Kubuki, N. Oka, *Pure Appl. Chem.* **89** (2017) 419.
- [9] T. Nishida, Y. Fujita, S. Shiba, S. Masuda, N. Yamaguchi, T. Izumi, S. Kubuki, N. Oka, *J. Mater. Sci.: Mater. Electron.* **30** (2019) 8847.
- [10] T. Nishida, N. Oka, T. Sakuragi, S. Matsusako, R. Imamura, Y. Sato, *J. Mater. Sci.: Mater. Electron.* **31** (2020) 22881.

Spent LiFePO₄ Batteries Management: Towards Direct Recycling Strategies

Moulay Tahar Sougrati^{1,2}

¹ICGM, Université Montpellier, CNRS, ENSCM, 34090, Montpellier, France

²Réseau sur le Stockage Electrochimique de l'Energie (RS2E), FR CNRS 3459, Amiens, France

Moulay-tahar.sougrati@umontpellier.fr

The linear economic model, based on extraction, production, consumption, and disposal, is no longer sustainable. A transition toward a circular economy is essential, particularly to support the deployment of renewable energy and the reduction of the overall energy footprint. In this context, electric mobility plays a central role, driven by electric vehicles (EVs) that rely on high-energy-density batteries. Among lithium-ion technologies, lithium iron phosphate (LFP) batteries stand out due to their safety, long cycle life, and the use of abundant and widely distributed elements such as iron and phosphorus. However, large-scale deployment of this technology demands efficient, cost-effective, and sustainable recycling strategies for electrode materials at end-of-life. Beyond conventional recycling methods (pyro- and hydrometallurgy), direct recycling approaches are emerging, aiming to restore the performance of active materials while significantly reducing energy use and chemical consumption. In this work, we report two innovative methods for the direct regeneration of end-of-life LFP cathodes, both avoiding high-temperature treatments: (A fast, solvent-free (FSF) dry method and a mild aqueous route using ascorbic acid as a reducing agent). An advanced multi-analytical characterization strategy was employed to assess the effectiveness of these processes. In particular, Mössbauer spectroscopy played a key role in identifying iron oxidation states, thus indirectly quantifying lithium loss, and diagnosing failure mechanisms in aged cathode materials. Our results show that end-of-life LFP is typically oxidized by ~33%, corresponding to lithium loss through parasitic reactions (Figure 1a). After relithiation, all Fe³⁺ species are reduced back to Fe²⁺ via lithium reinsertion, restoring the LFP structure (Figure 1b) and its electrochemical performance. Notably, the regenerated materials exhibit electrochemical properties comparable to pristine LFP (Figure 1c). These findings demonstrate that direct recycling offers a promising pathway toward a low-energy, low-impact, and potentially competitive solution for the sustainable management of LFP batteries within a circular economy framework.

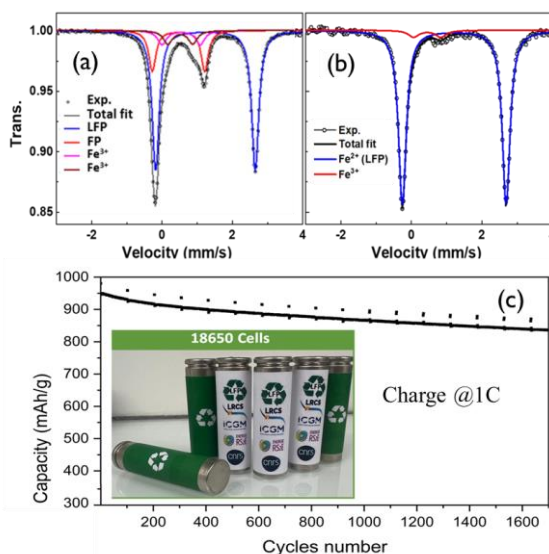


Figure 1. RT Mössbauer spectra before (a) and after (b) regeneration of spent LFP. Typical performance obtained in 18650 cells. (c)

A Global Mössbauer Spectrum for Martian Soil

Paulo de Souza

School of Engineering, Edith Cowan University, Joondalup, Australia

p.desouza@ecu.edu.au

The mineralogical and elemental composition of Martian soil provides valuable insights into chemical and physical weathering processes. Data from the Mars Exploration Rovers suggest that bright dust deposits on opposite sides of the planet belong to a global unit rather than being influenced by local rock compositions [1, 2]. Dark soil deposits at both sites exhibit similar basaltic mineralogy, indicating either a global component or comparable local rock sources. The presence of olivine suggests limited aqueous alteration, while elevated nickel concentrations imply that the upper soil layers may contain up to one percent meteoritic material, reinforcing the overall homogeneity of Martian surface soil.

Physical weathering, driven by extreme temperature fluctuations and strong winds, plays a significant role in soil formation, with global storms facilitating its uniform distribution [3]. Mössbauer analyses from MIMOS II data collected on Mars [e.g., 4, 5] provided breakthrough insights into iron mineralogy of the planet's surface. Resulting from limited measurement time, science operations were divided among multiple instruments, restricting the detection of minor Fe-bearing mineral phases (below 5% WSA). MIMOS II records Mössbauer spectra at 10K intervals, and to enhance signal-to-noise ratios, spectra from different intervals were combined, when applicable [6]. For instance, temperature variations between -10°C and -40°C in basaltic samples do not significantly impact the spectra, allowing data from all intervals to be integrated.

By combining MIMOS II data from various soil samples and over different temperature ranges, global Mössbauer spectrum for Martian soil is proposed, aiming to identify potential minor Fe-bearing mineral phases on the planet's surface.

- [1] A. Yen et al. *Nature* **436** (2005) 49.
- [2] W. Goetz et al., *Nature* **436** (2005) 62.
- [3] R. Greeley et al., *JGR-Planets* 111 (2006) E02S09.
- [4] G. Klingelhöfer et al. *Science* 306 (2004) 1740.
- [5] R. V. Morris et al. *Science* 305 (2004) 833.
- [6] G. Klingelhöfer et al. *JGR-Planets* **151** (2003) 125.

Notes

Abstracts of Oral Contributions



ICAME Invited Lectures

ICAME-INVITED-T01

Complex Structural, Mössbauer Spectroscopy and Magnetic Investigations of Rare-Earth Iron Garnets Obtained by Different Processing Routes

Cristina Bartha

National Institute of Materials Physics, Atomistilor str. 405A, Bucharest-Magurele, Romania

cristina.bartha@infim.ro

Recent advances in spintronic ultrafast spin storage devices have increasingly focused on ferrimagnetic rare-earth iron garnets close to the compensation temperature, Θ_C . In this respect, sintering such materials with a compensation temperature near room temperature, RT, is essential. However, tuning Θ_C in general and over RT in particular, is highly challenging due to its critical dependence on the structural, magnetic, and stoichiometric properties of the material. Its precise control requires a thorough understanding of how atomic arrangement, cation interactions, and rare earth content modify exchange interactions and magnetic configuration of the material, with direct influence on the magnetization compensation conditions. This study presents an in-depth analysis of the stoichiometry of rare-earth iron garnets synthesized by distinct routes and its influence on the magnetic configurations and compensation temperatures, promoting various magneto-functionalities. The proposed materials were obtained by three different methods, two of them being used for the first time for this type of compounds: (i) an original processing route that combines a cheap and facile surfactant assisted hydrothermal method to prepare mesoporous garnet nano-powders followed by sintering, (ii) Spark Plasma Sintering (SPS) and post-annealing to obtain high-density nano-structured bulks, and (iii) solid state reaction. Samples were investigated with respect to morpho-structural and magnetic properties. X-ray diffraction and Rietveld analysis confirm for all analyzed samples the presence of only garnet phases with different stoichiometries, which differ from the ideal one. The ideal structure of a rare-earth iron garnet type ($\text{RE}_3\text{Fe}_5\text{O}_{12}$) is cubic, with 2 iron atoms on the octahedral positions and 3 iron atoms on the tetrahedral positions, the 3 RE atoms being on the dodecahedral position according to the formula unit: $\text{RE}_3^{3+}\text{Fe}_2^{3+}\text{Fe}_3^{3+}\text{O}_{12}$. The changes in stoichiometry are due to the presence of small cationic inversions, as well as to defects, both generated by processing technologies. To note that the stoichiometry closest to the ideal one was observed in samples processed by SPS. Local electronic and magnetic configurations in the analyzed samples were investigated by temperature-dependent Mössbauer Spectroscopy. Magnetic properties and some related magneto-functionalities were investigated by magnetometry and magneto-electric measurements, and finally correlated to the local structure. The regularly observed two components in the Mössbauer spectra, directly connected to the two components derived from Rietveld analysis, highlight the formation of two garnet phases, one with ideal stoichiometry and the second one with cationic inversion. For the phase with cationic inversion, Fe^{3+} ions from the octahedral positions migrate partially to the position of RE and vice versa, generating a structure of the type $(\text{RE}_{3-x}\text{Fe}_x)(\text{Fe}_{2-x}\text{RE}_x)\text{Fe}_3\text{O}_{12-x}$, fully elucidated from Mössbauer and magnetic investigations. It has been proven that the magnetic properties, including the compensation temperature as well as the related magneto-functionalities, can be understood only on the basis of the Mössbauer spectroscopy data.

ICAME-INVITED-T02

Spectroscopic and Computational Studies of Unique Spin States in Biological Iron-Sulfur Clusters and Their Synthetic Congeners

Jin Xiong¹, Divya Prakash², Anupkuar Rai², Mengshan Ye³, Daniel Suess³, Emile L. Bominaar¹, and Yisong Guo^{1*}

¹ Department of Chemistry, Carnegie Mellon University, PA, US

² Chemical and Biomolecular Sciences, Southern Illinois University, IL, US

³ Department of Chemistry, Massachusetts Institute of Technology, MA, US

*ysguo@andrew.cmu.edu

Iron-sulfur (Fe-S) clusters exist in all life forms and play critical and versatile roles as electron transport units, catalytic centers, structural components, or regulators in numerous biological pathways. As one of the most common and important family members, 4Fe-4S clusters formally can show four oxidation states, $[4\text{Fe-4S}]^{0,1+,2+,3+}$, with a common ground spin state of $S = 0$ for the 2+ state, and $S = 1/2$ for the 1+ and 3+ states. However, an enzymatic $[4\text{Fe-4S}]^+$ intermediate in group 4 ferredoxin: thioredoxin reductase (AFTR) exhibits an $S = 7/2$ ground state. Similarly, a synthetic $[4\text{Fe-4S}]$ model complex, MP^{2+} , was also found to adopt an $S = 7/2$ state. Herein, we report a comprehensive spectroscopic analysis centered around Mössbauer spectroscopy and theoretical investigation using density functional theory of the $S = 7/2$ $[4\text{Fe-4S}]^{1+}$ intermediate of AFTR, with MP^{2+} serving as a spectroscopic model. Our results indicate that the $S = 7/2$ ground state originates from chemical modification of one of the acid-labile sulfide bridges, leading to the formation of a $\mu_3\text{-SR}^-$ moiety ($\text{R} = \text{H}$ in AFTR, or C in MP^{2+}). Specifically, the $[4\text{Fe-3SSH}]^{2+}$ intermediate in AFTR provides the first direct evidence for an Fe-S cluster acting as a proton transfer unit in biological systems.

ICAME-INVITED-T03

How Do the Synthesis Conditions Influence the Final Properties of Nanoparticles

Beata Kalska-Szostko^{1*}, Urszula Klekotka¹, Magda Bielicka², Anna Wasilewska²,
Dariusz Satuła³, Wojciech Olszewski³

¹University of Białystok, Faculty of Chemistry, Ciołkowskiego 1K, 15-245, Białystok, Poland

²Doctoral School, University of Białystok, Ciołkowskiego 1K, 15-245, Białystok, Poland

³University of Białystok, Faculty of Physics, Ciołkowskiego 1L, 15-245 Białystok, Poland

* kalska@uwb.edu.pl

The properties of nanoparticles strongly depend not only on their composition but also on the synthesis routine and used stabilizers. Therefore, factors such as: the nature of the rigid core precursor, synthesis conditions, as well as selected nanoparticles coating are important issues, since they determine the final products. Each of these parameters influences according to its own rule; therefore, a detailed and systematic study of these allows us to draw some conclusions. The choice of core composition primarily determines the magnetic properties, which are expected due to the foreseen application. Synthesis conditions are very often rigorously monitored or limited due to economic issues, favoring low cost and the most effective one. The study of surface stabilization is of great significance, since many characteristics, e.g., blocking temperature, particle interactions, etc., strongly depend on particle size, morphology, and therefore, the type of surfactants used.

In the presented studies, nanostructures were obtained by modified thermal decomposition of iron(III) acetylacetonate precursor in an organic solvent, co-precipitation of iron chlorides in an ammonia solution, or green chemistry processes. Selected long-chain carboxylic acids (eg, oleic, lauric, palmitic, stearic, and caprylic acids) or amines (e.g., oleylamine, hexylamine, dioctylamine, trimethylamine, and trioctylamine) were tested for their effectiveness in stabilizing nanoparticles. The obtained nanoparticles were examined by XRD, TEM, and FTIR. Their magnetic properties were characterized by Mössbauer spectroscopy.

The presented studies show: (I) how the ration of surfactant to inorganic core precursors influences on the nanoparticles growth, morphology, and its final properties; (II) whether the characteristics of the doping element have impact on positioning in magnetite structure; and (III) are the green chemistry routines suitable for magnetite synthesis.

The work was partially financed by EU funds via project with contract number POPW.01.03.00-20-034/09-00, POPW.01.03.00-20-004/11-00.

ICAME-INVITED-T01

Altermagnetism: A Conceptional Overview and What We Learn with Mössbauer Spectroscopy and Other Local Probes

Hans-Henning Klauss^{1*}, Felix Seewald¹, Tillmann Weinhold¹, Rajib Sarkar¹, Mengli Hu², Oleg Janson², Jeroen van den Brink², Sabine Wurmehl², Shandra Shekhar³, Claudia Felser³

¹IFMP, Faculty of Physics, TU Dresden, Germany

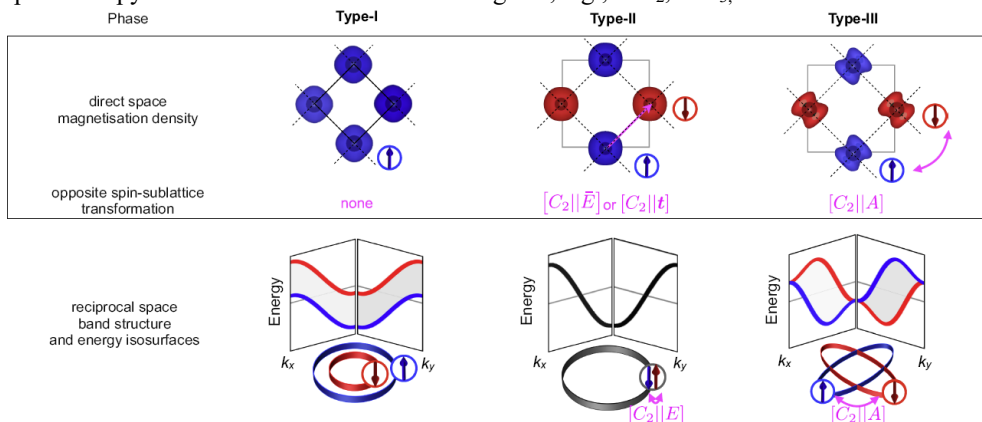
²Leibniz Institute for Solid State and Materials Research IFW Dresden, Germany

³Max-Planck-Institute for Chemical Physics of Solids, Dresden, Germany

*henning.klauss@tu-dresden.de

Altermagnetism is a new form of long-range magnetic order different from ferromagnetism and antiferromagnetic, and ferrimagnetic magnetic orders known. New functionalities arise mainly for semimetallic or metallic systems with long-range altermagnetic order. These systems show spin-split bands in an antiferromagnetic system [1,2]. In my talk, I present an illustrative picture to understand why spin-split bands are formed in such antiferromagnets [3] and the systematic classification of altermagnets.

So far, about 50 possible altermagnetic systems are identified from symmetry considerations and band structure calculations [2]. Several of these compounds exist for decades. I will discuss what are characteristic signatures of altermagnets in Mössbauer and NMR spectroscopy and why they are often not observed. In my talk, I will focus on Mössbauer spectroscopy of some of the Fe-based altermagnets, e.g., FeF₂, FeF₃, and FeSb.



[1] L. Šmejkal, J. Sinova, and T. Jungwirth, *T. Phys. Rev. X* **12** (2022) 031042.

[2] Y. Guo, H. Liu, O. Janson, I. C. Fulga, J. v. d. Brink, *Mat. Today Phys.* **32** (2023) 100991.

[3] S. S. Fender, O. Gonzales, D. K. Bediako, *J. Am. Chem. Soc.* **147** (2025) 2257.

ICAME-INVITED-T08

Mössbauer Spectroscopy of Nanoparticle Suspensions

Denisa Kubániová^{1,2*}, Tomáš Kmječ^{2,1}

¹Institute of Physics CAS, Na Slovance 1999/2, Prague, 182 21, Czech Republic

²Department of Low Temperature Physics, Faculty of Mathematics and Physics, Charles University, V Holešovičkách 2, Prague, 180 00, Czech Republic

*denisa.kubaniova@matfyz.cuni.cz

A comprehensive understanding of the fundamental physical characteristics and the intricate relationships among composition, microstructure, magnetic properties, and relaxation characteristics is crucial for the rational design of well-defined magnetic nanoparticle systems for both material research and industrial applications.

Whenever possible, it is advantageous to study the nanoparticles using complementary methods in their as-prepared state, as the purification process and other sample treatments can alter the original product, especially for highly reactive species.

The application of Mössbauer spectroscopy to study nanoparticle suspensions presents several significant challenges, particularly when dealing with thermal anchoring of the sample volume to the heater in various cryogenic experimental setups and ensuring a sufficient concentration of resonant nuclei in the cross-section of the incident γ -beam while minimizing the non-resonant absorption. Particles subjected to temperature gradient within the sample volume can exhibit spectral characteristics that may lead to physical misinterpretation of the data. This issue is particularly pronounced in materials with strong temperature dependence of hyperfine parameters or in voluminous suspension of particles with distributions of particle size and/or magnetocrystalline anisotropy.

This presentation delves into the experimental methodologies developed to overcome these challenges and the novel data analysis methods designed to extract meaningful information from complex spectra of nanoparticles with particle size distribution subjected to superparamagnetic relaxation. Several case studies, including validation of the method, will be presented to illustrate the capabilities and limitations of Mössbauer spectroscopy in the context of nanoparticle suspensions.

ICAME-INVITED-T03

Mössbauer Study of Iron Nitrides: Exploring Biomedical and Thermoelectric Applications

Lenka Kubičková^{1,2*}, Jaroslav Kohout², Tomáš Kmječ², Karel Knížek¹, Štefan Hricov^{1,3}, Ondřej Kaman¹, Jamila Kuličková¹, Yevhen Ablets⁴, Robin Kidangan Paul⁴, Stanislav Mráz⁵, Jochen Schneider⁵, Oliver Gutfleisch⁴, Imants Dirba⁴

¹FZU - Institute of Physics of the Czech Academy of Sciences, Praha, Czech Republic

²Faculty of Mathematics and Physics, Charles University, Praha, Czech Republic

³Faculty of Science, Charles University, Praha, Czech Republic

⁴Functional Materials, Institute of Materials Science, TU Darmstadt, Darmstadt, Germany

⁵Materials Chemistry, RWTH Aachen University, 52074 Aachen, Germany

*kubickol@fzu.cz

Mössbauer spectroscopy has proven to be a powerful tool for probing the local electronic and magnetic properties of materials containing Mössbauer isotopes. We will present selected examples of iron nitrides studied by ^{57}Fe Mössbauer spectroscopy, employing both traditional transmission geometry and conversion electron Mössbauer spectroscopy (CEMS). First, we will show spectra of air-sensitive Fe_3N nanoparticles, which exhibit a high degree of structural disorder. Moreover, we will discuss the formation of an oxide layer by their passivation, whose nature and extent are difficult to assess from other methods, but are crucial for medical applications. Second, room-temperature CEMS spectra of $\text{Fe}_{4-x}\text{Ge}_x\text{N}$ ($x = 0, 0.5$, and 1) crystalline thin films not only demonstrate the magnetic dilution effect with increasing content of Ge, but also allow us to determine the direction of magnetization in the film of the undoped phase. In addition, together with the DFT calculations, the position of the Ge atom in the Fe_4N structure can be determined based on the hyperfine parameters of the neighboring ^{57}Fe nuclei. Such local insights are valuable for designing and optimizing iron-based films, e.g., for their magnetic or thermoelectric applications.

Acknowledgement

Funding by the TERAfit project - CZ.02.01.01/00/22_008/0004594 is gratefully acknowledged.

ICAME-INVITED-T01

Interplay between Structural, Electronic, and Magnetic Properties of Iron Oxides at Extreme Conditions

Xiang Li^{1,2}

¹ESRF-The European Synchrotron (ESRF), Grenoble, France)

² Institute for Mineralogy, University of Münster, Münster, Germany)

* xiang.li@esrf.fr

Iron-bearing minerals play a fundamental role in basic science, applied technologies, and geoscience. Traditionally, FeO, Fe₂O₃, and Fe₃O₄ were considered the primary stoichiometries of iron oxides. Over the past decade, high-pressure and high-temperature studies have identified new phases of these oxides and have led to the discovery of novel binary iron oxides with unconventional stoichiometries, such as Fe₄O₅, Fe₅O₆, and so on [1, 2]. Most of them are fundamentally related and can be described by the homologous series $n\text{FeO}-m\text{Fe}_2\text{O}_3$ [3]. While substantial research has been conducted on these iron oxides, limited information exists about their structural, electronic, and magnetic properties under extreme pressure-temperature conditions. Notably, the interplay between these properties remains largely unexplored, despite its potential implications for understanding a wide range of oxides.

We will present our recent investigation on the pressure and temperature dependence of the electronic, magnetic, and structural properties of iron oxide, using the FeO end-member as an example, by means of Single-Crystal X-ray diffraction and Synchrotron Mössbauer Source spectroscopy in diamond anvil cells at pressures up to 200 GPa and temperatures up to 3000 K. The potential implications for the planetary interiors and other complex oxides systems will be discussed.

[1] B. Lavina, et al., *Proc. Natl Acad. Sci. USA* **108** (2011) 17281–17285.

[2] B. Lavina and Y. Meng, *Sci. Adv.* **1** (2015) e1400260.

[3] E. Bykova, et al., *Nat. Commun.* **7** (2016) 10661.

ICAME-INVITED-T02

Mössbauer Studies on Catalysts for H₂ Storage Using Dibenzyltoluene

Kuo Liu^{1*}, Junhu Wang², Yanqiang Huang², Xuning Li², Tao Zhang^{2,3}

¹Institute of Process Engineering, Chinese Academy of Sciences, Beijing, China

²Dalian Institute of Chemical Physics, Chinese Academy of Sciences, Dalian, China

³University of Chinese Academy of Sciences, Beijing, China

* kuoliu@ipe.ac.cn

Hydrogen (H₂) is considered as a clean and efficient secondary energy, and the use of H₂ to generate electricity won't cause any harmful emissions. However, how to store and transport H₂ safely remains a challenge. The technology using liquid organic hydrogen carries (LOHCs) could transport H₂ at ambient conditions and is a safe way of H₂ storage and transportation [1-3]. The core of this technology is the catalysts. Until now, Mössbauer study on the catalysts for H₂ storage using LOHCs is still rare, although Mössbauer spectroscopy is a powerful tool for clarifying the catalytic reaction mechanism based on quasi in situ, in situ, and operando techniques [4-8]. In this report, application of Mössbauer spectroscopy in H₂ storage using dibenzyltoluene (DBT, a promising LOHC with theoretical 6.2 wt% hydrogen storage capacity) is presented. PtFe-containing catalysts could achieve high degrees of DBT hydrogenation at 150 °C. The addition of Fe in Pt/Al₂O₃ was found to benefit the dehydrogenation of perhydro-dibenzyltoluene (H18-DBT), and the dehydrogenation degree on the catalyst with an Fe loading of 1 wt% was > 80% at 300 °C. By combining Mössbauer spectroscopy, XRD, and XPS studies, the change of the Fe species during the reaction was studied in detail, and the active Fe species were identified. The presence of low valent Fe species and modification of Pt by Fe species accounted for the high activity of H18-DBT dehydrogenation.

- [1] H. Jorschick, P. Preuster, S. Dürr, A. Seidel, K. Müller, A. Bösmann, P. Wasserscheid, *Energy & Environment Science* **10** (2017) 1652.
- [2] T.W. Kim, M. Kim, S.K. Kim, Y.N. Choi, M. Jung, H. Oh, Y.-W. Suh, *Applied Catalysis B: Environment and Energy* **286** (2021) 119889.
- [3] N. Lei, S. Qiu, L. Zhang, G. Zhao, S. Wang, K. Liu, *Industrial & Engineering Chemistry Research* **64** (2025) 4761.
- [4] K. Liu, A. Wang, W. Zhang, J. Wang, Y. Huang, J. Shen, T. Zhang, *The Journal of Physical Chemistry C* **114** (2010) 8533.
- [5] K. Liu, W. Zhang, J. Wang, A. Wang, Y. Huang, C. Jin, J. Shen, T. Zhang, *Chinese Journal of Catalysis* **31** (2010) 1335.
- [6] K. Liu, A.I. Rykov, J. Wang, T. Zhang, *Advances in Catalysis* **58** (2015) 1.
- [7] Y. Deng, J. Zhao, S. Wang, R. Chen, J. Ding, H.-J. Tsai, W.-J. Zeng, S.-F. Huang, W. Xu, J. Wang, F. Jaouen, X. Li, Y. Huang, B. Liu, *Journal of the American Chemical Society* **145** (2023) 7242.
- [8] K. Liu, J. Wang, T. Zhang, *Mössbauer Spectroscopy Applications in Chemistry and Materials Science*, published by WILEY-VCH (2023) 145.

ICAME-INVITED-T06

Application Of Mössbauer Spectroscopy To Study Metamict Minerals And Their Thermally-Induced Recrystallization Process

Dariusz Malczewski^{1*}, Agnieszka Grabias², Maria Dziurawicz¹

¹University of Silesia, Institute of Earth Sciences, 41-200 Sosnowiec, Poland

²Łukasiewicz Research Network - Institute of Microelectronics and Photonics, 02-668 Warszawa, Poland

*dariusz.malczewski@us.edu.pl

This presentation summarizes recent research findings of representative metamict minerals using ^{57}Fe Mössbauer spectroscopy. Metamict minerals contain radioactive elements (^{238}U , ^{232}Th , and ^{235}U) that degrade their crystal structures over geologic time ($\sim 10^9$ years) due to recoil nuclei from α -decays of U and Th series [1]. The main factors influencing susceptibility to amorphization (metamictization) of a given mineral are the total absorbed α -dose (D) expressed as the number of alpha decays per g or mg of the mineral mass and the internal complexity of crystal structure (number of cationic positions, bond types, atomic packing). Most silicates become metamict after the cumulative α -dose of about 10^{16} α -decays mg^{-1} , whereas metamict oxides require an amorphization dose above 10^{17} α -decays mg^{-1} [2]. The original crystalline structure of a metamict mineral may be restored with high-temperature annealing. These minerals are widely used in geochronology and can be natural analogs for radiation effects in high-level nuclear waste (HLW). The rare earth elements (REE) content in metamict minerals may exceed 50%. Changes in hyperfine parameters observed in ^{57}Fe Mössbauer spectra of annealed iron-bearing metamict minerals are sensitive indicators of recrystallization. Results presented here demonstrate the use of Mössbauer spectroscopic data to track the transformation of the local crystal structure around Fe ions in metamict phases and to determine the activation energy for the thermally-induced recrystallization process[3]. The higher the activation energy for recrystallization, the easier a mineral phase may be amorphized by internal radiation damage.

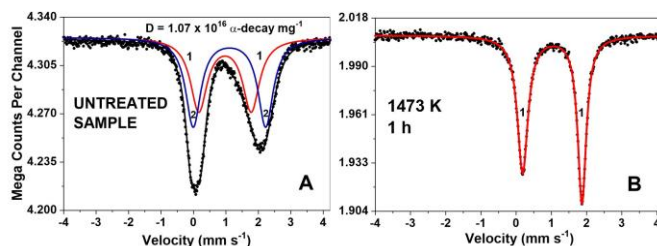


Figure 1. ^{57}Fe Mössbauer spectra of (A) Untreated fully metamict gadolinite sample ($\text{REE}_2\text{Fe}^{2+}\text{Be}_2\text{Si}_2\text{O}_{10}$), and (B) Gadolinite sample after one-hour annealing in argon at 1473 K.

Acknowledgments. This work was supported by the National Science Centre of Poland, grant no. 2018/29/B/ST10/01495.

- [1] R.C. Ewing, *Nuclear Instruments and Methods in Physics Research B* **91** (1994) 22.
- [2] D. Malczewski, M. Dziurawicz, *American Mineralogist* **100** (2015) 1378.
- [3] D. Malczewski et al, *Journal of Geosciences* **65** (2020) 37.

ICAME-INVITED-T01

***Operando* Mössbauer Spectroscopy Under Reversible Strain for Magneto-Strictive Materials**

Jun Okabayashi

Research Centre for Spectrochemistry, The University of Tokyo, Japan

jun@chem.s.u-tokyo.ac.jp

The large magnetostriction (MS) effect has garnered attention for device applications involving sensors or vibrational power generation [1]. Although most significant MS effects depend on materials containing rare-earth elements, Fe₃Ga (Galfenol) modifies Fe-based materials to achieve a large MS of 300 ppm, which is ten times greater than that of conventional alloy compounds. However, the reason for the large MS in Fe₃Ga remains unclear. The doping of Ga atoms into pure bcc-Fe enhances the MS by altering the electronic structures [2,3]. The piezoelectric control of Fe₃Ga/ferroelectric materials has also gained interest through the introduction of reversible strain. From the perspective of electronic structures, the spin and orbital states under applied reversible strain must be examined. We have developed electric field (E)-induced operando Mössbauer spectroscopy techniques to apply E to the ferroelectric substrate Pb(Mg_{1/3}Nb_{2/3})O₃-PbTiO₃ (PMN-PT), which reversibly tunes the interfacial lattice constants of the Fe₃Ga magnetic layer [4]. In this study, we discuss the microscopic origin of inverse magnetostriction effects or orbital-elastic effects in Fe₃Ga concerning the orbital magnetic moments (morb) using Mössbauer and X-ray magnetic circular dichroism (XMCD) spectroscopies, comparing the Fe₃Ga and Fe₃Si cases.

We prepared samples of a 10-nm-thick Fe₃Ga (422) layer grown on single-crystal PMN-PT (011) substrates using molecular beam epitaxy. To apply an E to the PMN-PT substrate, the electrode was deposited on the backside of the PMN-PT substrate. Operando Mössbauer spectroscopy was performed at BL11XU, SPring-8, using a 14.4 keV linearly polarized beam with grazing incident setup.

The magnetization measurements indicated that the magnetic easy axis rotates 90° in the in-plane direction when E is applied, due to the modulation of in-plane lattice strain of approximately 0.1% in PMN-PT. By applying an E of −8 kV/cm, the Mössbauer spectra were modulated as the magnetization direction changes. When the beam aligns with the easy axis, all hyperfine peaks appear. In contrast, when the beam is orthogonal to the easy axis, only the 2nd and 5th peaks are observed. The hyperfine field also changed, affecting the morb since the hyperfine field includes the Fermi contact, dipole interaction, and orbital angular momentum. The changes in the hyperfine field of 1.2 T correspond to a variation of 0.02 μB in morb [5]. This value is comparable to the operando XMCD using a similar setup. These multimodal detections enable the observation of changes in morb, which is a microscopic origin of MS in Fe₃Ga. Furthermore, in the case of Fe₃Si on PMN-PT, it is not morb but quadrupole formation that becomes essential for the modulation of magnetic anisotropy by strain. These results suggest guidelines for designing functional magneto-strictive materials.

The author acknowledges the collaborations with Kohei Hamaya, Takamasa Usami, Seiji Sakai, Kousuke Fujiwara, Yasuhiro Kobayashi, and Takaya Mitsui.

- [1] T. Ueno and S. Yamada, *IEEE Trans. Magn.* **47** (2011) 2407.
- [2] R. Wu, *J. Appl. Phys.* **91** (2002) 7358.
- [3] P. B. Meisenheimer et al., *Nature Commun.* **12** (2021) 2757.
- [4] J. Okabayashi et al., *Nature Partner Group NPG Asia Materials* **16** (2024) 3.
- [5] G. Y. Guo and H. Ebert, *Phys. Rev. B* **53** (1996) 2492.

ICAME-INVITED-T06

Use of Nuclear Resonance in Studies of Space Returned Samples from Ryugu and Bennu Asteroids

Roskosz Mathieu^{1*}, Beck Pierre², Viennet Jean-Christophe¹, Amano Kana¹, Nakamura Tomoki³, Lavina Barbara⁴, Hu Michael⁴, Zhao Jiyong⁴, Yaroslavtsev Sergey⁵, Bessas Dimitrios⁵, Chumakov Aleksandr⁵, Esen E. Alp⁴,

¹IMPMC, MNHN, Paris, France. ²IPAG, Grenoble, France. ³Tohoku University, Sendai, Japan. ⁴APS, Argonne National Laboratory, Argonne, USA. ⁵ESRF, 38000 Grenoble, France

*mathieu.roskosz@mnhn.fr

Iron occurs under multiple valence state in meteorites. It reflects the origin and evolution of primitive bodies in the solar system. It is used to trace geological processes that occurred on asteroids. Observations of the mineralogy of carbonaceous chondrites (some of the most pristine rocks formed in the solar system) have revealed the presence of mineral assemblages that are barely in thermodynamic equilibrium. Even at the micron-scale, iron is often present under multiple valence state in a wide range of minerals, including silicates, oxy-hydroxide, sulfides, sulfates, clays, and carbonates. Furthermore, since most Fe-bearing phases are redox-sensitive, exposure to terrestrial atmosphere also induce iron oxidation and late modifications of the iron mineralogy. It is therefore tricky to disentangle the different processes recorded by the iron mineralogy of chondritic materials.

In this context, Hayabusa 2 (JAXA) and OSIRIS-REx (NASA) missions recently sampled Ryugu and Bennu, two asteroids that did not suffer extensive thermal metamorphism. These spacecrafts returned rocks to Earth with no air exposure. This is a unique chance to study the redox state of the most oxidized primitive rocks of the solar system.

An analytical framework was developed to investigate their iron mineralogy and valence state at the micron scale by combining X-ray Diffraction, Conventional Mössbauer (MS), Nuclear Forward Scattering (NFS), and Synchrotron Mössbauer (SMS) spectroscopies. An array of standard minerals was analysed and cross-calibrated between MS and NFS. Then, MS, SMS, and NFS spectra several Ryugu and Bennu grains were collected at the bulk and the micron scales together with other related meteorites available in our collections.

We provide the bulk and local estimates of the mineralogy, relative abundances, distributions, and redox state of iron-bearing minerals from Ryugu and Bennu [1]. Contrary to Orgueil or Tagish Lake meteorites, magnetites are stoichiometric and are not anomalously oxidized. The same holds for pyrrhotite, that do not show trace of oxidation. Furthermore, clays from Ryugu and Bennu are more reduced than typical carbonaceous meteorites in collection, with the notable exception of the recently found OC002 [2]. This strongly suggests that the terrestrial alteration of most primitive samples is more pervasive than previously suggested. The Hayabusa 2 and OSIRIS-REx samples are the most pristine chondritic material analysed to date and may represent the initial state of CI chondritic material.

Our results show that the formation environments of carbonaceous chondrites are much less oxidizing than previously assumed, and possibly not so different from those of non-carbonaceous chondrites. This work demonstrates that CIs are not an oxidized end-member of extraterrestrial rocks. Instead, it most certainly marks the redox state of the dust present in the outer part of the protoplanetary disk before the accretion in planets.

[1] Roskosz, *MAPS* (2023) 1.

[2] Gattacceca, *MAPS* (2025) In Press.

ICAME-INVITED-T01

Exploring Valence and Magnetic Order Using ^{151}Eu Mössbauer Spectroscopy

D. H. Ryan

Physics Department and Centre for the Physics of Materials,
McGill University, Montreal, Canada

dhryan@physics.mcgill.ca

Although ^{57}Fe is, and will likely remain, the preeminent Mössbauer isotope, ^{151}Eu provides access to one of the most interesting elements on the periodic table. Europium occurs in two (generally) well-defined valence states: Eu^{2+} and Eu^{3+} with *very* different properties. Divalent europium has a half-filled $4f$ shell, giving it a large, low-anisotropy $7\mu_B$ magnetic moment. By contrast, trivalent europium is smaller and typically carries zero moment. These features set up a rich phenomenology whereby small changes in volume (pressure) or electron count can lead to extreme changes in valence and magnetism. Furthermore, in systems where the energy difference between Eu^{2+} and Eu^{3+} is comparable to $k_B T$ at reasonable temperatures, one can observe spontaneous changes in valence with temperature, and dynamic electron hopping between europium ions or between them and the crystal environment.

The 21.6keV Mössbauer transition in ^{151}Eu is remarkably well matched to the phenomenology evident in europium compounds. The two valence states yield fully distinct and well-resolved isomer shifts, typically more than 10 linewidths apart, and magnetic ordering in divalent europium yields well-split patterns with hyperfine fields of 20–40 Tesla. The 87-year half-life of the source (^{151}Sm) makes the source an investment rather than a panic, and the low gamma energy means that useable spectra can be recorded up to around 800K. Finally, the transition is well matched to current synchrotron sources, enabling nuclear resonance scattering studies in diamond anvil pressure cells to investigate the interplay of volume, valence, and magnetism in high-pressure environments.

In what follows, I will review examples of spontaneous and pressure-driven valence changes in systems both where the two valence states co-exist and others where one transforms into the other. Magnetic ordering in europium compounds also turns out to be remarkably complex, given the essentially spherical form of the half-filled $4f$ shell in Eu^{2+} . While many simple ferromagnetic and antiferromagnetic systems exist, incommensurate modulated magnetic structures frequently occur. Bulk methods (magnetization, susceptibility...) are largely blind to such structures, but they provide clear signatures in the ^{151}Eu Mössbauer spectrum, and the evolution through modulated ordering is readily tracked. Unfortunately, ^{151}Eu Mössbauer spectroscopy can only tell you *whether* the magnetic structure is modulated; it cannot tell you *how* it is modulated. For that, we must turn to diffraction-based techniques such as resonant magnetic x-ray scattering or neutron diffraction.

ICAME-INVITED-T04

Collective Atomic Dynamics in Glass Revealed by Mössbauer Time-Domain Interferometry

Makina Saito^{1*}, Takeaki Araki²

¹Department of Physics, Tohoku University, Sendai, Japan

²Department of Physics, Kyoto University, Kyoto, Japan

*makina.saito.d6@tohoku.ac.jp

Many soft matter and glass-forming systems exhibit atomic motions on the nanosecond time scale, which are the microscopic origin of various material properties and functionalities. On the 100 ns time scale, atomic dynamics have been studied by quasi-elastic gamma-ray scattering (QEGS) experiments based on the neV energy resolution of ⁵⁷Fe Mössbauer gamma rays emitted from a ⁵⁷Co source [1]. However, due to the low brilliance of gamma rays, radioactive source-based QEGS has been of limited use. Nowadays, high-brilliance gamma rays generated by synchrotron radiation (SR) allow more efficient QEGS measurements. By constructing a time-domain interferometer (TDI) of the Mössbauer gamma rays, atomic dynamics can be efficiently measured in the time domain around 100 nanoseconds [2,3].

TDI has been used to study glass-forming materials. In particular, it promotes the study of the Johari-Goldstein (JG) relaxation, which is the microscopic origin of the impact strength of glasses, although its physical picture remains controversial. Using TDI, a strong wavenumber dependence of the relaxation time has been observed for the JG relaxation [4]. Although the strong wavenumber dependence is a key to revealing the physical picture, there is no consensus on its interpretation [4,5]. To reveal the physical picture, we studied a model glass-forming material, the ionic glass Ca_{0.4}K_{0.6}(NO₃)_{1.4} (CKN), by TDI-QEGS in combination with molecular dynamics simulations [6]. The simple structure of the constituents of CKN, atomic Ca²⁺ and K⁺ ions, and triangular NO₃⁻ ions, facilitates the simulation study. The structure and dynamics of the experiments and simulations were in good agreement, thus validating the simulation results. The real-time and real-space picture of the JG relaxation dynamics from the validated simulation results showed for the first time that the collective local motion of the particles contributes to the JG relaxation. In addition, similar collective motions have recently been observed for well-equilibrated model glass-forming systems, confirming the universality of the results. Thus, TDI has made a significant contribution to the understanding of the origin of the JG relaxation, which is one of the major problems in glass-related physics. Along with these research results using TDI, future research prospects using a new quasi-elastic scattering measurement system with the µeV-energy resolution will also be presented [7]. This work is supported by JST-CREST grant number JPMJCR2095, Japan.

[1] D. C. Champeney and F. W. D. Woodhams, *J. Phys. B* **1** (1968) 620.

[2] A. Q. R. Baron, *et al.*, *Phys. Rev. Lett.* **79** (1997) 2823.

[3] M. Saito, *et al.*, *Sci. Rep.* **7** (2017) 12558.

[4] M. Saito, *et al.*, *Phys. Rev. Lett.* **109** (2012) 115705.

[5] F. Caporaletti, *et al.*, *Nat. Commun.* **12** (2021) 1867.

[6] M. Saito, T. Araki, Y. Onodera, K. Ohara, M. Seto, Y. Yoda, Y. Wakabayashi, *Acta Mater.* **284** (2025) 120536.

[7] M. Saito, *et al.*, *Phys. Rev. Lett.* **132** (2024) 256901.

ICAME-INVITED-T07

Lattice Dynamics of Ultrathin Films and Nanostructures from *in situ* Nuclear Inelastic Scattering and *ab initio* Theory

Svetoslav Stankov

Institute for Photon Science and Synchrotron Radiation, Karlsruhe Institute of Technology,
Karlsruhe, Germany

svetoslav.stankov@kit.edu

The systematic determination of lattice dynamics, thermodynamic, and elastic properties upon the transition from bulk materials to ultrathin films and nanostructures remains a challenge in the experimental condensed matter physics. Classical methods, such as inelastic neutron and x-ray scattering, are bulk-sensitive and not suitable for mapping phonon dispersions of nanoscale materials. Helium atom scattering and high-resolution electron energy loss spectroscopy are surface-sensitive methods and not applicable to bulk materials. The limited momentum transfer of methods based on inelastic scattering of visible or infrared light prohibits the determination of the vibrational thermodynamics. The large penetration depth of the X-ray, combined with the high values of the nuclear resonant absorption cross-section, promoted nuclear resonant inelastic X-ray scattering [1,2] to a perfectly suitable method for a systematic determination of the phonon density of states from bulk to ultrathin films and nanostructures containing Mössbauer isotopes [3]. Applied *in situ*, i.e., under ultrahigh vacuum conditions, and combined with *ab initio* calculations, this method provides a direct access to the lattice dynamics, thermodynamic, and elastic properties of nanoscale materials, which are often not accessible otherwise.

In this talk, the basis of the experimental and theoretical methods will be presented. Applications of this combined approach will be illustrated with systematic lattice dynamics studies of endotaxial [4,5,6] and epitaxial [7,8] silicide thin films, nanoislands, and nanowires.

We acknowledge the financial support over the years by the Helmholtz Association (VHNG-625) and the Federal Ministry of Education and Research BMBF (05K16VK4, 05K22VK2).

- [1] M. Seto et al., *Phys. Rev. Lett.* **74** (1995) 3828.
- [2] W. Sturhahn et al., *Phys. Rev. Lett.* **74** (1995) 3832.
- [3] S. Stankov et al., *Phys. Rev. Lett.* **99** (2007) 185501.
- [4] J. Kalt et al., *Phys. Rev. B* **106** (2022) 205411.
- [5] J. Kalt et al., *Phys. Rev. B* **102** (2020) 195414.
- [6] J. Kalt et al., *Phys. Rev. B* **101** (2020) 165406.
- [7] S. Stankov et al., *submitted* (2024).
- [8] A. Seiler et al., *Phys. Rev. Lett.* **117** (2016) 276101.

ICAME-INVITED-T08

Velocity Moments and Tensor Properties of Mössbauer Spectra

K. R. Szymański^{*}, P. Butkiewicz, D. Satuła, W. Olszewski

University of Białystok, Poland

^{*}k.szymanski@uwb.edu.pl

The analysis of Mössbauer spectra provides valuable insights into the orientation of hyperfine fields. Although transition probability formulas for describing spectral lines are well-established, their practical application is hindered by two significant challenges: algebraic complexity and result ambiguity, where different parameter sets can produce indistinguishable spectra. This work demonstrates that the velocity moments of Mössbauer spectra correspond to their tensor properties, incorporating hyperfine fields and the photon direction relative to the sample. The velocity moments formalism simplifies the analysis by eliminating explicit dependence on transition probabilities in absorption line amplitudes. The electric field gradient tensor can be obtained as the first velocity moment. This approach is also effective in examining magnetic and crystalline textures, offering insights into sample structure and symmetry. Synchrotron radiation sources provided ideal conditions for precise measurements of spectra under varying beam directions. Initial experimental results obtained at Spring-8 are presented, highlighting the utility of the velocity moments formalism.

ICAME-INVITED-T04

Iron-Based Zeolite Heterogeneous Catalysts: Insights into Active Centers and Reaction Pathways through Mössbauer Spectroscopy

Edyta Tabor

J. Heyrovský Institute of Physical Chemistry, Czech Academy of Sciences, Prague, Czech Republic

edyta.tabor@jh-inst.cas.cz

Iron-containing zeolites represent a vital class of heterogeneous catalysts, extensively studied for their role in N₂O decomposition and hydrocarbon oxidation.^{1,2} The efficient conversion of excess CH₄ into oxygenated compounds is of significant importance, as these products serve as versatile platform chemicals and are more easily transportable. However, only a specific subset of iron species in zeolites actively participates in reactant activation and product formation during catalytic transformations.

Mössbauer spectroscopy emerges as an indispensable tool for characterizing the valence state, coordination environment, and geometry of iron species in zeolites, providing comprehensive insights into their structural and electronic properties, as well as monitoring in situ processes. This study combines Mössbauer spectroscopy with XAS and FTIR techniques to investigate the nature of extra-framework iron centres in zeolites and their role in facilitating CH₄ oxidation using various oxidants, such as N₂O, O₂, and CO₂.

Special emphasis is placed on correlating spectroscopic data with catalytic performance to identify and quantify the specific iron species responsible for catalytic activity.^{2,3} The entire redox cycle of methane oxidation is systematically studied using in-situ Mössbauer and FTIR spectroscopy, in conjunction with catalytic analysis, to elucidate the mechanisms of oxidant activation and product formation. Additionally, the influence of reaction mixture composition on the formation and stabilization of active iron centres in zeolites is examined in detail.

The combined spectroscopic results, including Mössbauer, XAS, and FTIR spectroscopy, enable the determination of the structure, geometry, and cooperative interactions of iron active centres in zeolites. These findings contribute to a deeper understanding of the catalytic activity of iron-containing zeolites, advancing the development of more efficient catalysts for methane transformation into value-added oxygenated products.

Acknowledgments:

The authors thank the Czech Science Foundation #24-14387L and the National Science Centre, Poland, 2022/47/I/ST4/00607, for the financial support.

[1] Q. Zhang, J. Yu, A. Corma, *Adv. Mater.* **32** (2020) 2002927A.

[2] K. Mlekodaj, M. Lemishka, A. Kornas, D. K. Wierzbicki, J. E. Olszowka, H. Jirglová, J. Dedeczek, E. Tabor, *ACS Catal.* **13** (2023) 3345A.

[3] A. Kornas, E. Tabor, D. K. Wierzbicki, J. E. Olszowka, R. Pilar, J. Dedeczek, M. Sliwa, H. Jirglova, S. Sklenak, D. Rutkowska-Zbik, K. Mlekodaj, *Appl. Catal. B: Environ.* **336** (2023) 122915.

ICAME-INVITED-T02

Study of Single-Atom Catalysts with *in-situ/operando* Mössbauer Spectroscopy

Tao Zhang

State Key Laboratory of Catalysis, Dalian Institute of Chemical Physics, Chinese Academy of Sciences, Dalian 116023, China

* taozhang@dicp.ac.cn

Single-atom catalysts (SACs), distinguished by their isolated metal centers, provide unique platforms for probing genuine active sites and underlying reaction mechanism. However, the dynamic structural and electronic evolution and the origin of the intrinsic activity of SACs during reactions remain unclear, largely due to the lack of atomically resolved *operando* techniques and the single-atom model catalytic system. Herein, we employ state-of-the-art *operando* techniques to systematically investigate the structural and electronic evolution of a model SAC featuring a high-spin (HS) Fe(III)N₄ center during the electrochemical CO₂ reduction reaction (CO₂RR). *Operando* ⁵⁷Fe Mössbauer and X-ray absorption spectroscopy reveal a distinct transition from HS Fe(III)N₄ to HS Fe(II)N₄ centers, accompanied by the capture of FePc-CO₂⁻ reactive intermediates during CO₂RR. By contrast, in Ar-saturated electrolytes, lacking such axial catalytic intermediates, the initial HS Fe(III)N₄ species undergoes irreversible reduction to metallic iron. *Operando* Raman spectroscopy as well as cyclic voltammetry confirm that the phthalocyanine (Pc) ligand coordinated to the Fe center acts as an electron reservoir, undergoing a one-electron reduction under CO₂RR conditions to form Fe(II)Pc⁻. Density functional theory (DFT) calculations further elucidate that this Pc ligand reduction adjusts both the d-band center and CO₂ adsorption affinity of the HS Fe(II)Pc⁻ species, enhancing its catalytic activity towards CO₂RR. These findings establish a structure-function paradigm wherein ligand-driven electronic modulation synergizes with active site geometry to enhance CO₂RR activity. Furthermore, this mechanism is broadly applicable to a variety of spin-configured systems, in particular the covalently oxygen-bridged low-spin (LS) FeN₄ with significantly enhanced intrinsic activity.

- [1] B. Qiao, A. Wang, X. Yang, L.F. Allard, Z. Jiang, Y. Cui, J. Liu, J. Li, T. Zhang, *Nature Chemistry* **3** (2011) 634.
- [2] X.-F. Yang, A. Wang, B. Qiao, J. Li, J. Liu, T. Zhang, *Accounts of Chemical Research* **46** (2013) 1740.
- [3] A. Wang, J. Li, T. Zhang, *Nature Reviews Chemistry* **2** (2018) 65.
- [4] Y. Zeng, J. Zhao, S. Wang, X. Ren, Y. Tan, Y. Lu, S. Xi, J. Wang, F. Jaouen, X. Li, Y. Huang, T. Zhang, B. Liu, *Journal of the American Chemical Society* **145** (2023) 15600.
- [5] R. Chen, J. Zhao, Y. Li, Y. Cui, Y. Lu, S. Hung, S. Wang, W. Wang, G. Huo, Y. Zhao, W. Liu, J. Wang, H. Xiao, X. Li, Y. Huang, B. Liu, *Journal of the American Chemical Society* **145** (2023) 20683.
- [6] R. Chen, J. Zhao, X. Zhang, Q. Zhao, Y. Li, Y. Cui, M. Zhong, J. Wang, X. Li, Y. Huang, B. Liu, *Journal of the American Chemical Society* **146** (2024) 24368.

Abstracts of Oral Contributions



ICAME Young Session

ICAME-YOUNG-T08

Interactions of Gamma Photons with Ensemble of Nuclei Described by Quantum Mechanical Model

Michal Hausner^{1*}, Vlastimil Vrba¹, Vít Procházka¹

¹Department of Experimental Physics, Faculty of Science, Palacký University Olomouc, Olomouc, Czech Republic

*michal.hausner01@upol.cz

In this presentation, a one-dimensional quantum mechanical description (based on coherent path model [1]) of interaction of a gamma photon with a nuclear ensemble is extended for the following situations: **I.** nuclear resonant forward scattering on multiple single spectral line absorbers, **II.** scattering on ^{57}Fe absorber in magnetic field, including the polarization effects, **III.** scattering on an ultra-acoustically vibrating single-line absorber (acoustic coherent control), **IV.** combination of acoustic coherent control and polarization effects in ^{57}Fe absorber in magnetic field, and **V.** interaction of a gamma photon with an excited nucleus describing a simplified model of stimulated emission. The model of the stimulated emission was developed with assumptions which enable a specific experimental arrangement for simultaneous detections of pairs of gamma photons.

In the presented models, the absorbers are described as an ensemble of effective nuclei. The model of forward scattering on multiple single spectral line absorbers serves as the first step in deriving the scattering on ^{57}Fe absorber in magnetic field including the polarization effects. The presented model demonstrates that while multiple absorbers with the same spectral line act as a single absorber with increased thickness, multiple absorbers with different spectral lines exhibit more complex time structure of the photon detection probability.

Nuclei in the magnetic field exhibit polarization dependent interaction with photons. Such polarization phenomena could be further used for the construction of polarizers and analyzers of gamma radiation. Additionally, the vibration of the absorber in magnetic field results in the formation of pulses of polarized gamma radiation.

Furthermore, a photon can interact with an excited nucleus. This interaction can lead to stimulated emission of gamma radiation. This could be utilized in the creation of a coherent source of gamma radiation. The presented model predicts the time structure of 14 keV photon pairs emitted by excited ^{57}Fe nuclei under the condition of simultaneous coincidence detection of 122 keV photons. The model shows distinctions between the time structure of spontaneous emission of a pair of photons and stimulated emission, which could be utilized for observation of the latter phenomenon.

[1] G. R. Hoy, *Journal of Physics: Condensed Matter* **9** (1997) 8749.

ICAME-YOUNG-T02

Nuclear Forward Scattering and Density Functional Theory Studies of Photo- and Catalytically Active Iridium Complexes

Maren H. Hoock^{1,*}, Olaf Leupold², Alexander Haag¹, Yanik Becker¹,
Andreas Omlor¹, Jonathan Oltmanns¹, Lukas Knauer¹, Tim Hochdörffer¹,
Konstantin Gröpl¹, Marco A. M. Tummeley¹, Deepak Prajapat²,
Réne Steinbrügge², Atefeh Jafari², Ilya Sergueev², Ralf Röhlberger^{2,3},
Werner R. Thiel¹, Hans-Jörg Krüger¹, Juliusz A. Wolny¹, Volker Schünemann¹

¹University of Kaiserslautern-Landau, Kaiserslautern, Germany

²Deutsches Elektronen Synchrotron (DESY), Hamburg, Germany

³Helmholtz Institut Jena and Friedrich-Schiller Universität Jena, Jena, Germany

*hoock@rptu.de

Iridium complexes are used in many different applications due to their photochemical, photophysical, and catalytic properties. For example, they are used in organic light-emitting diodes (OLEDs) [1] and automotive exhaust catalysts [2]. Iridium complexes have also been used to initiate water oxidation reactions [1]. They also show promise as photosensitizers and photocatalysts for targeted photodynamic cancer therapy (PDT) [1]. Recently, nuclear forward scattering (NFS) of ^{193}Ir at 73 keV has been established at beamline P01, PETRA III, DESY, Hamburg [3]. We have used ^{193}Ir -NFS to obtain information on the electronic properties of selected iridium complexes via the quadrupole splitting (Fig. 1(a)). By the additional introduction of an iridium foil as a reference, the isomer shift can be determined (Fig. 1(b)). Using iridium dioxide as a reference, it is even possible to determine the sign of the isomer shift (Fig. 1(c)). To theoretically interpret the experimentally determined Mössbauer parameters, we also performed density functional theory (DFT) calculations to calculate the Mössbauer parameters of the studied complexes.

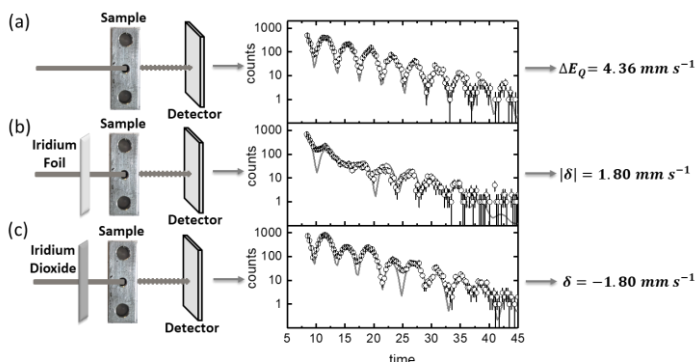


Figure 1. NFS-data taken at 12 K of the complex $[\text{Cp}^*\text{Ir}^{\text{III}}\text{Cl}_2]$ (denoted as Sample) without (a), with an iridium foil (b), and with iridium dioxide (c) in the synchrotron beam. Simulations (grey line) were performed with CONUSS [4].

[1] M. L. P. Reddy, *J. Photochem. Photobiol. C: Photochem* **29** (2016) 29.

[2] Haneda, *Catal. Sci. Technol.* **5** (2015) 1792.

[3] P. Alexeev, *Sci. Rep.* **9** (2019) 5097.

[4] W. Sturhahn, *Hyperfine Interact.* **125** (2000) 149.

ICAME-YOUNG-T02

Solvent-Dependent Two-Step Spin Crossover Behavior in 3D Coordination Frameworks

Xiaochun Li¹, Mariusz Wolff², Aurelian Rotaru³, Dominik Maskowicz⁴, Wioletta Kopec⁴, Serhiy Demeshko⁵, Mirosław Sawczak⁴, Rafał Jendrzewski⁴, Franc Meyer⁵, Yann Garcia^{1*}

¹Institute of Condensed Matter and Nanosciences, Molecular Chemistry, Materials and Catalysis (IMCN/MOST), Université catholique de Louvain, Place L. Pasteur 1, 1348 Louvain-la-Neuve, Belgium

²Institute of Functional Materials and Catalysis, Faculty of Chemistry, University of Vienna, Währinger Strasse 38-42, 1090 Vienna, Austria

³Department of Electrical Engineering and Computer Science and MANSiD Research Center, “Stefan cel Mare” University, University Street, 13, Suceava 720229, Romania

⁴Photophysics Department, The Szwalski Institute of Fluid-Flow Machinery, Polish Academy of Sciences, Fiszerka 14, 80-231 Gdańsk, Poland

⁵Institute für Anorganische Chemie, Universität Göttingen, Tammannstrasse 4, D-37077 Göttingen, Germany

*xiaochun.li@uclouvain.be

Some transition metal complexes, particularly those of the first transition series with configurations $3d^4$ to $3d^7$, can undergo a spin crossover (SCO) when induced by an external stimulus such as light, temperature, pressure, electric field, or guest molecules.[1] SCO compounds have been studied extensively over the last few decades for potential applications in high-density information storage devices, quantum computers, and spintronics.[2]

In this work, new 3D iron(II) complexes based on tris(4,4'-bis-1,2,4-triazole) have been synthesized with the formula $[\text{Fe}(\text{btr})_3](\text{anion})_2 \cdot n\text{H}_2\text{O}$. Crystallographic analysis shows two crystallographically independent iron sites. The magnetic properties were studied using SQUID. $[\text{Fe}(\text{btr})_3](\text{anion})_2 \cdot \text{H}_2\text{O}$ shows incomplete SCO, while $[\text{Fe}(\text{btr})_3](\text{anion})_2$ shows two-step complete transition. The SCO occurs in two steps with a ca. 67 K plateau, each involving around 50% of the Fe^{2+} ions. The low-temperature step is abrupt and undergoes thermal hysteresis with a width of 12 K from 116 K to 128 K. The high-temperature step, centered on $T_2 = 187$ K, without thermal hysteresis. ^{57}Fe Mössbauer spectra were obtained at different temperatures. At 80 K, where the sample is expected to be LS, a unique doublet with an isomer shift $\delta^{LS} = 0.57 \text{ mm s}^{-1}$ and a low quadrupole splitting of $\Delta E_Q = 0.17 \text{ mm s}^{-1}$ are detected. A spectrum collected at 160 K on the plateau confirmed the mixed spin state situation with $\delta^{LS} = 0.54 \text{ mm s}^{-1}$ and $\Delta E_Q^{LS} = 0.22 \text{ mm s}^{-1}$, and $\delta^{HS} = 1.11 \text{ mm s}^{-1}$ and $\Delta E_Q^{HS} = 1.83 \text{ mm s}^{-1}$, corresponding to a ~45/55% LS/HS ratio. At 250 K, the spectrum shows a unique quadrupole doublet of HS $\text{Fe}(\text{II})$ ions, thus delineating a complete spin transition. Differential scanning calorimetry and variable-temperature Raman spectroscopy confirm a two-step spin crossover with thermal hysteresis. These findings highlight the crucial role of solvent molecules in modulating spin crossover properties.

[1] L. Sun, X. Li, Y. Garcia *et al.*, *Mater. Adv.* **21** (2024), 8564-8574.

[2] W. Li, X. Li, Y. Garcia, *et al.*, *Dalton Trans.* **4** (2024), 1449-1459.

ICAME-YOUNG-T01

¹⁵¹Eu Mössbauer Spectroscopy and Magnetic Studies of EuSnP Single Crystals

Karolina Podgórska^{1*}, Kamila Komędera¹, Jan Żukrowski¹, Michał Babij², Lan
Maria Tran², Łukasz Gondek¹, Janusz Przewoźnik¹, Czesław Kapusta¹, Wojciech
Tabiś¹, Damian Rybicki¹

¹AGH University of Krakow, Kraków, Poland

²Institute of Low Temperature and Structure Research, Polish Academy of Sciences,
Wrocław, Poland

*klpodgor@agh.edu.pl

EuSnP is an antiferromagnetic material in which the europium magnetic moments order at $T_N = 21$ K, although it is likely not a 'simple' (A or B type) antiferromagnet [1-3]. Previous study has suggested that in this compound, Eu can be of the mixed valence [3]. To gain deeper insight into its magnetic properties and ordering of europium's magnetic moments, the measurements as a function of temperature and applied magnetic field, such as heat capacity, AC susceptibility, magnetization, and Mössbauer spectroscopy (on ¹⁵¹Eu), were performed. The study was conducted on obtained high quality, homogeneous single crystals grown from Sn flux. The quality and composition of the crystals were confirmed by energy dispersive X-ray spectroscopy (EDS) and X-ray diffraction analysis. Differently from the suggestions in the literature, our ¹⁵¹Eu Mossbauer results indicate that europium is in a divalent (Eu²⁺) state and its magnetic moments align along or very close to the crystallographic *c*-axis below the T_N . Small amount of Eu³⁺ visible in the spectra is most likely an impurity phase. During the presentation, the detailed results of our study will be presented and discussed.

Acknowledgements: We acknowledge financial support by National Science Centre, Poland (Grants No. 2018/30/E/ST3/00377 and 2021/41/B/ST3/03454). The research project was partly supported by the program "Excellence initiative—research university" (projects 9907 and 6387) for the AGH University of Krakow.

- [1] A.C. Payne et al., *J. Alloys Compd.* **338** (2002) 229-234.
- [2] W. Iha et al., *JPS Conf. Proc.* **29** (2020) 012002.
- [3] T. Fujiwara et al., *Physica B* **378–380** (2006), 1122-1123.

ICAME-YOUNG-T01

Mössbauer Investigations of FeCoNiZn_x System

A. Sławek^{1*}, K. Berent², J. Cieślak¹

¹Faculty of Physics and Applied Computer Science, AGH University, Krakow, Poland

²Academic Center for Materials and Nanotechnology, AGH University, Krakow, Poland

*annaslawek@agh.edu.pl

The concept of medium and high entropy alloys (MEA, HEA) has garnered significant interest from both scientific and technological perspectives. These alloys consist of multiple elements with comparable molar fractions, maximizing configurational entropy and stabilizing a simple crystal structure. The literature provides numerous examples of HEAs and MEAs based on FeCoNi, which remain single-phase (*fcc*) even when doped with other elements, such as palladium or chromium. In many cases, these systems exhibit intriguing magnetic properties.

The FeCoNiZn_x ($x < 0.75$) system demonstrates good solubility of zinc and remains single-phase up to approximately $x = 0.5$. Due to the significant difference in melting points between zinc and the other alloying elements, sintering was the only effective technique for obtaining these alloys. However, the resulting materials proved to be thermally unstable, ruling out potential high-temperature studies.

This study investigates the effect of Zn concentration on the microstructure, hyperfine parameters, and, in particular, the magnetic properties of this system. X-ray diffraction (XRD), scanning electron microscopy (SEM-EDX), and Mössbauer spectroscopy were employed in the analysis. Mössbauer spectroscopy, in particular, revealed different orientations of the hyperfine field in multiphase systems in cold-rolled samples.

[1] J. Cieślak, M. Calvo-Dahlborg, K. Berent, U. Dahlborg, *J. Magn. Magn. Mater.* **518** (2021) 167371.

[2] G. Chandra Mohanty, C. Chowde Gowda, P. Gakhad, M. Sanjay, A. Singh, Koushik Biswas, C. Sekhar Tiwary, *Energy Adv.* **12** (2024) 2972-2985.

[3] O. Yakovenko, V. Sokolskii, P. Švec, I. Janotová, P. Švec Sr, T. Kulik et al., *J. Alloys Compd.*, **1002** (2024) 175312.

ICAME-YOUNG-T03

Preparation and Physico-Chemical Characterization of AISI 304 Stainless Steel Film Deposited by DC Magnetron Sputtering

Samuel Tomko^{1,2}, Jiří Pechoušek¹, Jiří Tuček³, Ernő Kuzman⁴, Vítězslav Heger¹, Stanislaw M. Dubiel⁵, and Libor Machala¹

¹Department of Experimental Physics, Faculty of Science, Palacký University, 17. listopadu 1192/12, 779 00 Olomouc, Czech Republic

²Hella Autotechnik Nova s.r.o., Družstevní 16, 789 85 Mohelnice, Czech Republic

³Research Centre, Faculty of Electrical Engineering and Informatics, University of Pardubice, Studentská 95, 530 02, Pardubice, Czech Republic

⁴Institute of Chemistry, Eötvös Loránd University, 1117 Budapest, Pázmány Péter sétány 1/A, Hungary

⁵Faculty of Physics and Applied Computer Science, AGH University of Krakow, Al. A. Mickiewicza 30, 30-059 Kraków, Poland

samuel.tomko01@upol.cz

The present study reports on the preparation and physico-chemical investigation of a 2 μm thick film produced from AISI 304 stainless steel by DC magnetron sputtering. A phase transformation from the conventionally non-magnetic face-centered cubic (FCC) phase of austenite ($\gamma\text{-Fe}$) nature to a predominantly body-centered cubic (BCC) ferromagnetic single phase ($\alpha\text{-Fe}$) during the deposition is observed upon the deposition process. The deposited films are characterized by various experimental techniques, including scanning electron microscopy (SEM) with energy-dispersive X-ray spectroscopy (EDX), X-ray powder diffraction (XRD), grazing-incidence X-ray powder diffraction (GIXRD), and Mössbauer spectroscopy (MS) in both transmission and back-scattered geometry. For the interpretation of the Mössbauer spectra of the film, a physico-chemical model based on distinct micromagnetic environments evolved due to alloying elements is suggested. The results, presented within this study, may stimulate further and detailed research in identifying the causes for the phase transition from both theoretical and experimental perspectives and understanding the underlying mechanisms.

Notes

Abstracts of Oral Contributions



ICAME Oral Contributions

ICAME-ORAL-T01

Pressure-Induced Electronic and Magnetic Transitions in the Iron(IV) Oxide Sr_2FeO_4

Peter Adler^{1*}, Sergey A. Medvedev¹, Quingge Mu¹, Dimitrios Bessas², Aleksandr Chumakov², Sergey Yaroslavtsev², Martin Jansen¹, and Claudia Felser¹

¹Max Planck Institute for Chemical Physics of Solids, Dresden, Germany

²ESRF – The European Synchrotron, Grenoble, France

*adler@cpfs.mpg.de

Oxides with 3d transition metal (TM) ions in a high oxidation state exhibit strong electronic correlations as well as pronounced covalency of TM-oxygen bonding. In such compounds, peculiar electronic and magnetic phenomena emerge, including insulator-metal transitions, charge or bond disproportionation, non-collinear magnetic ordering that in some cases is associated with topological spin textures, and high spin (HS) to low spin (LS) transitions. High pressure (HP) is a clean way to induce electronic and magnetic transitions in these systems, as it allows one to tune the balance of electronic interactions and the coupling of electronic states to the lattice. An example of contemporary interest is the mixed-valent (formally $\text{Ni}^{2+}/\text{Ni}^{3+}$) nickelate $\text{La}_3\text{Ni}_2\text{O}_7$ featuring superconductivity at pressures above 14 GPa with critical temperatures up to ~ 80 K.

Here, we present our investigations on the HP electronic and magnetic states of the K_2NiF_4 -type iron(IV) oxide Sr_2FeO_4 [1], which is a covalent insulator without charge disproportionation of Fe^{4+} at ambient pressure and exhibits an elliptically modulated cycloidal spin structure giving rise to a peculiar shape of the Mössbauer spectra [2]. The synchrotron Mössbauer source (SMS) at beamline ID18 of ESRF, Grenoble, was used to obtain energy-domain Mössbauer spectra at pressures up to 89 GPa at variable temperature and magnetic field conditions. Our results allow us to sketch an electronic/magnetic phase diagram of Sr_2FeO_4 and extend previous work reporting laboratory Mössbauer and transport studies on Sr_2FeO_4 up to ~ 30 GPa [3].

Combining the results from the present and the previous study, several electronic regimes can be identified. Below ~ 7 GPa, the spiral spin texture is retained. In this region, we could successfully model field-dependent SMS spectra by applying the anharmonic spherical modulation (ASM) model [1]. Between 8 and 18 GPa, the system adopts a ferromagnetic semiconducting state with a moderate increase in magnetic ordering temperature T_m from 56 K at 0 GPa to ~ 100 K at 13 GPa. Above the metallization pressure near 18 GPa, a ferromagnetic metallic state emerges featuring a dramatic increase in T_m to above room temperature. Beyond 50 GPa, T_m decreases again, and a phase coexistence with indications for a partial HS ($t_{2g}^3 e_g^1$, $S = 2$) to LS (t_{2g}^4 , $S = 1$) transition was observed.

Our study nicely illustrates the unique potential of SMS spectroscopy for exploring HP electronic states and magnetism in complex materials and provides the experimental basis for critically discussing a recent theoretical study on the HP state of Sr_2FeO_4 [4]. Our results may be relevant for understanding the electronic situation in unconventional superconductors as the nickelates or the K_2NiF_4 -related oxide Sr_2RuO_4 .

[1] P. Adler et al., *Phys. Rev. B* **110** (2024) 054444.

[2] P. Adler et al., *Phys. Rev. B* **105** (2022) 054417.

[3] G.K. Rozenberg et al., *Phys. Rev. B* **58** (1998) 10283.

[4] A. Kazemi-Moridani et al., *Phys. Rev. B* **109** (2024) 165146.

ICAME-ORAL-T01

Quasi-two-dimensional Magnetism and Antiferromagnetic Ground State in $\text{Li}_2\text{FeSiO}_4$

W. Hergett¹, N. Boudi², M. Jonak¹, C. Neef¹, C. Ritter³, M. Abdel-Hafiez^{1,4,5},
F. Seewald⁶, H.-H. Klauss^{6*}, M. W. Haverkort², R. Klingeler¹

¹Kirchhoff Institute of Physics, Heidelberg University, D-69120 Heidelberg, Germany

²Institute for Theoretical Physics, Heidelberg Univ., D-69120 Heidelberg, Germany

³Institut Laue-Langevin, 38042 Grenoble, France

⁴Physics Department, Faculty of Science, Fayoum Univ., Fayoum 63514, Egypt

⁵Department of Applied Physics and Astronomy, Univ. of Sharjah, United Arab Emirates

⁶Institute for Solid State and Materials Physics, TU Dresden, D-01069 Dresden, Germany

*henning.klauss@tu-dresden.de

The quasi-2D orthosilicate $\gamma\text{-Li}_2\text{FeSiO}_4$ has been intensively studied in polycrystalline form as a high-capacity cathode material for lithium-ion batteries [2]. We present neutron diffraction, Mössbauer spectroscopy, magnetic susceptibility, specific heat, and numerical studies on the evolution of short- and long-range magnetic order in $\gamma\text{-Li}_2\text{FeSiO}_4$. Our study suggests a quasi-two-dimensional (2D) nature of magnetism [3]. In this presentation, we focus on the importance of nuclear local probe spectroscopy in inhomogeneous magnetic ordering phenomena.

The magnetic susceptibility data on single crystals imply long-range antiferromagnetic order below $T_N = 17$ K. A broad maximum in magnetic susceptibility χ at $T_m \sim 28$ K, and the observation of magnetic entropy changes up to 100 K are indicative of low-dimensional magnetism and suggest short-range magnetic correlations up to 200 K.

Neutron diffraction shows that long-range antiferromagnetic order is characterized by the propagation vector $k = (1/2, 0, 1/2)$. The ordered moment, $\mu = 2.50(2) \mu_B/\text{Fe}$ at $T = 1.5$ K, is along the crystallographic a axis.

In Mössbauer spectroscopy, we observed a low temperature static hyperfine field of $B_{\text{hyp}} = 14.8(3)$ T, which indicates significant orbital contributions. The temperature dependence of B_{hyp} yields the critical exponent $\beta = 0.116(12)$, which is in the regime of the 2D Ising behavior.

LSDA+U studies exploiting the experimental spin structure suggest dominating magnetic exchange coupling within the ac layers (i.e., $J_3 \sim -6$ K and $J_6 \sim -2$ K) while interlayer coupling is much smaller and partly frustrated.

[1] C. Gong and X. Zhang, *Science* **363** (2019) eaav4450.

[2] M.S. Islam et al., *J. Mater. Chem.* **21** (2011) 9811.

[3] W. Hergett et al., *Phys. Rev. B* **111** (2025) 024414.

High-entropy Magnetism of Murunskites

Kamila Komędera^{1,2,*}

¹Faculty of Physics and Applied Computer Science, AGH University of Krakow, Poland

²Department of Physics, Faculty of Science, University of Zagreb, Croatia

*komedera@agh.edu.pl

Murunskite ($K_2FeCu_3S_4$) and its derivatives represent a novel family of materials that, in many respects, can be viewed as a bridge between the two only known ambient-pressure high- T_c superconducting families: cuprates and iron pnictides. Structurally, murunskite is isostructural to the 122-type iron pnictides, while electronically, it behaves as an insulator, similar to the parent compounds of cuprate superconductors [1].

In addition, murunskite exhibits a cascade of intriguing electronic and magnetic transitions, including an antiferromagnetic-like ordering around 100 K, followed by the emergence of full magnetic and orbital order below 30 K [2]. Notably, its magnetic ordering remains exceptionally robust against structural disorder. Altogether, the murunskite family offers a unique platform to explore the interplay between lattice, spin, and orbital degrees of freedom, with promising implications for uncovering new mechanisms relevant to high-temperature superconductivity.

To investigate the magnetic ground state of murunskites, we conducted systematic Mössbauer spectroscopy measurements on $K_2FeCu_3X_4$ ($X = S, Se, Te$). Spectra were collected in transmission geometry over a temperature range of 4.2 K to 300 K, using the 14.41 keV resonant line of ^{57}Fe . Our results indicate the emergence of a modulated magnetic structure associated with Fe ions, with magnetic order persisting up to approximately 100 K. Moreover, the complex magnetic pattern revealed by Mössbauer spectroscopy, when considered alongside recent DFT calculations, suggests that while the magnetic structure in murunskites differs from that of ferropnictides, it nonetheless offers valuable insights into their magnetic behavior.

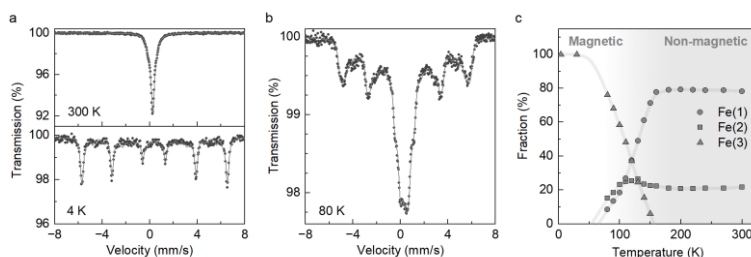


Figure 1. Selected ^{57}Fe Mössbauer spectra of $K_2FeCu_3S_4$ (a,b) and temperature evolution of the contribution from each of the nonequivalent Fe sites(c)[2].

[1] D. Tolj, et al., *Appl. Mat. Tod.* **24** (2021) 101096.

[2] D. Tolj, et al, *arXiv:2406.17108v1*

This work was supported by the Croatian Science Foundation under the project number [HRZZ-IP-2022-10-3382] and the National Science Centre, Poland, grant OPUS: UMO-2021/41/B/ST3/03454.

ICAME-ORAL-T01

Synchrotron-radiation-based Mössbauer Spectroscopy for Europium Hydrides under Hydrogen Pressure up to 80 GPa

Ryo Masuda^{1*}, Takahiro Matsuoka², Kosuke Fujiwara³, Kitao Shinji⁴, Yoshin Hara¹,
Kaito Murakami¹, Takaya Mitsui³, Makoto Seto⁴

¹Hirosaki University, Hirosaki, Japan

²University of the Philippines Diliman, Quezon, Philippines

³National Institutes for Quantum Science and Technology, Sayo, Hyogo, Japan

⁴Kyoto University, Kumatori, Osaka, Japan

*masudar@hirosaki-u.ac.jp

Hydrogen atoms are absorbed by various metals and alloys. Such hydrides often show properties different from their base materials, such as magnetism, conductivity, and crystal structure. The states of absorbed hydrogen atoms also vary, depending on the electronegativity, atomic size of the base materials, and so forth. Europium also absorbs hydrogen, and EuH_2 is a well-known stable hydride phase [1]. In 2011, the EuH_3 -like phase was discovered under high hydrogen pressure of about 10 GPa [2]. Since 2017, further different hydride phases have been discussed under higher high hydrogen pressure up to 400 GPa [3-5].

Synchrotron radiation (SR)-based Mössbauer spectroscopy method [6] is useful to elucidate the electronic structure of such Eu hydrides, since highly brilliant SR with ^{151}Eu energy has high penetrating power and is very suitable for the study using a diamond anvil cell for the high hydrogen pressure [2]. Recently, we studied the electronic states of Eu hydride under high hydrogen pressure between 20 and 80 GPa at room temperature by ^{151}Eu SR-based Mössbauer spectroscopy. Among this pressure range, the Mössbauer spectra could be understood by a single site without hyperfine splitting; this result agrees with the XRD study, showing the EuH_3 -like hydride phase [2,5]. The isomer shift values were in the region of the Eu^{3+} state, but gradually increased as the hydrogen pressure increased, as shown in Fig. 1.

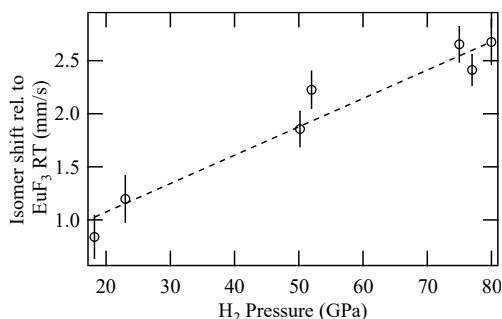


Figure 1. Hydrogen pressure dependence of ^{151}Eu Isomer shifts of Eu hydrides. The circles are experimental data, and the dotted line is a line fitting for eye guides.

- [1] Y. Fukai, The Metal-Hydrogen System 2nd Ed., Springer (2010).
- [2] T. Matsuoka et al., *Phys. Rev. Lett.* **107** (2011) 025501.
- [3] F. Peng, et al., *Phys. Rev. Lett.* **119** (2017) 107001.
- [4] D.V. Semenok, et al., *J. Phys. Chem. Lett.* **12** (2021) 32.
- [5] L. Ma, et al., *Phys. Rev. Res.* **3** (2021) 043107.
- [6] M. Seto et al., *Phys. Rev. Lett.* **102** (2009) 217602.

ICAME-ORAL-T01

Successive Transitions in $\text{Ca}_5\text{Ir}_3\text{O}_{12}$ Revealed by ^{193}Ir Synchrotron-Radiation-Based Mössbauer Spectroscopy

Satoshi Tsutsui^{1,2*}, Hiroki Hanate³, Keisuke Kadohiro³, Takashi Honda^{4,5},
Ryo Masuda⁶, Nobumoto Nagasawa¹, Yoshitaka Yoda¹, Satoru Hayami⁷,
Hisatomo Harima⁸, and Kazuyuki Matsuhira³

¹Japan Synchrotron Radiation Research Institute (JASRI), SPring-8, Sayo, Hyogo, Japan

²Institute of Quantum Beam Science, Graduate School of Science and Technology, Ibaraki University, Hitachi, Japan

³Graduate School of Engineering, Kyushu Institute of Technology, Kitakyushu, Japan

⁴Materials and Life Science Division, J-PARC Center, Tokai, Ibaraki, Japan

⁵Institute of Material Structural Science, High Energy Accelerator Research Organization, Tsukuba, Japan

⁶Faculty of Science and Technology, Hirosaki University, Hitosaki, Aomori, Japan

⁷Graduate School of Science, Hokkaido University, Sapporo, Hokkaido, Japan

⁸Graduate School of Science, Kobe University, Kobe, Hyogo, Japan

*satoshi@spring8.or.jp

A series of $5d$ -transition metals contains many Mössbauer nuclei. Among them, the 73 keV transition of ^{193}Ir is useful for applying to material sciences. Recent development of nuclear resonant scattering techniques at synchrotron radiation facilities allows us to measure Mössbauer spectra using synchrotron radiation X-rays instead of radioactive sources [1]. We succeeded in the nuclear excitation of the 73 keV ^{193}Ir Mössbauer transition and its application to some materials [2].

$\text{Ca}_5\text{Ir}_3\text{O}_{12}$ undergoes two successive transitions at 105 K and 7.8 K [3]; the higher transition is caused by a structural change [4]; the lower one is caused by a magnetic ordering [3,5]. We performed ^{193}Ir synchrotron-radiation-based (SR-based) Mössbauer spectroscopy at BL09XU and BL35XU of SPring-8 to elucidate the origin of the successive transitions.

^{193}Ir SR-based Mössbauer spectra obtained between 120 and 90 K clearly demonstrate that Ir charge disproportionation is accompanied by the structural transition at 105 K [2, 4]. On the other hand, the ^{193}Ir SR-based Mössbauer spectrum at 4 K demonstrates the absence of any hyperfine magnetic field [6]. Although we also conducted neutron diffraction at BL21 NOVA of J-PARC MLF, we failed to observe any magnetic reflections. These results imply a higher-rank magnetic order like that in NpO_2 [7-9]. These successive transitions in $\text{Ca}_5\text{Ir}_3\text{O}_{12}$, including the results in this work, can be explained theoretically by electric and magnetic toroidal moments [5]. The details will be discussed in the presentation.

[1] M. Seto et al., *Phys. Rev. Lett.* **102** (2009) 217602.

[2] S. Tsutsui et al., *J. Phys. Soc. Jpn.* **90** (2021) 083701.

[3] M. Wakeshima et al., *Solid State Commun.* **125**, (2003) 311.

[4] H. Hanate et al., *J. Phys. Soc. Jpn.* **90** (2021) 063702.

[5] I. Franke et al., *Phys. Rev. B* **83** (2011) 094416.

[6] S. Hayami et al., *J. Phys. Soc. Jpn.* **92** (2023) 033702.

[7] D.E. Cox et al., *J. Chem. Solids* **28** (1967) 1649.

[8] B.D. Dunlap et al., *J. Phys. Chem. Solids* **29** (1968) 1365.

[9] W. Copmann et al., *J. Alloys Compd.* **271** (1998) 463.

ICAME-ORAL-T01

Aromatic Substituent Effects on the Spin Crossover Properties of $[\text{Fe}(\text{H}_2\text{Bpz}_2)_2(\text{bipy-R})]$ Complexes

Mengmeng Wang¹, Youssef Draoui¹, Xiaochun Li¹, Koen Robeyns¹, Aurelian Rotaru², Yann Garcia^{1*}

¹Institute of Condensed Matter and Nanosciences, Molecular Chemistry, Materials and Catalysis (IMCN/MOST), Université catholique de Louvain, Place L. Pasteur 1, 1348 Louvain-la-Neuve, Belgium

²Department of Electrical Engineering and Computer Science and MANSiD Research Center, “Stefan cel Mare” University, University Street, 13, Suceava 720229, Romania

*mengmeng.wang@uclouvain.be

Spin crossover (SCO) compounds are promising for applications in data storage, sensors, and molecular electronics due to their ability to reversibly switch state between high-spin (HS) and low-spin (LS) in response to changes in temperature, pressure, or light, accompanied by variations in electronic structure, magnetism, conductivity, and color [1]. The spin transition behavior is mainly governed by ligand field strength and cooperative interactions, necessitating systematic studies to understand the structure–SCO property relationship [2]. Aryl groups, characterized by their unique π -conjugation, steric effects, and fluorescence properties, play a crucial role in modulating the structure, electronic behavior, and photophysical properties of complexes. In this work, we introduce phenyl (phen), 1-naphthyl (1-nap), 2-naphthyl (2-nap), and anthryl (an) groups into the model spin crossover (SCO) complex $[\text{Fe}(\text{H}_2\text{Bpz}_2)_2(\text{bipy})]$ (H_2Bpz_2 = dihydrobis(1-pyrazolyl)borate, bipy = 2,2'-bipyridine) in the C5 and C5' position of the bipy ligand connected by C=N imine bond to afford four Fe(II) complexes $[\text{Fe}(\text{H}_2\text{Bpz}_2)_2(\text{bipy-R})]$ (R = phen, **1**; R = 1-nap, **2**; R = 2-nap, **3**; R = an, **4**) and investigated their SCO properties (Figure 1). Complexes **1** and **3** undergo one-step spin transition with $\sim 57\%/50\%$ completeness and $T_{1/2} = 139\text{ K}/152\text{ K}$. Complexes **2** and **4** exhibit two-steps gradual SCO with $\sim 45\%/30\%$ completeness ($T_{1/2} = 242\text{ K}/289\text{ K}$) for the first step and $\sim 29\%/50\%$ completeness ($T_{1/2} = 137\text{ K}/176\text{ K}$) for the second step revealed by magnetic susceptibility measurements. Unique crystal stacking patterns, rich $\pi \cdots \pi$ interactions raised by aromatic substituent, and their influence on SCO behavior in the series complexes were discussed.

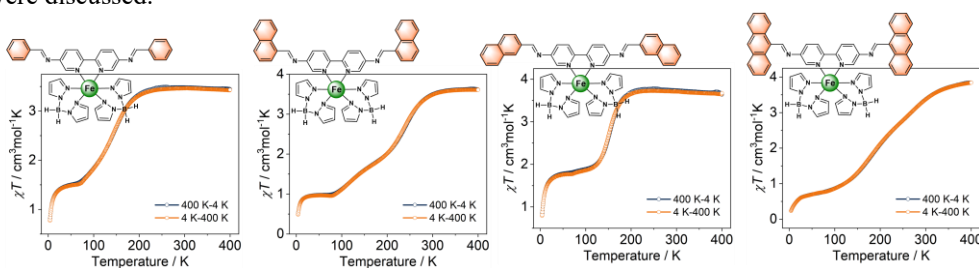


Figure 1. The complexes referred to in this work and their χ_{MT} vs. T plots.

[1] P. Gütllich et al., *Beilstein J. Org. Chem.* **9** (2013) 342.

[2] M. A. Halcrow, *Chem. Soc. Rev.* **40** (2011) 4119.

ICAME-ORAL-T02

Unraveling the Sodium Storage Mechanism of Atomically Dispersed Sn on Hard Carbon via Mössbauer Spectroscopy

Changchang Dong^{1,2*}, Junhu Wang^{1,2}

¹CAS Key Laboratory of Science and Technology on Applied Catalysis, Dalian Institute of Chemical Physics, Chinese Academy of Sciences, Dalian 116023, China

²Mössbauer Effect Data Center, Dalian Institute of Chemical Physics, Chinese Academy of Sciences, Dalian 116023, China

*ccd9165@dicp.ac.cn

Sodium-ion batteries (SIBs), as a new type of high-energy-density green energy battery, have become a core focus in the fields of energy transformation and technological innovation. Tin single-atom anode electrode materials have been applied in the field of SIBs due to their unique physicochemical properties, but they still face two key issues that urgently need to be addressed: difficulties in controllable preparation and unclear working mechanisms. In response to these two bottlenecks, this work utilizes a high-energy-resolution and highly selective in-situ Mössbauer spectroscopy characterization system to guide the synthesis of tin single atoms and the deep analysis of reaction mechanisms. By collaborating with various in-situ characterization techniques such as X-ray diffraction, Raman spectroscopy, and X-ray absorption spectroscopy, the charge/discharge mechanism, capacity decay mechanism, and interfacial layer state of tin single-atom negative electrodes were researched. Through optimizing the material in terms of the carrier, coordination environment, and dispersion, a strategy for the controllable preparation of highly dispersed tin single-atom negative electrode materials was established, achieving a first-cycle coulombic efficiency greater than 90% and a reversible capacity greater than 400 mAh/g at a rate of 0.1 C. This work lays a foundation for the sodium storage mechanism using Mössbauer spectroscopy and provides a method for preparing high-performance anode materials.

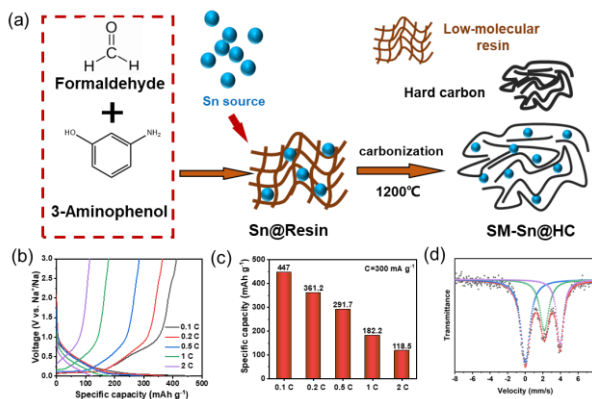


Fig. 1. (a) Scheme of Atomically Dispersed Sn on Hard Carbon, (b,c) the battery performance test, (d) the Mössbauer spectroscopy.

[1] Li Y, Li Y, Lu J, et al. *Adv. Mater.* (2025): 2415026.

[2] Ai L, Zhao Z, Song X, et al. *Adv. Mater.* (2024), 2412592.

Real-Time Insights into Amorphous NiFeB Catalysts for Water Oxidation: An operando Mössbauer Study

Sumbal Farid^{1*}, Junhu Wang¹

¹CAS Key Laboratory of Science and Technology on Applied Catalysis, Dalian Institute of Chemical Physics, Chinese Academy of Sciences, Dalian 116023, China

*sumbalfarid@outlook.com

The transition to sustainable energy relies on developing efficient and durable oxygen evolution reaction (OER) catalysts for water electrolysis, a key process in green hydrogen production.[1] Nickel-iron (NiFe) catalysts have gained significant attention due to their high efficiency and cost-effectiveness. However, critical challenges remain, particularly in understanding the relationship between material properties and catalytic performance and the underlying mechanisms governing activity and degradation [2]. Iron (Fe) is widely recognized as a crucial component in enhancing catalytic efficiency, yet its precise role and interactions during OER remain poorly understood [3]. While crystalline NiFe alloys have been extensively studied, their amorphous counterparts remain underexplored, despite offering potential advantages such as improved active-site accessibility and superior corrosion resistance. Moreover, the incorporation of non-metallic elements like boron (B) has shown promise in further enhancing OER activity and stability, yet the fundamental mechanisms driving these improvements remain unclear [4]. Addressing these gaps is essential for optimizing NiFe-based catalysts and advancing next-generation water-splitting technologies.

Herein, we present the synthesis and detailed characterization of amorphous B-doped NiFe-hydroxide ($\text{Ni}_{0.8}\text{Fe}_{0.2}\text{BOH}$) nanoparticles, highlighting the role of B-doping in enhancing OER performance. Employing a combination of *operando* spectroscopic techniques, including Mössbauer, X-ray absorption (XAS), and Raman spectroscopies, as well as reaction pathway simulation, we elucidate the role of high-valent Ni and Fe species in the catalytic mechanism in the presence of B. Our findings reveal that introducing B not only modifies the metal ion oxidation states but also promotes the formation of active sites involving the *in-situ* formation of NiFeB@NiFeO_x , significantly improving the electrocatalytic efficacy. *Operando* Raman and XAS studies validate the reconstruction of $\text{Ni}_{0.8}\text{Fe}_{0.2}\text{BOH}$ at 1.35 V vs. RHE, while *operando* Mössbauer studies confirm the emergence of high-valent Fe species, fluctuating from 1.4% at 1.35 V vs. RHE to 0.6% at 1.40 V, peaking at 5.8% at 1.55 V, slightly dropping to 5.1% at 1.60 V, and returning to zero post-OER. Reaction pathway simulations reveal a lower water dissociation energy (ΔG_1) for $\text{Ni}_{0.8}\text{Fe}_{0.2}\text{BOH}$ (0.5446 eV) compared to $\text{NiFe}_{0.2}\text{O}_x\text{H}_y$ (0.5738 eV), indicating that B doping promotes easier water activation. The optimized NiFeB and $\text{Ni}_{0.8}\text{Fe}_{0.2}\text{BOH}$ achieve 10 mA/cm² current densities at overpotentials as low as 242 mV and 254 mV, respectively, in 1.0 M KOH solution, while exhibiting remarkable stability over 24 hours. Moreover, the Tafel slopes of the NiFeB alloy and its hydroxide derivatives were found to be 57 mV/dec and 58 mV/dec, respectively, indicating fast reaction kinetics and a more favorable OER pathway compared to pure NiFe-based catalysts. This study offers key insights into optimizing NiFe-based OER electrocatalysts through B-doping, advancing their potential in water splitting and energy conversion technologies.

[1] Chengli Rong, *Advanced Materials* **37** (2025) 2416362.

[2] Daire Tyndall, *Journal of Materials Chemistry A* **11** (2023) 4067–4077.

[3] Peijia Liu, *Catalysis Surveys from Asia* **28** 2024, 361–374.

[4] Zonghua Pu, *Small Methods* **5** (2021) 2100699.

Magnetic and Vibrational Properties of a Molecular $\text{Fe}_{18}\text{Dy}_6$ Wheel

Konstantin Gröpl¹, Andreas Omlor¹, Juliusz A. Wolny¹, Jonathan Oltmanns¹, Tim Hochdörffer¹, Maren H. Hooch¹, Hagen Kämmerer², Jiyong Zhao³, Michael Hu³, Thomas Toellner³, Ercan E. Alp³, Yan Peng^{2,4}, Christopher E. Anson^{2,4}, Ilya Sergueev⁵, Annie K. Powell^{2,4}, Volker Schünemann^{1*}

¹University of Kaiserslautern-Landau, Kaiserslautern, Germany

²Karlsruhe Institute of Technology (KIT), Karlsruhe, Germany

³Advanced Photon Source, Argonne National Laboratory, Argonne, IL, USA

⁴Institute for Quantum Materials and Technologies (IQMT), Karlsruhe, Germany

⁵Deutsches Elektronen Synchrotron (DESY), Hamburg, Germany

*schuene@rptu.de

Single-molecule magnets (SMMs) show a stable magnetization and magnetic hysteresis at low temperature. Potential applications of SMMs are data storage with higher storage densities than today's devices. The molecular wheel $\text{Fe}^{\text{III}}_{18}\text{Dy}^{\text{III}}_6$ is the largest known molecule with a toroidal arrangement of the anisotropy axes of the Dy [1]. We have explored the magnetic properties of this system with temperature and field-dependent ^{57}Fe Mössbauer spectroscopy. The molecular vibrational modes involving Fe movement have been studied with nuclear inelastic scattering (NIS). Since it is expected that the Dy magnetic moments determine the magnetism of the Fe ions temperature-dependent ^{161}Dy nuclear forward scattering (NFS) has been performed. In addition, ^{161}Dy -NIS experiments have shed light on the molecular modes involving Dy movement. Accompanying density functional theory (DFT) calculations give further insights into the interplay of magnetic relaxation and vibrational modes in this system.

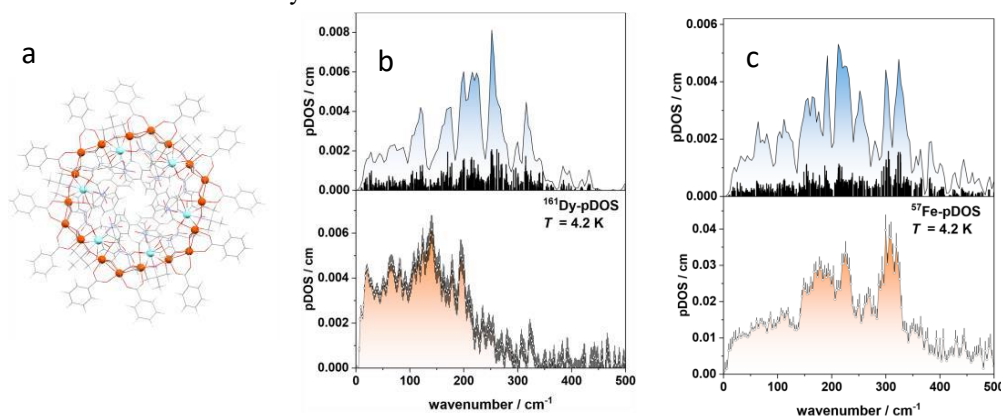


Figure 1. a) Structural representation of $[\text{Fe}_{18}\text{Dy}_6(\mu\text{-OH})_6(\text{ampd})_{12}(2\text{-amino-2-methyl-1,3-propanediol})_{12}(\text{PhCO}_2)_{24}] (\text{NO}_3)_6 \cdot 38\text{MeCN}$ [1]; b) ^{161}Dy partial density of vibrational states (pDOS) (lower panel) measured at 3-ID beamline, APS, Argonne National Laboratory, Argonne, and DFT simulated ^{161}Dy -pDOS (upper panel); c) ^{57}Fe -pDOS measured at beamline P01, PETRA III, DESY Hamburg, (lower panel) and DFT simulated ^{57}Fe -pDOS (upper panel).

[1] H. Kämmerer et al. *J. Am. Chem. Sci.* **42** (2020) 14838.

ICAME-ORAL-T03

Mössbauer Spectroscopy Study of Sn-doped α -Fe₂O₃ Nanoparticles

Stjepko Krehula^{1*}, Marijan Marcijuš¹, Luka Pavić¹, Ljerka Kratočil Krehula²,
Zoltán Homonnay³, Ernő Kuzmann³, Shiro Kubuki⁴

¹ Division of Materials Chemistry, Ruđer Bošković Institute, Zagreb, Croatia

² Faculty of Chemical Engineering and Technology, University of Zagreb, Zagreb, Croatia

³ Faculty of Natural Sciences, Eötvös Loránd University, Budapest, Hungary

⁴ Graduate School of Science and Engineering, Tokyo Metropolitan University, Tokyo, Japan

*krehul@irb.hr

Doping iron oxide α -Fe₂O₃ (hematite) with Sn⁴⁺ ions has proven to be an effective way to improve its performance in several advanced applications, such as photoelectrochemical water splitting [1], photocatalytic degradation of toxic organic compounds [2], or detection of toxic and flammable gases [3]. Very small Sn-doped hematite particles could be suitable for these applications due to the large active surface area and the short average distance of the site of the e⁻-h⁺ pair formation by light absorption from the particle surface.

In this study, pure and Sn-doped hematite nanoparticles were prepared by a simple solvothermal method. Effects of Sn doping on the properties of hematite nanoparticles were investigated using Mössbauer spectroscopy, SEM, XRD (Figure 1), and other techniques.

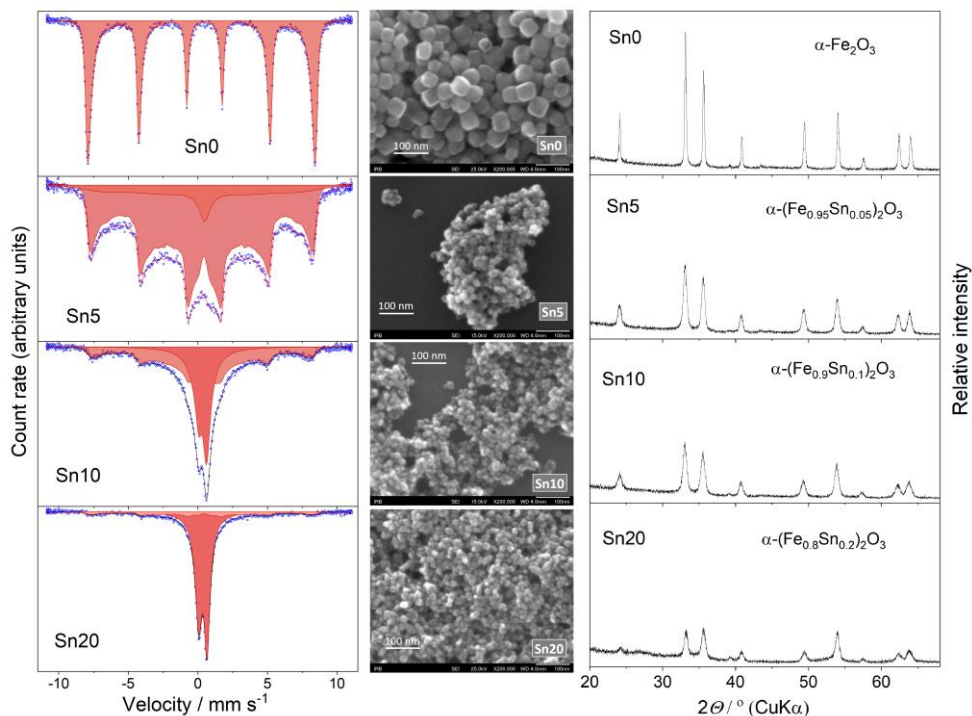


Figure 1. ⁵⁷Fe Mössbauer spectra, SEM images and XRD patterns of pure and Sn-doped hematite nanoparticles.

- [1] A.G. Hufnagel et al., *Adv. Funct. Mater.* (2018) 1804472.
- [2] N. Popov et al., *J. Phys. Chem. Solids* **161** (2022) 110372.
- [3] Q. Xia et al., *Sens. Actuators B: Chem.* **399** (2024) 134874.

ICAME-ORAL-T03

Stabilizing Non-collinear Spin Structures in Thin Flms: A Novel Approach Using Oblique Incidence Deposition for Precise Control and Detection via NFS

Anjali Panchwanee^{1*}, Lars Bocklage¹, Sven Velten¹, Sakshath Sadashivaiah², Ilya Sergeev¹, Ralf Rohlsberger,^{1, 2, 3, 4} and Kai Schlage¹

¹Deutsches Elektronen-Synchrotron DESY, 22607 Hamburg, Germany

²Helmholtz-Institut Jena, 07743 Jena, Germany

³Institut für Optik und Quantenelektronik, Friedrich-Schiller-Universität Jena, 07743 Jena, Germany

⁴Helmholtz Centre for Heavy Ion Research (GSI), 64291 Darmstadt, Germany

*anjali.panchwanee@desy.de

The development of advanced spintronic devices relies heavily on the precise engineering of specific magnetic spin structures in thin films at the nanoscale [1]. Achieving this goal presents a significant challenge, requiring the development of novel techniques for creating, stabilizing, and detecting controlled non-collinear spin arrangements. In this work, we present an innovative approach using oblique incidence deposition (OID) to induce and stabilize magnetic spin spiral structures in iron thin films at room temperature, with precise control over spin spiral profile achieved by tuning magnetic OID surface anisotropy strengths and their orientation [2].

The depth-dependent spin configuration was probed using nuclear forward scattering (NFS) of synchrotron radiation, offering high sensitivity and precision in resolving intrinsic spin spirals [3]. This technique confirmed the stabilization of spin spirals and provided insights into their tunability, validating the feasibility of our OID-based fabrication approach.

Our findings, along with the demonstrated ability to precisely control spin configurations, open new opportunities for engineering custom spin spirals in next-generation energy storage, magnetic sensors, and FMR spin filters, paving the way for advanced spintronic and magnetic nanotechnology applications. The combination of the OID fabrication technique and NFS detection method presented in this work provides a robust and adaptable approach to designing and characterizing tailored non-collinear spin structures, marking a significant step toward room-temperature functional spintronic devices.

[1] A.A. Khajetoorians et al., *Science* **332**, 1062–1064 (2011).

[2] K. Schlage et al., *Adv. Funct. Mat.* **26**, 7423–7430 (2016).

[3] R. Röhlsberger, "Nuclear condensed matter physics with synchrotron radiation: Basic principles, methodology and applications." Vol. 208 (Springer Science & Business Media, 2004).

ICAME-ORAL-T03

New Insights into the Crystal and Magnetic Structure of Hematite

Alberto Martinelli^{1,3}, Sawssen Slimani^{1,2}, Nader Yaacoub⁴, Davide Peddis^{1,2*}

¹Department of Chemistry and Industrial Chemistry & Genova, INSTM RU, nM2-Lab, University of Genova, 16146 Genova, Italy

²Institute of Structure of Matter, National Research Council, nM2-Lab, Via Salaria km 29.300, Monterotondo Scalo 00015, Roma, Italy

³CNR-SPIN Corso Perrone 24, I-16152 Genova, Italy

⁴Institut des Molécules et Matériaux du Mans CNRS UMR-6283, Le Mans Université, Avenue Messiaen, 72085 Le Mans, France

*davide.peddis@unige.it

Hematite (α -Fe₂O₃) is a particularly interesting antiferromagnetic material because its Morin transition (T_m) is influenced by size, surface, and microstructural defects. Below T_m , hematite behaves as a uniaxial antiferromagnet, with magnetic moments aligned along the (111)*c* hexagonal axis. Above T_m , it becomes a canted antiferromagnet ("weak ferromagnet"), with moments lying in the basal (111) plane and slightly canted ($\sim 11^\circ$), producing a small net magnetization. This study investigates the structural and magnetic behavior of hematite nanoparticles, using synchrotron X-ray powder diffraction (XRPD), neutron powder diffraction (NPD), and Mössbauer spectrometry to unravel the interplay between bulk and surface magnetic phases in hematite (α -Fe₂O₃) nanoparticles. The nanoparticles were synthesized through the auto-combustion sol-gel method (SH sample), followed by thermal treatment at 1100 °C for 2 h (ASH sample). NPD identifies magnetic ordering fulfilling the Γ_3 irreducible representation at 300 K, with spins lying in the hexagonal *ab* plane for both samples. Remarkably, the Γ_3 model allows a canted antiferromagnetic arrangement of the magnetic moments, giving rise to a weak ferromagnetic component in the plane, in full agreement with the Dzyaloshinskii theory. On cooling, a WF-to-antiferromagnetic transition occurs around ~ 265 K. Our NPD data collected at 1.5 K indicate that magnetic ordering fulfills the Γ_1 irreducible representation, with spins antiferromagnetically aligned along the hexagonal *c*-axis (AF antiferromagnetic phase). Interestingly, the intensity of the magnetic peak 003 at $\sim 1.35 \text{ \AA}^{-1}$ decreases on cooling, but it is not fully suppressed at the lowest temperature, although it is observed with different intensities in the two samples. This peak does not pertain to the Γ_1 symmetry. This suggests that distinct magnetic phases (AF and WF) coexist in separate domains below the Morin transition. Domain size analysis from NPD peak broadening reveals that crystallographic domains in the ASH are 10–20% larger than AF magnetic domains at 1.5 K. This implies that particles are not single magnetic domains, with WF ordering coexisting as a secondary phase. The nanostructured nature of the samples suggests a core-shell configuration, where the core exhibits AF order and the surface supports WF canted moments. This scenario is supported by Mössbauer spectrometry measurements performed at 12 K and under an applied magnetic field (8 T), that confirms the presence of two magnetic phases: WF component (57% in SH, 48% in ASH) with canting angles ($\theta = 80^\circ$ in SH, 71° in ASH) and the AF phase (43% in SH, 52% in ASH). The reduced WF fraction and canting angle post-annealing align with NPD's observation, indicating that annealing suppresses surface-driven spin canting and stabilizes bulk AF order.

Nuclear GISAXS on Self-assembled Magneto-resistive Multilayer Nanowires

K. Schlage^{1*}, S. Velten¹, N. Colomer¹, L. Bocklage^{1,3}, S. Sadashivaiah^{2,4},
G. Meier^{3,5} and R. Röhlberger^{1,2,4,6}

¹DESY, Hamburg, Germany

²Helmholtz Institute Jena, Jena, Germany

³The Hamburg Centre for Ultrafast Imaging, Hamburg, Germany

⁴Institute for Optics and Quantum Electro., Friedrich Schiller University, Jena, Germany

⁵Max Planck Institute for the Structure and Dynamics of Matter, Hamburg, Germany

⁶Helmholtz Centre for Heavy Ion Research (GSI), Darmstadt, Germany

*kai.schlage@desy.de

Complex nano-structuring routines on magnetic multilayers are frequently applied in data storage and sensor technology to functionalize devices via shape anisotropy. Here we test if sputter deposition onto nano-faceted surfaces can be applied to form self-assembled, high-quality nanowires with adjustable size and anisotropy.

Fe/Cr superlattices with intended antiferromagnetic order were deposited in oblique incidence (Fig. a) onto a nano-faceted Al₂O₃ wafer (facet height 25 nm) where the facet morphology was adjusted via high-T annealing. Due to a shadowing effect, separated nanowires are expected to form on the surface. A precise nanoscopic characterization, however, is challenging with lab-based techniques. To investigate the structural quality and magnetic properties of the wires, we perform conventional and nuclear grazing incidence small-angle x-ray scattering. While GISAXS (b) is used to extract the relevant parameters of the multilayer morphology, nuclear GISAXS at the 14.41 keV Fe resonance is applied to determine the spin structure of the wires. Fig. c) shows resonant detector line scans along the multilayer GISAXS pattern. In addition to the structural Bragg peak, magnetic superstructure peaks appear, whose intensity is coupled to the strength of antiferromagnetic order. Field-dependent hysteresis curves and nuclear time at these scattering maxima were analysed to extract the magnetic reversal.

These elegant ways for flexible multilayer nanowire formation and novel characterization are highly interesting for potential sensor and device applications requiring tunable magnetic anisotropies.

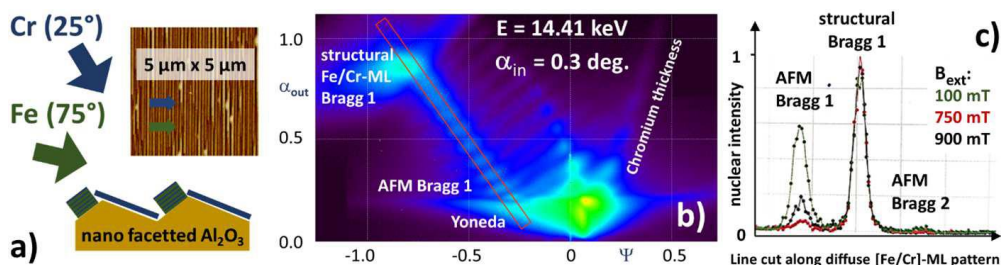


Figure 1. a) Sketch of the multilayer nanowire fabrication. b) Conventional (non-resonant) GISAXS image of the nanowire array bearing information about the nanoscopic multilayer morphology. c) Field-dependent nuclear resonant line scans with superstructure Bragg peaks due to an antiferromagnetic spin alignment.

ICAME-ORAL-T03

Magnetic Structure of Hollow Nanoarchitectures

Sawssen Slimani^{1,4*}, Marianna Vasilakaki², Kalliopi N Trohidou²,
Gurvinder Singh⁴, Nader Yaacoub³, and Davide Peddis^{1,4}

¹Department of Chemistry and Industrial Chemistry & Genova, INSTM RU, nM2-Lab,
University of Genova, 16146 Genova, Italy

²Institute of Nanoscience and Nanotechnology, NCSR “Demokritos”, 15310 Agia Paraskevi,
Attiki, Greece

³Institut Des Molécules Et Matériaux du Mans (IMMM) CNRS UMR-6283, Le Mans
Université, Avenue Messiaen, 72085, Le Mans, France

⁴Institute of Structure of Matter, National Research Council, nM2-Lab, Via Salaria km
29.300, Monterotondo Scalo 00015, Roma, Italy

⁵The University of Sydney Nano Institute, The University of Sydney, Sydney, New South
Wales, 2006, Australia

*sawssen.slimani@unige.it

At the nanometer scale, the surface-to-volume ratio ($R = S/V$) of nanoparticles increases significantly, playing a crucial role in altering or introducing novel magnetic properties compared to their bulk counterparts. Among these, hollow nanoparticles (NPs) stand out as a particularly intriguing class, as they possess both internal and external surfaces, further enhancing the surface-to-volume ratio and amplifying their unique magnetic behaviour [1]. Here, we present a comparative study of the morpho-structural and magnetic properties of full and hollow maghemite ($\gamma\text{-Fe}_2\text{O}_3$) nanoparticles, characterized by a big surface to volume ratio, of corresponding sizes 5.0(5) nm, 7.4(7) nm, and 13(1) nm. These systems have been thoroughly characterized by means of DC and AC magnetization measurement and in-field ^{57}Fe Mössbauer spectrometry. The in-field hyperfine structure analysis suggested the presence of a non-collinear spin structure (i.e., spin casting) for both hollow NPs, originating from the increased surface effects due to the presence of inner surface (IS) and outer surface (OS) (i.e., hollow morphology). Interestingly, after field cooling, a horizontal shift of the hysteresis loop was observed. Monte Carlo (MC) simulations show that the spins canted in the OS and IS are strongly antiferromagnetically exchange-coupled, leading to a decrease of their saturation magnetization (M_s). At the interface, this strong exchange coupling results in a strong exchange bias, inducing an increase in the coercive field, in agreement with the experimental and Mössbauer findings.

[1] F. Sayed et al., *J. Phys. Chem. C* **122** (2018)

ICAME-ORAL-T04

Mössbauer Characterization of Low Temperature Iron-based Fischer-Tropsch Catalysts

Yassir A. Abdu^{1*}, P. Julius Pretorius², and Frank C. Hawthorne³

¹Department of Applied Physics and Astronomy, University of Sharjah, Sharjah, United Arab Emirates

²Saskatchewan Research Council, Saskatoon, Canada (Current address: Sherritt Technologies, Fort Saskatchewan, Canada)

³Department of Earth Sciences, University of Manitoba, Winnipeg, Canada

*yabdu@sharjah.ac.ae

Fischer-Tropsch (FT) synthesis is the process of producing hydrocarbons from syngas over a transition metal catalyst. There has been renewed interest in FT synthesis due to its ability to produce clean fuels and sustainable energy. Here we use Mössbauer spectroscopy to characterize low-temperature Fe-based FT catalysts prepared by two methods: the historical Ruhrchemie method (by precipitation from a copper-containing iron nitrate solution) and an organic acid method that uses a mixture of iron and formic acid. Mössbauer spectroscopy measurements were done in transmission mode (at room temperature) using a ⁵⁷Co(Rh) source. The spectra were fitted, using Voigt-based line shapes, to two paramagnetic doublets and five magnetic sextets. The doublets are assigned to Fe²⁺ (larger quadrupole splitting) and Fe³⁺, whereas the sextets are ascribed to the Fe-carbide χ -Fe₅C₂ (fitted with three sextets having hyperfine magnetic fields of ~ 22, 18, and 10 T) and magnetite Fe₃O₄ with its characteristic two-sextet pattern with hyperfine magnetic fields of ~ 48 T (A-site) and ~ 45 T (B-site). The Mössbauer relative areas, which give the relative proportions of Fe-containing phases, indicate that the catalyst samples prepared by the historical Ruhrchemie method contain large amounts of Fe-carbide (up to ~ 60% relative area) compared to those prepared by the organic acid method, consistent with their large FT activity. On the other hand, the spectra of the catalyst samples prepared by the organic acid method are dominated by magnetite. The results will be discussed in connection with the observed synthesis outcomes and compared with published Mössbauer data on Fe-based FT synthesis.

ICAME-ORAL-T04

High Throughput Nuclear Resonant Time Domain Interferometry: NR-TDI

Esen Ercan Alp^{1*}, Marc Pavlik¹, Michael Hu¹, Jiyong Zhao¹, Barbara Lavina¹,
Dennis E. Brown², Larry Lurio²

¹Advanced Photon Source, Argonne National Laboratory, USA

²Northern Illinois University, De Kalb, Illinois, USA

*eea@anl.gov

We introduce a high-throughput nuclear resonant time domain interferometry to measure relaxation time in liquid-glass or liquid-solid transformations, as well as to measure diffusion in solids as a function of temperature and different length scales. We have implemented a golden annular slit concept to improve the data collection rate by a factor up to 100, which enables systematic measurements of temperature and length dependent dynamical changes.

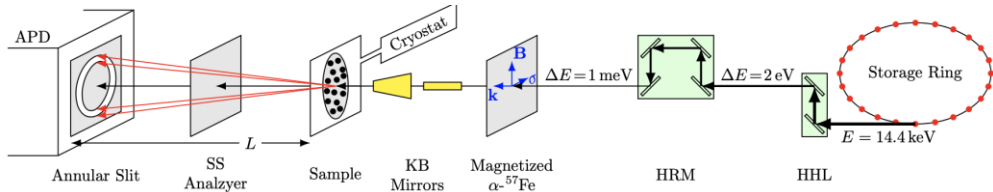


Figure 1: The idea behind the experiment is to produce a longitudinally coherent beam (using magnetized ^{57}Fe foil), and an analyzer (Stainless Steel) to check on the remaining fraction of the coherent beam after being scattered by the sample. Here, HHL is High Heat Load monochromator, HRM is high resolution monochromator, KB is Kirkpatrick-Baez Mirror, and APD is the time-resolved Avalanche Photo Diode detector.

The time development of such an experiment is best described by the following equation:

$$I(\mathbf{q}, t) = 2 \left| G_{\text{Fe}}(t) \right|^2 \left(1 + \cos[\Omega t] \right) + f_{\Delta E} \left| G_{\text{SS}}(t) \right|^2 + 4 G_{\text{Fe}}(t) G_{\text{SS}}(t) f_q e^{-\left(\frac{t}{\tau_k} \right)^\beta} \cos \left[\frac{\Omega}{2} t \right] \cos[\omega_{\text{IS}} t]$$

The stretched exponential term above can be extracted from the analysis of the time decay data. Here, $G_{\text{Fe}}(t)$ and $G_{\text{SS}}(t)$ represent the nuclear resonant response function of the iron foil and the stainless steel analyzer. The cross term $G_{\text{Fe}}(t) G_{\text{SS}}(t)$ is the interference term that provides contrast due to loss of coherence in the liquid sample. The samples can be anything that does not contain iron.

[1] M. Pavlik, E. Alp et al, *J. Synchrotron Rad.* **29** (2022) 677,

[2] M. Kaisermayr, E. Alp et al, *Eur. Phys. J. B20*, 355 (2001)

ICAME-ORAL-T04

Mössbauer Spectroscopy Investigation of Crystallization in (FeCoCrNi)-(B,Si) High-Entropy Metallic Glasses

Leila Panahi¹, Pere Bruna^{2,3,4*}

¹Methodology Group, ALBA Synchrotron, Cerdanyola del Vallès, Barcelona, Spain

²Universitat Politècnica de Catalunya · BarcelonaTech (UPC), EEBE/Dept. of Physics, Spain

²UPC, Barcelona Research Center in Multiscale Science and Engineering, Spain

³UPC, Institute of Energy Technologies (INTE), Spain

*pere.bruna@upc.edu

High-entropy alloys (HEAs) and high-entropy metallic glasses (HEMGs) have attracted significant attention due to their exceptional mechanical, thermal, and magnetic properties, making them promising candidates for structural and functional applications. HEAs, characterized by multi-principal element compositions, exhibit outstanding strength, corrosion resistance, and thermal stability, while HEMGs combine the disordered atomic structure of metallic glasses with the high-entropy effect, enhancing their glass-forming ability and wear resistance. These materials have been extensively studied for their unique phase stability and crystallization behavior [1]. Understanding the crystallization process in HEMGs is critical for optimizing their performance in advanced applications.

In this study, the crystallization behavior of (FeCoCrNi)-(B,Si) high-entropy metallic glasses was investigated using Mössbauer spectroscopy and X-ray diffraction. Mössbauer analysis provided insight into the local atomic environments and magnetic properties of Fe-containing phases during thermal treatment. The as-prepared amorphous phase exhibited paramagnetic characteristics with a broad distribution of hyperfine fields, indicative of significant atomic disorder. Upon annealing, the formation of crystalline phases resulted in a progressive increase in hyperfine field strength, suggesting the development of Fe-containing nanocrystalline structures. The Mössbauer spectra revealed the coexistence of residual amorphous and newly formed crystalline phases through the presence of sextet patterns, confirming partial crystallization. These findings highlight the role of Fe atoms in the structural evolution and magnetic behavior of high-entropy metallic glasses, providing valuable insights into their thermal stability and potential technological applications [2].

[1] J. Li et al., *Mater. Des.* **95** (2016) 183-187.

[2] L. Panahi et al. , *J. Non-Cryst. Sol.* **547** (2020) 120301.

Effect of Partial Pressures of Oxygen on Oxidation States and Coordination Structures of Iron Ions and on Iron Oxide Activity Coefficients in Silicate Slags

Miyuki Hayashi^{1*}, Shiro Kubuki², Masahiro Susa¹

¹Institute of Science Tokyo, Tokyo, Japan

²Tokyo Metropolitan University, Tokyo, Japan

*hayashi.m.ac@m.titech.ac.jp

The effect of partial pressures of oxygen on the oxidation states and coordination structures of iron ions and on iron oxide activity coefficients in $\text{Na}_2\text{O-SiO}_2\text{-FeO-Fe}_2\text{O}_3$ and $\text{CaO-SiO}_2\text{-FeO-Fe}_2\text{O}_3$ slags. The melts were placed in Pt containers at 1573 K and equilibrated at partial pressures of oxygen (P_{O_2}) in the range between 10^{-9} atm and 10^{-4} atm, and the activities were derived from Fe concentrations in the Pt containers using the activity coefficient of Fe in Pt-Fe alloys reported as a function of molar fraction of Fe. At the same time, the percentages of Fe^{2+} , Fe^{3+} in octahedral symmetry ($\text{Fe}^{3+}(\text{oct})$) and Fe^{3+} in tetrahedral symmetry ($\text{Fe}^{3+}(\text{tetr})$) were also measured by Mössbauer spectroscopy. With increasing P_{O_2} , the Fe^{2+} pct. decreases while the $\text{Fe}^{3+}(\text{oct})$ pct. increases and the $\text{Fe}^{3+}(\text{tetr})$ pct. moderately increases in both $\text{Na}_2\text{O-SiO}_2\text{-FeO-Fe}_2\text{O}_3$ and $\text{CaO-SiO}_2\text{-FeO-Fe}_2\text{O}_3$ slags. The activity coefficients of FeO (γ_{FeO}) are larger than those of $\text{FeO}_{1.5}$ ($\gamma_{\text{FeO}_{1.5}}$) in $\text{Na}_2\text{O-SiO}_2\text{-FeO-Fe}_2\text{O}_3$ melts, i.e., $\gamma_{\text{FeO}} > \gamma_{\text{FeO}_{1.5}}$, and the hierarchy of the activity coefficients, i.e., $\gamma_{\text{FeO}} > \gamma_{\text{FeO}_{1.5}(\text{oct})} > \gamma_{\text{FeO}_{1.5}(\text{tetr})}$, holds in the $\text{CaO-SiO}_2\text{-FeO-Fe}_2\text{O}_3$ melts. The magnitude of effective ionic radii is in the hierarchy of $\text{Fe}^{2+} > \text{Fe}^{3+}(\text{oct}) > \text{Fe}^{3+}(\text{tetr})$, and thereby the bond strength between iron ion and oxide ion is in the hierarchy of $\text{Fe}^{3+}(\text{tetr}) > \text{Fe}^{3+}(\text{oct}) > \text{Fe}^{2+}$. This suggests that Fe^{2+} are more loosely and $\text{Fe}^{3+}(\text{tetr})$ are more rigidly bound to the silicate skeleton, which situation would be reflected in the hierarchy of the activity coefficients, i.e., $\gamma_{\text{FeO}} > \gamma_{\text{FeO}_{1.5}(\text{oct})} > \gamma_{\text{FeO}_{1.5}(\text{tetr})}$. The values of $\gamma_{\text{FeO}_{1.5}}$ in the $\text{CaO-SiO}_2\text{-FeO-Fe}_2\text{O}_3$ melts are much larger than the values of $\gamma_{\text{FeO}_{1.5}}$ in the $\text{Na}_2\text{O-SiO}_2\text{-FeO-Fe}_2\text{O}_3$ melts. The result may be explained by the difference in the number of valences of cation, i.e., divalent ion Ca^{2+} and monovalent ion Na^+ maintaining electrical neutrality of FeO_4^{5-} tetrahedra. Figure 1 shows the schematic representation in 2-dimension of the structure of (a) $\text{Na}_2\text{O-SiO}_2\text{-FeO-Fe}_2\text{O}_3$ melt and (b) $\text{CaO-SiO}_2\text{-FeO-Fe}_2\text{O}_3$ melt. As shown in Fig. 1(b), Ca^{2+} ion requires two FeO_4^{5-} tetrahedra nearby, accordingly, resulting in the agglomeration of FeO_4^{5-} , i.e., larger $\gamma_{\text{FeO}_{1.5}}$ values.

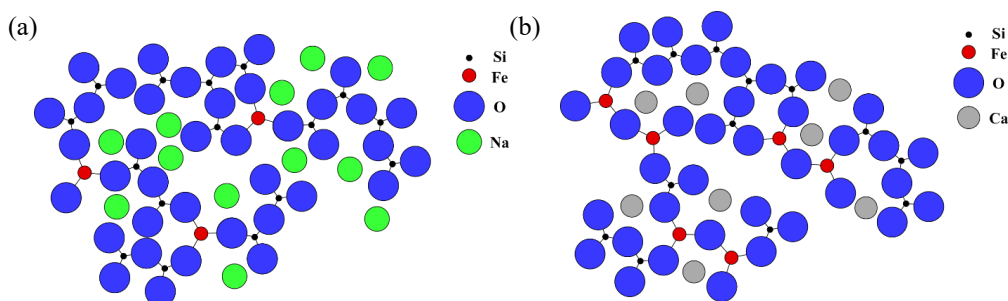


Figure 1. Schematic representation in 2-dimension of structure of (a) $\text{Na}_2\text{O-SiO}_2\text{-FeO-Fe}_2\text{O}_3$ melt and (b) $\text{CaO-SiO}_2\text{-FeO-Fe}_2\text{O}_3$ melt.

ICAME-ORAL-T04

Influence of Eu-doping on the Magnetic Structure of Goethite: A Mössbauer Study

Z. Homonnay^{1,*}, A. Doumae², K. Tani², Y. Arita², K. A. Béres^{1,5}, M. Kudor¹,
K. Süvegh¹, E. Kuzmann¹, S. Krehula³, M. Marciuš³, L. Pavić³,
M. Mirosavljević³, A. Šantić³, B. Zhang⁴,
L. Zhang⁴, S. Kubuki²

¹Institute of Chemistry, Eötvös Loránd University, Hungary

²Graduate School of Science, Tokyo Metropolitan University, Japan

³Division of Materials Chemistry, Ruđer Bošković Institute, Croatia

⁴School of Environmental and Safety Engineering, Jiangsu University, China

⁵Institute of Materials and Environmental Chemistry, HUN-REN Research Centre
for Natural Sciences, Hungary

*homonnay.zoltan@ttk.elte.hu

Synthetic goethites doped with lanthanides (e.g., La^{3+} , Lu^{3+} , Gd^{3+} , Eu^{3+}) are the focus of research in order to achieve improvements in novel battery electrode fabrication as well as in the preparation of new photo-active catalysts for wastewater treatment. The presence of lanthanides has an influence on the band structure of the insulator goethite, giving rise to electronic transitions that can turn goethite into a photoactive catalyst.

Mössbauer Spectroscopy can sensitively detect changes in the environment of the iron sites in goethite by measuring hyperfine interactions. From among these interactions, the hyperfine magnetic field is most sensitive to minor changes in the lattice.

We report studies on Eu-doped goethites synthesized by the solvothermal method. The initial molar ratio of Eu relative to Fe in the synthesis was set from zero to 50 %.

The reference pristine goethite, synthesized the same way as the doped materials, showed a continuous distribution of the internal hyperfine magnetic field. Incorporation of Eu resulted in rather discrete field distributions at room temperature, with one of the individual fields resembling that in hematite.

There was only one single iron environment found at 90 K for the samples with 40 % and 50 % initial Eu-fraction. More interestingly, this field at 90 K was lower than the largest (hematite-like) field observed at room temperature (Fig. 1). A Substantial paramagnetic component was found only for 5% and 10% initial Eu content.

It is proposed that Eu doping creates magnetic sublattices with well-separated and characteristic antiferromagnetic couplings in the goethite structure that collapse into a uniform (or two-component, at maximum) magnetic structure at 90 K. It will also be discussed why this temperature dependence depends on the amount of excess Eu applied in the synthesis.

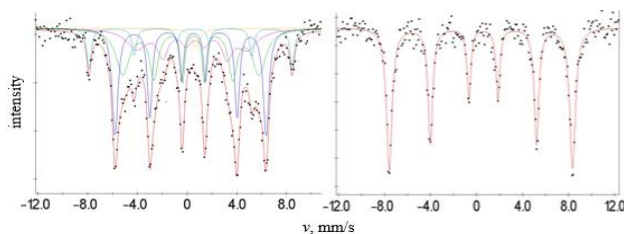


Figure 1. Mössbauer spectra of Eu-doped goethite recorded at room temperature (left) and at 86 K (right).

ICAME-ORAL-T04

Eu-Activated SiAlON Studied by Synchrotron-Radiation-Based ^{151}Eu Mössbauer Spectroscopy

S. Kitao^{1*}, R. Degawa², R. Masuda³, Y. Kobayashi¹, H. Yamashita⁴, N. Nagasawa⁵,
Y. Yoda⁵, T. Masuda⁶, K. Yoshimura⁶, M. Seto¹

¹Institute for Integrated Radiation and Nuclear Science, Kyoto Univ., Kumatori, Osaka 590-0494, Japan

²Denka Company Limited, Omuta, Fukuoka 836-8510, Japan

³Graduate School of Science and Technology, Hirosaki Univ., Hirosaki, Aomori 036-8561, Japan

⁴Graduate School of Science, Kyoto Univ., Kyoto 606-8502, Japan

⁵Japan Synchrotron Radiation Research Institute, Sayo, Hyogo 679-5198, Japan

⁶Research Institute for Interdisciplinary Science, Okayama Univ., Okayama 700-8530, Japan

*kitao.shinji.5s@kyoto-u.ac.jp

Nitride phosphors have been attracting great attention as fluorescent substances for lighting devices such as white light-emitting diodes(LEDs). Among these substances, Eu-activated silicon aluminum oxynitride (SiAlON) is one of the most widely used substances in recent industry because of its excellent fluorescent properties. The doped Eu in the SiAlON plays an important role in the fluorescent mechanisms. However, the relationship between the electronic state of Eu and the fluorescent properties has not been well understood yet.

Mössbauer spectroscopy is one of the most powerful tools for the investigation of a specific element. The ^{151}Eu is the most commonly used Mössbauer isotope after ^{57}Fe and ^{119}Sn , because it has a long-life Mössbauer source of ^{151}Sm . However, Eu Mössbauer spectroscopy using the radioactive source for Eu-activated SiAlON is sometimes difficult since it requires a long measurement time because of the quite small composition rate of Eu. On the contrary, synchrotron-radiation(SR)-based Mössbauer spectroscopy can be widely used for most Mössbauer isotopes. Different from conventional spectroscopy, the SR-based Mössbauer spectroscopy has unique properties of SR, such as high photon flux, small beam size, time-pulsed property, and so on. High photon flux is quite effective for reducing the measurement time. Moreover, the time-pulsed property of SR enables us for time-resolved experiments using the newly developed system, recording event-by-event signals with time and energy information [1].

In this study, an experiment of Eu-activated SiAlON using SR-based ^{151}Eu Mössbauer spectroscopy performed at BL35XU beamline at SPring-8 is reported. Electronic properties from the Mössbauer parameters of Eu in the SiAlON have been well evaluated at a temperature of 20 K. In addition, an attempt with irradiation of LED light during the measurement is discussed.

[1] S. Kitao et al., *J. Phys. Conf. Ser.* **2380**, 012136 (2022).

ICAME-ORAL-T04

Relationships among Structure, Photocatalytic and Electrical Properties of Lanthanide-Substituted Goethite Nanoparticles

A. Doumae¹, K. Tani¹, Y. Arita¹, K. A. Béres^{2,3}, M. Kudor², K. Süvegh²,
Z. Homonnay², E. Kuzmann², S. Krehula⁴, M. Marciuš⁴, L. Pavić⁴, A. Baftić⁵,
A. Šantić⁴, M.V. Ushakov⁶, M. I. Oshtrakh⁶, B. Zhang⁷, L. Zhang⁷,
S. Kubuki^{1*}

¹Graduate School of Science, Tokyo Metropolitan University, Tokyo, Japan

²Institute of Chemistry, ELTE Eötvös Loránd University, Budapest, Hungary

³Institute of Materials and Environmental Chemistry, HUN-REN

Research Centre for Natural Sciences, Budapest, Hungary

⁴Division of Materials Chemistry, Ruđer Bošković Institute, Zagreb, Croatia

⁵Faculty of Chemical Engineering and Technology, University of Zagreb, Zagreb, Croatia

⁶Department of Experimental Physics, Institute of Physics and Technology, Ural Federal
University, Ekaterinburg, Russian Federation

⁷School of Environmental and Safety Engineering, Jiangsu University, Jiangsu, China

*kubuki@tmu.ac.jp

The relationships among local structure, photocatalytic ability, and electrical conductivity, including cathode and anode performances in Na-ion battery of La-, Gd-, and Lu-substituted goethite nanoparticles (NPs) with the substitution ratio (x) of lanthanide elements from 0 to 50 mol.%, abbreviated as Lnx before and after heat treatment at 300 °C for 30 min, were investigated by X-ray Diffractometry (XRD), X-ray absorption fine structure (XAFS), ⁵⁷Fe-Mössbauer Spectroscopy (MS), Brunauer-Emmett-Teller (BET) method, electrical impedance spectroscopy (EIS), and UV-Vis spectroscopy (UV-Vis). The XRD patterns of Lnx showed a crystalline phase mainly derived from α -FeOOH in all samples. An increase in the peak intensities attributed to La(OH)₃ and Gd(OH)₃, respectively, was observed from the XRD pattern of Lax and Gdx with x equal to or larger than 10 mol.%, while that of Lux shows only the peaks attributed to α -FeOOH. The MS of α -FeOOH NPs is composed of several sextets due to Ln-doped α -FeOOH in addition to a minor doublet in Lax and Gdx and a major doublet in Lux. For Lax and Gdx, the doublets are considered as a sign of superparamagnetic Ln-doped goethite. In the case of Lux, the major doublet, which grows significantly with increasing Lu content, is assigned to iron-doped amorphous Lu-hydroxide. Compared with the specific surface area of 40.4 m²·g⁻¹ recorded for lanthanide-free α -FeOOH, remarkable increases in the specific surface area were measured for Lax, Gdx, and Lux NPs. In the methylene blue decomposition test, the reaction rate constant (k) decreased from 6.9×10^{-3} to 2.6×10^{-3} , 3.1×10^{-3} min⁻¹, and 1.6×10^{-3} min⁻¹ when evaluating for Lax, Gdx, and Lux NPs with x from 0 to 50 mol.%, respectively. The decreasing k values with the lanthanide concentration of Lnx NPs are caused by the decrease in the goethite content and the formation of the lanthanide hydroxides. Due to the high electrical conductivity of 1.05×10^{-5} S·cm⁻¹ and the large cathode and anode capacities of 216.7 and 500.0 mAh·g⁻¹ recorded for the SIB containing the heat-treated Lu10 NPs, it is concluded that the heat-treated Lu10 NPs is the best sample among the investigated Lnx NPs because of the highest electrical conductivity.

M.I.O. and M.V.U. were supported by the Ministry of Science and Higher Education of the Russian Federation, project № FEUZ-2023-0013, and by the Ural Federal University Program of Development within the Priority-2030 Program (research funding from the Ministry of Science and Higher Education of the Russian Federation).

ICAME-ORAL-T04

Structure, Microstructure, and Hyperfine Interactions in Hf- and Ni-Substituted TiFe Alloy for Hydrogen Storage

K. Komędera¹, J. M. Michalik^{1,*}, K. Sworst¹, Ł. Gondek¹

¹AGH University of Krakow, Faculty of Physics and Applied Computer Science, Department of Solid State Physics, Mickiewicza 30, 30-059 Kraków, Poland

*jmichali@agh.edu.pl

Hydrogen storage in metallic materials is of utmost importance for hydrogen energy applications. In this contribution, we address the issue of finding cost-effective materials for large-scale usage. One such material is TiFe, which requires high H₂ pressure and temperature above 400 °C to activate and start reversibly absorbing/desorbing hydrogen. To facilitate the aforementioned processes, the alloy must be subjected to doping by other elements. We report research on the Ti_{1-x}Hf_xFe_{1-y}Ni_y compounds and their hydrides investigated by means of X-ray diffraction, electron microscopy, and Mössbauer spectroscopy. The data show that for Ti_{0.9}Hf_{0.1}Fe_{0.9}Ni_{0.1}, the activation temperature is reduced to 200 °C, with a slightly reduced total hydrogen absorption. According to Mössbauer spectroscopy results, hydrogenation of the synthesized alloys leads to a significant decrease in the electronic state of the compounds, as could be expected for hydrides. It also proves the existence of structural disorder introduced to facilitate the activation of the alloys, complementary to X-ray diffraction and electron microscopy.

This work was partially supported (synthesis, X-ray diffraction, electron microscopy studies, data consolidation) by the National Science Centre, Poland, number: 2023/05/Y/ST3/00249 under the M-ERA.NET 3 Call 2023 (project acronym “HY-PHAD” Horizon 2020 grant agreement No. 958174).

[1] K. Komędera et al., *Acta Phys. Pol. A* **146(3)** (2024) 215-221.

ICAME-ORAL-T04

Hybrid Iron-based Nanoadsorbents: Morphological, Structural, Magnetic and Hyperfine Properties

Edson C. Passamani^{1*}, Camila N. Pinotti¹, Willbrynnner P. Marques², J. R. Capua Proveti¹, Adriano da Silva², J. C. C. Freitas¹, F. Jochen Litterst³, and Juan Adrian Ramos-Guivar⁴

¹Universidade Federal do Espírito Santo, Vitória 29075-910, ES, Brazil

²Universidade Federal de Santa Catarina, Florianópolis, 88040-900, SC, Brazil

³Technische Universität Braunschweig, 38106, Braunschweig, Germany

⁴Universidad Nacional Mayor de San Marcos, Lima, 15081, Peru

*edson.caetano@ufes.br

Magnetic remediation has emerged as a suitable method for effluent treatments that were severely contaminated with toxic metals (Pb, As, Cd, etc.), borates, phosphorates, among others [1-4]. In this regard, magnetic adsorbents are still an essential key for a correct application of this method with an expected high efficiency on contaminant removal and low impact of the adsorbent on living organisms naturally found in effluents. Nanomaterials show high specific BET (Brunauer, Emmett, and Teller theory) surface areas by which their catalytic properties could be enhanced either in their natural states or with surface functionalization with specific materials, resulting in nanohybrids or metamaterials. Thus, the main focus, at this moment, is based on the development, characterization, and tests of magnetic nanomaterials that could yield remarkable results in removal efficiency concomitantly with low toxic impacts in the bioenvironment. Magnetic iron-oxide-based (MIOB) nanohybrids have shown potential features to cover some of the above main requests [3-4].

In this conference, we will discuss the results of MIOB nanoadsorbents that were effectively synthesized by the co-precipitation route and were systematically characterized by several experimental methods to comprehend their structural, morphological, hyperfine, and magnetic properties before and after adsorption processes. The MIOB nanoadsorbents are nanoparticles of maghemite ($\gamma\text{-Fe}_2\text{O}_3$) or Mg-ferrite (MgFe_2O_4) functionalized with MgO and/or zeolites, where the former phase is responsible for their magnetic properties, whereas the latter ones cover the adsorption properties for pollutant removal. Kinetics and isothermal adsorption models were applied to describe the types of adsorption mechanisms. Thus, in this presentation, we will correlate the hyperfine properties seen by ^{57}Fe Mössbauer spectroscopy and Nuclear Magnetic Resonance of MIOB, responsible for the efficiency of the water treatment.

We would like to thank FAPES and CNPq for the financial support.

- [1] W.P. Marques et al., *J. Clean. Prod.* **470** (2024) 143184-143216.
- [2] C.N. Pinotti et al., *Mat. Chem. Phys.* **308** (2022) 128313-128332.
- [3] C.A. Tamanaha-Vegas, *Adv. Pow. Tech.* **33** (2022) 103395-103402.
- [4] J.A. Ramos-Guivar, *Nanomat.* **11** (2021) 2310-2341.

ICAME-ORAL-T04

Structural Modifications across Dielectric Maxima in Lead-free BaTiO₃-based Relaxors: ¹¹⁹Sn Hyperfine Interaction Study

V. Raghavendra Reddy^{1*}, Meenal Dhanetwal¹, Akash Surampalli², Deepak Prajapat³, Anjali Panchwanee³, Sven Velten³, Ilya Sergeev³

¹UGC-DAE Consortium for Scientific Research, Khandwa Road, Indore 452001, India

²Department of Materials Science and Engineering, University of California, Berkeley, California 94720, USA

³Deutsches Elektronen-Synchrotron - A Research Centre of the Helmholtz Association, 22607 Hamburg, Germany

*varimalla@yahoo.com / vrreddy@csr.res.in

Lead-free relaxors, particularly those based on barium titanate BaTiO₃ (BTO), have received a lot of attention due to their nontoxic nature, high dielectric permittivity, several phase transitions, and the possibility of tuning transition temperature close to room temperature. It is noteworthy that doped BTO materials exhibit relaxor behavior even in the absence of charge disorder. This characteristic distinguishes them from traditional lead-based relaxors, such as PbMg_{1/3}Nb_{2/3}O₃, which typically display nominal charge disorder. With complementary experimental methods such as Raman spectroscopy, x-ray absorption spectroscopy (XAS), Mossbauer measurements, etc., unambiguous signatures of structural modifications across the dielectric maxima in iso-valent (Sn⁴⁺) substituted BTO relaxor are reported, and hence providing inputs for a deeper understanding of the dipole dynamics in such relaxors [1-3].

The present work deals specifically with the ¹¹⁹Sn hyperfine interaction study of 30% substituted BTO relaxor (BTS30). The presence of quadrupole splitting (QS) below the dielectric maxima (T_m) of BTS30 is confirmed unambiguously using synchrotron radiation perturbed angular correlation (SRPAC) experiments [3]. Further, temperature-dependent ¹¹⁹Sn nuclear forward scattering (NFS) data clearly depict the development of QS below T_m [3]. Finite values of QS with temperature, below T_m , unambiguously indicate the development of electric field gradient around Sn/Ti sites in BaTi_{0.7}¹¹⁹Sn_{0.3}O₃ relaxor, emphasizing the applicability of conventional ferroelectric models in explaining relaxor properties of iso-valent substituted BTO-based materials.

[1] A. Surampalli et al., *Phys. Rev. B* **100**, 134104 (2019)

[2] A. Surampalli et al., *Phys. Rev. B* **104**, 184114 (2021)

[3] M. Dhanetwal et al., *Phys. Rev. B* **110**, 054205 (2024)

ICAME-ORAL-T04

Quality Inspection of 3D Printed Steel Elements, Marine Engine Crankshafts, Wind Turbine Shafts and Nanomagnetic Ferrofluids with Mössbauer Spectrometry

Tadeusz Szumiata^{1*}, Zbigniew Siemiątkowski¹, Mirosław Rucki¹

¹Department of Physics, Faculty of Mechanical Engineering,
Casimir Pulaski Radom University, Radom, Poland

*t.szumiata@urad.edu.pl

The main goal of the lecture is to demonstrate the effectiveness of the Mössbauer spectroscopy technique for industrial applications in the quality assessment of steel and iron oxide products. The transmission Mössbauer spectrometry analysis of hyperfine magnetic field distributions proved that the selective laser melting (SLM) did not change considerably the martensite structure at an atomic level of sleeves made out of maraging steel [1].

The conversion electron Mössbauer spectrometry (CEMS) method confirmed a high phase purity, homogeneity, and isotropy of the marine diesel engine crankshaft (Fig. 1) fabricated of carbon-saturated ferritic steel of martensite structure [2]. Similarly, CEMS pointed to a high purity and isotropy of the 42CrMo4 steel dominated by the phase of bcc α -Fe type and used for the manufacturing of wind turbine main shafts [3].

On the other hand, in the case of oil-nanomagnetite ferrofluids, the transmission Mössbauer measurements in the external magnetic fields enabled the investigation of spin relaxation effects and confirmed that low hyperfine magnetic field components in the spectra can be assigned to the finest fraction of the nanoparticles [4].

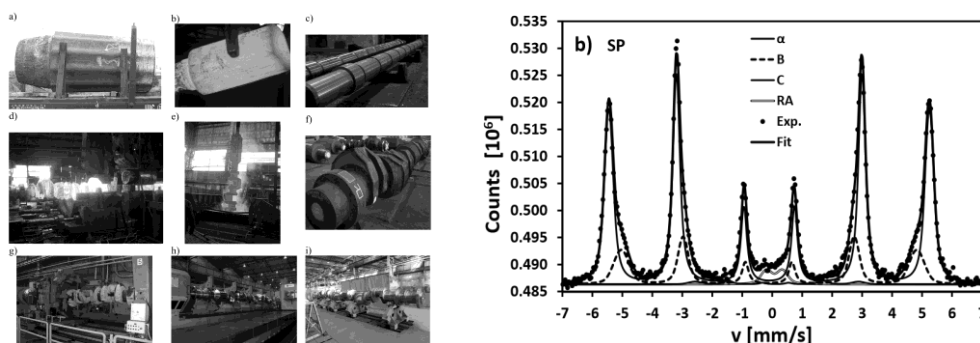


Figure 1. The sequence of actions when manufacturing a monolithic marine engine crankshaft and the CEMS spectrum.

- [1] P. Tyczyński et al., *Mat.* **13** (2020) 3408.
- [2] Z. Siemiątkowski et al., *J. Marine Eng. Tech.* **17** (2018) 160.
- [3] Z. Siemiątkowski et al., *Nukleonika* **62** (2017) 171.
- [4] T. Szumiata et al., *Acta Phys. Pol. A* **134** (2018), 1007.

ICAME-ORAL-T05

Hypertension Development May Be Impacted by Gold, Silver, and Titanium Oxide Nanoparticles

Kvetoslava Burda^{1*}, Joanna Fiedor¹, Magdalena Peter¹, Aleksander Siniarski²,
Jarosław Kiecana², Józef Korecki³, Grzegorz Gajos²

¹Faculty of Physics and Applied Computer Science, AGH-University of Krakow, Krakow, Poland

² John Paul II Hospital, Department of Coronary Disease, Krakow, Poland

³Jerzy Haber Institute of Catalysis and Surface Chemistry, Polish Academy of Sciences, Krakow, Poland

*burda@agh.edu.pl

Over the last two decades, the focus of both nano- and bio-technologies has been on nanoparticles (NPs). TiO₂, Ag, and Au NPs belong nowadays to the most commonly used nanomaterials. This is due to their unique electronic, photonic, catalytic, and therapeutic properties. However, humans are exposed to a particularly high level of these NPs' action due to the extensive range of their use in everyday life. In the medical field, they can be used as a means to carry drugs and as containers.

The aim of the study was to examine their potential toxicity on red blood cells. We investigated size and shape changes, stability, and functionality of erythrocytes resulting from the action of NPs using optical microscopy, spectrophotometry, atomic force microscopy, absorption, and Mössbauer spectroscopy, respectively. We observed morphological changes in erythrocytes treated with NPs. These changes were due to the reorganization of their membrane skeleton. The osmotic resistance curves demonstrated differing behaviour and a marked reliance on the type and concentration of NPs utilised. This suggests that these NPs interact complexly with the membrane structures of red blood cells. Additionally, we found that all the NPs used were capable of modifying haemoglobin's affinity for O₂.

We will present a comparison of the effects of these nanoparticles on erythrocytes isolated from healthy individuals and individuals with type 2 diabetes. This will demonstrate the similarities and differences in the impact of NPs on erythrocytes from healthy donors and those with diabetes. Based on these findings, we will discuss the potential impact of TiO₂, Ag, and Au NPs on erythrocyte function and the development of primary hypertension.

This work was partially supported by the National Science Centre, Poland, grant No. 2019/33/B/NZ7/02724.

ICAME-ORAL-T05

Exploring the Magnetic Moment of Iron in Oxyhaemoglobin - A Story Still Unfolding

Katarzyna Dziedzic-Kocurek^{1*}, Jakub Dybaś², Jan J. Stanek¹

¹M. Smoluchowski Institute of Physics, Jagiellonian University, Kraków, Poland

²Jagiellońskie Centrum Rozwoju Leków JCET, Jagiellonian University, Kraków, Poland

*k.dziedzic-kocurek@uj.edu.pl

Due to its widespread presence and vital role in biological systems, the nature of Fe–O₂ bonding in hemoproteins has been a topic of scientific debate for decades [1–3]. A Mössbauer spectrum of oxidized human red blood cells, recorded at 5 K under an external magnetic field of 8 T, reveals a hyperfine field at the ⁵⁷Fe nuclei of 8.6 T, approximately 7.5% higher than the applied field. This indicates a residual magnetic moment in the nominally low-spin Fe²⁺ state of oxyhaemoglobin. We interpret this as evidence for rapid spin-state relaxation between the ground low-spin (LS, S = 0) and an excited intermediate-spin (IS, S = 1) state.

In the case studied, the electric field gradient (EFG) tensor at the iron nucleus has a negative sign, in contrast to myoglobin, where the dominant species is high-spin (HS) Fe²⁺. In myoglobin, the EFG primarily originates from valence contributions, particularly from a single 3d electron in the 3d⁶ configuration of HS Fe²⁺. Conversely, the positive EFG observed in our system suggests a lattice-originated EFG, consistent with a LS Fe²⁺ configuration.

Based on these findings, we propose the following mechanism for oxygen binding in oxyhaemoglobin: (1) at low temperatures, iron exists in a LS Fe²⁺ state, while O₂ remains in an excited singlet state; (2) as temperature increases, iron gradually transitions to an intermediate-spin state (IS, S = 1), accompanied by a singlet-to-triplet conversion of O₂. The two are antiferromagnetically coupled [4]; (3) this thermally induced spin transition resembles behaviour commonly observed in various iron-based organometallic compounds [5].

This research was partially supported by the grant NCN/DEC-2019/03/X/NZ1/01631.

[1] L. Pauling and C. D. Coryell, *Proc. N. A. S.* **22** (1936), 210.

[2] G. Lang and W. Marshall, *Proc. Phys. Soc.* **87** (1966), 3.

[3] S. Mayda et al., *Sci. Rep.* **10** (2020), 8569.

[4] D. Kurokawa et al., *ACS Omega.* **3** (2018), 9241.

[5] M. Magott et al., *Chem. Sci.* **14** (2023), 9651.

ICAME-ORAL-T05

Identification of Heme and Non-heme Iron in Foods: Mössbauer Spectroscopy Study

Mariola Kądziołka-Gawel^{1*}, Marcin Wojtyniak²

¹Institute of Physics, University of Silesia, 75 Pułku Piechoty 1, 41-500 Chorzów, Poland

²Institute of Physics, Silesian University of Technology, Konarskiego 22B, 44-100 Gliwice, Poland

*mariola.kadziolka-gawel@us.edu.pl

Iron is a multifunctional trace element that plays a key role in the growth and development of the human body at all stages of its life. This element plays a significant role in the oxygen transport system and is a cofactor in enzymatic and non-enzymatic operations [1]. Iron is a nutrient that the human body does not synthesize and must be supplied with food. Dietary iron present in food is in two forms as heme and non-heme iron. Although plant materials contain only non-heme iron, animal products contain both heme and non-heme iron [2]. Furthermore, heme iron has a higher bioavailability (> 15%) than non-heme iron (< 5%) [2]. Iron deficiency develops when the amount of iron in the diet is below the required value and causes anemia and other pathological changes in the body. Iron is an ingredient of many food products, so with a bit of willingness, there is no problem in providing the body with the right amount of it and avoiding this necessity. Limited research has examined the mineral content of plant or animal-based foods, especially iron. For this reason, using Mössbauer spectroscopy and X-ray fluorescence method, this paper aimed to examine the concentration and properties of iron in foods. The information on heme and non-heme iron content based on their concentration in foods is necessary for predicting the total amount of iron available in a meal. Additionally, such knowledge is particularly relevant in the current environment, with growing numbers of people adopting a plant-based diet. Our research is based on products readily available in supermarkets or butcher shops. Among others, we used products such as black olives (Figure 1b), soy, spleen, and dried beef and pork blood (Figure 1a) for the research.

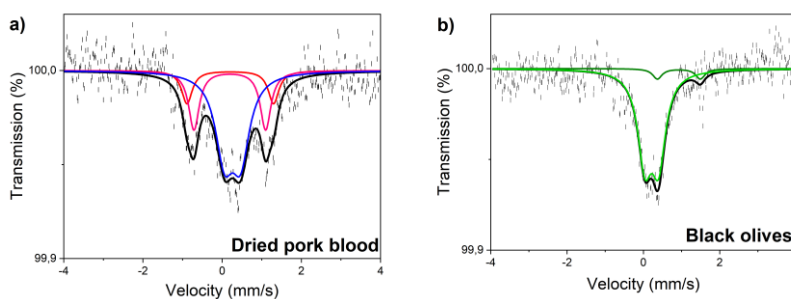


Figure 1. Room temperature Mössbauer spectra for dried pork blood a) and black olives b). The experimental points, fitting curves, and spectral components corresponding to iron sites are presented.

[1] U. Malhotra et al., *Food Bioeng.* **2** (2023) 53.

[2] R. Kongkachuichai et al., *J. Food Comp. Analys.* **15** (2002) 389.

ICAME-ORAL-T05

Application of Nuclear Resonant Scattering at High Pressure and High Temperature at Advanced Photon Source

Jiyong Zhao^{1*}

¹Advanced Photon Source, Argonne National Laboratory, Lemont, IL 60439, US

*jzhao@anl.gov

Nuclear resonant scattering (NRS) using synchrotron radiation is a powerful technique that provides extensive information about materials, including hyperfine interactions, magnetism, vibrational density of states, and sound velocities. These capabilities make NRS widely applicable in materials science research. Furthermore, NRS under high-pressure and high-temperature conditions has unique applications in geophysics and geochemistry, enabling the study of geo-materials in extreme environments.

This presentation will discuss recent novel applications of NRS at the Advanced Photon Source (APS), including studies on the melting behavior of Fe-alloys under extreme conditions [1] and investigations into magnetism in quantum materials [2]. Additionally, the talk will highlight recent upgrades to the APS storage ring and NRS beamlines, which have significantly enhanced experimental capabilities. Key advancements, such as the implementation of a micro-focusing system and an updated laser-heated diamond anvil cell system, will be presented, showcasing how these upgrades enable cutting-edge research in materials science, geophysics, and quantum materials.

[1] V.V. Dobrosavljevic et al., *Nature Commun.* **14** (2023), 7336.

[2] J.C. Greeshma et al., *J. Phys. Condens. Matter* **36** (2024), 255802.

ICAME-ORAL-T06

Classification Method of Ordinary Chondrites Based on Mössbauer Spectroscopy - What Can It Tell Us About Meteorites?

M. Jakubowska¹, M. Woźniak², J. Gałązka-Friedman¹

¹Warsaw University of Technology, Faculty of Physics, Koszykowa 75, 00-662 Warsaw, Poland

²University of Warsaw, Faculty of Biology, Miecznikowa 1, 02-096, Warszawa, Poland

*martyna.jakubowska@pw.edu.pl

Mössbauer spectroscopy with the ⁵⁷Fe isotope is widely applied in meteorite analysis. It is particularly useful for ordinary chondrites, the most common meteorites that fall to Earth, which contain 19–30 wt.% of iron.

Mössbauer spectroscopy can serve as a basis for the classification of ordinary chondrites for example through the 4M method [1], which is based on Mössbauer spectroscopy results and multidimensional discriminant analysis. It relies on a database of Mössbauer data from meteorites of known petrographic types.

The classical classification method of ordinary chondrites is based on determining the fayalite and ferrosilite content in silicates, while the 4M method focuses on the distribution of iron in the main mineral phases. Both methods give comparable classification results.

In this study, we present classification results obtained using the 4M method and compare them with those derived from the classical method. For each sample, based on literature data, the molar percentage of fayalite and ferrosilite was determined. A database consisting of 4709 samples was used to calculate the distances to the centers of clusters corresponding to groups H, L and LL. For the 4M method, the percentage similarity to each of these groups was also computed.

Table 1. Comparison between the classical classification method and the 4M method

	Distance from Cluster Center			Percentage Similarity to			Classification Result Using	
	H	L	LL	H	L	LL	4M Method	Classical Method
Aiquile	1.0	8.1	13.6	49.1%	3.0%	0.0%	H	H
Campos Sales	8.0	0.7	4.8	35.6%	41.5%	0.1%	L	L
Kheneg Ljouâd	14.9	7.6	2.2	0.8%	4.3%	14.3%	LL	LL

Mössbauer spectroscopy also enables the assessment of the oxidation state of a meteorite resulting from terrestrial weathering during its residence on the Earth's surface [2]. This process leads to the oxidation of Fe⁰ and Fe²⁺ ions to Fe³⁺ ions. The metallic phase is the first to oxidize — its relative contribution to the Mössbauer spectrum decreases [3].

One of the significant advantages of Mössbauer spectroscopy is its ability to distinguish troilite from its terrestrial counterpart, pyrrhotite. This distinction is of considerable importance for meteorite identification, as the presence of troilite supports the extraterrestrial origin of the studied sample.

[1] M. Woźniak, *et al.*, *Meteorit. Planet. Sci.* **54** (2019) 1828–1839.

[2] M. Jakubowska, *et al.*, *Acta Soc. Metheor. Polon.* **8** (2017) 63–72.

[3] H.C. Verma, *et al.*, *Hyperfine Interact.*, **186** (2008) 141–145.

ICAME-ORAL-T06

Two-Dimensional Mössbauer Spectroscopy – New Horizons in Molecular Magnetism and Space Exploration

Franz Renz^{1*}, Kevin Tran¹, Maximilian Seydi Kilic¹, Rene Lucka¹, Justus Pawlak¹, Mathias Blumers¹

¹Institute of Coordination Chemistry, Leibniz University Hannover, Callinstraße 9, D-30167 Hannover, Germany

* franz.renz@acd.uni-hannover.de

Mössbauer Spectroscopy enables the determination of spin states and oxidation states in coordination compounds, making it a powerful tool for analyzing products in inorganic chemistry [1,2].

In our research group, we are at the forefront of developing the miniaturized Mössbauer Spectrometer (MIMOS) and improving the recording of Mössbauer spectra. Recently, we introduced a two-dimensional data recording system, where we detect the energy of each counted photon and store it alongside the velocity of the Mössbauer drive. This approach allows us to obtain an energy spectrum that can be post-processed to extract the different Mössbauer spectra [2,3]. For iron-57 Mössbauer spectroscopy, using energy ranges of 14.4 keV, 6.4 keV, and 7.0 keV with SD detectors in transmission and reflection, we are opening new frontiers, especially in light of the growing interest in molecular magnetism [4,5]

[1] C. M. Grunert, S. Reiman, H. Spiering, J. A. Kitchen, S. Brooker, P. Gülich, *Angew. Chem. Int. Ed.*, **47** (2008) 2997-29.

[2] M. Jahns, S. Klimke, D. Natke, R. Sindelar, U. Schrewe, R. Patzke, F. Renz, *Nucl. Inst. Methods Phys. Res. A*, **940** (2019).

[3] M. Jahns, J. Pawlak, S. Klimke, R. Sindelar, U. Schrewe, R. Patzke, F. Renz, *Nucl. Inst. Methods Phys. Res. A*, **1031** (2022) 166529.

[4] C. Rajnák, J. Titis, J. Moncol, F. Renz, R. Boca, *Chem. Comm.*, **55** (2019) 13868.

[5] C. Rajnák, R. Micova, J. Moncol, L. Dhan, C. Krüger, F. Renz, R. Boca, *Dalton Trans.*, **50** (2021) 472.

ICAME-ORAL-T07

NRIXS and Atomic Dynamics Simulations

Michael Y. Hu ^{1*}

¹Argonne National Laboratory, United States of America

*myhu@anl.gov

Nuclear Resonant Inelastic X-ray Scattering (NRIXS) is an advanced spectroscopic technique used primarily to study the vibrational dynamics of solids. Ab initio atomic dynamics simulations based on Density Functional Theory (DFT) are also widely used to investigate and predict the vibrational properties of materials at the atomic scale. They can provide benchmarks and interpretations of features in measured spectra and thus derived phonon Density of States (DOS). We present a research combining both methods closely to gain better understanding of materials and their properties. Using SnSe as an example, we study its anharmonicity and thermal transport properties ("Onset of anharmonicity and thermal conductivity in SnSe", Hu et al., PRB 104, 184303, 2021).

ICAME-ORAL-T08

Nuclear Resonance Scattering Beamline ID14 at the European Synchrotron Radiation Facility

Dimitrios Bessas^{1*}, Ilya Kupenko¹, Jean-Philippe Celse¹, Rudolf R  ffer¹,
Aleksandr I. Chumakov¹

¹European Synchrotron Radiation Facility, Grenoble, France

*bessas@esrf.fr

The Extremely Brilliant Source upgrade of the European Synchrotron Radiation Facility is a large-scale facility upgrade that brought into the scientific community a first-of-a-kind, low-emittance, high-energy synchrotron light source and new cutting-edge beamlines.

The Nuclear Resonance Scattering beamline at the European Synchrotron Radiation Facility, which operated with great success for around 30 years at the ID18 straight section [1], has recently been relocated at the ID14 straight section and profits from all the merits of the Extremely Brilliant Source upgrade of the facility.

A new cryogenically cooled permanent magnet undulator already in use at ID14 results in an increase by about an order of magnitude more photons at energies above 50 keV. A second in-vacuum undulator to be used simultaneously with the existing cryogenically cooled permanent magnet undulator is under development and will lead to about 60% enhancement in the photon flux at 14.4 keV, *i.e.*, the nuclear resonance energy for ⁵⁷Fe. The high-heat-load monochromator now operates in horizontal scattering geometry. As a result, all irregularities induced by the heat load of the white synchrotron radiation X-ray beam, the static deformation from the crystal holders, and from mechanical vibrations, affect much less the downstream high-resolution optics that scatter in the vertical plane. The overall thermal stability at the sensitive high-resolution X-ray optic elements is significantly enhanced, down to the 0.1 K level, and leads to practically no X-ray optics adjustment throughout the course of a user experiment. The high-resolution spectroscopy using a spectrograph [2] is now routinely offered to the user community. A thermally stabilised experimental hutch, with stability down to 0.1 K level, is operational, dedicated to X-ray nanoscopy [3]. Several other auxiliary tools have been added at ID14, including white and monochromatic X-ray beam translocators for collimation, a Pilatus 3 (2M) area detector for exploratory X-ray diffraction during nuclear resonance scattering experiments. The operation of an offline conventional M  ssbauer spectroscopy laboratory for sample pre-characterization is resumed.

In this presentation apart from showing the key elements of the brand-new nuclear resonance scattering beamline ID14 at the European Synchrotron Radiation Facility, the added value in terms of photon flux (up to about an order of magnitude for ⁶¹Ni and ⁹⁹Ru), energy resolution (down to 100 μ eV for phonon spectroscopy by ⁵⁷Fe), and beamsizes (down to 320 nm for X-ray nanoscopy by ⁵⁷Fe) will be shown. Room for potential development and collaborations will be given.

[1] R. R  ffer and A. I. Chumakov, *Hyperfine Interact.* **97** (1996) 589.

[2] A. I. Chumakov et al., *Phys. Rev. Lett.* **123** (2019) 097402.

[3] I. Kupenko et al., *High Pressure Res.* **44** (2024) 310.

ICAME-ORAL-T08

MinSight: Web-based Fitting for Mössbauer Spectroscopy

James M. Byrne^{1*}

¹School of Earth Sciences, University of Bristol, Bristol, United Kingdom

*james.byrne@bristol.ac.uk

This presentation focuses on the development of an application called MinSight, www.minsight.org, which has been designed to read, fit, and interpret Mössbauer spectroscopy data in a web browser. This project aims to deliver a framework to: (a) accelerate the analysis and interpretation of spectra; (b) simplify spectral analysis for new users of Mössbauer spectroscopy; (c) increase accessibility to both raw data as well as associated hyperfine parameters; (d) enable automation of data fitting and interpretation; (e) integrate other spectroscopy techniques to provide multimodal analytics.

MinSight is unique compared to other Mössbauer software in its offering of a browser-based approach to fitting spectra. It has been built using Python, with Streamlit providing the web interface and Firebase handling data storage. Data can be uploaded in a file management system, which also includes the ability to create many different projects, each of which may contain a number of different spectra. Simple annotation inputs enable users to provide basic metadata such as measurement temperature and describe samples such as type (e.g., thin film, powder), or collection environment (e.g., synthetic, sediment, soil, etc.).

Once data is on the server, the analysis page provides options to visualise and fit data using standard models (Lorentzian, Squared Lorentzian, Voigt, and extended Voigt), as with other more traditional software. What sets MinSight apart are its additional features. This includes the ability to load parameter guesses based on published literature. Users have the ability to directly compare their spectra against a spectral library, with a score ranking their similarity. If there is a satisfactory match, the parameters used for the original publication can be imported and used for fitting. This feature helps to provide a starting point for complex spectra such as those from environmental soils and sediments, and also enables users to quickly access relevant publications, which may help in their interpretations. This approach can also be used to support automated and batch fitting. Further support is provided for interpreting fits, including hyperfine parameter correlation plots (e.g., isomer shift vs. quadrupole splitting, or isomer shift vs. hyperfine field), helping users to visually inspect if sites fall within acceptable limits or need further refinement. Parameters can be matched against a hyperfine parameter database for sample identification, though the database is currently small and would benefit from expansion. With the possibility of loading multiple spectra within a project, more widespread comparisons can be made, including for relative abundances, which are compared in a bar plot and update automatically. Furthermore, a summary table can be easily downloaded, and a multi-panel figure can be constructed via a simple button. By embedding the software into a web browser, users gain flexibility. They can log in to their accounts, upload and store data on a server, and access it from any device, including mobile. Collaborative tools also allow users to share their data with project partners, enhancing teamwork.

Development of MinSight has initially focused on Mössbauer spectroscopy, but it is planned to expand into a range of spectroscopic methods, including FTIR, XANES, and Raman, amongst others. Such a combination of techniques in the same platform will enable multimodal analytics, which will cater to various research fields, including (bio)geochemistry, geophysics, paleomagnetism, geomicrobiology, and astrobiology, among countless others. This presentation will discuss the development of this project, as well as ongoing challenges and new opportunities.

ICAME-ORAL-T08

Single-shot Mössbauer Spectroscopy at X-ray Free-electron Lasers

Evers Jörg^{1*}, for the ⁵⁷Fe EuXFEL collaboration

¹Max Planck Institute for Nuclear Physics, Heidelberg, Germany

*joerg.evers@mpi-hd.mpg.de

Mössbauer spectroscopy is widely used to study the structure and dynamics of matter with a remarkably high energy resolution, provided by the narrow resonance line widths. However, theory and experiment so far are focused on the linear low-excitation regime with, on average, less than one resonant exciting photon per incident X-ray pulse, owing to a restriction of the experimentally available resonant photon flux.

This situation has changed with the availability of X-ray free-electron lasers, which may provide a large number of photons within the nuclear linewidth, either on average or per pulse. A first experiment demonstrated superradiance with up to 70 signal photons per X-ray pulse [1]. Further progress towards the high-excitation regime recently became possible with high-repetition-rate self-seeded hard X-ray free electron lasers, and is expected to open up several qualitatively new lines of research with Mössbauer nuclei. One of them is the exploration of ultra-narrow Mössbauer resonances, which has already been realized with the recent direct resonant X-ray excitation of the Mössbauer clock transition in ⁴⁵Sc [2], and which is based on the high average number of resonant photons.

In a parallel development, the ⁵⁷Fe EuXFEL collaboration (led by R. Röhlberger and J. Evers) has established nuclear resonance scattering on ⁵⁷Fe in a series of experiments at the European X-ray free-electron laser in Germany. In these experiments, up to several hundred signal photons were observed following a single x-ray excitation.

In this talk, I will discuss single-shot Mössbauer spectroscopy as a second application of NRS at XFELs, which relies on the high number of resonant photons per pulse in order to alleviate the need for time averaging [3]. I will introduce our approach, which is capable of also including repetitions with lower signal photon numbers into the single-shot analysis. Then, I will demonstrate its feasibility using data from a recent experiment at European XFEL.

[1] A.I. Chumakov et al., *Nature Phys.* **14** (2018) 261.

[2] Y. Shvyd'ko et al., *Nature* **622** (2023) 471.

[3] M. Gerharz et. al, *in preparation*

ICAME-ORAL-T08

Nuclear Resonant Scattering in Public Beamline of SPring-8

Nobumoto Nagasawa^{1*}, Yoshitaka Yoda¹, Alfred Q.R. Baron^{2,1}

¹Precision Spectroscopy Division, JASRI, SPring-8, Sayo, Hyogo, Japan

²Materials Dynamics Laboratory, RIKEN SPring-8 Center, Sayo, Hyogo, Japan

*nagasawa@spring8.or.jp

Nuclear Resonant Scattering (NRS) is one of the longest-running scientific programs at JASRI at SPring-8. Activity was started in 1997 at BL09XU, and it has extended to some other beamlines. In 2021, the main base of operation was moved from BL09XU to BL35XU, where the NRS program shares beamtime with the meV inelastic x-ray scattering (IXS) program [1]. The short-period undulator installed at BL35XU for meV IXS is also beneficial for NRS, providing higher flux (x2 to x3 on the sample, or more) compared to BL09XU. The BL35XU NRS setup has many high-resolution monochromators for various isotopes. Especially for ⁵⁷Fe, several energy resolutions are available in order to gain the best efficiency for each technique. In addition to the high-resolution monochromators for specific isotopes, a Si(nn0) channel-cut monochromator is installed for higher energies, such as for the ⁶¹Ni resonance at 67.4 keV. We choose a suitable reflection index, *n*, to match the sample size and its transmission.

NRS activities continue to develop. Not only are more quick measurements with the same techniques as BL09XU, but also adding other variables to the conventional techniques are available at BL35XU: e.g., energy-window for scattered process on the synchrotron Mössbauer spectroscopy with time-gating method [2] has been developed [3]. Higher flux at energies above 60 keV allows us to accelerate the investigation of science using the time-gated synchrotron Mössbauer spectroscopy, as for ⁶¹Ni, ¹⁹³Ir, ¹⁷⁴Yb, ⁹⁹Ru, *etc.*. Some developments without the synchrotron radiation bunch structure have been performed. A novel quasielastic scattering spectroscopy using an X-ray imaging detector, CITIUS, has been developed [4]. We note that the BL35XU ID is not tunable <14 keV and between 29 keV and 43 keV. However, NRS experiments in these energy regions are available at BL19LXU.

The presentation will show an overview of the beamline instrumentations and some research using the NRS techniques described above.

[1] Y. Yoda, et al., ICAME2021, Romania

[2] M. Seto, et al., *Phys. Rev. Lett.* **102** (2009) 217602.

[3] S. Kitao, et al., *J. Phys. Conf. Ser.* **2380** (2022) 012136.

[4] M. Saito, et al., *Phys. Rev. Lett.* **132** (2024) 256901.

Remote Control and Alarm Monitoring of Mössbauer Laboratories

Dénes Lajos Nagy^{1*}, László Deák¹, Zoltán Németh¹, Edit Szilágyi¹

¹HUN-REN Wigner Research Centre for Physics, Budapest, Hungary

*nagy.denes@wigner.hun-ren.hu

Remote control of Mössbauer laboratories has recently become an issue of great significance. The practically unlimited bandwidth nowadays available worldwide on desktops, tablets, and mobile phones makes possible on-line controlling many functions of spectrometers even from the home office. An increasing number of Mössbauer groups offer open-access collaboration using mail-in samples, and it is expected that this approach will gain currency. This will widen the scope of accessible isotopes and experimental techniques for the co-workers. The remote partners may also wish to control their experiments live as much as possible. We present the experiences collected at the HUN-REN Wigner Research Centre for Physics and its predecessors (Wigner RCP) since 2015 in remote controlling Mössbauer laboratories and related facilities like the helium gas recovery system. Special emphasis is laid on handling unexpected electric blackouts and notifying the experimenters of such events.

Two Mössbauer laboratories are running in one building of the Wigner RCP. Experiments are controlled by personal computers (PC) operating under MS Windows 10. The PCs can be accessed by remote desktop applications. Remote access to PCs is subject to SSH tunnelling, for which a valid user account at HUN-REN Wigner RCP is required.

Cameras connected to the experiment-controlling PCs are watching instruments in the laboratory and, by logging into the given PC, can be accessed remotely. Unplanned electric blackouts (even of a few seconds or less) need special attention. Indeed, immediately continuing the experiments could damage some instruments, e.g., Mössbauer drives, field-effect transistors of preamplifiers, or turbopumps. Therefore, the electric feed pipe of the laboratory has been divided into two parts. Sensitive instruments are protected by an auto-release magnetic switch. We refer to this part of the electric feed pipe as “magnetic-switch-protected grid” (MSPG). Conversely, pieces of equipment that should operate continuously (lighting, refrigerators, etc.) are fed from the lighting power grid (LPG) and will remain working. Spectra are collected in autonomous USB-controlled MSPCA® Mössbauer analyser units. Experiment-controlling PCs are fed from the LPG and become immediately reachable remotely after the blackout. A router installed in the laboratory and fed from the MSPG is pinged every minute by a Linux server fed from the LPG. The server sends an alarm mail to all experimenters if the router is not reachable, indicating a signature of the electrical blackout. Having restored normal operation, a reassuring email is sent to the experimenters.

Details on unplanned electric blackouts affecting Mössbauer laboratories of the Wigner RCP have been available since 2015. All blackouts lasted less than one second. Statistical analysis of these events shows that they were not independent from each other; they rather accumulated in each other’s vicinity. In fact, the time difference between two independent events follows an exponential distribution. Nevertheless, the registered events followed this behaviour only up to about 250 days, while in the range of 250–450 days, a significant increase in the time difference of such events was observed. This indicates that the unplanned electric blackouts probably had common (in different periods, possibly different) technical causes, a conclusion with implications for the management of research organizations operating Mössbauer laboratories, especially open-access ones.

ICAME-ORAL-T08

PolMoss: A User-friendly Software for ^{57}Fe Mössbauer Spectra Simulation and Fitting

Tomasz Pikula^{1*}

¹Lublin University of Technology, Lublin, Poland

*t.pikula@pollub.pl

Fitting complex Mössbauer spectra (MS) can be a challenging and time-consuming task, especially for young scientists who are beginning their journey with Mössbauer spectroscopy. This presentation introduces a simple, user-friendly software designed for the simulation and fitting of ^{57}Fe Mössbauer spectra. While it is primarily aimed at young researchers, experienced users may also find it beneficial.

The main goal of this project is to provide free software with an intuitive graphical user interface (Fig. 1) that accelerates the modelling and analysis of ^{57}Fe MS. This software allows young scientists to observe in real-time how changes to specific parameters affect the shape of the calculated spectrum.

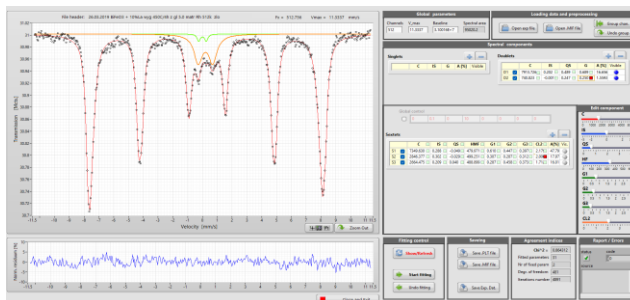


Figure 1. Graphical user interface of the PolMoss software.

The PolMoss software offers the ability to simulate MS based on known hyperfine interaction parameters or fit experimental data using an assumed model. The key features that make the program user-friendly include:

- graphical presentation of experimental and calculated spectra with easy toggling of component visibility,
- mouse-driven zooming in and out of the graph for identifying subtle details in the analyzed spectrum,
- insertion of spectral components (singlets, doublets, sextets) with a single click,
- customization of spectral components by using sliders or by editing a table, with real-time updates to the graph,
- reduction of the number of channels for experimental spectra with poor statistics,
- fitting capabilities for up to 5 singlets, 5 doublets, and 10 sextets corresponding to specific iron sites,
- quick and convenient fixing of hyperfine interaction parameters during the fitting process,
- easy saving and exporting of data to programs like Origin, Excel, etc., by a single click,
- storing and loading sets of hyperfine interaction parameters,
- all functions are accessible via a straightforward user interface.

In PolMoss, the fitting of experimental spectra relies on least squares minimization, which is implemented using the Levenberg–Marquardt algorithm. The software was developed using the LabVIEW graphical programming framework, making it easy to modify, scale, and implement new models for MS fitting. There are plans to enhance the software functionalities soon by adding features for hyperfine interactions parameters distribution fitting and more advanced models, such as spin density waves and spin cycloids.

ICAME-ORAL-T08

A Mobile Mini-beamline for Mössbauer Spectroscopy at the European X-ray Free-Electron Laser

R. Röhlberger^{1,3,5,6*}, J. Evers², L. Bocklage³, C. Bömer³, U. Boesenberg⁴, G. A. Geloni⁴, M. Gerharz², M. Guetg³, J. Hallmann⁴, W. Hippler^{1,5}, R. Horn², D. Krebs³, S. Liu³, R. Loetzsch¹, L. M. Lohse⁶, A. Madsen⁴, B. Marx-Glowna¹, T. Pfeifer², J.-E. Pudell⁴, R. Rysov⁴, S. Sadashivaiah¹, K. Schlage³, I. Sergeev³, A. Siemens³, S. Velten³, C. L. Wessel⁵, L. Yagüe-Bosch², A. Zozulya⁴

¹Helmholtz Institut Jena, Jena, Germany

²Max-Planck-Institut für Kernphysik, Heidelberg, Germany

³Deutsches Elektronen-Synchrotron DESY, Hamburg, Germany

⁴European XFEL, Schenefeld, Germany

⁵Friedrich-Schiller-Universität Jena, Jena, Germany

⁶The Hamburg Centre for Ultrafast Imaging CUI, Universität Hamburg, Germany

*r.roehlsberger@hi-jena.gsi.de

After pioneering nuclear resonance experiments with X-ray laser radiation in Bragg scattering from $^{57}\text{FeBO}_3$ [1] and in fluorescence geometry to detect the ^{45}Sc resonance [2], we report here the first ^{57}Fe Mössbauer spectroscopic studies in coherent forward scattering at an X-ray laser. Discrimination of the resonantly scattered radiation was achieved by two Si(840) linear polarizers in a 90° crossed setting [3]. The enormous peak brilliance of the X-ray laser pulses leads to remarkable scattering effects that are absent under conventional excitation conditions; in addition, a complete time spectrum can be recorded with a single pulse. Our mobile setup enables efficient use of beamtime via pre-aligned instruments from one experiment to the next.

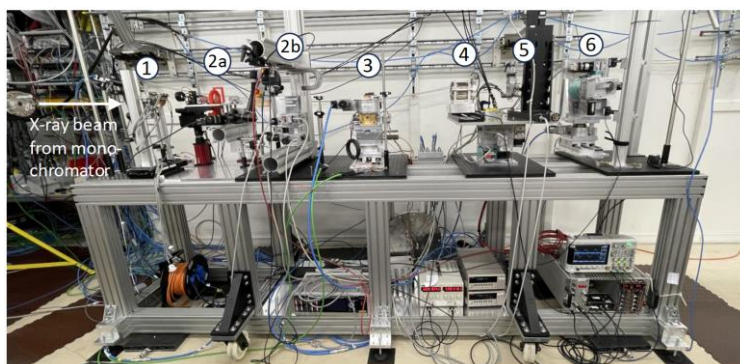


Figure 1. Setup at the MID station of the European XFEL [4]. Instruments are mounted on a mobile heavy-load table: (1) Si(840) polarizer, (2a,b) Sample stages for transmission and reflection, (3) Si(840) analyzer, (4) velocity transducer for Mössbauer spectral analysis, (5) APD detectors, (6) Bond stage for X-ray energy measurement.

[1] A. I. Chumakov et al., *Nature Phys.* **14** (2018) 261.

[2] Y. Shvydko et al., *Nature* **622** (2023) 471.

[3] B. Marx-Glowna et al., *J. Synchrotron Radiat.* **28** (2021) 120.

[4] A. Madsen et al., *J. Synchrotron Radiat.* **28** (2021) 637.

ICAME-ORAL-T08

Ultrafast Control of Coherence in Nuclear Resonant X-rays

Sakshath Sadashivaiah^{1*}, Willi Hippler^{1,2}, Anjali Panchwane³, Sven Velten³, Deepak Prajapat³, Dietrich Krebs³, Christina Bömer³, Berit Marx-Glowna^{1,2}, Robert Löttsch^{1,2}, Kai Schlage³, Lars Bocklage³, Olaf Leupold³, Ilya Sergueev³ and Ralf Röhlsberger^{1,2,3}

¹Helmholtz Institute Jena, Fröbelstieg 3, 07743 Jena, Germany

²GSI Helmholtzzentrum für Schwerionenforschung GmbH, Planckstraße 1, 64291 Darmstadt, Germany

³Deutsches Elektronen-Synchrotron DESY, Notkestrasse 85, 22607 Hamburg, Germany

*s.sadashivaiah@gsi.de

The ultranarrow linewidths of Mössbauer resonances enable the preparation of well-defined nuclear quantum states, whose energies are addressed by accelerator-driven light sources [1, 2]. Qualitatively new opportunities emerge if the dynamics of these states can be tuned using the electromagnetic field of light pulses. These nuclear states are affected by ultrashort visible laser pulses due to the changes induced in hyperfine interactions, for example, across light-induced phase transitions [3].

Here, we explore optical control of the quantum states using nuclear resonant diffraction in materials such as epitaxial ⁵⁷FeRh(100) thin films in the L1₀ phase, which exhibit an isostructural metamagnetic phase transition from the antiferromagnetic (AFM) to ferromagnetic (FM) phase. Upon femtosecond laser excitation, the coherent nuclear forward scattering (NFS) signal from the thin films in the AFM phase is suppressed instantaneously (Figure 1). We find that the Bragg-diffracted coherent nuclear resonant photons are redirected in an ultrafast process from the AFM state to that of the FM state, indicating coherent control. Thus, new avenues in ‘transient’ x-ray scattering can be accessed. As a first application, we demonstrate on-demand occurrence of nuclear resonant X-ray pulses of tunable pulse widths. This provides perspectives for adaptive x-ray optical elements such as transient nuclear resonant gratings, whose properties can even change dynamically.

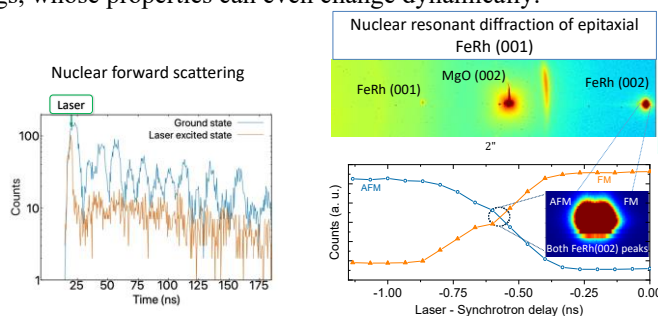


Figure 1. The Time spectrum of NRS from a ⁵⁷FeRh thin film, showing the laser-induced suppression of the coherent emission is shown on the left. The green arrow shows the temporal position of the laser pulse relative to the synchrotron pulse, which occurs at $t = 0$. On the right, the diffraction peaks of the ⁵⁷FeRh(001) film are depicted in the top panel. The bottom panel shows the position of the (002) peak along the AFM or FM as a function of the laser-synchrotron delay, where the emergence of the AFM state is seen.

- [1] R. Röhlsberger et al, *Science* **328** (2010) 1248.
- [2] J. P. Hannon and G. T. Trammel, *Physica B* **159** (1989) 161.
- [3] S. Sadashivaiah et al, *J. Phys. Chem. Lett.* **3** (2021) 573.

ICAME-ORAL-T08

Recent Results and Development at the P01 Beamline, PETRA III, DESY

Ilya Sergeev^{1*}, Sven Velten¹, Deepak Prajapat¹, Olaf Leupold¹,
Hans-Christian Wille¹, Rudolf Ruffer²

¹Deutsches Elektronen-Synchrotron DESY, Hamburg, Germany

²European Synchrotron Radiation Facility, Grenoble, France

*ilya.sergeev@desy.de

Nuclear Resonance Scattering (NRS) is one of the three key techniques currently available at the High Resolution Dynamics Beamline P01 at the PETRA III synchrotron facility. The beamline operates over a broad photon energy range of 2.5 keV to 75 keV, enabling users to explore Mössbauer transitions of several isotopes, including ⁵⁷Fe, ¹¹⁹Sn, ¹²¹Sb, ¹²⁵Te, and ¹⁹³Ir. Recently, a new high-resolution monochromator was developed for the ¹⁶⁹Tm Mössbauer transition at 8.4 keV, making it possible to perform both Nuclear Forward Scattering (NFS) and Nuclear Inelastic Scattering on this isotope [1].

Another major development at the beamline is the Synchrotron Mössbauer Source (SMS), which became available to users in 2024 [2]. Since NRS experiments are primarily conducted in timing mode, it is feasible to combine SMS and NFS techniques on the same sample, even with beam focusing down to a few micrometers. This allows the power of NFS to be efficiently integrated with the simplicity of SMS within a single experiment. Examples of such combined studies will be presented.

[1] S. Velten et al., in preparation.

[2] I. Sergeev et al., accepted for publication in *J. Phys: Conf. Ser.*

ICAME-ORAL-T08

Research Opportunities at SOLARIS Synchrotron

Marcin Sikora^{1*}

¹SOLARIS National Synchrotron Radiation Centre, Jagiellonian University,
Czerwone Maki 98, 30-392 Krakow, Poland

*marcin1.sikora@uj.edu.pl

The SOLARIS synchrotron in Krakow is a third-generation light source operating at 1.5 GeV electron energy. The first synchrotron light from SOLARIS was observed in 2016, while the first user experiments were performed in 2018 using soft X-ray absorption spectroscopy and angle-resolved photoelectron spectroscopy beamlines. Since SOLARIS is expanding its activities, developing new end-stations, and providing complementary infrastructure such as cryo-electron microscopes [1]. The experimental techniques offered by SOLARIS, the only synchrotron in Central-Eastern Europe, can well complement the outcomes of Mossbauer spectroscopy and hyperfine methods in basic and applied interdisciplinary research projects.

It should be emphasized that access to the research infrastructure at SOLARIS is free of charge and provided based on the assessment of the beamtime applications by the international review panel. Financial support to user visits is provided through EU projects NEPHEWS, ReMade@ARI, and RIANA, as well as the CERIC-ERIC consortium.

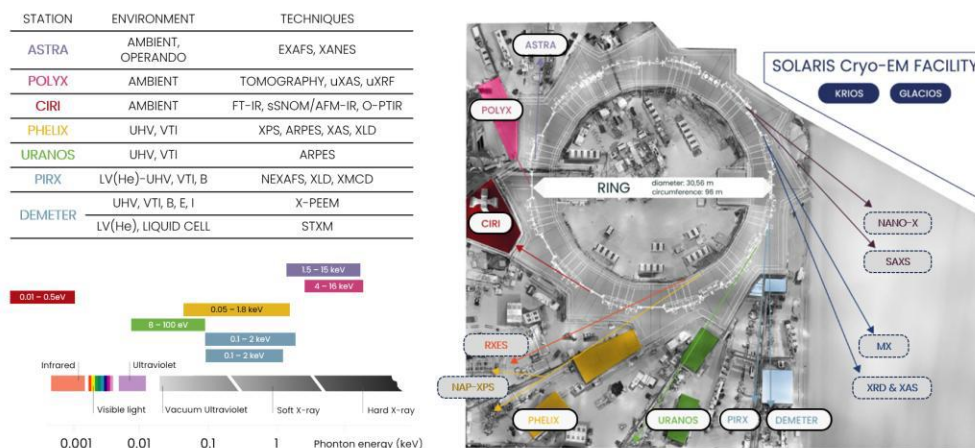


Figure 1. (top left) List of synchrotron beamlines operating at SOLARIS, including typical sample environment and main experimental techniques. (bottom left) Photon energy range covered by each beamline. (right) Aerial view of the experimental hall of SOLARIS Centre with the synchrotron tunnel and infrastructure of the existing beamlines (names on a white background) as well as schematically marked location of the cryo-electron facility and beamlines under construction and design (techniques listed on gray background).

We acknowledge the entire team of the SOLARIS Centre and the supporting research groups. SOLARIS operation is financed by the Polish Ministry and the Higher Education project: “Support for research and development with the use of research infrastructure of the National Synchrotron Radiation Centre SOLARIS” under contract nr 1/SOL/2021/2.

[1] J. Szlachetko et al., *Eur. Phys. J. Plus* **138** (2023) 10.

ICAME-ORAL-T08

Flexible Intensity Control of Resonantly Scattered Gamma-Rays Using Multi-Frequency Vibrating Resonant Absorber

Aleš Stejskal^{1*}, Vlastimil Vrba¹, Tomáš Krátký¹, Vít Procházka¹

¹Faculty of Science of Palacký University Olomouc, Olomouc, Czech Republic

*ales.stejskal@upol.cz

Extending the concepts of classical optics to the gamma-ray regime (1-100 keV) is of interest due to the unique properties of gamma photons, such as very short wavelength, deep material penetration, and high efficiency and low noise single photon detection. However, the performance of gamma optics experiments requires controllable coherent sources of gamma radiation. A recent study [1,2] demonstrated that a sinusoidally vibrating resonant absorber can coherently control recoilless gamma-ray intensity waveforms, producing gamma-ray pulses.

Based on these works, we have investigated further possibilities of coherent intensity control using more complicated motion profiles composed of multiple harmonics [3]. Specifically, triangular, square, trapezoidal, and bipolar pulse motion profiles composed of 12 harmonics were applied. We found out that different motion profiles, together with Doppler tuning of the energy of the incident radiation, allow shaping the gamma-ray intensity into various waveforms, including not only high-intensity single pulses or multi-pulse structures of different amplitudes and widths, but also short-time induced absorption. This approach enables the construction of a highly controllable tabletop gamma pulse source and paves the way to other gamma-optical or x-ray optical elements, such as delays, gates, or memories.

In this contribution, the numerical simulations and experimental results of the coherent control of gamma rays by a multi-frequency vibrating absorber will be presented. In addition, experimental details and problems related to the inhomogeneity of the picometer motion of the absorber will be described, and attempts to find the optimal motion profile to realize a given intensity waveform via an evolutionary optimization algorithm will be mentioned.

[1] F. Vagizov et al. *Nature* **508** (2014).

[2] R.N. Shakhmuratov et al., *Phys. Rev. A* **92** (2015).

[3] A. Stejskal et al., *Appl. Phys. Lett.* **126** (2025).

Abstracts of Oral Contributions



HYPERFINE Invited Lectures

HYPERFINE-INVITED-T05

μ^+ SR Investigations of Microporous Aluminosilicates: Probing Interactions with Pd Nanoparticles in Catalysis

Hiroko Ariga-Miwa

University of Electro-Communications, Tokyo, Japan

*h-miwa@uec.ac.jp

Hydrogen in heterogeneous catalysis exhibits dynamic behavior that is crucial for understanding and optimizing catalytic reactions, which includes the dissociation of hydrogen molecules on catalyst surfaces, the migration of hydrogen atoms (spillover and reverse spillover), and the influence of reaction conditions on catalyst structure and activity. Understanding these dynamic processes is essential for designing efficient and stable catalysts for various applications [1]. Despite its importance, directly probing hydrogen's behavior and charge state under catalytic reaction conditions remains notoriously difficult. However, in our research, we applied the μ^+ SR (Muon Spin Rotation/ Relaxation/ Resonance) method to study hydrogen dynamics in a bifunctional catalytic system comprising Pd nanoparticles supported on the outer surface of microporous aluminosilicates, developed for the direct alkylation of benzenes with alkanes (Figure 1(a)). The approach provided evidence that atomic hydrogen can form on the catalyst and persist for lifetimes in the submicrosecond range, which is long enough to participate in chemical reactions [2].

All pulsed μ^+ SR measurements were conducted in the D1 area of Materials and Life Science Experimental Facility (MLF) in Japan Proton Accelerator Research Complex (J-PARC), using a spin-polarized surface muon beam in the double bunch operation mode.

μ^+ SR time spectra recorded for H-mordenite under a transverse field (TF) of 0.10 mT are shown in Figure 1(b). The frequency of damped cosine signal, 1.44 MHz, is characteristic of the spin-triplet component of paramagnetic atomic Mu under 0.10 mT. The depolarization rate (λ_p) for the spin-triplet Mu signals can be expressed as $\lambda_p = \tau_{\text{Mu}}^{-1} + \lambda_0$, where τ_{Mu} represents the chemical lifetime of the initially formed atomic Mu and λ_0 accounts for depolarization contributions from all other sources. This relation indicates that the inverse of λ_p gives a lower limit of τ_{Mu} . The λ_p values are close to those for other sodium-type aluminosilicates. With this figure, it is revealed that the chemical lifetime of the atomic Mu formed upon implantation of μ^+ is in the submicrosecond range or longer at temperatures up to ~ 400 K.

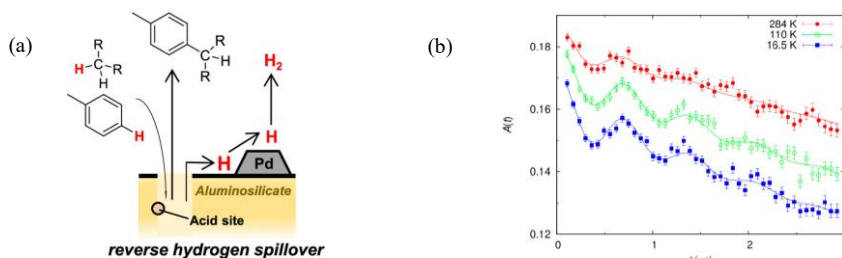


Figure 1. (a) Schematic illustration of the direct alkylation of benzenes with alkanes over Pd nanoparticles supported on the external surface of microporous aluminosilicates [2]. (b) μ^+ SR time spectra recorded for H-mordenite under a transverse field (TF) of 0.10 mT at 16.5, 110, and 284 K [2]. Copyright 2023 American Chemical Society.

- [1] D.R. Aireddy, *et al. ACS Catal.* **12** (2022) 4707., W. Karim, *et al. Nature* **541** (2017) 68.
 [2] S. Misaki, H. Ariga-Miwa, T.U. Ito *et al.*, *ACS Catal.* **13** (2023) 12281.

HYPERFINE-INVITED-T05

Nuclear Quantum Memory for Hard X Ray Photons

S. Velten^{1,2}, L. Bocklage^{1,2*}, X. Zhang³, K. Schlage¹, A. Panchwancee¹, I. Sergeev¹,
O. Leupold¹, A. I. Chumakov⁴, O. Kocharovskaya³, and R. Röhlberger^{1,2,5,6,7}

¹Deutsches Elektronen-Synchrotron DESY, Hamburg, Germany

²The Hamburg Centre for Ultrafast Imaging, Hamburg, Germany

³Department of Physics and Astronomy and Institute for Quantum Science and Engineering,
Texas A&M University, College Station, Texas, USA

⁴ESRF-The European Synchrotron, Grenoble, France

⁵Friedrich-Schiller Universität Jena, Jena, Germany

⁶Helmholtz-Institut Jena, Jena, Germany

⁷Helmholtz Centre for Heavy Ion Research (GSI), Darmstadt, Germany

* lars.bocklage@desy.de

Quantum optics concepts are rarely applied in the hard X-ray regime due to the extremely high electric field strengths required for coherent control of atomic transitions at these energies—conditions that are difficult to achieve experimentally. However, researchers have found alternative approaches using nuclear transitions, with the 14.41 keV Mössbauer transition of the ⁵⁷Fe nucleus being a notable example. These nuclear resonances offer exceptional coherence properties with its natural linewidth of ⁵⁷Fe ($\Gamma_0=5\text{neV}$) is about twelve orders of magnitude smaller than its resonance energy. Combined with the high number densities typically found in solid-state materials and a resonant cross-section that exceeds the purely electronic one by a factor of 400, these transitions have become central to observing quantum optics phenomena in the hard X-ray domain. Such phenomena include the collective Lamb shift [1], electromagnetically induced transparency [2], and the subluminal propagation of X-ray pulses [3]. Building on this foundation, a recent study by X. Zhang et al. proposes an advancement toward quantum information processing: by stacking multiple resonant absorbers moving at different velocities, they create a nuclear frequency comb potentially capable of storing single X-ray photons [4].

In this work, we report the experimental realization of the proposed concept. By exploiting Doppler shifts in stainless steel foils on multiple from Mössbauer drives, we successfully generated a well-defined frequency comb, leading to the periodic emission of X-ray photon pulses (Fig. 1). To demonstrate photon pulse storage, we integrated a thin-film cavity, which broadens the nuclear transition linewidth through the superradiance effect [1]. The frequency comb effectively samples this broadened transition, enabling repetitive emission of cavity photons with an efficiency of approximately 0.4 and a fidelity—defined here as the intensity overlap—of about 0.2. Looking ahead, the use of more advanced motion-control technologies, such as piezoelectric actuators, may allow for on-demand emission of X-ray photon pulses. This approach lays the groundwork for implementing quantum information processing schemes in the hard X-ray regime, not only at large-scale facilities like synchrotrons and free-electron lasers, but also in laboratory settings using radioactive sources, as proposed by X. Zhang et al. [4].

[1] R. Röhlberger et al, *Science* **328**, 1248 (2010).

[2] R. Röhlberger et al, *Nature* **482**, 199 (2012).

[3] K. P. Heeg et al., *Physical Review Letters* **114**, 203601 (2015).

[4] X. Zhang et al., *Physical Review Letters* **123**, 250504 (2019).

HYPERFINE-INVITED-T07

Teaching Hyperfine Interactions to the World: From the Good Old Internet to Artificial Intelligence (www.hyperfinecourse.org)

Stefaan Cottenier^{*1}

¹Ghent University, Belgium

^{*}stefaan.cottenier@ugent.be

How do we teach? Ideally, in the most effective way. Yet what counts as “effective” is quietly set by the technology at our disposal. It matters whether we have only an oral tradition, can produce handwritten manuscripts, or can use a printing press, audio discs, VHS tapes, or the internet. In the past two decades, broadband internet has boosted the role of video in education, alongside synchronous and asynchronous online learning [1]. Now we are witnessing the advent of another game-changer: artificial intelligence (AI). In this contribution, I ponder how AI might affect the delivery of our free and open online course on hyperfine interactions (www.hyperfinecourse.org). I will explore the potential of AI to lower access barriers -- language, disabilities, heterogeneity, ... -- and to enable radically different learning approaches, for instance, disposable learning resources. This will be illustrated by examples of how we are implementing this in the hyperfine course.

[1] I’ve reported at HYPERFINE-2019 how this enabled teaching hyperfine interactions online: https://youtu.be/_cMNuQB3fI

HYPERFINE-INVITED-T02

Nuclear Gamma-Ray Polarimetry Based on Multi-Layer Semiconductor Compton Cameras

Shintaro Go

National Research and Development Agency RIKEN, Japan

go@riken.jp

To detect and track structural changes in atomic nuclei, the systematic study of nuclear levels with firm spin-parity assignments is important. While linear polarization measurements have been applied to determine the electromagnetic character of gamma-ray transitions, the applicable range is strongly limited due to the low efficiency of the detection system. The multi-layer Cadmium-Telluride (CdTe) Compton camera can be a state-of-the-art gamma-ray polarimeter for nuclear spectroscopy with the high position sensitivity and the detection efficiency. We demonstrated the capability to operate this detector as a reliable gamma-ray polarimeter by using polarized 847-keV gamma rays produced by the $^{56}\text{Fe}(p, p'\gamma)$ reaction. By combining the experimental data and simulated calculations, the modulation curve for the gamma ray was successfully obtained. A remarkably high polarization sensitivity was achieved, compatible with a reasonable detection efficiency. Based on the obtained results, a possible future gamma-ray polarimetry is discussed in the presentation.

HYPERFINE-INVITED-T04

Quantum Critical Behavior in Heavy Fermion Superconductor Studied by μ SR

Wataru Higemoto^{1,2,3}

¹Advanced Science Research Center, Japan, Atomic Energy Agency, Tokai, Ibaraki, Japan

²J-PARC Center, Japan, Atomic Energy Agency, Tokai, Ibaraki, Japan

³Department of Physics, Institute of Science Tokyo, Meguro, Tokyo, Japan

higemoto.wataru@jaea.go.jp

Quantum critical phenomena are one of the central issues in condensed matter physics. In the vicinity of the quantum critical point (QCP) where two different interactions compete, quantum fluctuations play a major role in realizing unconventional superconductivity as well as other exotic ground states. This quantum critical phenomenon could be observed when the phase transition occurs at $T = 0$ by tuning parameters other than temperature, such as magnetic field, pressure, and chemical substitutions. For instance, in a heavy fermion system, the magnetic RKKY interaction conflicts with the nonmagnetic Kondo effect. Nontrivial quantum states can be realized in the vicinity of the QCP in many strongly correlated electron systems. In particular, an emergence of unconventional superconductivity around the QCP strongly suggests that the quantum critical fluctuations play a central role in the superconducting pairing mechanism. However, a clear signature of the direct coupling between the superconducting pairing states and the quantum criticality had not yet been elucidated by the microscopic probes.

Herein, we present muon spin rotation/relaxation (μ SR) measurements in the superconducting dome of $\text{CeCo}(\text{In}_{1-x}\text{Zn}_x)_5$. It was found that a magnetically ordered state develops at $x \geq 0.03$, coexisting with the superconductivity. The magnitude of the ordered magnetic moment is continuously reduced with decreasing x , and it disappears below $x \sim 0.03$, indicating a second-order phase transition and the presence of the QCP at this critical Zn concentration. Furthermore, the magnetic penetration depth diverges toward the QCP. These facts provide evidence for the intimate coupling between quantum criticality and Cooper pairing [1].

We also present recent μ SR results of the superconducting $\text{Ce}(\text{Co}_{1-y}\text{Ni}_y)\text{In}_5$, which is also located in the vicinity of the QCP.

[1] W.Higemoto, M.Yokoyama et al., PNAS **119** (49) e2209549119 (2022).

HYPERFINE-INVITED-T08

Positron Annihilation Lifetime Spectroscopy – Assumptions and Applications

Bożena Jasińska

Institute of Physics, Maria Curie Skłodowska University, 20-031 Lublin, Poland

bozena.jasinska@mail.umcs.pl

PET (Positron Emission Tomography) and PALS (Positron Annihilation Lifetime Spectroscopy) are two the most known techniques based on positron-electron annihilation.

PET is a commonly recognized diagnostic method enabling imaging of the metabolism of chosen substances in the living organism. One of the most important applications is imaging of patients tumour location and size, and aiming at the search for the possible, as metabolism rate rises significantly in these places, and in effect the number of annihilating positrons.

On the contrary, PALS allows following of processes leading to positron annihilation, as is known that o-Ps lifetime value reflects size of the free spaces in which it is trapped. In a vacuum o-Ps annihilate emitting three photons, while in the dense media some part of o-Ps can annihilate in pick-off process *via* the two photons. Size of the free volume leads to shortening the o-Ps lifetime value even below 1 ns. It is a reason the PALS is widely applied in material science to investigate free spaces size in a range from 0.1 to about 100 nm [1].

The new idea is to include the new imaging method, similar to this used in material science, to PET.

Preliminary investigation performed on real healthy and altered human tissues using PALS clearly indicates that it is possible to distinguish between healthy and diseased tissues and between different kinds of lesions of the some organ using techniques based on positron annihilation.

- [1] T. Goworek, K. Ciesielski, B. Jasińska, J. Wawryszczuk, *Chem. Phys. Lett.* **272** (1997) 91.
- [2] P. Moskal, B. Jasińska, E. Stępień, S. Bass, *Nature Rev. Phys.* **1**, (2019) 527.
- [3] B. Zgardzińska, G. Chołubek, B. Jasińska et al., *Sci.Rep.* **10(1)** (2020) 11890.

HYPERFINE-INVITED-T03

Exploring New Nuclear Magic Numbers with Continuous Beam Collinear Laser Spectroscopy at COLLAPS

Tim Enrico Lellinger^{1,2} for the COLLAPS collaboration

¹Max-Planck Institute for Nuclear Physics

²CERN

tim.enrico.lellinger@cern.ch

Over a decade ago, the first experimental evidence for the $N = 32$ subshell closure in the calcium isotopic chain emerged [1,2]. Subsequent experimental and theoretical investigations have confirmed this finding. However, in laser spectroscopy measurements extending up to ^{52}Ca ($N = 32$), no indications of this shell gap were apparent [3]. Crossing the shell gap with laser spectroscopy setups has proved difficult due to the simultaneous requirement of a sensitivity of approximately 10 ions/s and a measurement uncertainty on the order of MHz.

This contribution presents the first laser spectroscopy measurements of $^{53,54}\text{Ca}$, facilitated by an extension of the collinear laser spectroscopy technique employed at the COLLAPS setup at ISOLDE/CERN. This technique, termed as *radioactive detection after optical pumping and state selective charge exchange* (ROC), combines the high sensitivity of a particle detection scheme with the high resolution of low-power, continuous wave lasers utilized in a collinear geometry. The methodology of this technique will be explained, followed by the presentation and discussion of preliminary values for the magnetic dipole moment of ^{53}Ca and the charge radii of $^{53,54}\text{Ca}$ in the context of the robustness of the $N = 32$ subshell closure.

In the outlook, an ongoing effort to measure neutron rich fluorine isotopes around the emerging magic numbers $N=14$ and $N=16$ will be presented, for which a similar continuous beam technique, *state selective re-ionization*, is currently developed.

[1] Wienholtz, F. et al. *Nature* **498** (2013) 346-349.

[2] Steppenbeck, D. et al. *Nature* **502** (2013) 207-210.

[3] R.F. Garcia Ruiz et al, *Nat. Phys.* **12** (2016) 594-598.

HYPERFINE-INVITED-T02

β -decay Spectroscopy of ^{187}Ta and Recent Results at KISS

M. Mukai^{1*}, Y. Hirayama¹, Y. X. Watanabe¹, P. Schury¹, T. Hashimoto²,
N. Hinohara³, S. Ishizawa⁴, F. G. Kondev⁵, H. Koura⁶, G. J. Lane⁷, Yu. A. Litvinov⁸,
H. Miyatake¹, J. Y. Moon², T. Niwase⁹, Zs. Podolyák¹⁰, M. Reponen¹¹,
M. Rosenbusch¹², H. Ueno¹², M. Wada¹³, P. M. Walker¹⁰, H. Watanabe¹⁴

¹High Energy Accelerator Research Organization, Wako, Japan

²Institute for Basic Science, Daejeon, Korea

³University of Tsukuba, Tsukuba, Japan

⁴Tohoku University, Sendai, Japan

⁵Argonne National Laboratory, Argonne, USA

⁶Japan Atomic Energy Agency, Tokai, Japan

⁷Australian National University, Canberra, Australia

⁸GSI Helmholtzzentrum für Schwerionenforschung, Darmstadt, Germany

⁹Kyushu University, Fukuoka, Japan

¹⁰University of Surrey, United Kingdom

¹¹University of Jyväskylä, Jyväskylä, Finland

¹²RIKEN Nishina Center for Accelerator-Based Science, Wako, Japan

¹³Institute of Modern Physics, Lanzhou, China

¹⁴Beihang University, Beijing, China

*mmukai@post.kek.jp

To elucidate the astrophysical environments of the rapid neutron capture process – the origin of heavy elements – it is essential to resolve uncertainties in nuclear properties near $N = 126$ [1]. At the Wako Nuclear Science Center (KEK, IPNS), we have constructed the KEK Isotope Separation System (KISS), a facility that combines multinucleon transfer reactions with a gas-cell-based ISOL (Isotope Separation On-Line) technique to perform nuclear spectroscopy of neutron-rich nuclei around Pt [2]. In this facility, we have carried out β - γ decay spectroscopy, precision mass measurements using a multi-reflection time-of-flight mass spectrograph, and in-gas-cell laser ionization spectroscopy.

In this presentation, we discuss the β - γ decay spectroscopy of ^{187}Ta and recent measurements of neighboring nuclei. In the experiment of ^{187}Ta , we successfully observed the ground state β -decay [3], the internal transition of the first isomer [4], and the β -decay and internal transition of the second isomer [5]. We significantly updated the previously reported ground state half-life, and it was revealed that among the competing Gamow–Teller and forbidden transitions in this mass region, the first-forbidden transition is the dominant decay mode. In addition to these results, we will report on recent mass measurements [6] and in-gas-cell laser ionization spectroscopy at KISS in relation to nuclear shape transitions [7].

[1] M. R. Mumpower *et al.*, *Prog. Part. Nucl. Phys.* **86** (2016) 86.

[2] Y. Hirayama *et al.*, *Nucl. Inst. Meth. B* **353** (2015) 4, and B **412** (2017) 11.

[3] M. Mukai *et al.*, *Phys. Rev. C* **105** (2022) 032331.

[4] P. M. Waler *et al.*, *Phys. Rev. Lett.* **125** (2020) 192505.

[5] J. L. Chen *et al.*, *Phys. Rev. C* **111** (2025) 014304.

[6] M. Mukai *et al.*, *Phys. Rev. C* **111** (2025) 014322.

[7] G. G. Kiss and Zs. Podolyák, *Eur. Phys. J. A* **60** (2024) 175.

HYPERFINE-INVITED-T02

Exploring Nuclear Structure in Even-Even Er-W Isotopes in the Framework of IBM-1 with Intrinsic Triaxial Deformation

Polytimos Vasileiou^{1*}, Dennis Bonatsos², Theo J. Mertzimekis¹

¹Department of Physics, National and Kapodistrian University of Athens, Zografou Campus, Greece

²Institute of Nuclear and Particle Physics, National Centre for Scientific Research “Demokritos”, Aghia Paraskevi, Greece

*polvasil@phys.uoa.gr

The structure of low-lying quadrupole bands in even-even members of the Er-W isotopic chains is investigated by means of a microscopically derived IBM-1 Hamiltonian, with intrinsic triaxial deformation derived from fermionic proxy-SU(3) irreducible representations (irreps). Energy levels and B(E2) electric quadrupole transition strengths are calculated and compared with available experimental data. It is shown that the inclusion of a triaxial deformation, derived from the proxy-SU(3) irreps, leads to a significantly improved agreement between theoretical predictions and experimental data, compared to axially symmetric calculations. The results further point toward the preponderance of triaxiality over extended regions across the nuclear chart.

HYPERFINE-INVITED-T04

Measuring Spin Dynamics and Quantum Entanglement in Frustrated Spin Systems using μ SR

Francis Pratt

ISIS Neutron and Muon Source, STFC-Rutherford Appleton Laboratory, Didcot, U.K.

francis.pratt@stfc.ac.uk

The spin dynamics of frustrated magnetic systems, such as a 2D layered quantum spin liquid (QSL), can be probed via the longitudinal field dependence of the muon spin relaxation rate. This provides a measure of the frequency-dependent spectral density of spin fluctuations in the system. In these liquid-like magnetic states that lack magnetic order, the spectral density is found to have a diffusive character. Knowledge of the spectral density function allows us to derive a property known as the Quantum Fisher Information (QFI), which provides a witness of the degree of quantum entanglement, which increases significantly as the temperature becomes lower than the nearest-neighbour exchange coupling. Examples of this approach will be given for the cases of a triangular-lattice QSLs [1,2] and a kagome-lattice QSL [3].

[1] F. L. Pratt, F. Lang, W. Steinhardt, S. Haravifard, and S. J. Blundell, *Phys. Rev. B* **106** (2022) L060401

[2] H. C. H. Wu, F. L. Pratt, B. M. Huddart, D. Chatterjee, P. A. Goddard, J. Singleton, D. Prabhakaran and S. J. Blundell, arXiv:2502.00130v1.

[3] F. L. Pratt, D. López-Alcalá, V. Garcia-Lopez, M. Clemente-León, J. J. Baldoví and E. Coronado, *Phys. Rev. Res.* **7** (2025) 023007.

HYPERFINE-INVITED-T03

Local Probing of Structural Phase Transitions in Ferroelectric Layered Perovskite Systems Using PAC Spectroscopy

Pedro Rocha-Rodrigues^{1*}, I. P. Miranda², S. S. M. Santos³, G. N. P. Oliveira¹, M. L. Marcondes, J. G. Correia⁵, L. V. C. Assali⁴, H. M. Petrilli⁴, A. M. L. Lopes¹, J. P. Araújo¹

¹Institute of Physics for Advanced Materials, Nanotechnology and Photonics, Faculdade de Ciências da Universidade do Porto, Porto, Portugal

²Department of Physics and Astronomy, Uppsala University, Uppsala, Sweden

³Escola Politécnica, Universidade de São Paulo, São Paulo, Brazil

⁴Instituto de Física, Universidade de São Paulo, São Paulo, SP, Brazil

⁵C²TN, Centro de Ciências e Tecnologias Nucleares, Departamento de Engenharia e Ciências Nucleares, Instituto Superior Técnico, Universidade de Lisboa, Bobadela, Portugal

*pedro.da.r.rodrigues@gmail.com

Perturbed Angular Correlation (PAC) spectroscopy combined with ab initio electronic structure calculations provides a powerful, atomically precise tool for investigating structural, magnetic, and orbital phase transitions in complex materials. In this study, we apply γ - γ PAC spectroscopy to probe the structural phase transitions in the Ruddlesden-Popper (RP) ferroelectric compound $\text{Ca}_3\text{Ti}_2\text{O}_7$, a naturally layered perovskite.

In 2011, Benedek and Fennie identified the $\text{Ca}_3\text{Ti}_2\text{O}_7$ and $\text{Ca}_3\text{Mn}_2\text{O}_7$ systems as prototypical hybrid improper ferroelectric systems. [1] However, the detailed sequence of structural transitions these materials undergo to achieve polar symmetry remains a topic of debate. Our research aims to clarify this transition pathway by monitoring the evolution of the electric field gradient (EFG) at calcium lattice sites, using γ - γ PAC spectroscopy measurements following ^{111}mCd ion implantation at ISOLDE-CERN. [2-4]

Our results for the $\text{Ca}_3\text{Ti}_2\text{O}_7$ system reveal a transition from the polar $A2_{1am}$ phase to an orthorhombic $Acaa$ symmetry above 1057 K—challenging the widely accepted model of an avalanche transition to the tetragonal $I4/mmm$ aristotype phase. Additionally, the temperature-dependent EFG within the $A2_{1am}$ phase reveals a gradual decline in ferroelectric polarization between 500–800 K, preceding the paraelectric transition near 1057 K. These findings underscore PAC spectroscopy's unique sensitivity to local structural changes and provide compelling evidence for a more nuanced phase transition sequence in $\text{Ca}_3\text{Ti}_2\text{O}_7$ than previously recognized. [4]

Acknowledgments to FCT and IFIMUP, from projects UIDB/04968/2020 (<https://doi.org/10.54499/UIDB/04968/2020>) and UIDP/04968/2020 (<https://doi.org/10.54499/UIDP/04968/2020>).

- [1] N. A. Benedek and C. J. Fennie, *Phys. Rev. Lett.* **106** (2011) 107204.
- [2] P. Rocha-Rodrigues, et al., *Phys. Rev. B* **102** (2020) 104115.
- [3] P. Rocha-Rodrigues, et al., *Phys. Rev. B* **101** (2020) 064103.
- [4] P. Rocha-Rodrigues, et al., *Phys. Rev. B* **109** (2024) 224101.

HYPERFINE-INVITED-T03

Enhancement of Electrical Conductivity by Controlling the Chemical States of Impurity In in ZnO

W. Sato^{1,2*}, M. Takata², H. Shimizu³, S. Komatsuda⁴, Y. Yoshida⁵, A. Moriyama⁵, K. Shimamura⁶, and Y. Ohkubo⁷

¹Institute of Science and Engineering, Kanazawa University, Kanazawa, Japan

²Graduate School of Natural Science and Technology, Kanazawa University, Kanazawa, Japan

³Nishina Center, RIKEN, Wako, Japan

⁴Institute of Human and Social Science, Kanazawa University, Kanazawa, Japan

⁵Department of Physics, Kanazawa University, Kanazawa, Japan

⁶Engineering and Technology Department, Kanazawa University, Kanazawa, Japan

⁷Institute for Integrated Radiation and Nuclear Science, Kyoto University, Osaka, Japan

*wsato@se.kanazawa-u.ac.jp

Zinc oxide (ZnO) is one of the most promising compounds for next-generation electronic and spintronic materials. In addition to its intrinsic semiconducting property as a wide band-gap oxide, it is known that impurity doping with trivalent donor ions such as Al³⁺, Ga³⁺ and In³⁺ enhances its electrical conductivity. Achievement of high conductivity depends on the chemical states of the donor ions, and thus it is important to locate the impurities in defect-free Zn sites. In the present work, we have succeeded in establishing a simple method to introduce In³⁺ ions in the substitutional Zn site by controlling the association-dissociation processes of thermally activated In³⁺ ions in polycrystalline ZnO. The thermal behavior and eventual residential sites of In³⁺ ions were monitored on an atomic scale by means of time-differential perturbed angular correlation spectroscopy with the ¹¹¹In(\rightarrow ¹¹¹Cd) probe. Fig. 1 shows the room-temperature spectra obtained for 0.5 at.% In-introduced polycrystalline ZnO heat-treated (a) at 1373 K for 2 h in air and (b) at 1273 K for 14 h in vacuum, respectively. The present doping method of combined heat treatments in air and in vacuum enabled introduction of a great fraction of 0.5 at.% In donors into defect-free substitutional Zn sites. It was demonstrated that the In-containing ZnO samples show a clear positive correlation between the electrical conductivity and the concentration of In dopants, achieving the conductivity as high as five orders of magnitude compared with undoped ZnO [1, 2].

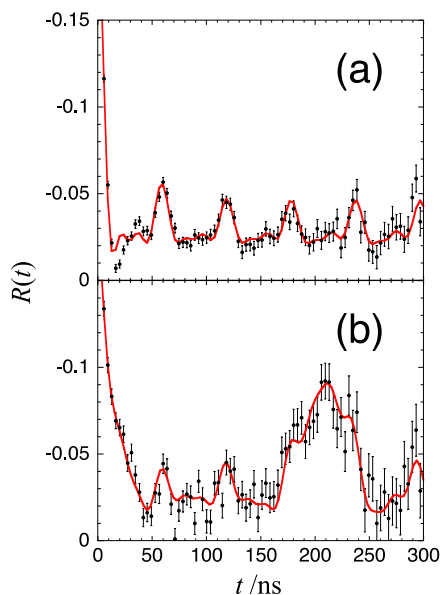


Figure 1. Room-temperature TDPAC spectra of the ¹¹¹In(\rightarrow ¹¹¹Cd) probe in 0.5 at.% In-introduced polycrystalline ZnO.

[1] W. Sato *et al*, *Phys. Rev. B* **90** (2014) 235204.

[2] W. Sato *et al*, *Phys. Rev. Mater.* **6** (2022) 063801.

Laser Mössbauer spectroscopy on Thorium-229

Schumm Thorsten^{1*}, Beeks Kjeld^{1,2}, Schaden Fabian¹, Morawetz Ira¹, Toscani de Col Luca¹, Pimon Martin¹, Leitner Adrian¹, Bartokos Michael¹, Schneider Felix¹, Pressler Martin¹, Kazakov Georgy¹, Sikorsky Tomas¹, Gerstenecker Benedikt¹

¹Atominstitut, TU Wien, Vienna, Austria

²École Polytechnique Fédérale de Lausanne (EPFL), Lausanne, Switzerland

*thorsten.schumm@tuwien.ac.at

Among all known isotopes, Thorium-229 has the lowest nuclear excited state, only 8.4 eV above the ground state. This so-called “isomer” is accessible to VUV laser excitation, and a plethora of applications at the interface of atomic and nuclear physics have been proposed, including a nuclear clock, a gamma laser, and a sensitive detector for variations of fundamental constants [1, 2].

After decades of attempts to determine the exact isomer energy and other nuclear properties, we report on three experiments which resonantly excite the isomer with lasers and spectroscopically resolve the nuclear quadrupole splitting in a CaF₂ single crystal [3, 4].

These measurements allow us to extract relevant nuclear properties, such as the change in electric quadrupole moment between ground and isomeric state, which is directly related to the transition’s sensitivity to variations of the fine structure constant [5].

We also extract information about the local chemical environment of the Thorium-229 nucleus in the solid-state matrix, identify several microscopic doping sites, and study the emerging nuclear quadrupole structure (line centres and linewidths) as a function of temperature and concentration. We find a remarkable reproducibility of nuclear transition frequencies on the 1e-12 level.

Finally, we present a new effect called “nuclear quenching”, which allows us to modify the lifetime of the Thorium-229 isomeric state by exposure to laser light or X-ray. This can be used to accelerate the readout cycle in a future solid-state nuclear clock.

[1] E. Peik, T. Schumm, M. S. Safronova, A. Palffy, J. Weitenberg and P. G. Thirolf, *Quantum Sci. Technol.* **6**, (2021) 034002.

[2] K. Beeks, T. Sikorsky, T. Schumm, J. Thielking, M. V. Okhapkin, E. Peik, *Nat. Rev. Phys.* **2** (2021) 238-248.

[3] J. Tiedau, M. V. Okhapkin, K. Zhang, J. Thielking, G. Zitzer, E. Peik, F. Schaden, T. Pronebner, I. Morawetz, L. Toscani De Col, F. Schneider, A. Leitner, M. Pressler, G. A. Kazakov, K. Beeks, T. Sikorsky, and T. Schumm, *Phys. Rev. Lett.* **132** (2024) 182501.

[4] C. Zhang, T. Ooi, J.S. Higgins, J.F. Doyle, L. v.d. Wense, K. Beeks, A. Leitner, G. Kazakov, P. Li, P.G. Thirolf, T. Schumm, J. Ye, *Nature* **633** (2024) 63-77.

[5] K. Beeks, G.A. Kazakov, F. Schaden, I. Morawetz, L.T.D. Col, T. Riebner, M. Bartokos, T. Sikorsky, T. Schumm, C. Zhang, T. Ooi, J.S. Higgins, J.F. Doyle, J. Ye, M.S. Safronova,

HYPERFINE-INVITED-T02

Towards High-Precision g -Factor Measurements on Stable and Radioactive Beams with the TDRIV Method

Konstantin Stoychev^{1*}, Georgi Georgiev², Andrew E. Stuchbery³,
Johan Ljungvall⁴, the IS628 and E845 collaborations

¹University of Guelph, Guelph, Canada

²IJCLab, Orsay, France

³Australian National University, Canberra, Australia

⁴IPHC, Strasbourg, France

*kstoyche@uoguelph.ca

The magnetic dipole moment of a nuclear state provides unique insight on the single-particle structure of the nucleus. Its experimental observable, the g factor, can yield valuable information, e.g., on the effective single-particle energies of proton and neutron orbitals, and shell evolution away from the valley of stability. One of the available methods for measuring g factors of excited nuclear states with picosecond lifetimes is the Time-Differential Recoil In Vacuum (TDRIV) method. This method is based on observing the Larmor frequency, proportional to the g factor, at which the nuclear and atomic spins precess around the total spin of the projectile as it recoils between the target and a secondary foil within a plunger device. The strong hyperfine fields experienced by the recoiling nucleus can be calculated from first principles, thus eliminating a significant source of systematic uncertainties, which improves the level of precision obtainable by g -factor measurements with the TDRIV method over alternatives methods.

Stuchbery, Mantica, and Wilson [1] proposed a modification of the TDRIV method designed to overcome one of its limitations, namely, applying it on radioactive ion beams. After a successful proof-of-principle experiment using a stable ^{24}Mg beam [2], the first application of the modified TDRIV method on a radioactive ^{28}Mg beam was performed at the HIE-ISOLDE facility to study the vicinity of the $N = 20$ Island of Inversion around ^{32}Mg . An additional TDRIV measurement was also performed using a stable ^{22}Ne beam in order to constrain some experimental parameters, making use of the precise literature value for the g factor of the first 2^+ state in this nucleus [3]. However, the results obtained from the ^{22}Ne measurement put into question the accuracy and precision of the adopted g -factor value, and in turn hindered the achievable precision for the g factor of the first 2^+ state in ^{28}Mg . This led to an initiative to develop better tools in order to reach new levels of precision for g -factor measurements in both stable and radioactive ion beam measurements. These improvements were incorporated in a dedicated TDRIV experiment on ^{22}Ne recently performed at GANIL that aimed at resolving the observed discrepancy.

Details on the above-mentioned experiments will be reported, and the implications of the obtained results on the transition towards the $N=20$ Island of Inversion in Mg isotopes will be highlighted. The directions for further advances with the TDRIV method, as well as plans for upcoming TDRIV measurements on radioactive ion beams will be discussed.

[1] A. E. Stuchbery, P. F. Mantica and A. N. Wilson, Phys. Rev. C **71** (2005) 047302.

[2] A. Kusoglu, A.E. Stuchbery, G. Georgiev *et al.*, Phys. Rev. Lett. **114** (2015) 062501.

[3] R. E. Horstman *et al.*, Nucl. Phys. A **275** (1977) 237.

HYPERFINE-INVITED-T03

Recent Studies of Exotic Nuclei Using High-Resolution Laser Spectroscopy

Xiaofei Yang

School of Physics and State Key Laboratory of Nuclear Physics and Technology,
Peking University, Beijing 100871, China

xiaofei.yang@pku.edu.cn

Exploring the properties and structure of exotic nuclei far from beta stability remains a central focus in modern nuclear physics [1]. High-resolution laser spectroscopy has emerged as a powerful tool for probing key nuclear observables, such as spin, electromagnetic moments, and charge radii [2]. These observables provide direct insights into the structure of unstable isotopes and serve as stringent benchmarks for modern nuclear many-body theories and effective interactions [3,4].

This presentation will highlight recent high-resolution laser spectroscopy studies of exotic nuclei across various mass regions. It will also present recent developments in high-resolution and high-sensitivity laser spectroscopy at the BRIF facility in China, along with preliminary results from measurements on unstable nuclei.

[1] Y.L. Ye, X.F. Yang, H. Sakurai, B.S. Hu, *Nat. Rev. Phys.* **7** (2024) 21 –37.

[2] X.F. Yang, S.J. Wang, S.G. Wilkins, R.F. Garcia Ruiz, *Prog. Part. Nucl. Phys.* **129** (2023) 104005.

[3] A. Koszorus et al., *Nat. Phys.* **17** (2021) 439.

[4] S.W. Bai et al., *Phys. Rev. Lett.* In press (2025).

HYPERFINE-INVITED-T06

New Frontiers of Mössbauer Spectroscopy – Phase Transitions of FePd Thin Alloy Films

Zarzycki Arkadiusz*, Marcin Perzanowski, Michał Krupiński, Marta Marszałek

Institute of Nuclear Physics Polish Academy of Sciences, Kraków, Polska

*arkadiusz.zarzycki@ifj.edu.pl

The FePd alloy is well known for its diverse magnetic properties, which depend on its stoichiometry and crystallographic structure. Among these, the most intriguing is the L1₀ phase, characterized by hard ferromagnetism and strong magnetocrystalline anisotropy. However, the range of crystallographic and magnetic phases in this alloy is so extensive that tracking the transformation leading to the L1₀ phase using standard structural techniques is challenging. A suitable solution is Mössbauer spectroscopy, which serves as an excellent tool for providing precise insights into structural and magnetic transformations due to its selectivity and unique ability to reveal the local atomic environment. This enables a broader understanding of the transformation pathways in binary alloys that result in the formation of the L1₀ structure.

In this lecture, we demonstrate how advanced analysis of Mössbauer spectra can be used to uncover the chemical ordering and phase formation processes that lead to the development of the FePd alloy with the L1₀ structure. The experiments began with thin Fe/Pd multilayers deposited on both flat and nanopatterned substrates. Through thermal treatment, we induced atomic intermixing, which gradually promoted chemical ordering and phase transformation. We investigated this process at various stages of annealing using Mössbauer spectroscopy, complemented by X-ray diffraction and scanning electron microscopy. These techniques allowed us to correlate morphological and structural changes with the evolving magnetic properties.

The analysis of the local structure revealed that the transformation to the L1₀ phase proceeds through a multiphase process. We identified two distinct transformation pathways, involving both stoichiometric and off-stoichiometric intermediate phases. A critical point in the transformation occurs when the sample loses continuity due to solid-state dewetting, observed as a rapid increase in the L1₀ phase growth ratio [1,2]. This dewetting process can be further influenced by the introduction of local curvature, as atomic intermixing behaves differently in patterned systems. Therefore, we focused on FePd systems deposited on patterned substrates and demonstrated that this approach can be used to control interatomic diffusion, phase transformation, and magnetic properties in thin alloy films. Specifically, we identified two opposing processes that affect the formation of the FePd L1₀ phase: enhanced interatomic diffusion induced by patterning, and a patterning-imposed limitation on the diffusion radius [3].

[1] A. Zarzycki *et al.*, *J. Phys. Chem. C* **128** (2024) 3907–3915.

[2] A. Zarzycki *et al.*, *Materials* **16** (2023) 92.

[3] A. Zarzycki *et al.*, *Nanoscale*, doi: 10.1039/D5NR00545K.

Notes

Abstracts of Oral Contributions



HYPERFINE Oral Contributions

HYPERFINE-ORAL-T01

Local Order-Disorder Phase Transition in Complex Perovskite Relaxor Lead Iron Tungstate $\text{Pb}(\text{Fe}_{2/3}\text{W}_{1/3})\text{O}_3$

Thien Thanh Dang^{1*}, Juliana Heiniger -Schell^{1,2}, Eva Kröll¹, Ian Chang Jie Yap¹, Björn Dörschell¹, Si Qi Jin³, Adeleh Mokhles Gerami⁴, Koen van Stiphout⁵, Doru Constantin Lupascu¹

¹Institute for Materials Science and Center for Nanointegration Duisburg-Essen (CENIDE), University of Duisburg-Essen, 45141 Essen, Germany

²European Organization for Nuclear Research (CERN), CH-1211 Geneva, Switzerland

³Institut für Anorganische Chemie, Georg-August-Universität Göttingen, Tammannstraße 4, 37077, Göttingen, Germany

⁴School of Particles and Accelerators, Institute for Research in Fundamental Sciences (IPM), P.O. Box 19395-5531, Tehran, Iran

⁵Georg-August-Universität Göttingen, Friedrich-Hund-Platz 1, 37077 Göttingen, Germany

*thien.dang@uni-due.de

This work presents a study of order-disorder phase transition at the atomic scale in complex perovskite relaxor Lead Iron Tungstate $\text{Pb}(\text{Fe}_{2/3}\text{W}_{1/3})\text{O}_3$ (or PFW) using Time Differential Perturbed Angular Correlation (TDPAC) spectroscopy. $^{111\text{m}}\text{Cd}$ (^{111}Cd) probe was used as a tracer ion for the investigation of local disorders at atomic sites. The resulting TDPAC spectra reveal that the local relaxor ferroelectric order exists in the whole tested temperature range (9-1073 K), and local electromagnetic coupling occurs in the relaxor antiferromagnetic state. X-ray diffraction (XRD) was employed to investigate how high-temperature TDPAC measurements influence the macroscopic structure and secondary phases. The experimental results agree well with calculations based on the TDPAC theory.

HYPERFINE-ORAL-T01

Enhancement of Spin Polarized RI and Muon Beam Imaging via Machine Learning Techniques

Yutaka Mizoi^{1*}, Mototsugu Mihara², Soshi Ishitani², Kenji M. Kojima³,
Ryo Fukushima², Miki Fukutome², Ryunosuke Imai², Syungo Ide²,
Masayoshi Kamon², Gen Takayama², Akira Sato², Suguru Shimizu², Ryo Taguchi²,
Keigo Yasuda²

¹Osaka Electro-Communication University, Neyagawa, Japan

²Osaka University, Toyonaka, Japan

³TRIUMF, Vancouver, Canada

*mizoi@osakac.ac.jp

At the HYPERFINE2023 conference, we reported a series of experiments demonstrating the feasibility of high-resolution imaging using spin-polarized radioactive isotopes (RI) and muon beams [1,2,3]. By injecting these polarized particles into a target material and employing position-sensitive detectors combined with fiber scintillators, we successfully traced anisotropic distributions of decay products—electrons and positrons—revealing underlying magnetic structures within the material. These initial results highlighted the potential of polarized beam imaging as a powerful, non-invasive diagnostic tool for probing spin-dependent interactions in complex systems.

Building upon this foundation, the present study aims to enhance the resolution and interpretability of polarized RI and muon imaging by integrating advanced machine learning techniques. While polarized beams offer directional sensitivity that can reveal fine details of magnetic and structural properties, the acquired data are often noisy and affected by nonlinear spin interactions. Traditional analysis methods struggle with these challenges, especially under low-statistics conditions.

To address this, we apply deep learning models such as convolutional neural networks (CNNs) [4] for denoising and spatial feature learning, physics-informed neural networks (PINNs) [5] for enforcing physical constraints, and generative models like GANs [6] and VAEs [7] for solving inverse problems. These techniques enable the reconstruction of clean, physically meaningful images and the extraction of key features that were previously difficult to isolate. Preprocessing steps—including temporal and spatial calibration, spin signal enhancement, and data imputation—further support this pipeline, ensuring high fidelity in both simulation and experimental datasets.

In summary, this work proposes a novel framework that combines spin-polarized beam imaging with machine learning to overcome conventional limitations. The approach opens up new possibilities for non-destructive material analysis and advanced imaging under challenging conditions, marking a step forward in the fusion of nuclear physics, materials science, and artificial intelligence.

- [1] Y. Mizoi et al., *Interact.* **245** (2024) 20.
- [2] T. Sugisaki et al., *Interact.* **245** (2024) 32.
- [3] G. Takayama et al., *Interact.* **245** (2024) 57.
- [4] Y. LeCun et al., *Journal Proc. of the IEEE* **86(11)** (1998) 2278.
- [5] M. Raissi et al., *J. Comput. Phys.* **378** (2019) 686.
- [6] I.J. Goodfellow et al., *Adv. Neural Inf. Process. Syst.* (2014) 2672.
- [7] D.P. Kingma et al., *arXiv preprint arXiv:1312.6114* (2013).

HYPERFINE-ORAL-T01

The Solid State Physics Programme at ISOLDE-CERN

Juliana Schell^{1,2*}, Hans Hofsaess³, Peter Schaaf⁴, Lukas Eng⁵, Sergiy Divinski⁶,
Anna Krawczuk⁷, Doru Lupascu²

¹Organization for Nuclear Research (CERN), CH-1211 Geneva, Switzerland

²Institute for Materials Science and Center for Nanointegration Duisburg-Essen (CENIDE),
University of Duisburg-Essen, 45141 Essen, Germany

³II. Physikalisches Institut, Georg-August-Universität Göttingen, Friedrich-Hund-Platz 1,
37077 Göttingen, Germany

⁴Chair Materials for Electrical Engineering and Electronics, Institute of Materials Science
and Engineering, Institute of Micro and Nanotechnologies MacroNano, TU Ilmenau,
Gustav-Kirchhoff-Strasse 5, 98693 Ilmenau, Germany

⁵Institut für Angewandte Physik, Technische Universität Dresden, 01062 Dresden, Germany

⁶Institute of Materials Physics, University of Münster, Wilhelm-Klemm-Str. 10,
48149 Münster, Germany

⁷Georg-August-Universität Göttingen, Institut für Anorganische Chemie, Tammannstraße 4,
D-37077 Göttingen, Germany

* juliana.schell@cern.ch

An important scientific challenge to obtain renewable energy-harvesting solutions for a sustainable future requires the investigation of materials functionalities down to the atomic scale. ISOLDE-CERN is the worldwide reference facility for the production and delivery of radioactive ion beams of high purity. Since the late 70s, the laboratory has been a pioneer in using nuclear techniques to study local properties of materials using high-technology equipment [1]. For instance, the brand-new ultra-high-vacuum implantation chamber called ASPIC's Ion Implantation chamber (ASCII) [2] decelerates the radioactive ion beam delivered at ISOLDE-CERN allowing to perform ultra-low energy ion implantations, and local measurements on the surface and interface of materials. The new MULTIPAC setup for Perturbed Angular Correlation Experiments in Multiferroic (and Magnetic) Materials [3] consists of a unique cryogenic magnetic system that simultaneously allows measuring local magnetic and ferroelectric properties of materials in magnetic fields up to 8.5 T. Last but not least, the eMIL-Setup [4] is an advanced emission Mössbauer spectrometer for measurements in versatile conditions of several classes of materials, thanks to the emission Magnetic Mössbauer Analyzer (eMMA) extension [5]. This presentation introduces the new setups as powerful tools and discusses the possibilities of investigations on the frontiers of solid-state physics research.

[1] K. Johnston et al., *J. Phys. G: Nucl. Part. Phys.* **44** (2017) 104001.

[2] K. van Stiphout et al., *Crystals* **12**(5) 2022 626.

[3] J. Schell et al., *Letter of Intent to the ISOLDE and Neutron Time-of-Flight Committee* (2023) CERN-INTC-2023-012 / INTC-I-249.

[4] D. Zyabkin et al., *Nucl. Instrum. Methods Phys. Res. A: Accelerators, Spectrometers, Detectors and Associated Equipment* **968** (2020) 163973.

[5] P. Schaaf et al., *Letter of Intent to the ISOLDE and Neutron Time-of-Flight Committee* (2020) CERN-INTC-2020-008 / INTC-I-211.

HYPERFINE-ORAL-T02

Nuclear Moments of Isomeric States around ^{132}Sn

Georgi Georgiev^{1,2*}, Franziskus Spee¹, Shintaro Go², Konstantin Stoychev³,
Megumi Niikura² for the NP1912-RIBF143R2 and the NP2212-RIBF225
collaborations

¹IJCLab, CNRS/IN2P3, Orsay, France

²RIKEN Nishina Center, Wako, Saitama, Japan

³University of Guelph, Guelph, Canada

*georgi.georgiev@ijclab.in2p3.fr

The nuclear electromagnetic moments provide essential information about the structure of the state of interest. They are very stringent tests to the nuclear theory. The magnetic dipole moments are especially sensitive towards the single-particle properties of the nuclear wave functions, while the electric quadrupole moments give insight into nuclear deformation and collectivity.

Experimental nuclear moments studies of microsecond isomeric states constitute a special challenge for the neutron-rich nuclei far from stability. Often, those isomeric states are populated in projectile fragmentation reactions, and specific techniques are applied in order to obtain spin-oriented ensembles of nuclei. The peculiarities of those techniques will be touched upon.

From a nuclear structure perspective, the region around ^{132}Sn represents a special interest and is often considered in conjunction with the ^{208}Pb region. The nuclear wave functions are expected to demonstrate clear single-particle properties; thus, the nuclear magnetic moments are expected to be well in agreement with the extreme single-particle shell model. Indeed, this has been observed experimentally for the case of ^{131}In [1], a single proton hole in ^{132}Sn , for which the experimental ground-state magnetic moment has been reproduced by the theory using free-nucleon g factors.

A campaign of two experiments, aiming at magnetic moment studies in ^{132}Sn and ^{130}Sn , was performed at the RIKEN Nishina Center in December 2024. The 10^+ isomeric state in ^{130}Sn ($E_x = 2435$ keV, $t_{1/2} = 1.6$ μs) has been populated in a two-step projectile fragmentation reaction following the two-neutron removal from the ^{132}Sn secondary beam. The Time Dependent Perturbed Angular Distribution (TDPAD) technique has been applied. In the second experiment, the 6^+ ($E_x = 4715$ keV, $t_{1/2} = 20$ ns) isomeric state in ^{132}Sn has been populated following the gamma-ray decay of the 8^+ ($t_{1/2} = 2.1$ μs) isomeric state in the same nucleus. The Time Dependent Perturbed Angular Correlations (TDPAC) technique has been used for the moment study of the short-lived isomeric state.

The experimental details and the status of the data analysis for the two experiments will be presented, and the results will be compared to theoretical models. The experimental challenges and the future perspectives will be discussed as well.

[1] A. Vernon et al., *Nature* **607** (2022) 260.

HYPERFINE-ORAL-T02

Measurement of Charge Radii in Neutron-Rich Regions Using Charge-Changing Cross Sections

M. Fukutome¹, M. Tanaka², G. Takayama³, M. Fukuda³, D. Nishimura⁴, M. Takechi¹, T. Suzuki⁵, R. Taguchi³, S. Ishitani³, T. Yamaguchi⁵, T. Ohtsubo¹, T. Moriguchi⁶, A. Ozawa⁶, A. Yano⁶, M. Mihara³, T. Naito⁷, T. Izumikawa¹, K. Adachi¹, S. Bagchi⁹, K.-H. Behr⁹, S. Endo⁴, N. Fukuda⁸, H. Geissel⁹, H. J. Ong¹⁰, N. Inabe⁸, C. Inoue⁴, K. Itabashi⁸, Y. Ka⁴, R. Kageyama⁴, Y. Kikuchi⁵, H. Kobayashi⁶, Z. Korkulu⁸, K. Kusaka⁸, K. Maeda⁴, K. Matsuyama⁴, M. Mikawa⁶, M. Mitsui⁶, D. Nagae⁸, S. Nishizawa⁵, M. Ohtake⁸, A. Prochazka⁹, H. Sakurai⁸, R. Sasamori¹, F. Sato⁴, C. Scheidenberger⁹, T. Shimamura¹, Y. Shimizu⁸, T. Sumikama⁸, H. akeda⁸, I. Tanihata¹⁰, K. Tezuka¹, K. Watanabe⁵, Y. Yanagisawa⁸, K. Yasuda³, I. Yasuda⁵, K. Yoshida⁸

¹Niigata University, Niigata, Japan, ²Kyushu University, Fukuoka, Japan, ³The University of Osaka, Toyonaka, Japan, ⁴Tokyo City University, Tokyo, Japan, ⁵Saitama Univ., Saitama, Japan, ⁶Univ. Tsukuba, Tsukuba, Japan, ⁷RIKEN iTHEMS, Wako, Japan, ⁸RIKEN Nishina Center, Wako, Japan, ⁹GSI, Darmstadt, Germany, ¹⁰RCNP, Univ. Osaka, Ibaraki, Japan

*miki.fukutome.1207@niigata-u.ac.jp

A charge radius is a fundamental physical quantity that reflects the charge distribution of a nucleus and the proton distribution radius. Therefore, the neutron distribution radius can be derived by combining the charge radius with the matter radius. For stable nuclei, charge radii have been measured for many isotopes using electron scattering, but this traditional method is difficult for unstable nuclei due to their short lifetimes and low production yields. Currently, the isotope shift method using high-resolution laser spectroscopy is an established technique for measuring the charge radii of unstable nuclei. Nevertheless, this method faces technical challenges, such as the difficulty in producing low-energy secondary beams with sufficient intensity and in developing appropriate laser systems tailored to each element. In contrast, the measurement of charge-changing cross sections has recently attracted attention as a universal and efficient method for determining the charge radii of unstable nuclei. The charge-changing cross section is a physical quantity corresponding to the probability of a change in the proton number Z of a given nuclide AZ . In recent years, a strong correlation has been found between charge-changing cross sections and charge radii of both stable and neutron-rich nuclei [1,2].

In this study, we measured the charge-changing cross sections of nickel isotopes ($^{58-77}\text{Ni}$) and reproduced the experimental results using a simple Glauber model that incorporates the effect of charged-particle evaporation. Based on this approach, we will report these results and discuss a method for extracting the charge radii of neutron-rich unstable nuclei.

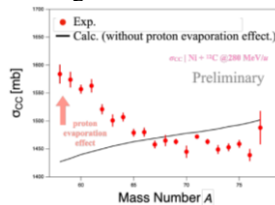


Figure 1. Charge-changing cross sections for Ni isotopes.

- [1] T. Yamaguchi, et al., *Phys. Rev. Lett.* **107** (2011) 03250 2.
 [2] M. Tanaka, et al., *Phys. Rev. C* **106** (2022) 014617.

HYPERFINE-ORAL-T02

Precision Measurements of the Ground State Hyperfine Splitting of Antihydrogen

Jay Suh^{1*}, Timothy Friesen¹, The ALPHA Collaboration²

¹University of Calgary, Calgary, Canada

²European Council for Nuclear Research, Geneva, Switzerland

*jay.suh@ucalgary.ca

Antihydrogen, the antimatter counterpart of hydrogen, provides a unique platform for testing fundamental symmetries in nature. One of its key properties, the hyperfine splitting, arises from the interaction between the antiproton and the orbiting positron and serves as a crucial probe for Charge-Parity-Time (CPT) symmetry. Precise measurements of antihydrogen's hyperfine splitting offer direct comparisons with hydrogen, where the splitting is known to a precision of 1.4 parts in 10^{12} [1]. In searching for possible CPT violations, the absolute precision of a measurement is considered more significant as opposed to its relative precision, making the hyperfine spectroscopy of antihydrogen a particularly sensitive test for possible Standard Model Extensions [2].

The ALPHA Collaboration, an international research team at CERN, leads efforts to investigate the fundamental properties of antihydrogen using its specialized trapping apparatus and innovative experimental techniques. Among their various objectives, one of ALPHA's primary experiments focuses on the hyperfine splitting of antihydrogen, with the aim of implementing novel measurement techniques to match or exceed the precision reached with the hydrogen atom [3]. Recent improvements in ALPHA's magnetic field and microwave infrastructure have revealed new opportunities for increased precision measurements, with better control of systematics and enhanced sensitivity to potential CPT-violating effects in antihydrogen's hyperfine splitting.

This presentation will report on recent advancements in antihydrogen hyperfine spectroscopy, the novel methods employed, and the latest results from the ALPHA Collaboration in our pursuit of testing fundamental symmetries with increasing precision.

[1] H. Hellwig, et al., *IEEE Trans. Instrum. Meas.* **19** (1970) 200-209.

[2] V. A. Kostelecký, A. J. Vargas, *Phys. Rev. D.* **92** (2015) 056002.

[3] M. Ahmadi, et al., *Nature*, **548** (7665) 66–69.

HYPERFINE-ORAL-T03

Local Structural Order in Layered Perovskite Solid Solutions

A. Cesário^{1*}, S. S. M. Santos², P. Rocha-Rodrigues¹, P. N. Lekshmi¹, J. G. Correia³,
L. V. C. Assali⁴, H. M. Petrilli⁴, M. S. Senn^{5,6}, J. P. Araújo¹, A. M. L. Lopes¹

¹IFIMUP, Departamento de Física e Astronomia da Faculdade de Ciências da Universidade do Porto, Rua do Campo Alegre, 687, 4169-007 Porto, Portugal

²Instituto Federal de Educação, Ciência e Tecnologia de Rondônia-Campus Colorado, Brazil

³C2TN, Centro de Ciências e Tecnologias Nucleares, Universidade de Lisboa, Estrada Nacional 10, 2695-066 Bobadela LRS, Portugal

⁴Instituto de Física, Universidade de São Paulo, CP 66318, 05315-970, São Paulo-SP, Brazil

⁵Department of Chemistry, University of Oxford, Inorganic Chemistry Laboratory, South Parks Road, Oxford, OX1 3QR, U.K.

⁶Department of Chemistry, University of Warwick, Gibbet Hill, Coventry CV4 7AL, U.K.

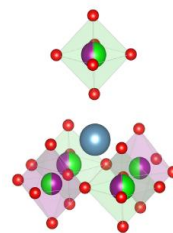
*antonio.duarte.neves.cesario@cern.ch

In this study, we investigate the nanoscopic structural properties of $\text{Ca}_2\text{Mn}_{1-x}\text{Ti}_x\text{O}_4$ Ruddlesden-Popper (RP) perovskites by combining experimental and computational approaches. Atomic-scale measurements were conducted at ISOLDE/CERN with Perturbed Angular Correlation (PAC) spectroscopy with ^{111}mCd (48 min) probes at substitutional Ca-sites [1]. This method has provided insights into structural phase transitions (10-1200K) and Mn/Ti site distributions across different compositions, with Density Functional Theory (DFT) calculations playing a crucial role in interpreting the experiments.

Our findings indicate that incorporating Ti into the Ca_2MnO_4 lattice creates two distinct local environments rather than a continuous Electric Field Gradient (EFG) distribution. This arises from the reduced number of Mn/Ti nearest neighbors (Fig. 1), which limits the possible local configurations when compared to the simple ABO_3 perovskites, where the A-cations have eight equidistant B-cations. PAC spectroscopy, with its sensitivity to atomic-scale variations, effectively resolves these site-specific interactions and cation ordering. By shedding light on the structural organization within the CaO rock-salt layer, this study advances our understanding of local structural effects in RP perovskites.

Beyond this specific system, our findings have broader implications for materials exhibiting correlated electronic and structural properties. PAC proves to be a valuable tool for distinguishing subtle local environments, making it relevant for studying similar layered perovskites. These materials are of practical interest due to their tunable properties, including superconductivity, magnetoelectric coupling, and negative thermal expansion [2]. Chemical substitution, as explored in this work, offers a pathway to optimize, control or even combine these effects in solid solutions [3].

Figure 1. Illustration of the ^{111}mCd local environment at a Ca-site in a Ruddlesden-Popper perovskite, surrounded by its five nearest Mn/Ti atoms (inside octahedra).



[1] P. R. Rodrigues et al., *Phys. Rev. B* **102** (2020) 104115.

[2] M. S. Senn et al., *Phys. Rev. Lett.* **114** (2015) 035701.

[3] C. Ablitt et al., *Front. Chem.* **6**, (2018) 455.

HYPERFINE-ORAL-T03

Evaluation of Local Chemical Environment via PAC Spectroscopy Using ^{111}In -Labeled Radiotracers: From Quantification to Cell-Based Validation

Boyu Feng^{1*}, Pietro Caradonna¹, Tomoko Mineo¹, Toshifumi Tatsumi², Ayaka Otsuka¹, Moh Hamdan¹, Sotaro Tokunaga¹, Akira Sugiyama², Takeshi Sato¹, Noriko Nakamura¹, Seiichi Ohta¹, Mizuki Uenomachi³, Kenzo Yamatsugu⁵, Sachiyo Nomura⁶, Ryohei Terabayashi¹, Hideki Tomita⁷, Tetsu Sonoda⁸, Yudai Shigekawa⁸, Takuya Yokokita⁴, Kenji Shimazoe¹

¹The University of Tokyo, Tokyo, Japan

²Isotope Science Center, The University of Tokyo, Tokyo, Japan

³Tokyo University of Science, Tokyo, Japan

⁴Tohoku University, Sendai, Japan

⁵Chiba University, Chiba, Japan

⁶Hoshi University, Tokyo, Japan

⁷Nagoya University, Nagoya, Japan

⁸RIKEN, Wako, Japan

*e-fengboyu@g.ecc.u-tokyo.ac.jp

Nuclear medicine imaging visualizes the distribution of radiopharmaceuticals by detecting emitted radiation. While PET and SPECT are widely used, they mainly reflect tracer accumulation and lack sensitivity to the local physicochemical environment. To access higher-order functional information, such as environmental pH, alternative imaging approaches are needed.

Perturbed angular correlation (PAC) is a nuclear spectroscopy technique sensitive to the probe's microenvironment via cascade gamma emissions. We investigated the pH-dependent PAC behaviour of two ^{111}In -labeled systems: an antibody-based tracer (Psyche-DOTA- ^{111}In) and a PEG-modified gold nanoparticle (AuNP-PEG-DOTA- ^{111}In), the latter known for efficient tumor accumulation due to the EPR effect.

PAC measurements under various pH conditions revealed an approximately linear increase in anisotropy coefficient from pH 1 to 7, indicating changes in local coordination. Around pH 5, corresponding to the lysosomal environment, a detectable shift suggests the potential to probe intracellular uptake.

Cell-based experiments further support the feasibility of this method in biological contexts. These findings highlight PAC as a promising complementary technique for functional imaging beyond conventional PET and SPECT.

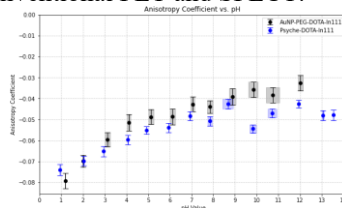


Figure 1. pH-dependent anisotropy coefficients for two tracers, showing distinct responses to the local environment.

[1] K. Shimazoe et al., *Commun. Phys.* **5**, (2022) 24.

[2] A. Sugiyama et al., *Proc. Jpn. Acad.*, B **95** (2019) 602–611.

HYPERFINE-ORAL-T03

High-Resolution and High-Sensitivity Collinear Resonance Ionization Spectroscopy of Rb and Cs Isotopes

Y. F. Guo^{1*}, H. R. Hu¹, X. F. Yang¹, Z. Yan¹, W. C. Mei¹, S. J. Chen¹, Y. S. Liu¹, P. Zhang¹, S. W. Bai¹, D. Y. Chen¹, Y. C. Liu¹, S. J. Wang¹, Y. L. Ye¹

¹ State Key Laboratory of Nuclear Physics and Technology, School of Physics, Peking University, Beijing, China

*yfkuo@pku.edu.cn

The fundamental properties of exotic nuclei offer crucial insights into nuclear structure and nucleon-nucleon interactions [1]. By measuring hyperfine structure and isotope shifts in atomic or ionic spectra, laser spectroscopy enables precise determination of nuclear spin, electromagnetic moments, and charge radii in a nuclear model-independent way [2].

To investigate nuclear properties and exotic structures of unstable nuclei at existing and forthcoming RIB facilities in China, we developed a high-resolution and high-sensitivity collinear resonance ionization spectroscopy offline system named PLASEN, as shown in Fig.1[3]. This system was first tested with ^{85, 87}Rb isotopes, achieving an overall efficiency exceeding 1:200 with a spectral resolution of 100 MHz. Using this system, we also developed the laser ionization scheme for cesium and identified the most efficient scheme. Under these conditions, the extracted hyperfine structure parameters and isotope shifts were in excellent agreement with literature values. These results pave the way for upcoming studies of neutron-rich ⁹⁸⁻¹⁰⁰Rb and ¹⁴⁷⁻¹⁵⁰Cs isotopes at BRIF in China to be conducted in a few months.

In this presentation, the details of the PLASEN system, including the beamline and laser system, as well as the results from the offline experiments and the planned online experiments on neutron-rich Rb and Cs isotopes at BRIF, will be presented.

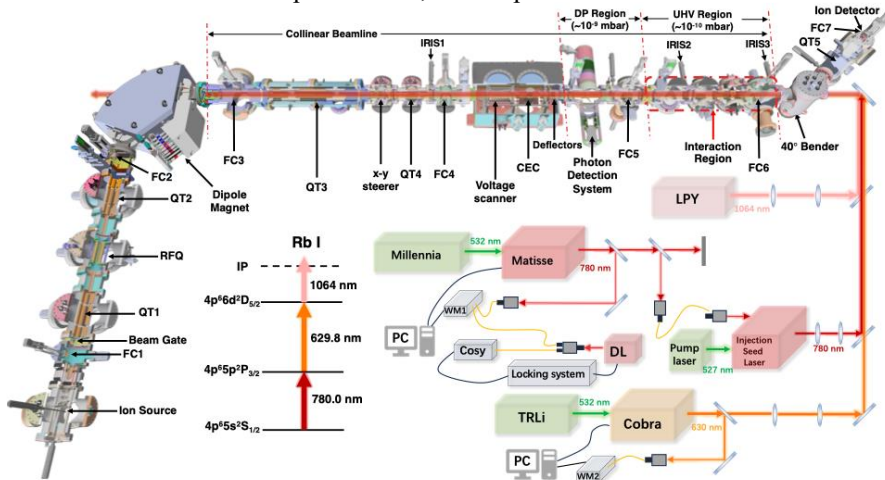


Figure 1. A schematic view of the PLASEN system, and the ionization scheme used for the test experiment [3].

- [1] Y. Ye et al., *Nat. Rev. Phys.* **7** (1) (2025)
- [2] X.F. Yang et al., *Prog. Part. Nucl. Phys.* (2022).
- [3] H. R. Hu, Y. F. Guo, X. F. Yang, et al., (2025) arXiv:2503.20637.

HYPERFINE-ORAL-T03

Laser Resonant Ionization Spectroscopy at Kiss

Y. Hirayama^{1*}, M. Mukai¹, Y.X. Watanabe¹, P. Schury¹, T. Hashimoto², S. Iimura³,
H.N. Kim², S. Kimura¹, H. Miyatake¹, J.Y. Moon², T. Niwase⁴, M. Rosenbusch⁵,
A. Takamine⁴, A. Taniguchi⁶, M. Wada¹

¹Wako Nuclear Science Center (WNSC), Institute of Particle and Nuclear Studies (IPNS),
High Energy Accelerator Research Organization (KEK), Wako, Saitama 351-0198, Japan

²Rare Isotope Science Project, Institute for Basic Science (IBS), Daejeon 305-811,
Republic of Korea

³Rikkyo University, Department of Physics, Tokyo 171-8501, Japan

⁴Kyushu University, Department of Physics, Fukuoka, 819-0395, Japan

⁵RIKEN Nishina Center for Accelerator-Based Science, RIKEN, Wako, Saitama 351-0198,
Japan

⁶Institute for Integrated Radiation and Nuclear Science, Kyoto University (KURNS),
Kumatori, Osaka 590-0494, Japan

*yoshikazu.hirayama@kek.jp

We have been performing nuclear spectroscopy, including laser spectroscopy, at the KEK Isotope Separation System (KISS) [1] installed in RIKEN, Japan, to study the nuclear structure of the nuclei in the vicinity of neutron magic number $N = 126$ to reveal the astrophysical sites for synthesizing heavy elements such as gold and platinum. These neutron-rich nuclei have been produced by using multinucleon transfer reactions [2] with the combinations of the low-energy $^{136}\text{Xe}/^{238}\text{U}$ beams and the production targets of W, Ir, and Pt.

At the KISS facility, radioisotopes are ionized by applying an in-gas-cell laser ionization technique. In the ionization process, we can perform laser ionization spectroscopy of the refractory elements with the atomic number $Z = 70-78$, such as Hf, Ta, W, Re, Os, Ir, and Pt, which cannot be performed in other facilities. Laser spectroscopy can be used to effectively investigate the nuclear structure through the measured magnetic moments, isotope shifts (IS) $\Delta\nu$, changes in the mean-square charge radii $\delta\langle r^2 \rangle$, and quadrupole deformation parameters $|\langle \beta_2^2 \rangle|^{1/2}$ [3,4,5].

We have performed in-gas-cell laser ionization spectroscopy of neutron-rich rhenium isotopes ($Z = 75$), which exit in the nuclear shape transition region from prolate to oblate through triaxial deformation. From the measured hyperfine spectra, we clearly observed the change of proton orbit, which strongly correlates with the shape transition.

To promote precise laser spectroscopy, we have started to develop collinear resonant laser ionization spectroscopy (CRIS) beam line and the relevant laser system. In this conference, we will report the results of laser ionization spectroscopy of rhenium isotopes and discuss the perspective of the CRIS project at KISS.

[1] Y. Hirayama et al., *Nucl. Inst. Meth.* B353, **4** (2015), and B412, **11** (2017).

[2] Y.X. Watanabe et al., *Phys. Rev. Lett.* **1** (2015) 172503.

[3] Y. Hirayama et al., *Phys. Rev. C* **96** (2017) 014307, and **106** (2022) 034326.

[4] M. Mukai et al., *Phys. Rev. C* **102** (2020) 054307.

[5] H. Choi et al., *Phys. Rev. C* **102** (2020) 034309.

HYPERFINE-ORAL-T03

First Principles and Experimental Local Probe Study of Ge-based Clinopyroxene Series

Ricardo P. Moreira^{1*}, E. Lora da Silva^{1,2}, Gonçalo N. P. Oliveira¹,
P. Neenu Lekshmi¹, Pedro Rocha-Rodrigues¹, Claire V. Colin³, Céline Darie³,
João G. Correia⁴, Lucy V. C. Assali⁵, Helena M. Petrilli⁵, Armandina M. L. Lopes¹,
João P. Araújo¹

¹IFIMUP, Institute of Physics for Advanced Materials, Nanotechnology and Photonics,
Departamento de Física e Astronomia da Faculdade de Ciências da Universidade do Porto,
Rua do Campo Alegre s/n, 4169-007 Porto, Portugal

²High Performance Computing Chair, University of Évora, Rua Romão Ramalho 59,
7000 671 Évora, Portugal

³Université Grenoble Alpes, CNRS, Institut Néel, 38000, Grenoble, France

⁴C2TN, DECN, Instituto Superior Técnico, Universidade de Lisboa, Bobadela, Portugal

⁵Instituto de Física, Universidade de São Paulo, CP 66318, 05315-970, São Paulo-SP, Brazil

*up201202493@edu.fc.up.pt

Pyroxenes are a class of materials with general formula AMX_2O_6 , where A is a monovalent or a divalent cation, M is a trivalent or a divalent cation, and X is either Si or Ge, well known in mineralogy and geology as one of the main rock-forming minerals of the Earth's crust [1]. Within this rich family of compounds, monoclinic pyroxenes (clinopyroxenes), with a $3d$ transition metal at the M -site, have recently been the subject of interest in condensed matter physics due to the diversity of their magnetic properties.

The electronic properties of the Ca/Sr and Mn site substitution of $CaMnGe_2O_6$ and $SrMnGe_2O_6$ clinopyroxene systems, obtained through *ab-initio* Density Functional Theory (DFT) calculations are presented. By combining DFT calculations and experimental results from Perturbed Angular Correlation Spectroscopy (PAC) measurements, compositions such as $(Ca,Sr)_{1-x}Cd_x MnGe_2O_6$ and $(Ca,Sr)Mn_{1-x}Cd_xGe_2O_6$ ($x=0.125, 0.25$) were predicted to be stable. Also, we proved that implanted Cd impurities can replace either the Ca/Sr or the Mn sites in the structures. Additionally, DFT calculations showed that Cd substitution is expected to lead to a reduction in the band gap width.

Guided by these findings, for the first time, the Cd-doped systems were successfully synthesized, and experimental results evidencing opportunities for potential band-gap engineering are presented.

[1] S. V. Streltsov, D. I. Khomskii, *Phys. Rev. B* **77** (2008) 064405.

HYPERFINE-ORAL-T03

Phase Transitions and Uniaxial Negative Thermal Expansion in CsNdNb₂O₇: Combined Local Probe and Diffraction Study

Pedro A. Sousa^{1*}, P. N. Lekshmi¹, António N. Cesário¹, P. Rocha Rodrigues¹, Lucy Assali², Helena M. Petrilli², E. Lora da Silva¹, S. S. M. Santos³, J. G. Correia⁴, J. P. Araújo¹, A. M. L. Lopes¹

¹IFIMUP, Faculdade de Ciências da Universidade do Porto, Portugal

²Instituto de Física da Universidade de São Paulo, São Paulo, Brazil ³Instituto Federal de Educação, Ciência e Tecnologia de Rondônia, Campus Colorado, Brazil ⁴C2TN, Centro de Ciências e Tecnologias Nucleares, Universidade de Lisboa, Portugal

*up201704307@edu.fc.up.pt

Zhu et al. [1] report that the CsNdNb₂O₇ system undergoes two phase transitions: a polar-to-antipolar structural change at 625 K followed by a transition to the aristotype at 800 K, resulting in three distinct phases—P2₁am (#26), C2/m (#12), and P4/mmm (#123). Their study attributes these transitions to rotations and tilts of NbO₆ octahedra, which not only stabilize the polar ferroelectric phase but also induce negative thermal expansion (NTE) in the c-axis lattice parameter during the 625 K transition.

Building on these findings, our work employs a multimodal strategy to systematically investigate the phase behaviour and structural evolution of CsNdNb₂O₇. Synchrotron X-ray diffraction (SXRD) provides high-precision measurements of lattice parameters and confirms the occurrence of NTE [1]. However, due to SXRD's limited sensitivity to light elements and subtle local distortions, we incorporate three complementary techniques:

- Perturbed Angular Correlation (PAC) Spectroscopy: A local probe is highly sensitive to atomic-scale dynamics, measuring the electric field gradient (EFG) at specific sites to capture information on local symmetry and NbO₆ rotational environments.

- Neutron Powder Diffraction (NPD): Leveraging the large neutron scattering cross-section of oxygen, NPD accurately determines oxygen positions, enabling detailed quantification of temperature-dependent distortions in both the perovskite and rock-salt layers, which are directly linked to the NTE mechanism.

- Density Functional Theory (DFT): Utilizing structural data from NPD, DFT calculations provide theoretical EFG values and offer an in-depth analysis of the electronic and structural intricacies underlying the phase transitions.

By integrating local (PAC), long-range and oxygen-sensitive (NPD), and theoretical (DFT) methodologies, our approach delivers critical new insights into the underlying mechanism of negative thermal expansion (NTE).

Our findings not only confirm the previously proposed structural evolution in CsNdNb₂O₇ but also underscore the importance of a multimodal characterization strategy in understanding phase transitions and thermal expansion anomalies in layered perovskites, particularly within the Dion-Jacobson family.

[1] T. Zhu, et al., *Chem. Mater.* **32**(10) (2020) 4340–4346

HYPERFINE-ORAL-T04

Performance Evaluation of Improved Muon Spin Imaging Device Using Charged Particle Trackers in μ -e Decay Process

M. Mihara^{1,9*}, S. Ishitani^{1,9}, K. M. Kojima^{2,9}, A. Sato¹, K. Yasuda¹, G. Takayama¹, T. Sugisaki^{1,9}, Y. Kimura^{1,9}, M. Fukuda¹, M. Fukutome³, R. Taguchi¹, S. Shimizu¹, K. Horie¹, R. Imai¹, S. Ide¹, K. Shimizu¹, M. Kamon¹, R. Fukushima¹, Y. Mizoi^{4,9}, A. Koda⁵, S. Kanda^{5,9}, W. Sato⁶, D. Nishimura⁷, M. Tanaka^{8,9}

¹The University of Osaka, Toyonaka, Japan, ²TRIUMF, Vancouver, Canada, ³Niigata University, Niigata, Japan, ⁴Osaka Electro-Communication University, Neyagawa, Japan,

⁵High Energy Accelerator Research Organization (KEK), Tsukuba, Japan, ⁶Kanazawa University, Kanazawa, Japan, ⁷Tokyo City University, Tokyo, Japan, ⁸Kyushu University, Fukuoka, Japan, ⁹Open-it

*mihara@phys.sci.osaka-u.ac.jp

The muon spin rotation/relaxation/resonance (μ SR) spectroscopy has been used in various research fields including material and life sciences as an extremely versatile measurement method. However, the conventional μ SR spectroscopy is difficult to apply to small sample volumes or to samples confined in small spaces such as high-pressure cells due to the difficulty in minimizing the muon beam size. In order to realize measurements under such special sample environments or furthermore 3D imaging of various objects such as biological samples, meteorites, archaeological materials and so on, we have started to develop an imaging technique we call “muon spin imaging” that adds spatial resolution to the conventional μ SR spectroscopy.

In the present study, significant improvements were made to our muon spin imaging device based on the previous results [1,2], which is shown in Figure 1. One of the improvement was to minimize the misalignment of the scintillation fibers used for tracking μ -e decay positrons, which was the main cause of image blurring. Another was to significantly reduce the dead time for data acquisition by incorporating the Kalliope system [3]. Third was to add a drift chamber for muon beam tracking, which enables 3D imaging combined with the positron tracking. We have tested the performance of the improved device using a surface DC muon 25 beam at TRIUMF and succeeded in creating a clear 2D image as shown in Figure 2. Analysis of 3D imaging is in progress and we will report on the details of the performance including the spatial image resolution.

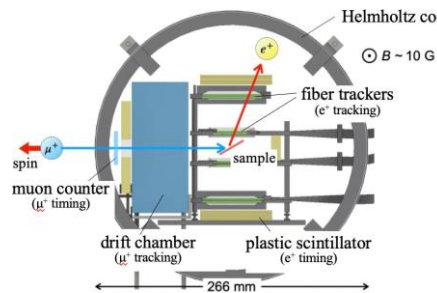


Figure 1. Setup of the muon spin imaging experiment.

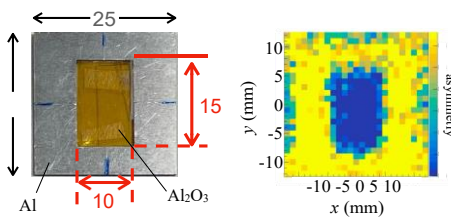


Figure 2. Test sample and an example of 2D μ SR image.

[1] T. Sugisaki et al., *Interactions* **245** (2024) 20.

[2] G. Takayama, *Interactions* **245** (2024) 32.

[3] K. M. Kojima et al., *J. Phys.: Conf. Ser.* **551** (2014) 012063.

Transient μ SR with High-Field μ SR Spectrometer at J-PARC

Shoichiro Nishimura^{1,2,3*}, Shigekazu Ito⁴, Hirotaka Okabe^{1,2}, Ryosuke Kadono^{1,2}, Akihiro Koda^{1,2,3}, Kenji M. Kojima⁵, Jumpei G. Nakamura^{1,2}, Masatoshi Hiraishi^{1,2}, Masanori Miyazaki⁶

¹Institute of Materials Structure Science, KEK, Tsukuba, Japan

²J-PARC Center, Tokai, Japan

³The Graduate University for Advanced Studies (SOKENDAI), Tsukuba, Japan

⁴Institute of Science Tokyo, Tokyo, Japan

⁵Research Scientist at Centre for Molecular and Materials Science (CMMS), TRIUMF, Vancouver, Canada

⁶Muroran Institute of Technology, Muroran, Japan

*nishimu@post.kek.jp

In recent years, the beam intensity at J-PARC has been significantly increased, and the operation of a 1 MW proton beam has finally been achieved. In muon spin rotation, resonance, and relaxation (μ SR) measurements, this increase in beam intensity has led to a reduction in measurement time. However, in standard μ SR experiment, it is necessary to keep the sample environment stationary during data acquisition. As a result, the time required to stabilize the sample environment is becoming longer than the actual measurement time.

To address this issue, we have developed a transient μ SR method in which sample environmental parameters such as temperature and magnetic field are recorded for each muon pulse, so that the time spectra corresponding to the desired parameter conditions can be extracted after the experiment. This method not only enables changes in the sample environment during measurement but also allows the observation of transient responses of the sample using μ SR [1]. Figure 1

illustrates the data analysis workflow employed in the transient μ SR method.

We conducted proof-of-principle experiment for the transient μ SR using the high-field μ SR spectrometer CYCLOPS (furnished with 5 Tesla superconducting magnet) installed in the S1 area at J-PARC MLF. This technique is particularly well-suited for superconducting magnets for which the magnetic field can be changed only gradually. Level crossing resonance spectra were measured on two organic samples while varying temperature and magnetic field, and resonance signals were successfully detected. In this presentation, we will report several results obtained by transient μ SR.

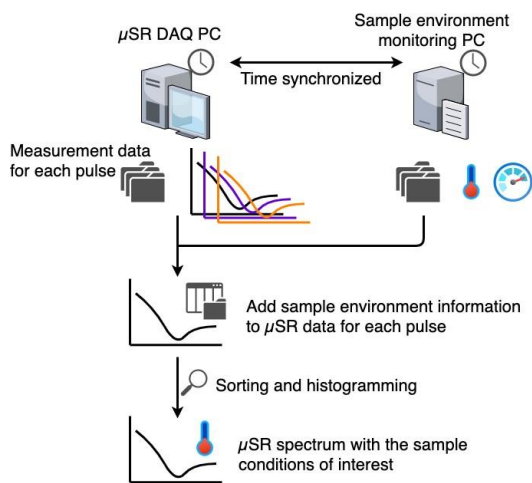


Figure 1. Workflow in the transient μ SR method.

[1] S. Nishimura et al., *Nucl. Instrum. & Meth. Phys. Res. A* (2023) **1056**, 168669.

HYPERFINE-ORAL-T04

Muon Spin Rotation and Relaxation Study in Albumin and Hemoglobin Derivatives

Amba Datt Pant^{1,2*}, Hiromi Sakai³, Akihiro Koda^{1,2}, Burkhard Geil⁴, Anup Shrestha⁵, Anjan Dahal⁵, Hari Shankar Mallik⁵, Katsuhiko Ishida^{1,2}, Masatoshi Hiraishi^{1,2}, Jumpei G. Nakamura^{1,2}, Shoichiro Nishimura^{1,2}, Koichiro Shimomura^{1,2}

¹Institute of Materials Structure Science, KEK, 1-1 Oho, Tsukuba, Ibaraki 305-0801, Japan ²Muon Section, Materials and Life Science Division, J-PARC center, 2-4 Shirane Shirakata, Tokai-mura, Naka-gun, Ibaraki 319-1195, Japan

³Department of Chemistry, Nara Medical University, Kashihara 634-8521, Japan

⁴Institut für Physikalische Chemie, Universität Göttingen, Tammannstrasse 6, 37077 Göttingen, Germany

⁵Central Department of Physics, Tribhuvan University, Kathmandu, Nepal

* pant@post.kek.jp

Hemoglobin (Hb) is a protein that plays an important role in transporting O₂ from the lungs to the tissues. Binding of O₂ with paramagnetic deoxyHb converts it into diamagnetic oxyHb. Since the muon, like a light proton ($m_{\mu} \sim 1/9 m_p$) with a magnetic moment greater than that of proton ($\mu_{\mu} = 3.2\mu_p$), acts as a sensitive local probe, and its bound state with an electron known as muonium ($\text{Mu} = \mu^+e^-$) interacts with O₂, the muon spin rotation and relaxation (μSR) method can be used to study the local electronic and dynamic states of the materials [1,2]. We apply μSR to study the Hb magnetism and the O₂ concentrations in the biosamples, as well as the dynamics of electron, protons, and ions in biosamples. In order to establish the fundamentals of muon in biology and applications in life sciences, we performed systematic μSR study starting from water [3], buffer, albumin, dilute protein aqueous solutions under controlled O₂ concentrations [4,5], and Hb derivatives under physiological concentrations. Even though several μSR studies are reported in water [6-8], we found new insights into μSR in water that help to understand the interactions of muon and its charge states with biomacromolecules by providing background information. Like in water, an isotropic Mu was observed in dilute aqueous solutions of albumin and Hbs in liquid state, and anisotropic Mu in the frozen state, but with different hyperfine interactions. We also found that the inter-Hb interaction and anisotropic behaviour of Mu changes with concentrations [9]. In the program, the study in albumin and derivatives (oxyHb, deoxyHb, COHb, and methHb) will be discussed.

[1] K. Nagamine, *Introductory Muon Science*, Cambridge Univ. Press, New York (2003).

[2] S. Blundell, et. al., *Muon Spectroscopy: An Introduction*, OUP, New York (2022).

[3] A. D. Pant, et. al., *Phys. Rev. B* **110** (2024) 104104.

[4] A. D. Pant, et. al., *J. Phys. Conf. Ser.* **551** (2014) 012043.

[5] A. D. Pant et. al., *Nucl. Instrum. Methods Phys. Res. A* **1011** (2021) 165561.

[6] P. W. Percival, et. al., *Chem. Phys. Lett.* **39** (1976) 333.

[7] K. Nagamine, et. al., *Chem. Phys. Lett.* **87** (1982) 186.

[8] S. F. J. Cox, et. al., *Hyperfine Interact.* **86**, 747 (1994).

[9] A. D. Pant, et. al., *in preparation*.

HYPERFINE-ORAL-T04

Muon Spectroscopy at the Swiss Muon Source SμS

Thomas Prokscha*

¹PSI Center for Neutron and Muon Sciences, 5232 Villigen PSI,
Switzerland

* thomas.prokscha@psi.ch

The Swiss Muon Source SμS [1] is one of the leading international user facilities for muon spectroscopy research. Six permanently installed instruments for muon spin spectroscopy (μSR) and one non-permanent instrument for Muon-Induced-X-ray-Emission (MIXE) are available. The μSR program typically uses positive muons as highly sensitive local magnetic probes to study a broad range of research topics in solid-state physics, chemistry, materials science, semiconductor, and energy research [2]. MIXE uses negative muons, which are captured by the target nuclei after implantation, emitting an element-specific cascade of X-ray radiation, which is two hundred times more energetic than in normal atoms due to the muon's higher mass than the electron. This allows non-destructive elemental analysis to be carried out on tuneable depths from 0.001 cm to > 1 cm [2]. The different instruments of the SμS facility offer a wealth of different experimental capabilities with respect to temperature, magnetic field, pressure, time resolution, measurement geometry, probing depth, and minimal sample size. SμS operates various unique instruments, such as the Low-Energy Muon LEM facility for the study of thin heterostructures and interfaces; the high-field instrument HAL-9500 for studies in magnetic fields up to 9.5 T and at low temperatures of 0.01 K; the high-energy muon instrument GPD with the combination of high pressures up to 2.8 GPa and sub-Kelvin temperatures of 0.3 K, and the DOLLY/VMS instrument with uniaxial pressure up to 1 GPa and low temperatures of 0.25 K. The latest addition to the facility is the GIANT instrument [3] for non-destructive elemental analysis using the MIXE method, which will be available to the muon user community from 2026.

Typical applications of μSR include a variety of topics in condensed matter research, with a focus on the investigation of novel and unconventional quantum materials. In addition to the traditional applications, μSR is used to investigate molecular dynamics, charge and spin transport phenomena, ion conduction in battery materials, as well as spectroscopic information on hydrogen levels, defect concentrations, and charge carrier profiles in technologically relevant semiconductor materials. MIXE extends the research field of muons further in the direction of applications through the elemental analysis of cultural heritage objects, such as archaeological artefacts and state-of-the-art battery devices. With the High-Intensity Muon Beams (HIMB) project, expected to be realized by mid-2028, a quantum leap in the applications of μSR towards much faster measurements, smaller samples, and much higher external stimuli (e.g., pressures) is expected [4], taking advantage of the huge benefits of particle tracking with state-of-the-art Si pixel detectors [5]. This contribution presents an overview of the facility and its future prospects.

[1] <https://www.psi.ch/smus> and <https://www.psi.ch/lmu>.

[2] A. Hillier et al., *Nat. Rev. Meth. Primer* **2** (2022) 1.

[3] L. Gerchow et al., *Rev. Sci. Instr.* **94** (2023) 045106.

[4] M. Aiba et al., *arXiv:2111.05788* (2022).

[5] L. Mandok et al., *arXiv:2503.08891* (2025).

HYPERFINE-ORAL-T04

Hyperfine Field Measurement and Local Structure of Muonic Organic Materials

Soshi Takeshita^{1*}, Tamiko Kiyotani², Masatoshi Hiraishi¹, Mio Yoshida³, Dai Tomono⁴, Yoshio Kobayashi³, Koichiro Shimomura¹

¹Institute of Materials Structure Science,
High Energy Accelerator Research Organization (KEK), Ibaraki, Japan

²Showa Pharmaceutical University, Tokyo, Japan

³The University of Electro-Communications, Tokyo, Japan

* soshi@post.kek.jp

Since the MUSE D-line at the J-PARC MLF is a decay muon beamline, it provides a high-intensity spin-polarized muon beam with both polarities, i.e., positive and negative. Positive muons implanted into polymers are known to form paramagnetic muons (muoniated radicals) and paramagnetic muons, while negative muons are captured by atomic nuclei to form muonic atoms. Thus, the sites for the positive muons in a sample are sometimes ambiguous, while those for the negative muons are clearly determined. This is one of the merits of a negative muon spin relaxation (μ^- SR) technique over a positive muon spin relaxation (μ^+ SR) technique, particularly for polymer science, as there are usually many possible μ^+ sites. However, to observe molecular dynamics in polymers with μ^- SR, it is essential to know the hyperfine interactions between μ^+ and nuclear spins of the nuclei on which μ^+ is captured.

In this study, we have performed μ^+ SR measurements on several simple organic materials to know the hyperfine fields and investigate the chemical states in the vicinity of the captured μ^- . The μ^- SR spectrum of organic materials under the zero-field often exhibits an oscillation at low temperatures due to the formation of two (or three) spin-1/2 system (Fig. 1). The oscillation frequency is well explained by the hyperfine interaction between the spin-1/2 μ^- captured by ^{12}C and one or two spin-1/2 H nuclei bound to the carbon. The bonding distance between the muonic carbon and hydrogen is estimated from the oscillation frequency: in the case of ethylene, the distance is estimated to be 1.202(9) Å.

We will discuss the structures around the captured μ^- based on these hyperfine interactions, including other simple organic materials.

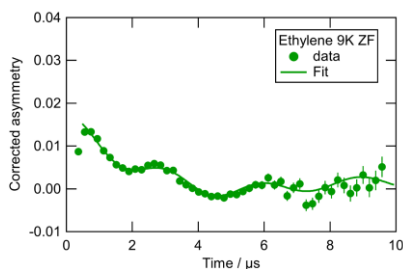


Figure 1. Time spectrum of μ SR in solid state ethylene measured at 9 K under the Zero magnetic field.

HYPERFINE-ORAL-T04

Hyperfine Spectroscopy of Muonium and Muonic Atoms for Precise Determination of the Muon Magnetic Moment

Hiroyuki A. Torii^{1*}, on behalf of the MuSEUM Collaboration

¹School of Science, The University of Tokyo, Tokyo, Japan

* torii@radphys4.c.u-tokyo.ac.jp

Muonium (Mu) is a hydrogenlike exotic atom composed of a positive muon and an electron (μ^+e^-). It is a suitable probe with its hyperfine structure (HFS) for a precise determination of the magnetic moment and thus the mass of the muon, a lepton particle, which leads to a rigorous test of bound-state quantum electrodynamics (QED) and weak interactions, as well as a search for new physics beyond the Standard Model of particle physics. MuSEUM collaboration has so far succeeded in measuring the ground-state HFS of the Mu atom under the zero magnetic field, and is now aiming at a precision of 2 ppb (2×10^{-9}) under strong magnetic fields to surpass the last world record, using a newly operational high-intensity muon beam line at J-PARC in Japan.

Figure 1 shows a schematic of our experiment. The pulsed muons polarized antiparallel to the beam direction are injected into a krypton (Kr) gas target and stopped inside. Each muon captures an electron after collisions to form a Mu atom. Microwave-induced resonant transition between hyperfine levels flips the μ^+ spin, manifesting itself as an increase in the number of positrons due to μ^+ decay to be detected downstream.

Over a decade, we have elaborated our experimental techniques with the gas chamber, microwave cavity, positron detectors, etc. In addition to our technical hardware developments to reduce systematic uncertainties, as well as our systematic studies on the energy shift of the hyperfine levels due to interatomic Mu–Kr collisions, we have made significant improvements in the data analysis. In contrast to standard spectroscopy, which determines the resonance centre frequency by fitting the resonance curve, our new technique, named Rabi-oscillation spectroscopy [1], does not require any frequency scanning, eliminating systematic uncertainties due to possible power fluctuations. The resonance frequency can be obtained directly from the time evolution of the Rabi oscillation at a fixed frequency of the applied electromagnetic wave.

We are also studying the muonic helium atom ($\mu^- \alpha e^-$), which is also hydrogenlike with a pseudo-proton composed of a negative muon and a helium nucleus ($\mu^- \alpha$), using the same method of hyperfine spectroscopy [2]. We have started our experiments for Mu under a strong and highly uniform magnetic field of 1.7 T produced by a superconducting solenoid, with satisfying spectroscopic results. Current achievements and near-future strategies of our experiments will be presented.

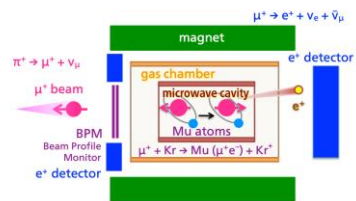


Figure 1. Schematic of the apparatus for the muonium atom spectroscopy experiment.

[1] S. Nishimura et al., *Phys. Rev. A* **104** (2021) L020801.

[2] P. Strasser et al., *Phys. Rev. Lett.* **131** (2023) 253003.

Muonium as a Probe of Point Defects in Type-Ib Diamond

K. Yokoyama^{1*}, J. S. Lord¹, H. Abe², and T. Ohshima²

¹ISIS Neutron and Muon Facility, Rutherford Appleton Laboratory, Didcot, United Kingdom

²National Institutes for Quantum Science and Technology, Takasaki, Gunma, Japan

* koji.yokoyama@stfc.ac.uk

Muonium, a bound state of a positively charged muon and an electron, can diffuse through crystal lattices and interact with defects and impurities. We utilised this property and measured their interaction with point defects in type-Ib diamond. Specifically, we have observed a Mu centre in tetrahedral interstitial sites (Mu_T^0) interacting with substitutional nitrogen atoms (N_s^0) and nitrogen-vacancy (NV) centres in type-Ib diamond samples. Figure 1(a) and (c) show muon spin asymmetry time spectra measured on pristine and NV diamond, respectively. In the pristine sample, the dominant point defect is N_s^0 , which has a single paramagnetic electron. In the NV diamond, part of the N_s^0 atoms in type-Ib diamond is converted to negatively charged NV centres with a pair of coupled electrons. The μSR time spectra were analysed with a simulation, which solves the time evolution of the muon spin using the density matrix method. In this modelling, we have identified the dynamically exchanging Mu system for the pristine and NV sample, as shown in Fig. 1(b) and (d). The electron spin relaxation rate Λ_T^0 carries information on Mu interaction with the paramagnetic N_s^0 centres, whereas the NV data requires a diamagnetic state in the model to take account of Mu abstracting an electron from the NV centres.

This work showcases a successful identification and application of Mu state exchange dynamics in diamond, following our previous work on n-type GaAs [1]. A talk was given on this work in the Hyperfine 2023 conference.

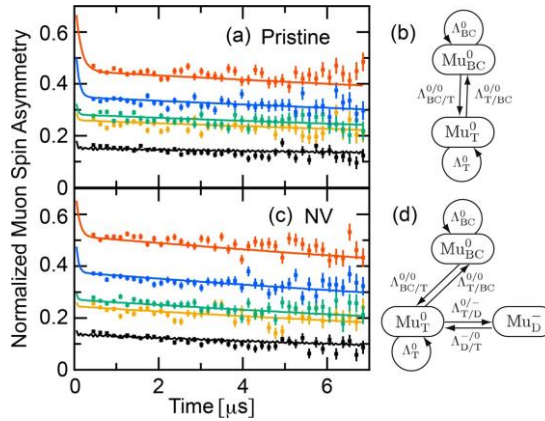


Figure 1. μSR time spectra measured on the (a) Pristine and (c) NV sample at 290 K under five representative longitudinal fields, i.e. 0, 200, 600, 2000, and 4000 G (from the smallest to largest curves in the graphs). Solid lines denote fit results based on the model in (b) and (d) for the pristine and NV sample, respectively.

[1] K. Yokoyama et al., *Phys. Rev. Res.* **6** (2024) 033140.

Interface Resolved Magnetism of Metal-Organic ($\text{Fe}^{57}/\text{C}_{42}\text{H}_{28}$) Thin Films; Studies under X-ray Standing Waves

Manisha Priyadarsini^{1*}, Sonia Kaushik¹, Ilya Sergeev², Dileep Kumar¹

¹UGC-DAE Consortium for Scientific Research, Indore, India

²Deutsches Elektronen-Synchrotron DESY, Notkestraße 85, 22607 Hamburg

*23manisha23@gmail.com

Ferromagnetic/Organic semiconductor (FM/OSC) interfaces, referred to as the spinterface (spin-interface), play a crucial role in achieving high spin polarization, long spin relaxation, and low impedance mismatch in organic spin valve devices [1]. In recent years, probing magnetic spinterface has gained significant interest due to some peculiar properties, such as local hybridization-induced interfacial anisotropy and organic overlayer-induced perpendicular magnetic anisotropy (PMA) [2]. Thus, it necessitates the study of FM/OSC interfaces. In the present study, the depth selective magnetism at the $\text{Fe}^{57}/\text{Rubrene}$ ($\text{C}_{42}\text{H}_{28}$) interfaces has been investigated in the presence of X-ray standing wave (XSW) using the synchrotron-based grazing incidence nuclear resonant scattering (GI-NRS) technique. Based on theoretical simulations utilizing the sample structure, we demonstrate that the antinode regions of XSW in waveguide structures allow for independent measurement of Fe-diffused and Fe-bulk components in the same sample just by changing the incident angle [3]. At these two angles, the time spectra measurements have been taken and fitted in REFTIM. The best fit to the data is obtained by considering three magnetic hyperfine fields (Bhf): 32.5 T, 28.5 T, and 25 T. Among these, the contribution of 32.5 T is maximum at the bulk FM layer, while the other two reduced Bhfs contribute to the diffused Fe layer. This decrease in the hyperfine field at the interface, as compared to bulk, is due to the formation of Fe nanoparticles inside the Rubrene matrix. Additionally, temperature-dependent studies are also conducted on the sample to see the temperature evolution of structure and magnetism. The present work also demonstrates the capability of the GI-NRS technique in depth-resolved magnetic studies, which is otherwise difficult using any other standard lab-based techniques.

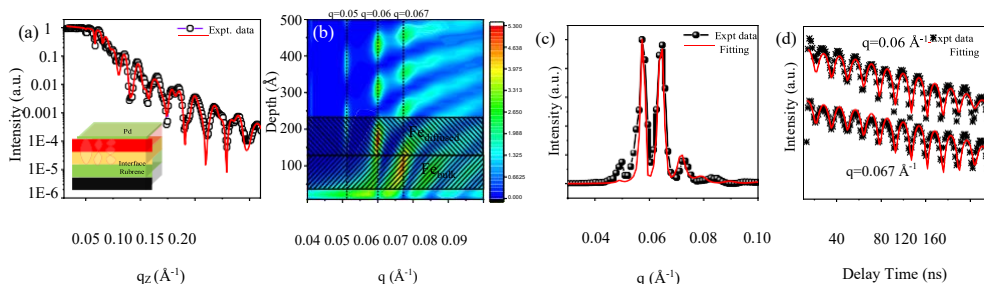


Figure 1. X-ray reflectivity (a), simulated X-ray standing wave structure (b), Nuclear Resonance Reflectivity (c), and time spectra (d), along with their corresponding fitting for the sample.

- [1] I. Bergenti et al., *Nano Mat. Sci.* **1** (2019) .
- [2] K. Bairagi et al., *Phys. Rev. Lett.* **114** (2015) 247203.
- [3] S. Kaushik et al., *Hyperfine Interact.* **242** 1 (2021).

HYPERFINE-ORAL-T06

Critical Temperature and Phonon Evaluation in Hydride Systems Using Computational Methods

Maria-Iulia Zai^{1,2*}, George Alexandru Nemnes^{1,3}, Lucian Ion¹, Victor Leca²

¹Faculty of Physics, University of Bucharest, 405 Atomistilor Street, 077125 Magurele, Romania

²Extreme Light Infrastructure - Nuclear Physics, "Horia Hulubei" National Institute for R&D in Physics and Nuclear Engineering, 30 Reactorului Street, 077125 Magurele, Romania

³"Horia Hulubei" National Institute for R&D in Physics and Nuclear Engineering, 30 Reactorului Street, 077125 Magurele, Romania

*iulia.zai@eli-np.ro

At or near room temperature, superconductivity is a hallmark of certain metallic hydrides, which have been researched extensively over the years [1]. The electron-phonon interactions that underpin the favourable transition temperatures (T_c) of Me_xH_y systems can be theoretically calculated, given sufficient computational resources, along with the structures of novel materials that could exhibit superconductivity. Unfortunately, most hydride compounds are stable only after the application of a pressure of dozens or even hundreds of GPa [2], which renders the experimental validation of their superconductivity difficult.

Using different DFT codes (such as CALYPSO, SIESTA, and ELK), alternative means of identifying the most promising hydride superconductor candidates were investigated via *ab initio* calculations. In the current work, we tested a series of input parameters (with different roles for each used code) derived from experimental superconductor studies in order to calculate the electron-phonon interactions and then estimate the T_c of different hydride compounds, e.g., Cr_xH_y , PdH , and $Pd_{1-x}Cu_xH_y$.

[1] A. M. Shipley et al., *Phys. Rev. B* **104.5** (2021): 054501.

[2] D. Duan et al., *Nat. Sci. Rev.* **4.1** (2017): 121-135.

HYPERFINE-ORAL-T08

Controlling the Isomeric State of Thorium-229 using X-rays

Koichi Okai^{1*}, Michael Bartokos², Kjeld Beeks², Hiroyuki Fujimoto³,
Yuta Fukunaga¹, Hiromitsu Haba⁴, Takahiro Hiraki¹, Yoshitaka Kasamatsu⁵,
Shinji Kitao⁶, Adrian Leitner², Takahiko Masuda¹, Ming Guan¹, Nobumoto
Nagasawa⁷, Ryoichiro Ogake¹, Martin Pimon², Martin Pressler², Noboru Sasao¹,
Fabian Schaden², Thorsten Schumm², Makoto Seto⁶, Yudai Shigekawa⁴, Kotaro
Shimizu¹, Tomas Sikorsky², Kenji Tamasaku⁸, Sayuri Takatori¹, Tsukasa Watanabe³,
Atsushi Yamaguchi⁹, Yoshitaka Yoda⁷, Akihiro Yoshimi¹ and Koji Yoshimura¹

¹Research Institute for Interdisciplinary Science, Okayama University, Okayama, Japan

²Institute for Atomic and Subatomic Physics, TU Wien, Vienna, Austria

³National Institute of Advanced Industrial Science and Techn. (AIST), Tsukuba, Japan

⁴RIKEN Nishina Center for Accelerator-Based Science, RIKEN, Wako, Japan

⁵Graduate School of Science, Osaka University, Osaka, Japan

⁶Institute for Integrated Radiation and Nuclear Science, Kyoto University, Osaka, Japan

⁷Japan Synchrotron Radiation Research Institute, Sayo-cho, Japan

⁸RIKEN SPring-8 Center, Sayo-cho, Japan

⁹RIKEN Center for Advanced Photonics, RIKEN, Wako, Japan

*k_okai@s.okayama-u.ac.jp

The nucleus of thorium-229 has an exceptionally low-lying first excited state at approximately 8 eV, which has been proposed as a promising candidate for a nuclear clock. Due to uncertainties in its transition energy and lifetime, direct excitation using VUV (vacuum ultraviolet) lasers has long been a challenge. In this study, we indirectly populated the isomeric state via X-ray excitation of the second excited state, and successfully determined both its energy and lifetime with sufficient accuracy to guide laser excitation studies. Our findings preceded a series of reports on laser-based direct excitation from other groups worldwide. Experiments were conducted at the SPring-8 synchrotron facility using thorium-doped CaF₂ crystals. The measurement system incorporates a VUV optical path to isolate the signal region and employs anti-coincidence techniques to suppress background events. Band-pass filters mounted before the photomultiplier tube allow wavelength selection. X-ray energies were tuned using a triple silicon monochromator system and evaluated *in situ* with an absolute energy reference, achieving ~50 meV accuracy. Systematic errors were minimized by alternating the X-ray energy between on- and off-resonance during measurement.

This work also reports the first observation of a quenching phenomenon affecting the isomer state [1]. Isomer quench is important to realize a nuclear clock because it enables fast interrogation. X-ray induces this quenching effect for thorium nuclei that are doped in the medium crystal. Our study was conducted using X-rays over a long period. Thus, we continuously investigated the dynamics of the isomeric state, which depends on several features: X-ray intensity, crystal temperature, and the difference between target crystals [2].

Moreover, we built a pulsed VUV laser to directly control the isomeric state and investigate the quenching effect by laser irradiation. Our laser system has already worked to realize direct laser spectroscopy for the nuclei. We are conducting the work to understand the isomeric state's dynamism. The latest progress of this work will be presented in this talk.

[1] T. Hiraki *et al.*, *Nat. Commun.* **15**, (2024) 5536.

[2] M. Guan *et al.*, *Nucl. Instrum. Methods in Phys. Res. B* **562** (2025) 165647.

HYPERFINE-ORAL-T08

Development of a Novel Nuclear Medicine Imaging Method with Local Microenvironment Sensing Based on Ultrasound-Guided Double-Photon Angular Correlation

Mizuki Uenomachi^{1*}, Yoshiki Tamai², Kenji Shimazoe², Ayumu Ishijima³

¹Institute of Science Tokyo, Japan, ²University of Tokyo, Tokyo, Japan

³Hokkaido University, Hokkaido, Japan

*uenomachi.m.4403@m.isct.ac.jp

Nuclear medicine modalities such as Positron Emission Tomography and Single Photon Emission Computed Tomography can visualize the distribution of radio tracers within the human body. However, these conventional methods cannot acquire local microenvironment information. Recently, we have proposed and demonstrated a novel nuclear medicine imaging method with pH sensing using cascade nuclides [1]. This method visualizes the accumulation of tracers using double-photon coincidence detection and mechanical collimators, while also extracting local microenvironmental information from the variations in angular correlation distribution based on the principle of perturbed angular correlation (PAC). Moreover, we have succeeded to demonstrate the variations in angular correlation distribution of $^{111}\text{InCl}_3$ solutions by irradiating ultrasound [2]. In this study, we propose a novel position localization method with local microenvironment sensing using pulsed ultrasounds and PAC.

The position is localised by measuring the time difference between the initiation of pulsed ultrasound irradiation and the timing of changes in angular correlation. The angular correlation of ^{111}In was measured using eight 8×8 array GAGG ($\text{Cd}_3(\text{Al,Ga})_5\text{O}_{12}(\text{Ce})$) detectors coupled with silicon photomultipliers arranged in a ring configuration. The frequency of ultrasound waves was set to 1 MHz [2]. A pulse repetition interval and a pulse width were set to 30 μs and 10 μs , respectively. The source position was shifted in 1.00 mm steps from 12.00 mm to

15.00 mm above the bottom surface (see Fig.1 (a)), corresponding to the focused ultrasound's approximate focal region. At each position, pulsed ultrasound was irradiated for 180 minutes. The results of position localization are shown in Fig.1 (b). Each colored point corresponds to a time window shift based on the ultrasound arrival time. The vertical axis represents the ratio of the angular correlation ratio values at 180 and 90 degrees. The horizontal axis positions were calculated assuming the speed of ultrasound in water to be 1,500 m/s. We successfully localised the position using pulsed ultrasound and variations in angular correlation.

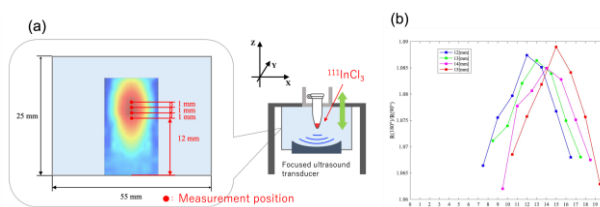


Figure 1.(a) Experimental setup. (b) Results of measurements of angular correlations and estimated positions.

[1] K. Shimazoe, et al., *Commun. Phys.*, **5**(1) (2022) 18.

[2] F. Sensui et al., *JINST*, **18**(04) (2023) C04001.

Abstracts of Poster Contributions



ICAME Posters

ICAME-T01-P1

High-pressure Studies on Zintl-type Europium Compounds with Unconventional Magnetic and Topological States

Ke Yuan Ma¹, Lifen Shi¹, Peter Adler¹, Sergey A. Medvedev¹, Claudia Felser¹,
Aleksandr Chumakov², Samuel Gallego-Parra²

¹Max Planck Institute for Chemical Physics of Solids, Dresden, Germany

²ESRF – The European Synchrotron, Grenoble, France

*adler@cpfs.mpg.de

Ternary Zintl-type europium compounds EuMX_2 exhibit a plethora of structural, electronic, and magnetic properties owing to the coexistence of an ionic magnetic sublattice of Eu^{2+} ions and a covalent $M\text{-X}$ sublattice. An important question is how the coupling between the two sublattices controls their physical properties. Complex electronic and magnetic properties may emerge if M is a magnetic transition metal (TM) ion, as for example in EuFe_2As_2 [1]. Recently, Eu compounds have found much interest as topological materials like Dirac or Weyl semimetals, as they present the possibility to tune the topology of the band structure through the magnetic structure of the Eu sublattice [2].

In this contribution, we present our high-pressure studies on the correlation between electronic behaviour, magnetic order, Eu valence, and structural properties of the two exemplary Zintl-type compounds EuMn_2P_2 and EuCuAs . Both compounds were investigated by transport studies, ^{151}Eu nuclear forward scattering (NFS), and by single crystal synchrotron x-ray diffraction (SXRD) experiments using diamond anvil cell techniques. At ambient pressure, EuMn_2P_2 is an insulator with a trigonal $P3\text{-}m1$ crystal structure and A-type antiferromagnetic ordering of the Eu^{2+} sublattice, while the Mn sublattice does not feature long-range magnetic order [3]. Near 5 GPa, EuMn_2P_2 starts to evolve towards a metallic state, and near 10 GPa, a structural phase transition and a valence transition from Eu^{2+} to Eu^{3+} are observed. The latter is accompanied by a loss of magnetic order at the Eu sites, as is evident from the NFS spectra in Figure 1, while the transport data suggest magnetic correlations at the Mn sites. EuCuAs is a semimetallic topological system exhibiting complex spin structures and a giant topological Hall effect [4]. Our SXRD studies reveal a structural phase transition near 13 GPa from $P63/mmc$ to $Pnma$, while our temperature and field-dependent NFS studies indicate a transition from antiferromagnetic to ferromagnetic order below 13 GPa and a change in spin structure in the $Pnma$ phase

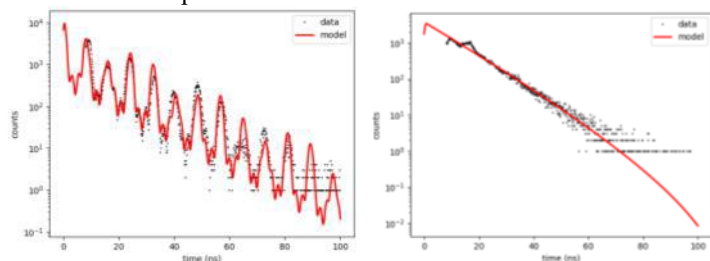


Figure 1. ^{151}Eu NFS spectra of EuMn_2P_2 . Left: At 4 K and 0.5 GPa. Right: at 4.8 K and 15.5 GPa.

[1] K. Matsubajashi et al. *Phys. Rev B* **84** (2011) 024502.

[2] N. H. Jo, *Phys. Rev. B* **101** (2020) 140402 (R).

[3] T. Berry et al., *J. Am. Chem. Soc.* **145** (2023) 4527.

[4] S. Roychowdhuri et al., *J. Am. Chem. Soc.* **145** (2023) 12920.

Structural and Magnetic Properties of Zn Doped CoFe_2O_4 Nanoparticles Prepared with Sol-Gel Auto-Combustion

M. Al-Maashani^{1*}, A.M. Gismelseed², K.A.M. Khalaf³, A.D. Al-Rawas²,
H.M. Widatallah², M.E. Elzain², A.A. Yousif²

¹ Department of Engineering and Technology, College of Engineering and Technology,
University of Technology and Applied Science, P.O. Box 211, Code 69, Oman

² Department of Physics, College of Science, Sultan Qaboos University, P.O. Box 36,
Code 123, Oman

³ Department of Mathematical and Physical Sciences, College of Arts and Sciences,
University of Nizwa, P.O. Box 33, Code 616, Oman

*mohammed.almaashani@utas.edu.om

Single phased nanocrystalline of zinc substituted cobalt ferrite with a formula ($\text{Zn}_x\text{Co}_{1-x}\text{Fe}_2\text{O}_4$, $x = 0.0, 0.2, 0.4, 0.6, 0.8$ and 1.0) were prepared via sol-gel auto-combustion method and the effect of zinc concentration on structural and magnetic properties were investigated using X-Ray Diffraction (XRD), Energy Dispersive Spectroscopy (EDS), Fourier Transfer Infra-Red (FTIR), Scanning Electron Microscopy (SEM), Transmission Electron Microscopy (TEM), , and Vibrating Sample Magnetometer (VSM). Hyperfine interactions of all samples were studied using Mössbauer Spectroscopy (MS). The unit cell parameter a increases significantly from 0.837 to 0.843 nm with increasing concentration of zinc due to the larger ionic radii of the Zn^{2+} ion. The FTIR spectra show a strong absorption band in the range of 545–575 cm^{-1} , corresponding to the tetrahedral site, and it seems to decrease by increasing zinc concentration, indicating the replacement of Co^{+2} (0.74 Å) and Fe^{+3} (0.67 Å) by Zn^{+2} (0.82 Å) in this site. SEM and TEM show a gradual segregation with zinc concentration and an increase in porosity, due to nonmagnetic ion Zn^{+2} ; also, the decrease in particle size distribution is noticed from 100 to 10 nm. The Mössbauer spectra at 295 K reveal the effect of zinc after $x = 0.4$ as a superparamagnetic doublet of zinc ferrite, shown in $x = 0.6$. Hysteresis loops show a significant change in saturation magnetization (M_s) and coercivity (H_c). M_s first increases from 39 to 49 emu/g at $x = 0.4$, and then decreases to reach about 3 emu/g for pure zinc ferrite. H_c shows a sudden decrease from 1450 Oe for pure cobalt ferrite to 60 Oe for pure zinc ferrite. The source of such behavior could be the variation of exchange interaction between the tetrahedral [A] and the octahedral [B] sites.

Evolution of Hyperfine Parameters of Spinel vs. Inversion Degree Parameter by DFT

V. Bilovol^{1*}, A.M. Mudarra Navarro^{2,3}, L.A. Errico^{2,3}

¹Academic Centre for Materials and Nanotechnology, AGH University of Krakow,
Al. Mickiewicza 30, 30-059, Krakow, Poland

²Departamento de Física, Facultad de Ciencias Exactas, Universidad Nacional de La Plata
(UNLP) and Instituto de Física La Plata, IFLP-CONICET CCT-La Plata, 1900, La Plata,
Argentina

³Universidad Nacional del Noroeste de la Provincia de Buenos Aires (UNNOBA),
Monteagudo 2772, 2700 Pergamino, Buenos Aires, Argentina

*vbilovol@agh.edu.pl

Cubic spinel ferrites ($M\text{Fe}_2\text{O}_4$, where M is usually a transition metal) are a class of magnetic semiconducting materials that have proven to be practically useful in a wide range of technological applications. Structurally, these systems exhibit two non-equivalent positions for the cations. Based on the number of surrounding oxygen atoms, the cationic sites are referred to as tetrahedral (A site) and octahedral (B site). The magnetic coupling in ferrites is governed by super-exchange interactions between the metal cations via oxygen atoms, resulting in A-O-A, B-O-B, and A-O-B couplings [1,2]. Consequently, the magnetic properties are strongly influenced by the distribution of the cations across the two magnetic lattices. Understanding this distribution is crucial for designing the material for specific applications.

Two types of ferrites can be distinguished: normal and inverted. In the former, the M ions occupy the A sites, and the Fe ones occupy the B sites. In inverted ferrites, the A sites are populated by Fe ions, while both M and Fe ions occupy the B sites in equal proportions. Between these two extremes, the more common cationic configuration is the partially inverse structure, where both cations occupy both sites in varying amounts. In such a scenario, the system exhibits structural and magnetic disorder, and multiple interactions may be observed. There are no straightforward interpretations, and crude assumptions about site assignments are often made, which can lead to incorrect conclusions. To unravel these complex cases, a realistic theory that assumes different structural and magnetic scenarios can be of great help in adequately interpreting the experimental Mössbauer spectra.

Two systems, CoFe_2O_4 (inverted structure) and ZnFe_2O_4 (normal structure), were theoretically studied to explore the degree of inversion using *ab initio* electronic structure full-potential linearized-augmented plane wave (FPLAPW) [3] calculations within the framework of density-functional theory DFT [4]. The dependence of the isomer shift, hyperfine field, quadrupole splitting, and the magnetic moment at the Fe sites on the number of divalent Co/Zn atoms in both tetrahedral and octahedral sites was calculated. Contrary to data often cited in the literature [5, 6], we found that the hyperfine field value of the Fe atom in the octahedral site increases with an increasing number of nearest divalent cations in both spinels.

- [1] Y. Suzuki, *Annu. Rev. Mater. Res.* **31** (2001) 265.
- [2] A. Goldman, in: *Modern Ferrite Technology*, 2nd Ed., Springer, Boston, MA (2006), 453.
- [3] P. Hohenberg and W. Kohn, *Phys. Rev.* **136**, B864 (1964).
- [4] S. H. Wei and H. Krakauer, *Phys. Rev. Lett.* **55**, 1200 (1985).
- [5] G.A. Sawatzky, F. van der Woude, A.H. Morrish, *Phys. Rev.* **187** (1969) 747-757.
- [6] G. Concas et al., *J. Magn. Magn. Mat.* **321** (2009) 1893-1897.

Influence of Cooling Conditions on Cubicity and Iron Distribution in Novel Copper Ferrites

A. G. Braunsperger^{1*}, M. Reissner¹, A. Tampieri², K. Föttinger²

¹Institute of Solid State Physics, TU Wien, Wien, Austria

²Institute of Materials Chemistry, TU Wien, Wien, Austria

*e11911522@student.tuwien.ac.at

Copper ferrites prepared by a novel combustion method are investigated by ^{57}Fe Mössbauer spectroscopy to get information about the influence of different cooling conditions on the formation of structure and the occupation of iron on the different crystallographic sites. Samples are prepared by a sol-gel combustion method followed by calcination at 950 °C, where they form cubic spinels, whereas at room temperature (RT), the tetragonal structure is more stable. Different cooling conditions are tested to check the completeness of the structure transition during cooling. The samples synthesised in such a method have a composition of $\text{Cu}_{0.87}\text{Fe}_{2.13}\text{O}_4$, as pure-phase stoichiometric CuFe_2O_4 is thermodynamically unstable; CuFe_2O_4 synthesised by a classical coprecipitation method and treated by the same cooling conditions is also investigated for comparison. ^{57}Fe Mössbauer spectra are taken in transmission geometry at room temperature. For one sample, measurements are also performed at 200, 300, and 400 °C. Spectra are analysed by two discrete subspectra according to the two crystallographic sites for iron, but also with hyperfine field distribution functions.

Concerning the structure transition, faster cooling results in a higher degree of cubicity at room temperature (visible in Fig. 1, the samples are arranged with increasing cooling rate). In-situ measurement at 400°C shows that at this temperature the cubic structure is still stable, whereas at 200 and 300°C the structure is tetragonal. This is in good accordance with the results of X-ray investigations.

To get information about the occupation of iron on the different crystallographic sites (A and B), the inversion parameter λ is determined, which gives the ratio of iron on the A and B sites. The tetragonal phase at room temperature forms an inverse spinel AB_2O_4 , where iron is equally distributed over A and B sites. Therefore, λ should be equal to one. At higher temperatures, a random distribution of iron over the two sites is expected, which should give an inversion parameter of two-thirds. The initial spectral analysis indicates deviations from these expectations. While in-situ measurements at higher temperatures show a λ of approximately one, the room temperature spectra indicate lower values. Further, the values are dependent on the cooling conditions of the samples. This unexpected result may point to a more complex diffusion process of iron between the two crystallographic sites.

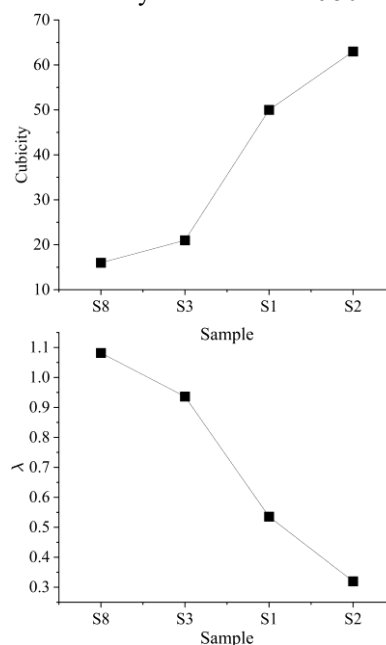


Fig. 1 Cub. and λ against increasing the cooling rate

ICAME-T01-P5

Magnetic and Mössbauer Spectroscopy Studies on the Effect of Oxygen Deficiency on the $\text{CoFe}_2\text{O}_{4-\delta}$ Spinel Ferrites

Benilde F.O. Costa^{1*}, Adel Benali^{1,2*}, Jhon Ipus³, Michael Zelger⁴, Anton Lerf⁴

¹ University of Coimbra, CFisUC, Physics Department, P-3004-516 Coimbra, Portugal

² Laboratoire de Physique Appliquée, Faculté des Sciences, Université de Sfax, B.P. 1171, 3000 Sfax, Tunisia

³ Departamento Física de la Materia Condensada, ICMSE-CSIC, Universidad de Sevilla, P.O. Box 1065, 41080 Sevilla, Spain

⁴ Physics Department, Technical University of Munich, D-85747 Garching, Germany

*benilde@uc.pt

In the present work, $\text{CoFe}_2\text{O}_{4-\delta}$ ($\delta = 0, 0.1, \text{ and } 0.3$) oxygen-deficient spinel ferrite nanoparticles have been synthesized through the auto-combustion method. The structural study, conducted by X-ray diffraction, revealed a cubic structure with the $Fd-3m$ space group. The crystallite size was found to be less than 40 nm for all studied materials. It was also found that the oxygen vacancy induces an increase in magnetization along with a decrease in the ferromagnetic-paramagnetic magnetic transition temperature (T_C).

The samples were studied by Mössbauer spectroscopy at room temperature (RT) and 4.2 K. At RT, besides the sextets ascribed to tetrahedral A and octahedral B sites of the spinel lattice, a quadrupole doublet, whose hyperfine parameters can be ascribed to Fe^{4+} coordination, was also determined. For all samples, the 4.2 K spectra show an asymmetric six-line pattern, fitted with two magnetic components corresponding to the A and B sites of the spinel lattice of the cobalt ferrite, plus a magnetic component corresponding to Fe^{5+} coordination. The observed Fe^{5+} can be due to temperature-dependent charge disproportionation. From the ratio of the intensities of each site, one can infer that the oxygen deficiency substitution increases the occupancy of octahedral B sites. The degree of inversion of the spinel compounds was also determined from those areas.

ICAME-T01-P6

Magnetic Coupling in $\text{MnCo}_{0.65}\text{Fe}_{0.35}\text{P}$ and $\text{MnFeP}_{0.5}\text{Si}_{0.5}$ from ^{57}Fe Mössbauer Spectroscopy

Piotr Fornal^{1*}, Jan Stanek¹, Daniel Fruchart³, Sonia Haj-Khlifa³,
Wiesław Chajec², Ryszard Zach²

¹Marian Smoluchowski Institute of Physics, Jagiellonian University, Łojasiewicza 11,
30-348 Cracow, Poland

²Institute of Physics, Technical University of Cracow, Podchorążych 1, 30-084 Cracow,
Poland

³Institut Néel, CNRS, BP 166, 38042, Grenoble Cedex 9, France

* piotr.fornal@pk.edu.pl

The intermetallic compounds $\text{MnCo}_{1-x}\text{Fe}_x\text{P}_y\text{Si}_{1-y}$ form a new series of materials exhibiting marked magneto-caloric characteristics, which may be proposed to develop environment-friendly cooling systems.

The present communication aims to extend previous works addressed to structural and magnetic investigations [1-3]. Mössbauer analyses in transmission mode for $\text{MnCo}_{0.65}\text{Fe}_{0.35}\text{P}$ and $\text{MnFeP}_{0.5}\text{Si}_{0.5}$ were performed at low temperature in the 80-310 K range. Besides, $\text{MnCo}_{0.65}\text{Fe}_{0.35}\text{P}$ was investigated at temperatures up to 773 K.

For $\text{MnCo}_{0.65}\text{Fe}_{0.35}\text{P}$, magnetically different Fe environments were accounted for, owing to the three different local Fe-Co configurations of the nearest metal sites Fe-Fe-Fe, Fe-Fe-Co, and Co-Fe-Co, with respective populations 0.12, 0.46, and 0.42. At 270 K, the magnetic sub-spectrum with relative intensity of 0.46 collapses into a single line, which points out the paramagnetic state due to the partial cancellation of the positive (Fe-Fe) and negative (Fe-Co) exchange interactions. The two other configurations, Co-Fe-Co and Fe-Fe-Fe, remain magnetic until 373 K and 573 K, respectively.

Fe is located within a site sharing 3f tetrahedra formed in $\text{MnFeP}_{0.5}\text{Si}_{0.5}$ around (Si,P) atoms. So five local configurations: Si_4 , Si_3P , Si_2P_2 , SiP_3 and P_4 can be distinguished. The probability of each configuration may be calculated from the binomial distribution, $p(i, x) = \binom{2}{i} x^i (1-x)^{2-i}$, where $i = 0, 1, 2, 3, 4$ is the number of P atoms forming the tetrahedron. So $p(0, 0.5) = p(4, 0.5) = 0.0625$, $p(1, 0.5) = p(3, 0.5) = 0.25$, and $p(2, 0.5) = 0.375$. Besides, the related five overlapping Zeeman sextets determine the complex Mössbauer spectra but their assignment to particular configurations is not obvious. However, reference to early works [2,3], substitution of P by Si appears leading to a minor impact on the overall iron magnetic couplings.

In summary, the broad distribution of the hyperfine fields in the studied single-phase ternary compounds appears related to the statistical distribution of Fe-Co and P-Si pairs around the 3f tetrahedral Fe site.

[1] R. Zach et al., *J. Phys. Cond. Matt.* **19**, (2007), 376201.

[2] S. Haj-Khlifa et al., *J. Alloys Compd.* **652** (2015) 322–330.

[3] D. Fruchart et al., *Crystals* **9** (2019) 37.

ICAME-T01-P7

Structural Analysis and Magnetic Properties of Nickel Doped Cobalt Nano-Ferrite

Abbasher. M. Gismelseed^{1*}, M. Al-Maashani², AD Al-Rawas¹, H. M. Widadallah¹, I Al Yahmadi¹, F. Bzour¹, and M.E. Elzain¹

¹ Department of Physics, College of Science, Sultan Qaboos University, P.O. Box 36, Code 123, Oman

² Department of Engineering and Technology, College of Engineering and Technology, University of Technology and Applied Science, P.O. Box 211, Code 69, Oman

*abbasher@squ.edu.om

A series of Nickel Doped Cobalt Nano-Ferrite $\text{Ni}_x\text{Co}_{1-x}\text{Fe}_2\text{O}_4$, (NCFO) ($0.2 \leq x \leq 1.0$) prepared by the sol-gel combustion method, have been studied using X-ray diffraction, scanning electron microscopy (SEM), transmission electron microscopy (TEM), vibrating sample magnetometer VSM, and Mössbauer spectroscopy (MS) techniques. X-ray diffraction patterns show that the samples have a cubic spinel structure. Using the MAUD program, the lattice constant obtained decreased from 8.368 to 8.334 Å for pure NFO, and the calculated crystallite size was in the range of 29–43 nm. The obtained average particle size was measured using transmission electron microscopy (TEM), and it was found to be decreased from 85 nm at $x = 0.2$ to 30 nm for $x = 1.0$.

Mössbauer spectra of all samples measured at 295 K and 78 K showed two resolved magnetic patterns, interpreted in terms of the octahedral [B] and tetrahedral [A] sites occupancies. The magnetic hyperfine field of the octahedral site is slightly increasing with increasing Ni contents, and it is almost constant for the tetrahedral site.

Hysteresis loops were measured at room temperature. A linear decrease in the saturation magnetization (M_s) and coercivity (H_c) with nickel concentrations was observed for NCFO nanoparticles. The abrupt decrease in blocking temperature was observed for the samples with $x \geq 0.8$. The linear increase in Curie temperature (T_c) from 814 to 841 K was observed when nickel concentration was increased from $x = 0.2$ to $x = 1.0$.

ICAME-T01-P8

⁶¹Ni Synchrotron-Radiation-Based Mössbauer Spectroscopy of Nd(Co_{1-x}Ni_x)₂P₂

Azumi Ishita^{1*}, Ryo Masuda², Nobumoto Nagasawa³, Yoshitaka Yoda³, Satoshi Tsutsui^{3,4}, Yoshio Kobayashi^{1,5,6}, Jin Nakamura¹

¹ Dept. Fundamental Sci. Eng., Univ. Electro-Commun., Chofu, Tokyo, Japan

² Grad. Sch. Sci. Tech., Hirosaki Univ., Hirosaki, Aomori, Japan

³ Japan Synchro. Radia. Res. Inst. (JASRI), SPring-8, Sayo, Hyogo, Japan

⁴ Inst. Quant. Beam Sci., Grad. Sch. Sci. Tech., Ibaraki Univ., Hitachi, Japan

⁵ Div. Arts Sci., Int. Christ. Univ., Mitaka, Tokyo, Japan

⁶ RIKEN Nishina Center, Wako, Saitama, Japan

*a.ishita@pac.pc.uec.ac.jp

The ThCr₂Si₂-type intermetallic compound NdCo₂P₂ consists of alternating Nd and Co₂P₂ layers. Both Nd and Co possess magnetic moments, resulting in a complex magnetic structure. M. Reehuis *et al.* have reported [1], based on magnetization and neutron diffraction measurements, that Co moments order antiferromagnetically at $T_N = 309$ K, and the Nd moments gradually order antiferromagnetically below 100 K. On the other hand, the temperature dependence of the inverse magnetic susceptibility in NdNi₂P₂ has been reported by W. Jeitschko and M. Reehuis [2], and the positive Curie-Weiss temperature of approximately 10 K suggests a possible ferromagnetic interaction between Nd moments.

In this study, polycrystalline samples of Nd(Co_{1-x}Ni_x)₂P₂ were synthesized by the solid-state reaction method. X-ray diffraction and magnetization measurements were carried out. In addition, ⁶¹Ni synchrotron-radiation-based (SR-based) Mössbauer spectroscopy was performed at beamline BL35XU of SPring-8 to investigate the electronic state of Ni substituted for the Co site in NdCo₂P₂, using samples with $x = 1$, 0.8, and natural Ni metal for comparison.

Figure 1 shows ⁶¹Ni SR-based Mössbauer spectra of NdNi₂P₂ at several temperatures. For the $x = 1$ sample, the spectra at 20 and 7 K were well reproduced using a single Ni component with a small electric field gradient interaction. The magnitude of the e^2qQ_g was estimated to be 0.62 ± 0.09 mm/s, in which the line width observed in the natural Ni experiment ($2\Gamma \sim 0.81$ mm/s) was used. In contrast, at 3.5 K, where magnetic ordering of Nd was observed in magnetization measurements, the spectrum was slightly broadened, which may be attributed to a magnetic hyperfine field transferred from the ordered Nd magnetic moment. The results of ⁶¹Ni SR-based Mössbauer spectroscopy will be discussed in relation to structure and magnetization measurements.

[1] M. Reehuis *et al.*, *J. Phys. Chem. Solids*.

54, 469 (1998).

[2] W. Jeitschko and M. Reehuis, *J. Phys.*

Chem. Solids **667**, 48 (1987).

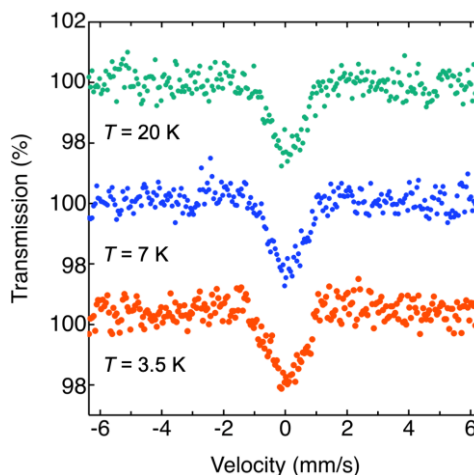


Figure 1. ⁶¹Ni SR-based Mössbauer spectra of NdNi₂P₂ at several

ICAME-T01-P9

Static and Dynamic Magnetic Properties in the Li-rich Antiperovskite (Li_2Fe)ChO (Ch = S, Se)

F. Seewald¹, F.L. Carstens², T. Schulze^{1,3}, N. Gräßler³, M.A.A. Mohamed³, S. Hampel³, L. Singer², R. Klingeler², H.-J. Grafe³, H.-H. Klauss^{1*}

¹IFMP, Faculty of Physics, TU Dresden, Germany

²Kirchhoff Institute for Physics, Heidelberg University, Germany

³Leibniz Institute for Solid State and Materials Research IFW Dresden, Germany

*henning.klauss@tu-dresden.de

Lithium transition metal (TM) oxides are standard electrode materials for Li-ion batteries [1]. The recently discovered lithium-rich antiperovskites (Li_2Fe)SeO and (Li_2Fe)SO host Li and Fe ions on the same atomic position, which octahedrally coordinate to central O^{2-} ions (see Fig. 1, left panel) [2,3]. In an antiperovskite, these sites form interpenetrating Kagome planes along $\langle 111 \rangle$ directions with triangular coordination, which, for a diluted magnetic lattice, are magnetically highly frustrated for antiferromagnetic exchange interactions. Despite their compelling properties as high-capacity Li-ion battery cathode materials, very little is known about their electronic and magnetic properties. We report static magnetization, Mössbauer, and NMR studies on both compounds.

Our data reveal a Pauli paramagnetic-like behaviour, a long-range antiferromagnetically ordered ground state below 50 K, and a regime of short-range magnetic correlations up to 100 K. Our results are consistent with a random Li-Fe distribution on the shared lattice position. In addition, Li-hopping is observed above 200 K with an activation energy of $E_a = 0.47$ eV. Overall, our data elucidate magnetism on a disordered frustrated magnetic lattice with thermally induced ion diffusion dynamics.

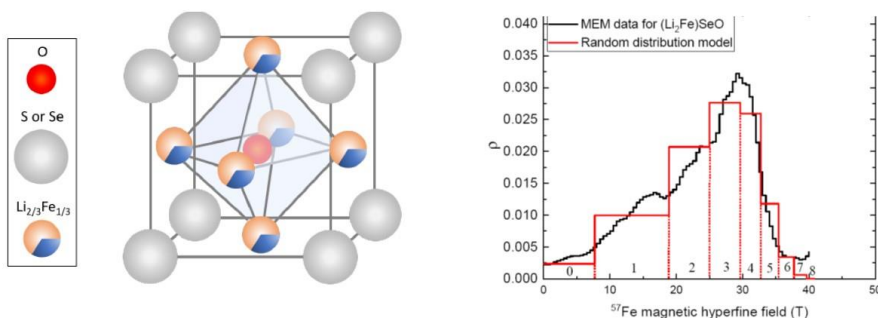


Figure 1. (left) lattice structure of (Li_2Fe) antiperovskite. (right) low temperature ^{57}Fe hyperfine field distribution compared with the frustrated random occupation model

- [1] A. Manthiram, *Nat. Commun.* **11**, 1550 (2020)
- [2] K. T. Lai, I. Antonyshyn, Y. Prots, and M. Valldor, *JACS* **139**, 9645 (2017)
- [3] M. A. A. Mohamed, H. A. A. Saadallah, I. G. Gonzalez-Martinez, M. Hantusch, M. Valldor, B. Büchner, S. Hampel, and N. Gräßler, *Green Chem.* **25**, 3878 (2023)

ICAME-T01-P10

Magnetic-field-induced Multiferroic BaHoFeO₄ - Mössbauer and NPD Spectroscopy Study

Tomáš Kmječ^{1*}, Jaroslav Kohout¹, D.P. Kozlenko²

¹ FMP, Charles University, V Holešovičkách 2, 180 00 Prague 8, Czech Republic

² Frank Laboratory of Neutron Physics, JINR, 141980 Dubna, Russia

* tomas.kmjec@matfyz.cuni.cz

Magnetic-field-induced multiferroic materials have drawn significant attention for fundamental physical research and their application potential.

Polycrystalline BaHoFeO₄ pellets were prepared by the solid-state method and ground in a ball mill. The Rietveld refinements of XRD and neutron diffraction data revealed that BaHoFeO₄ adopts the orthorhombic *Pnma* (No. 62) crystal structure, which remains unchanged upon cooling to 3 K. Fe³⁺ ions occupy two different crystal environments: FeO₅ square pyramids (site Fe¹) and FeO₆ octahedra (site Fe²).

The room temperature transmission Mössbauer spectrum of BaHoFeO₄ consists of two doublets, D₁ and D₂, with close values of isomer shift (δ), but with markedly different quadrupole splitting (Δ). The doublet D₁ corresponds to the ferric ions in the octahedral surrounding (Fe²O₆), and the second doublet D₂ can be attributed to the ferric ions in square pyramids (Fe¹O₅). Furthermore, Mössbauer spectra of BaHoFeO₄ were acquired at low temperatures ranging from 4.2 to 55 K. The paramagnetic doublets remain unchanged until $T_{N1} \sim 47$ K (in accordance with data in [1, 2]). The magnetic sextets appear in the spectra below T_{N1} as an indication of the onset of the magnetic ordering of iron ions. The spectra between T_{N1} and T_{N2} could be fitted by two sextets with very broad distributions of the hyperfine magnetic fields. This behaviour indicates the antiferromagnetic ordering of iron magnetic moments described as incommensurate spin-density waves [2]. Below the transition temperature $T_{N2} \sim 37$ K [1, 2] in zero external magnetic field, the respective lines of the spectra are narrowed. They could be decomposed into two well-resolved sextets, S₁ and S₂, corresponding to the two non-equivalent Fe³⁺ sites. Observation is consistent with a commensurate antiferromagnetic structure below T_{N2} [2].

To understand the magnetic origin in different temperature intervals, the magnetic ground state structures have been investigated by refining NPD patterns at selected temperatures around phase transitions. The NPD pattern at 42 K displays magnetic contributions at 2θ positions of 13.4°, 13.9°, and 20.7°, which can be indexed to an incommensurate magnetic propagation vector $k_1 = (0, 0, 0.329(7))$. Each unique Fe or Ho $4c$ site splits into two orbits, with magnetic symmetry coupling only between pairs separated by $\Delta z = 0.5$. The splitting suggests no symmetry coupling within individual Fe/Ho rings, while the interchain coupling is governed by magnetic symmetries within a given irrep. Upon further cooling, the NPD pattern at 25 K, below T_{N2} , shows sharp changes, including the appearance of new magnetic peaks. The Fe ions form a collinear AFM spin configuration within the Fe₄O₁₈ rings. Upon cooling to 15 K, the ordered magnetic moments of Fe ions and Ho₁/Ho₃ ions gradually increase, with insignificant deviations from their initial directions.

[1] A. A. Belik et al., *Journal of Alloys and Compounds* **922** (2022) 166297.

[2] C.H. Prashanth et. al. *Journal of Alloys and Compounds* **942** (2023) 169017

Acknowledgements: We thank Prof. N. T. Dang for providing the sample.

ICAME-T01-P11

Enthalpy of Solution of Palladium in Iron Studied by the ^{57}Fe Mössbauer Spectroscopy

Robert Konieczny^{1*}, Rafał Idczak¹

¹Institute of Experimental Physics, University of Wrocław, Wrocław, Poland

*robert.konieczny@uw.edu.pl

The room temperature ^{57}Fe Mössbauer spectra for binary iron-based $\text{Fe}_{1-x}\text{Pd}_x$ solid solutions, with x in the range $0.010 \leq x \leq 0.066$, were measured by using a constant acceleration POLON spectrometer of standard design. The spectra are presented in Fig. 1. They were analysed in terms of parameters of their components related to unlike surroundings of the iron probes, determined by different numbers of Pd atoms existing in the neighbourhood of iron atoms [1]. Based on the data, we determined the binding energy E_b [1-4] between two Pd atoms in the studied materials Fe-Pd. It was found that the energy is positive, which speaks in favour of the suggestion that palladium atoms interact repulsively in the α -iron (*bcc*) matrix. The obtained E_b values were used to calculate the extrapolated value of E_b for $x = 0$, and then the enthalpy of solution $H_{\text{Fe-Pd}}$ of Pd atoms in α iron. According to findings of [5], the $E_b(0)$ value is simply related to $H_{\text{Fe-Pd}} = -z \cdot E_b(0)/2$, where z is the coordination number of the α Fe crystalline lattice, amounted to 14.

It turned out that the value of $H_{\text{Fe-Pd}}$ determined on the basis of the ^{57}Fe Mössbauer spectra is in qualitative agreement with the corresponding value resulting from Miedema's model of alloys [6] and is at variance with the available calorimetric data [7] for the Fe-Pd system. All the mentioned $H_{\text{Fe-Pd}}$ data are displayed in Table I.

Table I: The enthalpy $H_{\text{Fe-Pd}}$ [eV/atom] of solution of palladium in iron.

Calorimetric data [7]	Miedema's model [6]	This work
0.353	-0.190	-0.381(26)

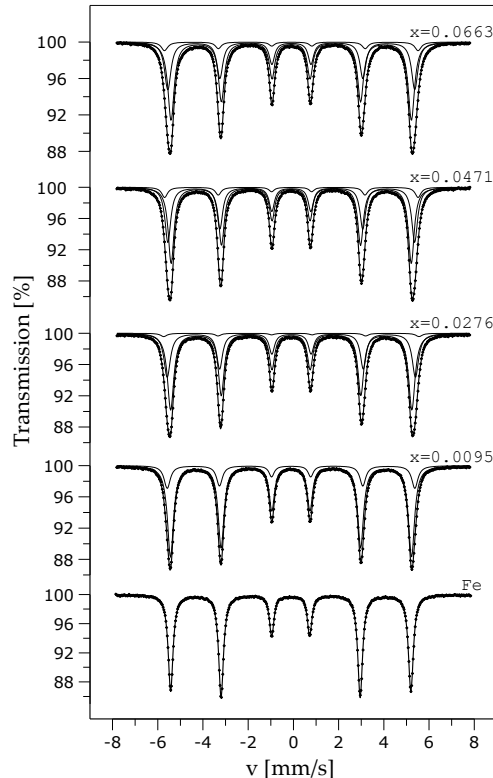


Figure 1. The room temperature ^{57}Fe Mössbauer spectra for $\text{Fe}_{1-x}\text{Pd}_x$ alloys prepared in an arc furnace filled with argon and then cold-rolled to the final thickness of about 0.04 mm, annealed in vacuum at 1270 K for 2 h and finally slowly cooled to room temperature during 6 h.

- [1] A. Błachowski, K. Ruebenbauer and J. Żukrowski, *Physica Scripta* **70** (2004) 368.
- [2] A. Z. Hryniewicz and K. Królas, *Phys. Rev. B* **28**, (1983) 1864.
- [3] J. Chojcan, *J. Alloys Compd.* **264** (1998) 50.
- [4] R. Konieczny, M. Sobota, R. Idczak, *Acta Physica Polonica A* **146** (2024) 239.
- [5] K. Królas, *Phys. Lett. A* **85** (1981) 107.
- [6] A. R. Miedema, *Physica B* **182** (1992) 1.
- [7] R. Hultgren, P. D. Desai, D. T. Hawkins, M. Gleiser, K.K Kelley, *American Society for Metals, MetalsPark (OH)* (197)

ICAME-T01-P12

Structural, Thermal, and Magnetic Characterization of the High-Entropy Alloy (FeCr)_{0.67}(MnNiCo)_{0.33}

Wojciech Nowak^{1,2*}, Dariusz Satuła³, Rafał Idczak¹

¹ Institute of Experimental Physics, University of Wrocław, pl. M. Borna 9, Wrocław, 50-204, Poland,

² Institute of Low Temperature and Structure Research, Polish Academy of Sciences, ul. Okólna 2, Wrocław, 50-422, Poland,

³ Faculty of Physics, University of Białystok, ul. K. Ciołkowskiego 1L, Białystok 15-245, Poland

*wojciech.nowak@uwr.edu.pl

High entropy alloys (HEAs), first proposed independently by Yeh *et al.* [1] and Cantor *et al.* [2], represent a novel class of metallic materials defined by their multi-principal-element compositions and the resulting high configurational entropy. This unconventional structural characteristic promotes the formation of simple solid-solution phases, often leading to unique mechanical, thermal, and functional properties not typically observed in conventional alloys.

The alloy studied in this work, (FeCr)_{0.67}(MnNiCo)_{0.33}, belongs to the family of 3d transition metal-based high-entropy alloys. The selected composition combines elements with distinct magnetic behaviors and varying atomic sizes, providing a platform to investigate the interplay between these characteristics and their effects on the alloy structural evolution, thermal stability, and magnetic response.

To characterize this material, several complementary experimental techniques will be employed. X-ray diffraction (XRD) will be used to identify the phase composition and crystal structure. Microstructural characteristics and elemental distribution will be examined by scanning electron microscopy with energy-dispersive X-ray spectroscopy (SEM-EDX). Calorimetric measurements will provide insight into the specific heat and possible low-temperature anomalies. DC magnetometry will allow investigation of the magnetic behavior, including temperature and field dependence. The ⁵⁷Fe Mössbauer spectroscopy will be applied to probe the local environment and magnetic interactions of iron atoms, offering valuable information on site occupancy, magnetic ordering, and electronic structure.

High-entropy alloys such as this one are promising systems for studying the interplay between composition, structure, and physical properties. Their potential to induce emergent phenomena makes them interesting not only from an application perspective but also as a platform for fundamental research in solid-state physics and materials science.

[1] J.W. Yeh *et al.*, *Adv. Eng. Mater.* **6**, 299 (2004).

[2] B. Cantor *et al.*, *Mater. Sci. Eng. A* **375–377**, 213 (2004).

Investigation of Asymmetrically Induced Magnetism in Pd/Fe/Pd Trilayer System

Bharti Pandit^{1,2*}, Sakshath Sadashivaiah^{2,3}, Anurag K⁴, Thomas Saerbeck⁵,
Sarathlal Koyiloth Vayalil^{4,6}, Ilya Sergeev⁶, Ralf Röhlsberger^{1,2,3,6}

¹Friedrich-Schiller Universität Jena, Institut für Optik und Quantenelektronik, Max-Wien-Platz 1, 07743 Jena, Germany

²Helmholtz-Institut Jena, Fraunhoferstrasse 8, 07743 Jena, Germany

³GSI Helmholtzzentrum für Schwerionenforschung GmbH, Planckstr. 1, 64291 Darmstadt, Germany

⁴Department of Physics, Applied Science Cluster, UPES, Dehradun 248007, India

⁵Institut Laue-Langevin, 71 Avenue des Martyrs, Grenoble Cedex 9 38042, France

⁶Deutsches Elektronen-Synchrotron DESY, Notkestrasse 85, 22607 Hamburg, Germany

*bharti.pandit@uni-jena.de

Magnetic proximity effect (MPE) is a crucial interface phenomenon that significantly influences the spin transport properties in spintronics devices [1]. It arises from the coupling interactions between ferromagnetic-non-magnetic materials exhibiting different long-range magnetic ordering. The strength and characteristics of this interaction are dependent on various factors, including the interfacial hybridization, thickness, and strain in the sample [2–4]. Therefore, it is essential to understand the effect of the structural properties on the MPE. Here, we investigate the MPE across the Pd-Fe interfaces in Pd/Fe/Pd trilayers, influenced by a Ta buffer layer on which the trilayers are grown. Using DC sputtering, Ta (5 nm)/Pd (2 nm)/⁵⁷Fe (2.5 nm)/Pd (4 nm)/Si (110) and Ta (5 nm)/Pd (2 nm)/⁵⁷Fe (2.5 nm)/Pd (4 nm)/Ta (3 nm) /Si (110) thin films were fabricated. Utilizing the polarized neutron reflectivity at instrument D17, ILL, Grenoble, we studied the magnetic moments of the Pd and Fe layers. The MPE is found to be asymmetric, where a higher magnetic moment is induced in the top Pd layer compared to that in the bottom Pd layer. Upon introduction of the Ta buffer layer, x-ray reflectivity indicates that the roughness at the Pd-Fe interfaces reduces. This results in a corresponding decrease in the induced magnetism in the bottom Pd layer. To explore the magnetic structure within the ⁵⁷Fe layer, we follow the changes to the hyperfine field distribution using grazing incidence nuclear resonance scattering performed at various angles of incidence at the beamline P01, PETRAIII, DESY, Hamburg. These changes are then correlated to the modifications of the interface structure. These findings can contribute to the understanding of interface-driven magnetism and offer potential avenues for optimizing spintronic device performance by controlling interface properties.

[1] H. Yang et al., *Nat. Electron* **8** (2024), 15–23.

[2] A. Mukhopadhyay et al., *Phys. Rev. B* **102** (2020), 144435.

[3] S. Mayr et al., *Phys. Rev. B* **101** (2020), 024404.

[4] O. Inyang et al., *Phys. Rev. B* **100** (2019), 174418.

ICAME-T01-P14

Inducing Dilute Magnetism in BaTiO₃ Nanoparticles Through Fe³⁺-doping and Tetragonal-to-Cubic Phase Transition

Sandeep Kumar Singh Patel*

Department of Chemistry, MMV, Banaras Hindu University, Varanasi, India

*skspatel@bhu.ac.in

This study details the sol-gel synthesis and characterization of Fe³⁺-doped BaTiO₃ nanoparticles (BaTi_{1-x}Fe_xO₃, $x = 0$ and 0.10). Fe³⁺-doping induced a structural phase transition from tetragonal to cubic, as evidenced by X-ray diffraction and Raman spectroscopy. X-ray diffraction, Raman, and Mössbauer spectroscopy confirmed that the ferromagnetism in the samples stemmed from defects, rather than secondary phases of metallic iron or iron oxide clusters. Specifically, Mössbauer studies showed a doublet and isomer shifts consistent with high-spin Fe³⁺ ions occupying Ti⁴⁺ sites, leading to changes in the local lattice environment. Room-temperature ferromagnetism was observed in Fe³⁺-doped BaTiO₃, a phenomenon attributed to oxygen vacancies and F-centers. While undoped BaTiO₃ exhibited diamagnetic behavior at room temperature, the Fe³⁺-doped counterparts were ferromagnetic. This induced magnetism in the Fe³⁺-doped BaTiO₃ nanoparticles is linked to a structural phase transformation from tetragonal to cubic, which increases the number of defects, specifically oxygen vacancies. Photoluminescence measurements further supported the presence of these defects. These findings highlight Fe³⁺-doped BaTiO₃ nanoparticles as promising materials for spin-based electronics.

[1] H. Ohno, *Science* **281** (1998) 951.

[2] T. Dietl, *Nature Materials* **9** (2010) 965.

Structural, Magnetic and Surface Characterization of $\text{Fe}_{11}\text{Mn}_2\text{Ga}_3$: an off-stoichiometric Heusler Alloy

O. Morales¹, V.A. Peña², V.M. Rojo^{3,*}, J.E. Prieto³, J.F. Marco³, F. Plazaola⁴, J. Z. Dávalos³

¹Universidad Nacional San Cristóbal de Huamanga, Escuela Profesional de Física y Matemáticas, Ayacucho, Perú

²Universidad Nacional Mayor de San Marcos, Facultad de Ciencias Físicas, Unidad de Post Grado–Ciencia de Materiales. Lima, Perú

³Instituto de Química Física Blas Cabrera. c/Serrano 119-28006, Madrid, Spain

⁴Departamento de Electricidad y Electrónica, Universidad del país Vasco UPV/EHU, Leioa, País Vasco, Spain

*vmrojo@iqf.csic.es

Ternary intermetallic X_2YZ and XYZ compounds, where X represents a transition metal or rare-earth element, Y is a transition metal, and Z is a main-group (p-block) element, are known as full-Heusler and half-Heusler alloys, respectively. In addition to these, Heusler compounds extend into inverse, binary, and quaternary structures, forming a fascinating class of materials with a wide range of versatile and intriguing properties. These properties make them highly relevant for both fundamental research and technological applications, including spintronics/magnetoelectronics, energy technologies, sensors, data storage, superconductors, thermoelectric semiconductors, permanent magnets, and multicaloric effects.

Among these, Fe-Mn-Ga alloys exhibit many of these desirable features and have been extensively studied. In particular, compounds near the stoichiometries of full-Heusler (Fe_2MnGa) and half-Heusler (FeMnGa) alloys have demonstrated intriguing properties, such as tunable topological insulators, ferromagnetic shape memory effects, and giant exchange bias. It is well known that Fe-Mn-Ga alloys exhibit polymorphic crystal and magnetic structures, which vary depending on the preparation conditions. For instance, Fe_2MnGa can crystallize in *fcc*, *bcc*, or hexagonal structures. However, despite numerous studies, the structural and magnetic properties of Fe-Mn-Ga alloys remain a subject of debate.

In this study, we investigate the structural, magnetic, and surface properties of $\text{Fe}_{11}\text{Mn}_2\text{Ga}_3$ a novel off-stoichiometric Heusler alloy synthesized by melting high-purity elements in an argon atmosphere by combining experimental techniques such as X-ray diffraction (XRD), ^{57}Fe transmission Mössbauer spectroscopy at different temperatures, vibrating sample magnetometry (VSM), and X-ray photoelectron spectroscopy (XPS).

ICAME-T01-P16

Magnetic Ordering in Hexagonal EuCuP

D. H. Ryan^{1*}

¹Physics Department and Centre for the Physics of Materials,
McGill University, Montreal, Canada

*dhryan@physics.mcgill.ca

EuCuP crystallizes in the BeZrSi-type hexagonal structure (Space group $P6_3/mmc$ #194) with triangular layers of Eu^{2+} separated by honeycomb CuP layers. These structural motifs have been associated with non-trivial topological states, and so the system has been subjected to an extensive bulk property work-up using commercial automated magnetic property measurement systems [1-3]. The order was shown to be ferromagnetic [1], but a more detailed analysis of the critical behaviour near T_c suggested that the ordering transition might be first-order [3].

Here we present a ^{151}Eu Mössbauer investigation of single-crystal EuCuP grown from tin flux. At 5 K, EuCuP exhibits a conventional magnetically split Eu^{2+} spectrum with $B_{\text{hf}} = 29.90(5)$ T, and an isomer shift (relative to EuF_3) equal to $10.65(2)$ mm/s, confirming the divalent state of the europium. With the quadrupole contribution constrained to the value obtained above T_c , we find the angle between V_{ZZ} and B_{hf} to be 90° , indicating basal-plane ordering. $B_{\text{hf}}(T)$ follows a conventional $J = 7/2$ mean-field model up to about 27 K and then breaks away. However, we do not see the development of a magnetic/non-magnetic coexistence that typically characterizes a first-order transition [4] but rather observe a rapid increase in apparent line width when we fit assuming a single europium site (see Fig. 1).

More detailed analysis [5] to be presented at the meeting shows that the order passes through an incommensurate modulated structure between 27 K and $T_c (= 32.6(1)$ K) to yield an ordering temperature of $34.4(1)$ K.

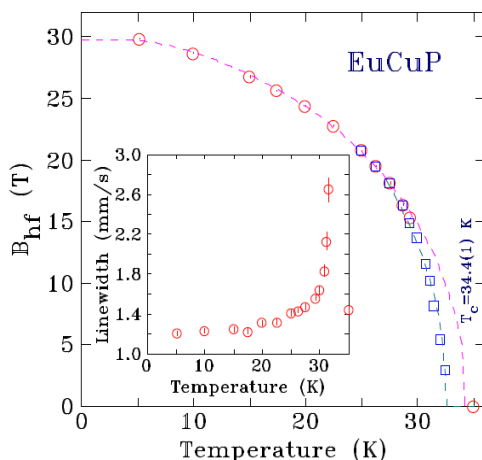


Figure 1. Hyperfine field (B_{hf}) and line width for EuCuP showing the break from $J = 7/2$ mean field behavior is associated with a rapid increase in linewidth.

- [1] Wataru Iha *et al.*, *J. Alloys and Compounds*. **788** (2019) 361.
- [2] Jing Wang *et al.*, *J. Alloys and Compounds*. **947** (2023) 169620.
- [3] Xiaojun Yang *et al.*, *J. Alloys and Compounds*. **1013** (2025) 178589.
- [4] C. Ritter *et al.*, *J. Alloys and Compounds*. **980** (2024) 173573.
- [5] P. Bonville *et al.* *Eur. Phys. J.* **B 21** (2001) 349

Structural and Magnetic Properties of High-entropy FeNiCoPd-X Alloys

A. Sławek^{1*}, K. Berent², J. Cieślak¹

¹Faculty of Physics and Applied Computer Science, AGH University, Kraków, Poland

²Academic Center for Materials and Nanotechnology, AGH University, Kraków, Poland

*annaslawek@agh.edu.pl

High-entropy alloys (HEA) represent a novel class of materials with unique structural and mechanical properties. Their ability to form stable phases with simple crystalline structures has made them a subject of extensive scientific investigation. Most studied HEAs exhibit a multiphase composition, with a few exceptions, such as FeCoNiPd-based systems, which crystallize in a single-phase (*fcc*) structure.

HEAs based on FeCoNiPd exhibit distinctive mechanical and magnetic properties that can be modified through appropriate doping. In this study, the influence of various elemental additions on the microstructure, phase stability, and magnetic properties of FeCoNiPd-X (X = Al, Mn, Ti, Cu, V) alloys was investigated. Special attention was given to doped alloys that retained their single-phase structure despite the introduction of additional elements.

The primary research techniques included X-ray diffraction (XRD), scanning electron microscopy (SEM-EDX), and Mössbauer spectroscopy. Mössbauer spectra were collected at both room temperature and liquid nitrogen temperature to evaluate the local atomic environment and changes in magnetic properties. Specific spectral features, such as significant broadening of the inner sextet lines and asymmetries in their amplitudes and widths, indicate the necessity of analyzing the spectra using three-dimensional distributions of the hyperfine field, isomer shift, and quadrupole splitting, incorporating additional correlations between these parameters.

The results indicate that most of the tested FeCoNiPd-X alloys exhibit a multiphase structure. However, alloys doped with vanadium and copper remain single-phase. The primary effect of doping is observed in the increase in the lattice parameter. Another notable observation is the transition from the magnetic to the paramagnetic state with increasing vanadium concentration.

The obtained results contribute to the broader research on high-entropy alloys, providing further evidence of the significant influence of doping on phase stability and magnetic properties. They confirm that the careful selection of alloying elements enables control over magnetic parameters, which may be crucial for future applications of these materials.

[1] S.A. Krishna et al., *J Manufactur Proc* **109** (2024) 583-606.

[2] J. Cieślak et al., *J Magn Magn Mat* **518** (2021) 167371

[3] J. Kitagawa, *J Magn Magn Mat* **563** (2022) 170024

ICAME-T01-P18

Magnetic Ordering in $(\text{CrFe})_{0.67}(\text{VMnNi})_{0.33}$ High-Entropy Alloy at Low Temperatures

Piotr Sobota^{1,2*}, Wojciech Nowak^{1,2}, Dariusz Satuła³, Rafał Idczak¹

¹Institute of Experimental Physics, University of Wrocław, pl. M. Borną 9, 50-204 Wrocław, Poland

²Institute of Low Temperature and Structure Research, Polish Academy of Sciences, ul. Okólna 2, 50-422 Wrocław, , Poland

³Faculty of Physics, University of Białystok, ul. K. Ciolkowskiego 1L, 15-245 Białystok, Poland

*piotr.sobota2@uwr.edu.pl

High-entropy alloys are the solid solutions of five or more elements mixed with non-negligible proportions (at least 5 at.% each). Contrary to other multi-element materials, high entropy of mixing stabilizes simple crystallographic phases, which in turn exhibit a high order of chemical disorder. These high-entropy effects can have profound consequences on magnetic ordering in the HEA.

Because high entropy can stabilize phases not enthalpically preferred, HEAs may exhibit magnetic orders in compositional ranges inaccessible to binary alloys. Slight compositional changes shift the balance of exchange couplings, allowing gradual tuning of Curie or Neel points over a wide range of temperatures. All of this makes magnetic high-entropy alloys objects of interest in material science and solid state physics.

Different element pairs (e.g., Fe–Cr, Fe–Ni, Cr–Mn) may prefer ferromagnetic, antiferromagnetic, or even diamagnetic coupling. In a disordered HEA lattice, these exchange interactions compete randomly, often preventing simple long-range ferromagnetic or antiferromagnetic order. The competition and randomness can freeze spins into frustrated, glass-like configurations at low temperature, with broad transitions and frequency-dependent AC susceptibility.

We present a comprehensive study of the magnetic behavior in a polycrystalline $(\text{CrFe})_{0.67}(\text{VMnNi})_{0.33}$ high-entropy alloy. The sample was obtained by conventional arc melting. The structure and homogeneity were studied using XRD and SEM-EDXS. Magnetic, specific heat, and Mössbauer spectroscopy measurements in the temperature range 1.8–400 K revealed the presence of magnetic orderings.

Mössbauer Spectrometric Study of SrTiO₃ Doped with Dilute ⁵⁷Fe and Sn

K. Nomura¹, M. Takahashi², Y. Kobayashi³, J. Pechoušek⁴, T. Naka⁵, Y. Koike⁶, J. Okabayashi⁷, C. Barrero⁸, S. Kubuki^{1*}

¹Graduate School of Science, Tokyo Metropolitan University, Tokyo, Japan

²Faculty of Science, Toho University, Chiba, Japan

³Institute for Integrated Radiation and Nuclear Science, Kyoto University, Kyoto, Japan

⁴Faculty of Science, Palacky University Olomouc, Olomouc, Czech Republic

⁵National Institute for Materials Sciences, Tsukuba, Japan

⁶School of Science and Technology, Meiji University, Kanagawa, Japan

⁷Graduate School of Science, The University of Tokyo, Tokyo, Japan

⁸Faculty of Exact and Natural Sciences, University of Antioquia-UdeA, Medellín, Colombia

* kubuki@tmu.ac.jp

Dilute magnetic semiconductors are required to have a Curie temperature above room temperature [1], and to achieve this, wide bandgap semiconductors doped with magnetic ions have been investigated [2]. In this study, we synthesized a strontium titanate (SrTiO₃: STO) doped with 1 at% ⁵⁷Fe³⁺ and several at% Sn⁴⁺ using a complexation/pyrolysis method. The local chemical states of iron were studied by Mössbauer spectrometry. At room temperature (RT), the two doublets due to the paramagnets and a broad relaxation peak were observed. The purpose is to clarify the origin of the broad peak in the low-temperature spectra. The samples were prepared by the decomposition of the ethylene glycol complexes at 500 °C for 2 hours and post-heating for 4 hours until 850 °C. The formation of STO doped with 1 at% ⁵⁷Fe³⁺ and with and without several at% Sn⁴⁺ was mainly confirmed by XRD. VSM and SQUID measurements were carried out for 1 at% ⁵⁷Fe and 0 ~ 4 at% Sn samples. We observed a very weak ferromagnetic behavior for 1 at% ⁵⁷Fe and 0~4 at% Sn co-doped samples. Mössbauer spectra of 1 at% ⁵⁷Fe co-doped STO at RT, 200, 75, 50, and 7 K are shown in Fig. 1. The Mössbauer spectra of doped STO consist of four Fe³⁺ sites; two paramagnetic components and two magnetic relaxation components with different internal fields (about 50 and 20 T). However, when doped with Sn, the larger peak at 50 T becomes broader, indicating that it is significantly affected by Sn. Introducing Fe³⁺ and Sn⁴⁺ to Ti⁴⁺ sites can cause oxygen defects and lattice distortion. The ferromagnetic behavior can be attributed to the formation of clusters incorporating the oxygen vacancies, two Fe³⁺ atoms, and the strain-inducing Sn⁴⁺. In some clusters, Fe³⁺ atoms achieved a long-range order [3,4].

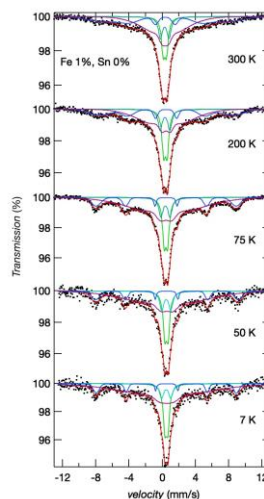


Fig. 1. Mössbauer spectra of 1% Fe-doped STO at 7, 50, 75, 200, and 300 K.

[1] J.M.D. Coey et al., *Nat. Mat.* **172**, 4 (2005).

[2] K. Nomura et al., *Hyp. Int.*, **241**, 6 (2020).

[3] A.M. Mudarra Navarro et al., *Interact.* **245**, 21 (2024).

[4] K. Nomura, et al., *J. Radioanalytic. Nuc. Chem.*, in press.

ICAME-T02-P1

Iron State in Some Dietary Supplements: Control by Mössbauer Spectroscopy

I.V. Alenkina¹, A.V. Chukin¹, G. Leitus², I. Felner³, K. Kovács⁴, E. Kuzmann⁴,
Z. Homonnay^{4*}, M.I. Oshtrakh¹

¹Institute of Physics and Technology, Ural Federal University, Ekaterinburg, Russian Federation

²Department of Chemical Research Support, Weizmann Institute of Science, Rehovot, Israel

³Racah Institute of Physics, The Hebrew University, Jerusalem, Israel

⁴Institute of Chemistry, Eötvös Loránd University, Budapest, Hungary

*homonnay.zoltan@ttk.elte.hu

Various anti-anemic pharmaceutical products contain iron, e.g., iron-containing vitamins and dietary supplements. These pharmaceuticals include different Fe^{2+} or Fe^{3+} compounds such as ferrous fumarate ($\text{FeC}_4\text{H}_2\text{O}_4$), ferrous sulfate (FeSO_4), ferrous gluconate ($\text{C}_{12}\text{H}_{24}\text{FeO}_{14}$), ferric pyrophosphate ($\text{Fe}_4(\text{P}_2\text{O}_7)_3$), etc. The iron state is very important for its efficacy in the body and related to its quality. ^{57}Fe Mössbauer spectroscopy is the most effective tool for determining the iron state based on the ^{57}Fe hyperfine parameters of various compounds and their relative iron fractions in the sample [1].

A study of some fresh dietary supplements containing ferrous fumarate, ferrous sulfate, ferrous gluconate, and ferric pyrophosphate was carried out using Mössbauer spectroscopy as well as X-ray diffraction and magnetization measurements. The results obtained by Mössbauer spectroscopy showed that many dietary supplements contain additional Fe^{2+} or Fe^{3+} compounds whose parameters are different from those announced by the manufacturers (see Figure 1). Observation of these additional compounds may be a result of the initial compounds oxidation or modifications, and instability.

The results obtained showed that Mössbauer spectroscopy is a powerful technique for the control of the iron state in various iron-containing pharmaceutical products.

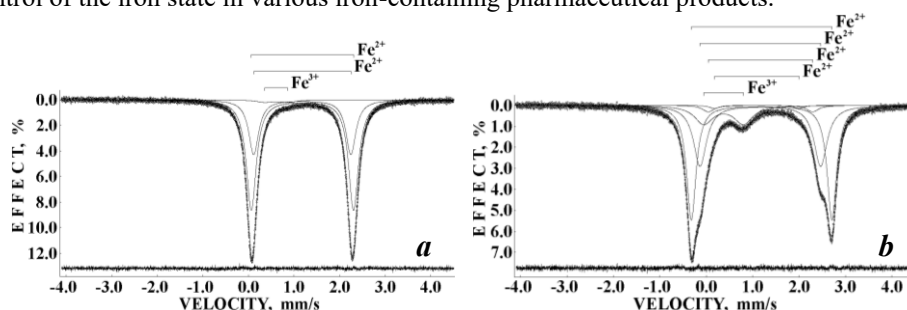


Figure 1. Mössbauer spectra of VAS & Folsav (BGB Interherb Kft., Hungary) with ferrous fumarate (a) and BioCo® (BioCo Magyarország Kft., Hungary) with ferrous gluconate (b). $T=295\text{ K}$.

This work was supported by the Ministry of Science and Higher Education of the Russian Federation, project № FEUZ-2023-0013. M.I.O. and I.V.A. gratefully acknowledge the Ural Federal University Program of Development within the Priority-2030 Program (research funding from the Ministry of Science and Higher Education of the Russian Federation). This work was carried out within the Agreement of Cooperation between the Ural Federal University (Ekaterinburg) and the Eötvös Loránd University (Budapest).

[1] I.V. Alenkina, M.I. Oshtrakh, *J. Pharm. Sci.* **113** (2024) 1426.

ICAME-T02-P2

Synthesis and Modification of Triazole Complexes for Optimized Spin Crossover Properties

Maximilian Seydi Kilic^{1*}, Rene Lucka¹, Justus Pawlak¹, Nele Pannewitz², Isabel Mae Merchant¹, Erika Elliott¹, Hikaru Yoshitake³, Taisei Suzuki³, Yu Odashima³, Takuya Shiga³, Nozomi Mihara³, Masayuki Nihei³, Franz Renz¹

¹Institute of Coordination Chemistry, Leibniz University Hannover, Callinstrasse 9, D-30167 Hannover, Germany

² Institute of Inorganic Chemistry, Leibniz University Hannover, Callinstrasse 9, D-30167 Hannover, Germany

³ Graduate School of Pure and Applied Sciences, University of Tsukuba, Tennodai 1-1-1, Tsukuba, Ibaraki 305-8577, Japan

*maximilian.kilic@acd.uni-hannover.de

Iron(II) triazole complexes offer a variety of possibilities to synthesize coordination compounds with customized spin crossover properties. They are known for their 1D chain structure, which results from the utilization of 1,2,4-triazoles. [1]

These complexes can be modified either by substituting the 4-position of the ligand, exchanging the metal cations, or by selecting the corresponding counterions. Ligands have also already been combined and brought into systems at different ratios. [2] The same applies to counterions. [3] However, these compounds are insoluble, which can make them difficult to incorporate into composite materials. However, previous approaches have shown that the choice of specific counterions can increase the solubility of these systems. [4]

In this study, we first tried to obtain a specific ligand and to combine it with 2-naphthalenesulfonate anions as an iron(II) complex. This should allow the complex to switch between high-spin and low-spin well above room temperature, but remain soluble. A complex was obtained which, according to Mössbauer spectroscopy, was in the low-spin state at room temperature. This newly obtained complex showed an irreversible spin transition, but opens up further possibilities for combining the obtained ligand with others.

[1] O. Roubeau, *Chem. Eur. J.* **18** (2012) 15230–15244.

[2] A. Sugahara, et al., *Inorganics* **5**(3) (2017) 50.

[3] M.S. Kilic et al., *F. European Journal of Inorganic Chemistry* **27**(35) (2024) 474.

[4] J. Brehme, et al., *R. F.* **245**(1) (2024), 10.

ICAME-T02-P3

Investigation of Novel Ethylenediamine-Based Iron(III) Complexes Exhibiting Spin Crossover Behavior by Mössbauer Spectroscopy

Rene Lucka^{1*}, Maximilian Seydi Kilic¹, Besnik Elshani¹, Philipp Buschmann¹, Franz Renz¹

¹Institute of Coordination Chemistry, Leibniz University Hannover, Callinstrasse 9, D-30167 Hannover, Germany

*rene.lucka@acd.uni-hannover.de

The unique spin crossover (SCO) effect has been a subject of intense research due to its fundamental and technological significance in areas such as molecular electronics, data storage, and sensor applications. The presented study focuses on the systematic synthesis, structural variation, and characterization of iron(III) complexes featuring multidentate ligands. In particular, recently reported ethylenediamine-based SCO complexes exhibit a thermally induced spin transition accompanied by a pronounced hysteresis around 150 K, making them highly attractive for potential applications. [1]

By systematically modifying the substitution patterns of the aromatic moieties as well as the structure of the diamine bridge, we aim to fine-tune the ligand field strength and consequently modulate the SCO properties of these compounds. The investigation employs a combination of spectroscopic and crystallographic techniques, with Mössbauer spectroscopy playing a crucial role in elucidating the electronic and spin states of the iron centers. Additionally, the interplay between ligand design and cooperative effects in the solid state is explored to gain deeper insights into structure-property relationships governing the SCO phenomenon.

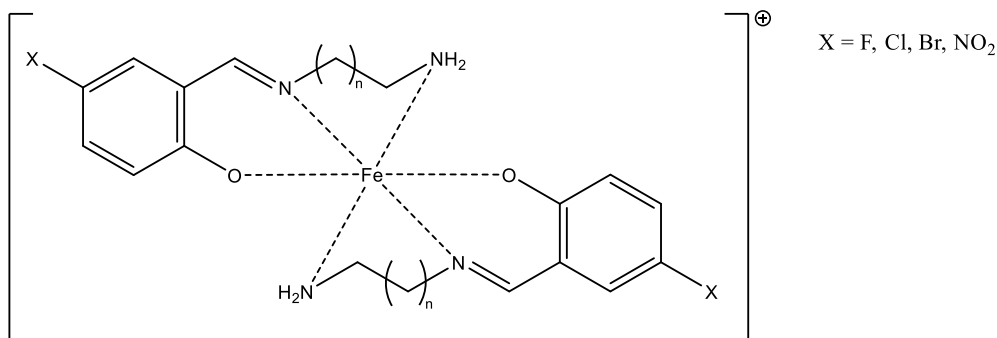


Figure 1. Structure of synthesized compounds.

[1] D. Tesfaye et al., *New J. Chem.*, **48** (2024) 17616-17622.

ICAME-T02-P4

Influence of Ga:Fe Ratio on Structural, Electrical, Magnetic, and Optical Properties of Uniform α -(Fe_{1-x}Ga_x)₂O₃ Particles

Marijan Marcius^{1*}, Stjepko Krehula¹, Luka Pavić¹, Ljerka Kratofil Krehula², Zoltán Homonnay³, Ernő Kuzmann³, Shiro Kubuki⁴

¹ Division of Materials Chemistry, Ruđer Bošković Institute, Zagreb, Croatia

² Faculty of Chemical Engineering and Technology, University of Zagreb, Zagreb, Croatia

³ Faculty of Natural Sciences, Eötvös Loránd University, Budapest, Hungary

⁴ Graduate School of Science and Engineering, Tokyo Metropolitan University, Tokyo, Japan

* mmarcus@irb.hr

Isostructural oxides α -Fe₂O₃ and α -Ga₂O₃ form solid solutions α -(Fe_{1-x}Ga_x)₂O₃ in the whole Ga:Fe range ($0 \leq x \leq 1$) [1]. α -(Fe_{1-x}Ga_x)₂O₃ particles can be transformed by calcination into gallium ferrite (Ga_xFe_{2-x}O₃) [1], Ga-Fe oxide with ferromagnetic and ferroelectric (multiferroic) properties [2]. In this study, α -(Fe_{1-x}Ga_x)₂O₃ particles were prepared by a simple solvothermal method using a 5:1 mixture of ethanol and water as the solvent and sodium acetate (CH₃COONa) as the precipitant. Effects of Ga:Fe ratio on various properties of α -(Fe_{1-x}Ga_x)₂O₃ particles were investigated using ⁵⁷Fe Mössbauer spectroscopy, SEM (Fig. 1) and other techniques.

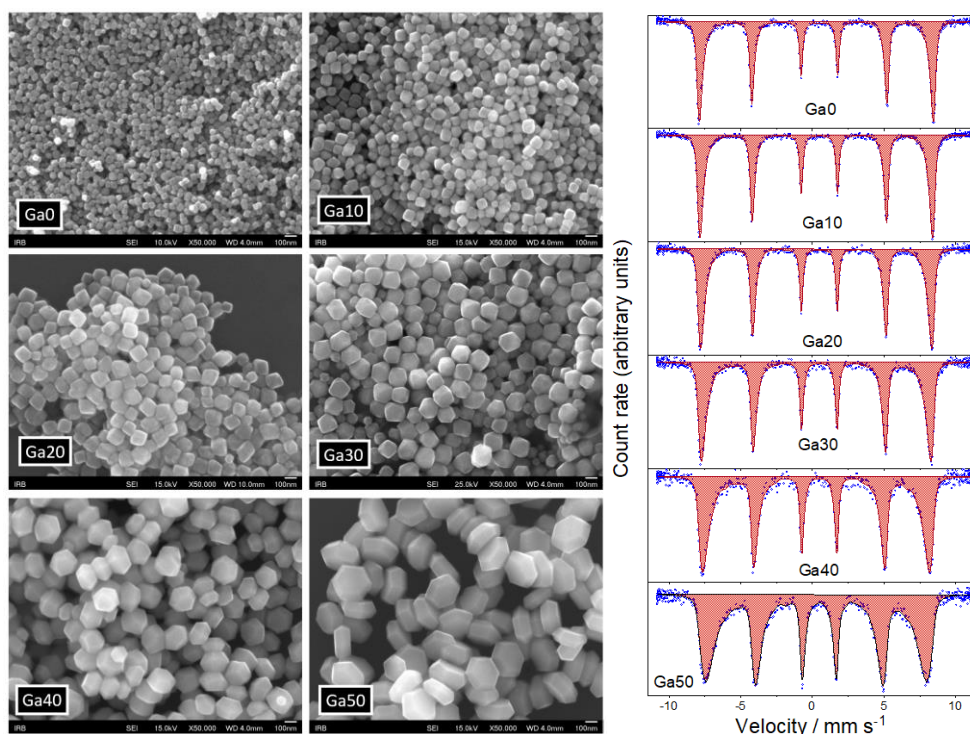


Figure 1. SEM images and ⁵⁷Fe Mössbauer spectra of α -(Fe_{1-x}Ga_x)₂O₃ particles (with 0, 10, 20, 30, 40 or 50 mol% Ga)

[1] S. Krehula et al., *J. Alloys. Compd.* **634** (2015) 130–141.

[2] T. Katayama et al., *Adv. Funct. Mater.* **28** (2018) 1704789.

ICAME-T02-P5

Mössbauer Characterization of Soluble Iron Triazole Complexes

Arthur Sander^{1*}, Samantha Jessica Stanton², Franz Renz¹

¹Inorganic Coordination Chemistry Research Group, Institute for Inorganic Chemistry,
Gottfried Wilhelm Leibniz Universität Hannover, Germany

*arthur.sander@acd.uni-hannover.de

Coordination compounds showing a change of their spin state through external stimuli are called spin crossover compounds. These materials can exist in two different stable spin states, low-spin (LS) and high-spin (HS), and are able to switch reversibly between them in response to external stimuli, including pressure, temperature, and light irradiation. Furthermore, the SCO is accompanied by a change of multiple properties, e.g., magnetism and color [1]. Of particular interest are polymeric complexes of the Fe^{II}Atrz₃ (Atrz = 4-amino-1,2,4-triazole) family because of their hysteretic spin transition at ambient conditions triggered by interesting stimuli like laser-irradiation and temperature [2].

In this work, several new triazole-based spin crossover compounds with an iron(II) center were synthesized and characterized. For this purpose, the salt Fe(NO₃)₂ was used together with novel triazole-based ligands to form complexes that have functional groups at the 4-position of the amino-triazole building block. These were chosen such that the resulting complex exhibited increased solubility in certain solvents. For this purpose, non-polar alkyl chains were selected, which should be soluble in solvents such as chloroform or diethyl ether. Furthermore, iron triazole complexes were prepared, which have linked chain structures due to multidentate ligands. As expected, the complexes synthesized here exhibited high solubility in chloroform, diethyl ether, ethanol, and methanol. The switching behavior of these complexes mostly exhibited a very gradual progression of the spin crossover effect over a very wide temperature range. The prepared ligands were analyzed by ESI-MS and ¹H-NMR to determine the purity. The resulting complexes were then investigated by IR and Mössbauer spectroscopy for their switching behavior. Furthermore, the solubility of these complexes was measured in different solvents.

[1] D. Unruh et al., *Dalton Trans.* **45** (2016) 14008

[2] O. Roubeau, *Chem. Eur. J.* **18** (2012), 15230-15244

ICAME-T03-P1

Fraction on ^{197}Au Mössbauer Spectroscopy of Au Particles Supported on TiO_2 and SiO_2

Yasuhiro Kobayashi^{1*}, Hironori Ohashi² and Makoto Seto¹

¹Institute for Integrated Radiation and Nuclear Science, Kyoto University, Kumatori, Osaka 590-0494, Japan

²Faculty of Symbiotic Systems Science, Fukushima University, Fukushima 960-1296, Japan

* kobayashi.yasuhiro.3x@kyoto-u.ac.jp

The recoilless fraction is a parameter that reflects lattice vibrations and provides important knowledge in physics, chemistry, etc. In ^{197}Au Mössbauer spectroscopy, the energy of γ -rays is higher than ^{57}Fe , so differences and changes in the recoilless fraction appear significantly. We have succeeded in estimating the Debye temperature not from the absolute amount of spectral absorption area but from its temperature dependence curve and estimated that of $\text{Au}(\text{OH})_3$ and Au_2S [1]. We applied this technique to Mössbauer measurements of Au-supported catalysts. The characteristics of Au-supported catalysts change depending on the supporters. To investigate the influences of the supporters on the Au particles, we measured the ^{197}Au Mössbauer spectrum and the recoilless fraction.

Prepared samples were Au particles on a TiO_2 supporter (Au/TiO_2) and Au particles on a SiO_2 supporter (Au/SiO_2). The Au contents were 2~10 wt% in Au/TiO_2 and 2 wt% in Au/SiO_2 . The TiO_2 or SiO_2 powder was put in the HAuCl_4 aqueous solution, and $\text{Au}(\text{OH})_3$ was precipitated on the powder surface by adjusting the pH while stirring. The obtained powder was dried and calcined at 300 °C for 4 hours to prepare the sample [2].

In the ^{197}Au Mössbauer spectra of the Au/TiO_2 and Au/SiO_2 samples, all components showed a single peak like metallic Au. It was found that Au was chemically in the metallic Au state in all samples. No interface or surface components were observed, even in the Au 2wt% Au/TiO_2 sample, which is considered the smallest Au particles.

The Debye temperatures of the Au/TiO_2 samples and the Au/SiO_2 sample obtained from the temperature change of the spectral absorption area. It was close to that of bulk metallic Au in the Au 10 wt% Au/TiO_2 sample. However, it was lower than metallic Au in the Au 2 wt% sample. This is thought to be due to a decrease in the recoilless fraction due to fine particle size. On the other hand, the Au 2 wt% Au/SiO_2 sample had a Debye temperature close to that of metallic Au, suggesting that the particles were not as small as those in Au/TiO_2 . In X-ray diffraction, the peaks of metallic Au were not observed in the 2 wt% Au/TiO_2 sample due to the fine particle size, whereas it was observed in the Au/SiO_2 sample. The results of the recoilless fractions are consistent with the X-ray diffraction. The lattice vibrations affect the adsorption and movement of adsorbed molecules on the Au particle surface. Therefore, it is thought to affect the catalytic activity.

[1] Y. Kobayashi et al., *Interactions*, **245** (2024) 42.

[2] L.X. Dien et al., *Applied Catalysis B: Environmental*, **241** (2019) 539.

ICAME-T03-P2

Magnetic Relaxation Effects in Nanosized Copper Ferrite

Alexander G. Braunsperger¹, Michael Reissner^{1*}, Alberto Tampieri², Karin Föttinger²

¹Institute of Solid State Physics, TU Wien, Wien, Austria

²Institute of Materials Chemistry, TU Wien, Wien, Austria

*e11911522@student.tuwien.ac.at

Magnetic relaxation processes in a copper ferrite sample, synthesized by the coprecipitation method, are investigated using ^{57}Fe Mössbauer spectroscopy, XRD, and magnetic measurements. XRD and Mössbauer investigations confirm a cubic spinel CuFe_2O_4 structure at room temperature. ^{57}Fe Mössbauer spectra are recorded in transmission geometry at various temperatures (Fig. 1). At 293 K, the spectra show a doublet with vanishing magnetic hyperfine field B_{hf} , whereas at 4.2 K and 15 K, distinct sextets with finite B_{hf} appear. With increasing temperature, the magnetic hyperfine splitting decreases and disappears around 40 K, leaving only quadrupole split spectra. This transition is typical for relaxation spectra. To get information about the relaxation process, the spectra are analysed by two different approaches, and the results are compared. The first approach is based on particle size distributions, where the distributions are discretized into 10 subspectra (M1 to M10), and for the fits, a time-independent Hamiltonian is used. The resulting particle size distribution follows a log-normal distribution in good agreement with the literature [2]. From the temperature dependence of B_{hf} for the ten subspectra (Fig. 2), a blocking temperature of approximately 33 K is determined. The second approach, based on a perturbative description of the interaction between the Fe nucleus and fluctuating electron spins, uses the solution of the relaxation Hamiltonian operator according to [1]. Since the cubic structure of a sample without superparamagnetic effects can be described by two sextets, this model is also used as a starting point for the relaxation Hamiltonian operator to determine the energy barrier and relaxation time. Both approaches show relatively good agreement in the calculated energy barriers.

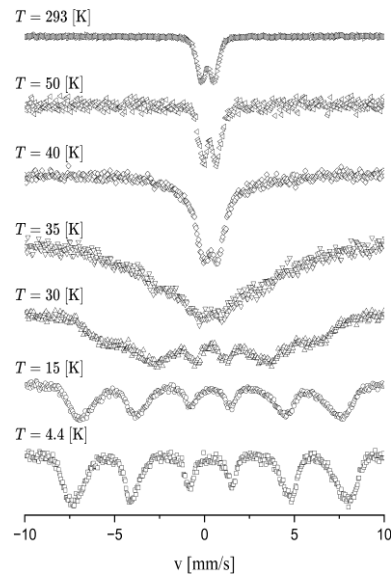


Fig. 1: MB spectra for different temperatures

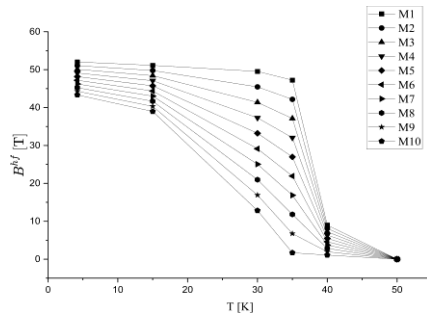


Fig. 2: Magnetic hyperfine fields for the ten subspectra

[1] M. Blume and J.A. Tjon, *Phys. Rev. B*, 165 1 (1968) 446–456.

[2] F. Bødker and M. Hansen, *Phys. Rev. B*, 61 10 (2000).

ICAME-T04-P1

Exploring Iron Precipitation for Understanding Phosphate Removal from Wastewater

Hannah Akhtar^{1*}, Marco A. M. Tummeley¹, Lukas Knauer¹, Maren H. Hoock¹, Konstantin Gröpl¹, Paul Hausbrandt¹, Tim Hochdörffer¹, Juliusz A. Wolny¹, Volker Schünemann¹

¹University of Kaiserslautern-Landau, Kaiserslautern, Germany

* hannah.akhtar@rptu.de

Phosphorus is a vital nutrient for agriculture and fertiliser production. However, it is in limited supply across Europe, resulting in heavy dependence on imports. Promising substitutes for phosphorus recovery have been found to be municipal sewage sludge and wastewater [1]. But present techniques of removal, mostly chemical precipitation with iron salts, cause non-bioavailable iron phosphate species [2]. The molecular mechanisms of the initial steps of phosphate fixation with iron salts remain unclear due to the complex nature of the process and the many possible nucleating species involved. It is evident that iron hydroxides ($\text{Fe}(\text{OH})_x$) play a crucial role in the mechanisms of phosphorus adsorption and precipitation [3]. Focusing on the early intermediates in iron hydroxide [4] precipitation and their reactivity towards phosphorus, this work seeks to clarify the molecular mechanisms underlying phosphorus fixation with iron salts during wastewater treatment. We examine the pH-dependent formation of iron hydroxide species and their subsequent conversion into iron phosphate compounds using ^{57}Fe Mössbauer spectroscopy and density functional theory (DFT) calculations. DFT calculations have been performed with Gaussian 16 [5] to optimize the geometries of the structures shown in Fig.1 using the B3LYP functional and the CEP-31G basis set. Mössbauer parameters for these structures have been calculated using ORCA 6.0. [6], by applying the B3LYP functional along with the CP(ppp) basis set to analyse the electronic properties of iron atoms. The calculation of partial density of states is ongoing, and the latest results will be presented.

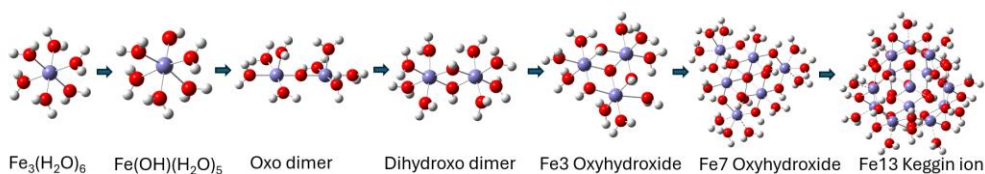


Figure 1. Structural stages of iron hydrolysis in water

- [1] T. Prot et al, *Water Res.* **182** (2020) 115911.
- [2] Y. Zheng et al, *Crit. Rev. Environ. Sci. Technol.* **53** **11** (2022) 1148–1172.
- [3] Y. Mochizuki, *J. Environ. Chem. Eng.* **9** **1** (2021) 104645.
- [4] J. Scheck et al, *J. Phys. Chem. Lett.* **7** **16** (2016) 3123–3130.
- [5] M. J. Frisch et al, *Gaussian 16 rev. C. 09.* (2016).
- [6] F. Neese et al., *J. Chem. Phys.* **152** (2020) 22.

ICAME-T04-P2

Study of Radiation-induced Processes in the Near-surface Layers of Nitride Coatings on HEA (AlTiZrYNb).

T. Aldabergenova^{1,2}, M. Vereshchak¹, S. Sakhiyev¹, S. Kislitsin¹

¹Institute of Nuclear Physics, Almaty, Kazakhstan

²Kazakh National Women's Teacher Training University

*tamaramus@inp.kz

High-entropy alloys (HEA) are a new class of materials with increased entropy when mixed. High entropy of mixtures prevents the formation of intermetallics and interstitial solid solutions during crystallization. Five or more components taken in equal or close proportions can form a single-phase crystalline alloy. HEA-based nitride coatings are a very perspective area of research. In this paper, the method of nuclear-resonance spectroscopy in the electron backscattering mode (EBS) was used to study HEA nitride coatings (AlTiZrYNb), produced by cathodic vacuum arc sputtering in a nitrogen atmosphere. Then the samples were implanted with ⁵⁷Fe ions with an energy of 200 keV to a fluence of $5 \cdot 10^{16} \text{ cm}^{-2}$ at the UKP-2-1 complex charge-exchange accelerator (INP, Almaty).

Irradiation was carried out with an ion beam current of $\sim 100 \text{ nA}$. The target temperature for the selected irradiation modes did not exceed 60°C . The projective range of ⁵⁷Fe ions in the coating was $\sim 100 \text{ nm}$; therefore, iron ions were implanted into the near-surface region commensurate in depth with the layer thickness available for analysis by the CEMS method. Ferritic-martensitic steel (Fe-12% Cr) was taken as a substrate.

Successive two-hour isochronous annealings of the samples were carried out in a vacuum furnace at temperatures of 870, 1070, 1170, 1220, and 1270 K. After each annealing stage, the coating structure was studied. The elemental composition and crystal structure. The electron environment of Fe⁵⁷ atoms after the completion of the implantation process was estimated using the KEMS method. Mössbauer studies were carried out on an MS-1104Em spectrometer at room temperature; Co⁵⁷ in a chromium matrix served as the source of γ -quanta. The Mössbauer spectra were processed by the model decoding method in the SpectrRelax program.

It is shown that iron ion implantations and the HEA nitride-based coating before annealing are represented by a significantly broadened paramagnetic line. This indicates a strong distortion of the electronic structure in the region of the Fe impurity atom, leading to an amorphization state of the HEA structure. Isochronous annealing leads to a monotonic decrease in the widths of the resonance lines. At the last stage of the annealing process ($T = 1270 \text{ K}$), the sample demonstrates a disordered substitution solid solution.

It was established that the group of Al, Ti, and Nb elements with a cubic structure of *fcc* and *bcc* syngony are responsible for the singlet; Zr and Y, having a hexagonal close packing (*hcp*) lattice, generated a doublet in the near-surface layers of the coating. The XRD data are in agreement with the CEMS studies. The substrate of the HEA coating was ferritic-martensitic steel Fe-12% Cr. On the diffraction pattern, it is represented by three reflections (110), (200), (211), and the coating is two sublattices of the *fcc* and *hcp* structure.

The work was carried out under the program “Development of complex scientific research in the field of nuclear and radiation physics based on Kazakhstani accelerator complexes” (IRN BP23891530).

ICAME-T04-P3

Structural and Mössbauer Studies of Nanocrystalline Mn²⁺/Zn²⁺-codoped Fe₃O₄ Particles

K.S. Al-Rashdi^{1,2*}, H.M. Widadallah², M. Elzain², A. Al-Rawas², A. Gismelseed²,
F. Al Ma'Mari^{2,3}, O. Cespedes³

¹Department of Applied Science and Pharmacy, University of Technology and Applied Science, P.O. Box 36, Al-Khuwair, Muscat 123, Oman

²Physics Department, College of Science, Sultan Qaboos University, Al-Khoudh, Muscat 123, Oman

³School of Physics and Astronomy, University of Leeds, Leeds LS2 9JT, UK

*khadija.alrashdi@utas.edu.om

We report on the effect of codoping nanocrystalline Fe₃O₄ particles with both Mn²⁺ and Zn²⁺ cations on their structural and magnetic properties using techniques such as XRD, TEM, Raman, and Mössbauer Spectroscopies. Highly crystalline single-phased Mn²⁺/Zn²⁺ codoped-Fe₃O₄ nanoparticles with an average size of $\sim 17 \pm 4$ nm, and a composition of Mn_xZn_{0.2}Fe_{3-y}O₄ ($y = \frac{2}{3}(x + 0.2)$, $x = 0.0, 0.1, 0.15, 0.2, 0.25$, and 0.3) are synthesized by the precipitation method as confirmed by the XRD and TEM. Raman spectroscopic data reveal that codoping with Mn²⁺ and Zn²⁺ suppresses the magnetite-to-maghemite phase transformation for the samples with $x \geq 0.2$. Consistent with the Raman results, Mössbauer spectroscopic data show a decrease in the γ -Fe₂O₃ phase as x increases, from about 12 % for $x = 0.0$ to approximately 6 % for $x = 0.15$, with the phase almost vanishing in samples with $x \geq 0.2$. The changes in isomer shifts, quadrupole shifts, and hyperfine fields with increasing x values are discussed. The cationic distribution attained from the XRD and Mössbauer data analysis indicates that both cations preferentially substitute for Fe³⁺ cations at the A-site. This is accompanied by the expulsion of some of the Fe³⁺ cations from the A-site to tetrahedrally-coordinated interstitial sites at low dopant concentrations ($x < 0.2$) and the octahedrally-coordinated interstitial sites as more dopants are added ($x \geq 0.2$).

[1] P.R. Graves et al., *Mat. Res. Bull.*, **23** (1988) 1651.

[2] N. Modaresi et al., *J. Magn. Magn. Mater.*, **482** (2019) 206.

ICAME-T04-P4

Structural, Magnetic, and Mössbauer Studies of $\text{PrFe}_x\text{Mn}_{1-x}\text{O}_3$ Perovskite Manganites

I. Z. Al-Yahmadi^{1*}, A.M. Gismelseed¹, H.M. Widatallah¹, F. Al Ma'Mari¹,
F. Albzour¹, M. E. Elzain¹

¹Physics Department, College of Science, Sultan Qaboos University, Muscat, Sultanate of Oman

*i.alyahmadi1@squ.edu.om

The effect of Fe-doping on the structural and magnetic properties of $\text{PrFe}_x\text{Mn}_{1-x}\text{O}_3$ ($x = 0.1, 0.3, 0.5, 0.7, 0.9$, and 1.0) nanocomposites was studied. The compounds were prepared using a modified auto-combustion sol-gel method. X-ray diffraction (XRD) refinement confirmed that all samples were indexed in a single-phase orthorhombic structure with a $Pbnm$ space group symmetry. The unit cell volume exhibited a linear increase with increasing Fe concentration (x). Zero-field-cooled (ZFC) and field-cooled (FC) magnetization measurements at an applied field of 0.02 T revealed that all samples undergo an antiferromagnetic (AFM) to paramagnetic (PM) transition as the temperature increases. While this magnetic behavior developed significantly with increasing Fe content, a signal of spin reorientation is observed with the sample $x = 0.7$. ^{57}Fe transmission Mössbauer spectroscopy was performed on all samples at room temperature (~ 295 K) and liquid nitrogen temperature (~ 78 K) to analyze their structure and magnetic ordering. The results indicated that the magnetic behavior strongly depends on Fe concentration. Compounds with low Fe concentrations ($x < 0.5$) exhibited a dominance of high-spin Fe^{3+} paramagnetic doublet at both 295 K and 78 K. In contrast, ^{57}Fe Mössbauer spectra of samples with higher Fe content ($x > 0.5$) showed well-resolved magnetic sextet patterns, with the hyperfine magnetic field increasing linearly as Fe content increased.

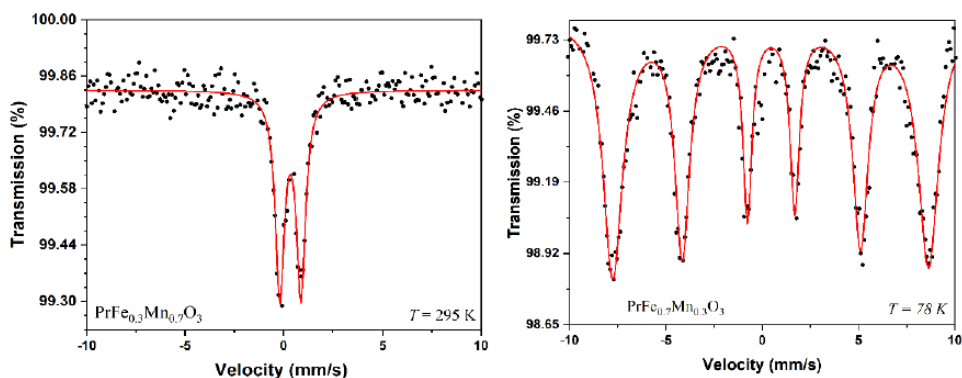


Figure 1. ^{57}Fe Mössbauer spectra of (left) $\text{PrFe}_{0.3}\text{Mn}_{0.7}\text{O}_3$ measured at 295 K and (right) $\text{PrFe}_{0.7}\text{Mn}_{0.3}\text{O}_3$ measured at 78 K. The dots represent the experimental data, and the red solid line indicates the corresponding fit.

ICAME-T04-P5

Structural, Magnetic, and Mössbauer Studies of $\text{ErFe}_x\text{Mn}_{1-x}\text{O}_3$

F. Bzour^{1*}, A. Gismelseed¹, I. Z. Al-Yahmadi¹, F. Al Ma'Mari¹, R. T. Al-Mamari¹,
A. Al-Rawas¹, H. M. Widatallah¹, M. Al-Maashani¹, and M.E. Elzain¹

¹Physics Department, College of Science, Sultan Qaboos University, Code 123, P.O. Box 36,
Al-Khoud, Oman

*fatenbzour@gmail.com

Iron-doped Erbium manganites $\text{ErFe}_x\text{Mn}_{1-x}\text{O}_3$ ($0.0 \leq x \leq 1.0$) compounds were synthesized using the sol-gel auto-combustion technique. Rietveld refinement of X-ray diffraction (XRD) patterns revealed a structural transition from the hexagonal ($P6_3cm$) phase to the orthorhombic ($Pbnm$) phase as the iron content increased, having a mixed hexagonal-orthorhombic phase in the concentration range of $0.2 \leq x \leq 0.6$. The Néel temperature (T_N) exhibited a shift towards higher temperatures with increasing Fe^{3+} content, reaching approximately 326 K at $\text{ErFe}_{0.2}\text{Mn}_{0.8}\text{O}_3$, near room temperature. The inclusion of Fe^{3+} also induced spin reorientation temperature (T_{SR}) at a specific iron concentration that exhibited a decreasing trend with increasing Fe^{3+} content, with values close to room temperature at 319 K and 275 K for $\text{ErFe}_{0.2}\text{Mn}_{0.8}\text{O}_3$ and $\text{ErFe}_{0.4}\text{Mn}_{0.6}\text{O}_3$, respectively. Mössbauer spectra showed considerable complexity due to the coexistence of orthorhombic and hexagonal phases, where the identification of many components in the spectra suggests the presence of different chemical environments around the Fe atoms. The magnitude of the hyperfine magnetic field (B_{hf}) demonstrated a linear increase with iron doping. The isomer shift values, measured at 295 K and 78 K, confirm the dominance of Fe in the trivalent oxidation state (Fe^{3+}).

Sustainable Recycling of End-of-life Nd-Fe-B Permanent Magnets

Zara Cherkezova-Zheleva^{1,*}, Daniela Paneva¹, Sabina Fironda², Marian Burada²,
Setareh Gorji Ghalamestani⁴, Olivier J⁵

¹Institute of Catalysis, Bulgarian Academy of Sciences, Sofia, Bulgaria

²National Research and Development Institute for Nonferrous and Rare Metals-IMNR, Ilfov, Romania,

³SIRRIS, Seraign, Belgium/Wallonia

⁴FADDTORY SPRL, FERNELMONT, Belgium/Wallonia

*zzhel@ic.bas.bg

The efficiency and high magnetic performance of Nd-Fe-B permanent magnets make them a strategic material for numerous emerging technologies in key sectors of the economy, technological evolution, green transition, defence, and space. Thus, the development of advanced and clean technologies, automation, green energy production, and manufacturing of different small devices leads to an extraordinarily high growth of consumption of Rare earth elements (REEs), mainly neodymium (Nd), dysprosium (Dy), and praseodymium (Pr). In this regard, REEs have been categorized as critical raw materials (CRMs) across the globe due to the combination of this high economic demand with significant supply risk. Recycling of the increasing stocks of end-of-life (EoL) Nd-Fe-B permanent magnets is a sustainable approach to address this problem and to balance the lack of REEs on the market. Nowadays, the research and innovative investigations are focused on the development of environmentally-friendly recycling technologies of waste products containing rare earth metals. Recently, the EoL Nd-Fe-B permanent magnets have been selected as a potential secondary source, able to meet the future demand of the critical REEs due to the huge production of these materials.

The paper presents our research activities on recycling and direct reuse of spent non-oxidized Nd-Fe-B permanent magnets from HDDs. Mechanical treatment is a widespread technique in material treatment, but the application of mechanochemistry for waste HDD recycling and REEs recovery still lacks a comprehensive investigation. The paper discusses the obtained optimal treatment conditions, appropriate for the direct reuse of the studied material. The application of the mechanochemical approach is focused on greening and optimization of the recycling of spent HDD permanent magnets under room-temperature, low-waste-emitting, energy-saving methodology, in consideration of the green and sustainable principles. Initial, intermediate, and treated products were characterized in detail by a complex of analytical methods, such as X-ray diffraction, Mössbauer spectroscopy, TEM, SEM/EDS analysis, and XPS. The treatment of materials was evaluated with an emphasis on structure–magnetic property relationships, as well as in the context of their further reuse for 3D printing of new magnets. The Mössbauer technique was used to analyse precisely the iron-bearing phases presented in the samples, and especially the evolution of the main Nd₂Fe₁₄B magnetic phase.

Acknowledgements: This article is based on the project activities of H2020 ERA-MIN3 Project № KII-06-ДO02-3/06/06/2022: Microwave enhanced recovery of REEs and plastic from WEEE and re-use in Additive Manufacturing of novel magnetic components (MW4REMAM).

Spectroscopic Investigation of Sublattice Occupancy and Magnetic Behavior of High-entropy Spinel Oxides

M. Szymczak^{1*}, V. Bilovol², M. Sikora³, K. Berent², J. Dąbrowa⁴, J. Cieślak¹

¹ Faculty of Physics and Applied Computer Science, AGH University of Krakow, Poland

² Academic Center for Materials and Nanotechnology, AGH University of Krakow, Poland

³ National Synchrotron Radiation Centre SOLARIS, Jagiellonian University, Poland

⁴ Faculty of Materials Science and Ceramics, AGH University of Krakow, Poland

* szymczak@agh.edu.pl

High-entropy spinel oxides combine the potential synergistic effects of the high-entropy approach with the versatility of properties offered by conventional spinel-structured systems [1]. However, these potential assets for designing functional materials also introduce significant complexity of the multi-component high-entropy oxides (HEOx), further convoluted by the coexistence of two non-equivalent cationic sites with low enthalpy barriers within the spinel space group. The insufficient understanding of the exact structure of HEOx hinders the intentional material design for specific applications. A study employing a wide array of techniques to unravel the cationic distribution and oxidation states of the original HEOx spinel (Co,Cr,Fe,Mn,Ni)₃O₄ points to an occupancy preference instead of the expected disorder [2]. The usefulness of Mössbauer spectroscopy as an element-specific probe has been showcased earlier for high-entropy and medium-entropy quaternary spinel oxides [3].

In this work, we assess the influence of specific elements and entropic contribution (i.e., number of elements) on atomic structure and magnetic properties. Starting with the well-studied, first-reported high-entropy spinel (Co,Cr,Fe,Mn,Ni)₃O₄, we eliminate one of the magnetic elements, either Co or Ni, or replace them with the non-magnetic Mg, obtaining (Cr,Fe,Mn,Ni)₃O₄, (Co,Cr,Fe,Mn)₃O₄, (Cr,Fe,Mg,Mn,Ni)₃O₄, and (Co,Cr,Fe,Mg,Mn)₃O₄.

We perform an extensive structural and magnetic study of the five spinel oxides. The single-phased spinel structure is verified through X-ray diffraction (XRD) with Rietveld analysis. We perform temperature-dependent Mössbauer spectroscopy measurements to analyze both local structure and magnetic behavior. The latter is further investigated through vibrating sample magnetometry (VSM). Oxidation states of cations and their occupancy distribution between tetrahedral and octahedral sites are investigated with X-ray absorption spectroscopy (XAS) and X-ray magnetic circular dichroism (XMCD).

The Mössbauer spectra exhibit features characteristic of the chemically disordered sublattices. The introduced modifications influence the temperature dependence of the hyperfine field values. The temperature of transition to a paramagnetic state is lower compared to the original composition in all the cases, except the Co-free quaternary oxide. The XAS and XMCD analyses indicate that elements adjusting their valency and occupancy distribution to the introduced modifications are Mn and Fe, respectively. Both experimental and theoretical results confirm the suppression of configuration entropy in the studied spinel HEOx.

[1] Q. Zhao, et al., *Chem. Rev.* **117** (2017).

[2] A. Sarkar, et al., *Acta Mater.* **226** (2022).

[3] J. Cieślak, et al., *Acta Mater.* **206** (2021).

This research was supported by the Polish National Science Center (NCN) under project no. UMO-2022/45/B/ST8/00617.

Temperature-driven Phase Transformations in a Pure and Nd-doped BiFeO₃ Prepared by the Sol-Gel Method

Karolina Czarnacka^{1*}, Karolina Siedliska¹, Kamila Komędera^{2,3}, Łukasz Gondek², Andrzej Kociubiński¹, Jakub Kisała¹, Tomasz Pikula¹

¹Lublin University of Technology, Lublin, Poland

²AGH University of Krakow, Kraków, Poland

³University of Zagreb, Zagreb, Croatia

*k.czarnacka@pollub.pl

In this study, we investigated the temperature-driven phase evolution of pure bismuth ferrite (BiFeO₃, BFO) and neodymium-doped bismuth ferrite (BNFO) ceramics synthesized by the sol-gel method. Whereas the thermal stability and structural transitions of BFO produced by conventional sintering are well known, the behaviour of sol-gel-derived materials remains largely unexplored. To fill this knowledge gap, we performed in-situ high-temperature X-ray diffraction measurements in the range of 300–1200 K for pure BFO and BNFO with 10% and 20% substitution of Bi by Nd. The results showed that pure α -BFO undergoes a partial decomposition into Bi₂Fe₄O₉ and Bi₂O₃ at 860 K. The remaining part of α -BFO transforms to orthorhombic *Pnma* structure (β -phase) at 1090 K. For Nd-doped samples, the presence of neodymium stabilises the orthorhombic *Pbam* structure, limiting phase transformations compared to pure BFO. Notably, for BNFO with 20% Nd, the orthorhombic *Pbam* phase remained dominant up to the highest investigated temperature, indicating enhanced thermal stability.

Mössbauer spectroscopy measurements were also performed, confirming the disappearance of cycloidal spin ordering with increasing Nd content. Mössbauer spectra revealed a transition from the cycloidal spin ordering characteristic of the *R3c* phase in pure BFO to an antiferromagnetic structure of the *Pbam* phase in BNFO with 20% Nd, correlating with the structural transformation observed in XRD. These findings complement previous studies, which demonstrate that Nd doping induces structural transitions and cycloid suppression at room temperature, which is accompanied by the thermal stability enhancement. The observed differences between sintered and sol-gel synthesized samples highlight the critical role of the synthesis method in defining the thermal and structural properties of multiferroic ceramics.

[1] K. Komędera et al., *Ceramics International* **51** (2025) 7208.

[2] R. Palai et al., *Physical Review B* **77** (2008) 014110.

ICAME-T04-P9

Structural, Magnetic, and Electrical Properties of Potentially Multiferroic $\text{Bi}_5\text{Ti}_3\text{Fe}_{1-x}\text{Co}_x\text{O}_{15}$ Aurivillius Compound

T. Pikula¹, J. Grotel^{1*}, B. Garbarz-Glos², D. Kamiński³, Z. Surowiec⁴,
M. Kowalczyk⁵ and E. Jartych¹

¹Department of Electronics and Information Technology, Lublin University of Technology,
Lublin, Poland

²Institute of Technology, Pedagogical University of Cracow, Cracow, Poland

³Department of Organic Chemistry and Crystallochemistry, UMCS, Lublin, Poland

⁴Department of Physics, UMCS, Lublin, Poland

⁵Faculty of Materials Science and Engineering, Warsaw University of Technology, Warsaw,
Poland

*j.grotel@pollub.pl

The $\text{Bi}_5\text{Ti}_3\text{FeO}_{15}$ (BTFO) is an Aurivillius compound which consists of four perovskite-like layers $[\text{Bi}_3\text{Ti}_3\text{FeO}_{13}]^{2-}$ alternating with fluorite-like layers $[\text{Bi}_2\text{O}_2]^{2+}$ along the c-axis. BTFO can be viewed as a combination of the three-layer Aurivillius phase $\text{Bi}_4\text{Ti}_3\text{O}_{12}$ (BTO) with diamagnetic fluorite-like layers and the well-known, antiferromagnetic multiferroic BiFeO_3 (BFO). Aurivillius phases have been proposed as candidates for single-phase, room-temperature multiferroics due to their favorable ferroelectric properties (e.g., Curie temperatures T_C above ambient level) and the possibility of incorporating foreign ions into their crystal structure [1]. The aim of the present work was to enhance magnetic properties of the compound via doping with Co ions in the range of concentration $x = 0 \div 0.5$ and investigate the magnetoelectric effect at room temperature.

The magnetoelectric effect describes a coupling between magnetic and ferroelectric order of a material. The magnetoelectric material exposed to an external magnetic (electric) field undergoes polarization (magnetization). The quantity that describes the relationship between the stimulus (field) and order parameter (polarization or magnetization) is called the magnetoelectric coupling coefficient α . Magnetoelectric materials have many potential applications in electronics, metrology, renewable energy engineering, and medicine [2].

The samples in the present study were synthesized via the standard ceramic method. The XRD structural analysis confirmed the successful synthesis of Co-doped BTFO samples. Small amount of non-magnetic secondary phase $\text{Bi}_{20}\text{TiO}_{32}$ was detected, as well as some structural changes were observed that can be attributed to the coexistence of three- and four-layered perovskite-like blocks. Magnetic measurements in $2 \div 400$ K range showed conflicting results. While the undoped sample is paramagnetic, Co doping induced behavior similar to spin-glass systems. Room-temperature VSM measurements point towards weak ferromagnetism that depends on the Co concentration. The greatest saturation magnetization was recorded for $x = 0.3$. On the other hand, Mössbauer spectra appear to be typical for paramagnetic systems. Ferroelectric hysteresis loops were observed utilizing the Sawyer-Tower circuit. Impedance spectroscopy was used to measure complex permittivity. Finally, magnetoelectric properties were investigated via the lock-in technique. A correlation between mechanical, electrical, and magnetic characteristics was detected, possibly attributed to the magnetoelectric coupling.

[1] X. Mao, H. Sun, W. Wang, Y. Lu, X. Chen, *Solid State Commun.* **152** (2012) 483-487.

[2] M. M. Vopson, *Crit. Rev. Solid State Mater. Sci.* **40** (2015) 223-250.

ICAME-T04-P10

Mössbauer Spectroscopy of Iron Phosphates with Relevance to Phosphorus Recovery from Sewage Sludge

Paul Hausbrandt^{1*}, Marco A. M. Tummeley¹, Linda Müller¹, Juliusz A. Wolny¹,
Luciana Ninni Schäfer¹, Heidrun Steinmetz¹, Volker Schünemann¹

¹University of Kaiserslautern-Landau, Kaiserslautern, Germany

*phausbra@rptu.de

Phosphorus is a raw material that is widely used in agriculture and industry. Widespread use can lead to increased levels of phosphorus in the environment, causing eutrophication. Targeted removal and recovery of phosphorus from wastewater is therefore important for environmental protection, but also for securing phosphorus as a resource. In wastewater treatment plants, P-elimination is often achieved by simultaneous precipitation with iron salts. In order to be able to extract phosphorus from the P-containing sewage sludge, it is important to know the iron phosphate compounds present in the sludge. Therefore, we have used Mössbauer spectroscopy to follow iron precipitation products in various treatment stages of a wastewater treatment plant (see Fig. 1).

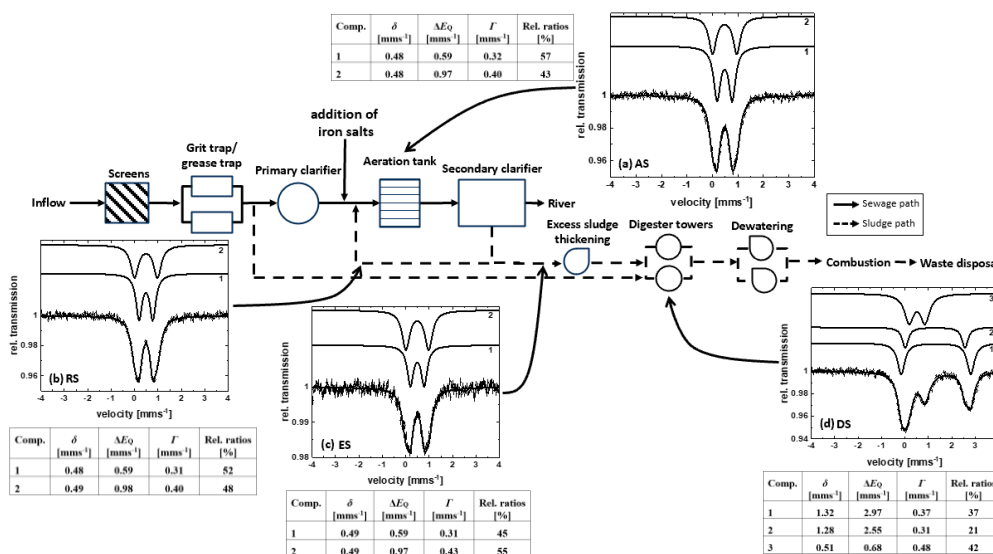


Figure 1.: Schematic representation of a sewage treatment plant with the corresponding Mössbauer spectra of sewage sludge in various treatment stages. (a) activated sludge (AS), (b) return sludge (RS), (c) excess sludge (ES), and (d) that of the digested sludge (DS). All spectra were recorded at 77 K.

The Mössbauer spectra show that, in contrast to the preceding stages, approximately 58 % of the iron in the digested sludge (DS) is present as iron(II), which could be bound in vivianite-like structures (see Fig. 1d). Vivianite is a paramagnetic iron phosphate mineral, and has been reported that it can be removed from the sludge by magnetic separation [1].

[1] P. Wilfert, *Environmental Science & Technology* **49** (2015), 9400.

ICAME-T04-P11

Characterization of Physicochemical Properties of Fe-Nb Alloys Prepared via Mechanical Alloying

Magdalena Sobota^{1,2}, Wojciech Nowak^{1,2}, Robert Konieczny¹, Wojciech Bartz³,
Rafał Idczak^{*,1}

¹Institute of Experimental Physics, University of Wrocław, pl. M. Borna 9, 50-204 Wrocław, Poland

²Institute of Low Temperature and Structure Research, Polish Academy of Sciences, ul. Okólna 2, 50-422 Wrocław, Poland

³Institute of Geological Sciences, University of Wrocław, ul. Cybulskiego 30, 50-205 Wrocław, Poland

*rafal.idczak@uwr.edu.pl

The most common element used to protect iron alloys from atmospheric and high-temperature corrosion is chromium, which forms a thin passive layer enriched with oxygen on the surface of the material. Recently, our group found that the addition of silicon to the Fe-Cr system significantly improves its anti-oxidation properties [1-3]. Another interesting element that could enhance the corrosion resistance of iron alloys is niobium. It was reported that Nb₂O₅ used as a coating deposited on the surface of the stainless steel 316L improves its anti-corrosion properties [4]. However, according to the Fe-Nb phase diagram, the solubility of Nb in Fe is very limited. In particular, binary Fe-Nb alloys with a content of Nb in the range 4–27 at.% at temperatures lower than 1273 K consist of two phases: a bimetallic substitutional random alloy that crystallises in body-centred cubic structure (bcc) and Fe₂Nb Laves phase.

In this work, we prepared the Fe_{0.95}Nb_{0.05} (nominal composition) powders using mechanical alloying (MA) with different milling time durations. MA is a technique developed in the 1960s that allows for the production of metastable materials. The process involves repeated cold welding, fracturing, and re-welding of powder particles. Since the synthesis was carried out at a temperature lower than 400 K, it is plausible to assume that during the milling, the Nb atoms will be introduced into the bcc Fe matrix. In the next step, the synthesised powders were oxidised at 870 K in air. Here, an interesting scenario is considered that, at high temperature, the low solubility of Nb in Fe, together with the possible surface segregation phenomenon of niobium atoms, may lead to the formation of a thin Nb-rich layer at the powder particles, which greatly enhances their corrosion resistance. To verify this hypothesis, the chemical composition of the oxidised powders was determined by ⁵⁷Fe Mössbauer spectroscopy.

[1] K. Idczak and R. Idczak, *Met. Mat. Trans. A* **51** (2020) 3076–3089.

[2] M. Sobota et al., *Met. Mat. Trans. A* **53A** (2022) 3083–3099.

[3] M. Sobota et al., *Coatings* **13** (10) (2023).

[4] M.O.A. Ferreira et al., *Mat. Chem. Phys.* **312** (2024) 128610.

Structural and Electrochemical Characterization of Perovskite-type LaFeO_3 Fabricated Using Solid-state Assisted by Low-energy Ball Milling

Juan A. Jaén^{1,2*}, Fernando Higuera³, Oscar Gil⁴, Eduardo Chung^{1,5}, Oscar Arnache⁶, Carlos Ostos⁶ and Griselda Caballero-Manrique^{1,2}

¹Grupo de Investigación de Materiales, Universidad de Panamá, Panamá

²Departamento de Química Física, Universidad de Panamá, Panamá

³Escuela de Física, Universidad de Panamá, Panamá

⁴Escuela de Química, Universidad de Panamá, Panamá

⁵Departamento de Física, Universidad de Panamá, Panamá.

⁶Grupo de Estado sólido, Instituto de Física, Facultad de Ciencias Exactas y Naturales, Universidad de Antioquia, Medellín, Colombia

* juan.jaen@up.ac.pa

Perovskite materials based on lanthanum orthoferrite (LaFeO_3) are of great importance due to their broad application potential in advanced technologies. The conventional solid-state reaction is a simple method and one of the most widely used routes for the synthesis of iron-based perovskite (LaFeO_3). Its pure form usually requires high temperatures ($\sim 1000^\circ\text{C}$) and long calcination times. Alternatively, high-energy mechanical milling improves the mixing and reduces calcination times and temperatures, enabling the synthesis of single-phase LaFeO_3 perovskite with high specific surface area, different particle sizes, and structural defects. We have used a solid-state technique assisted by low-energy ball milling procedures. A perovskite-type LaFeO_3 of high purity ($\sim 98\%$) (sample AO0) was successfully obtained. Without milling, both precursor materials and the perovskite phase are obtained, indicating an incomplete reaction during calcination. To reduce agglomeration, further milling was done for 5 hours (sample AO5). PXRD pattern analysis of both samples indicates a dominant crystalline phase of LaFeO_3 perovskite. Crystallite sizes were 97 nm and 90 nm, respectively. FESEM indicates the occurrence of a distribution of the particles of irregular grains with an agglomeration of nanometer-sized to micrometre-sized agglomerates. The ATR-FTIR spectra of the LaFeO_3 perovskite exhibit bands in the range of $310\text{--}398\text{ cm}^{-1}$ and at around 535 cm^{-1} . The higher frequency band corresponds to the intrinsic stretching vibrations of La–O and Fe–O. The RT Mössbauer spectra revealed the presence of a single sextet, which is in good agreement with those reported for this perovskite-type. Magnetic measurements were performed at 300K from -20 kOe to 20 kOe . The magnetization (M - H) curve of the AO0 sample exhibits an AFM response with a weak ferromagnetism, which is characteristic of LaFeO_3 , attributed to its canted antiferromagnetic structure resulting from Dzyaloshinskii-Moriya interaction. After milling, an increase in ferromagnetic behaviour was observed in sample AO5. Both samples exhibit a Morin-type transition at around 260 K. The ZFC-FC curves for sample AO5 show a spin glass-like behaviour, attributed to surface spin disorder introduced during the milling process. Finally, cyclic voltammetry studies were conducted using the voltammetry of immobilized microparticles technique. Both samples exhibit a pseudocapacitive behaviour in acidic media; notably, the capacitance of AO0 was around seven times higher than that of AO5. The electrochemical oxidation of methanol is currently under investigation and will be fully discussed.

ICAME-T04-P13

Structure, Mechanical, and Magnetic Properties of Co₂FeAl Heusler Alloy Prepared by Mechanosynthesis

Elżbieta Jartych^{1*}, Tomasz Pikula¹, Dariusz Oleszak²

¹Lublin University of Technology, Lublin, Poland

²Warsaw University of Technology, Warsaw, Poland

*e.jartych@pollub.pl

The ternary full Heusler-type alloys based on Co are known to exhibit high spin polarization and are good ferromagnets with relatively high Curie temperature and high saturation magnetization. Among them, Co₂FeAl alloy exhibits half-metallicity and large spin polarization, which makes this compound a suitable material to be used in spin-based electronic devices and spintronic THz emitters [1]. Recently, it has been reported that a highly ordered structure of Heusler alloys can be produced in non-equilibrium processes, like melt-spinning or mechanical alloying (MA) [2,3]. Solid solutions are often formed during the MA process, and only after heat treatment can the assumed phase be obtained. Moreover, the final product may be a pure phase or a mixture of ordered and disordered phases, which depends on the heating/annealing processes [4].

In the present study, we aimed to obtain the powdered Heusler alloy Co₂FeAl via the MA synthesis method and subsequent annealing. We propose Mössbauer spectroscopy to monitor the formation of the alloy at every stage of the milling process, together with X-ray diffraction. These two methods complement each other and allow us to recognize the phases and determine their magnetic state.

The disordered BCC solid solution was obtained after 20 h of milling, with an average crystallite size of 23 nm, a mean level of lattice strains of 0.75 % and microhardness 650 HV. After isothermal annealing, the assumed Co₂FeAl Heusler phase of B2 type was produced, without any secondary phases. The thermal process caused a slight increase in grain size (25 nm) and a significant decrease in lattice strains (0.3 %). Mössbauer spectroscopy revealed atomic disorder in the occupation of 1*b* and 1*a* sites by iron atoms in the crystalline *Pm-3m* phase, with a slight preference for filling the 1*b* positions. Macroscopic magnetic measurements showed soft magnetic properties of the milled and annealed powders. The obtained Co₂FeAl Heusler alloy is characterized by a high saturation magnetization value around 140 emu/g, which is equivalent to a magnetic moment of about 5.0 μ_B per formula unit. The results obtained correspond well with the high values of the hyperfine magnetic fields $30 \div 33$ T revealed by Mössbauer spectroscopy.

[1] R. Gupta et al., *Adv. Opt. Mat.* **9** (2021) 2001987.

[2] C.-H. Lee, *J. Nanosc. Nanotech.* **19** (2019) 888.

[3] F. Djaidi, et al., *Int. J. Mat. Res.* **111** (2020) 681.

[4] E. Jartych et al., *Nanomater.* **13** (2023) 3024.

ICAME-T04-P14

Fe₂(MoO₄)₃ as Catalyst for the Selective Oxidation of Ethanol

Lanjie Jiang^{1*}, Jan Welzenbach¹, Jonas Spielmann¹, Hannah Wilhelm¹, Kathrin Hofmann¹, Barbara Albert¹, Christian Hess¹, Ulrike I. Kramm¹

¹Eduard-Zintl-Institut für Anorganische und Physikalische Chemie, Technische Universität Darmstadt, Germany

*lanjie.jiang@tu-darmstadt.de

Iron molybdate (Fe₂(MoO₄)₃, noted as FMO) is used as an industrial catalyst for the methanol oxidative dehydrogenation (ODH) [1]. Recently, it was shown that it is also highly active and selective in the ODH of methanol towards acetaldehyde [2]. Hence, FMO catalysts represent a non-toxic and cheap substitutional catalyst for acetaldehyde production in comparison to the Pd catalysts used in the Wacker-Höchst process [3]. However, the exact role of Fe in the redox chemistry of the EtOH ODH is not clear so far. Mössbauer spectroscopy (MS) is a powerful tool to probe the Fe features in FMO, especially during ODH conditions.

We first performed lab-based *in situ* MS using a self-designed oven to discuss the influence of gas atmosphere and temperature on the Mössbauer parameters, as well as to deduce changes in the Lamb Mössbauer factor caused by a variation in gas atmosphere and temperature. These results are important for the concrete design of the experiment at the synchrotron facilities.

Based on these results, we developed a reactor design that enables simultaneous measurement of synchrotron-based Mössbauer spectroscopy (SMS), Raman spectroscopy, and product identification by mass spectroscopy. First experiments were performed by *in situ* and *operando* SMS and nuclear forward scattering (NFS) at the DESY and ESRF synchrotrons. In this presentation, we will focus on the proof-of-concept experiments that were used to verify the feasibility of our reactor. We will present and discuss what conclusions we can make regarding the iron speciation and its interplay with structural changes that are observed for molybdenum.

Acknowledgement: This work is financially supported by the German Research Foundation by the collaborative research center CRC1487, Iron, upgraded!

- [1] M. Bowker et al., *Top. Catal.* **48** (2008) 158–165.
- [2] N. Oefner et al., *Chem. Cat. Chem* **14** (2022).
- [3] J.C. Gebers et al., *ACS Eng. Au.* **3** (2023) 184–194.

Microstructure and Magnetic Properties of Amorphous Fe-Co-(Gd/Mo/Ti)-B Alloys

Agnieszka Łukiewska^{1*}

¹Department of Physics, Faculty of Production Engineering and Materials Technology,
Czestochowa University of Technology, 19 Armii Krajowej
Av., 42-200 Częstochowa, Poland

*agnieszka.lukiewska@pcz.pl

The Fe-Co-B-based amorphous alloys exhibit interesting soft magnetic properties, i.e., high magnetic saturation, high magnetic permeability, and extremely low coercivity [1], which are required for magnetic cores. It is well known that their microstructure and properties can be easily changed by additions such as atoms as Mo, Ti, Gd, [2] etc., or structural modifications that are introduced during their fabrication. In the present work, the effect of Ti and Mo additions on the microstructure and magnetic properties of Fe-Co-Gd-B alloy was studied in order to obtain a magnetically soft amorphous material with high saturation magnetization and relatively low Curie temperature. The microstructure and magnetic properties were investigated using Mössbauer spectroscopy and vibrating sample magnetometer, respectively.

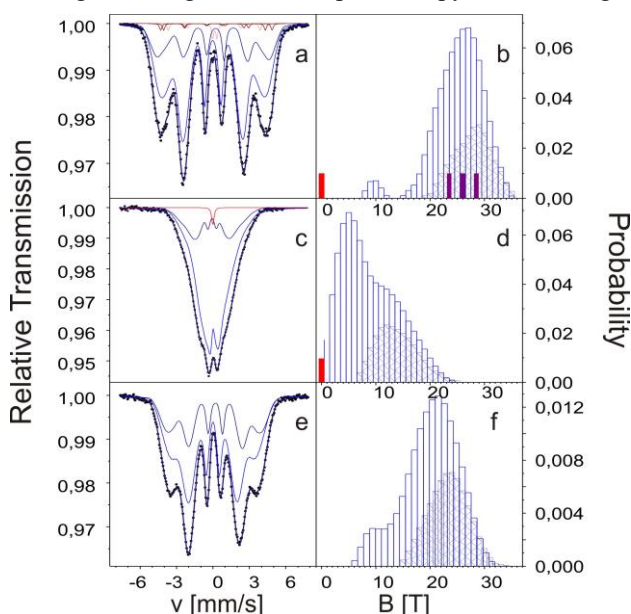


Figure 1. Transmission Mössbauer spectra (a, c, e) and corresponding hyperfine field distributions (b, d, f) for $\text{Fe}_{63}\text{Co}_{12}\text{Gd}_4\text{B}_{21}$ (a, b), $\text{Fe}_{60}\text{Co}_{12}\text{Gd}_4\text{Mo}_3\text{B}_{21}$ (c, d), and $\text{Fe}_{60}\text{Co}_{12}\text{Gd}_4\text{Ti}_3\text{B}_{21}$ (e, f) alloys.

- [1] F. Wang et al, *J. Alloy. Comp.*, **723** (2017) 376.
- [2] M.E. McHenry et al., *Prog. Mat. Sci.* **44** (1999) 291.

ICAME-T04-P16

Surface Characterization of Austenitic and Biphasic Fe-Mn-Al Alloys and Their Corrosion Behavior in a SO₂-polluted, Dry/Humid-cycled Atmosphere

V.F. Rodríguez Salcedo^{1,2,+}, M. Gracia¹, J.R. Gancedo¹, A. Bohorquez²,
G.A. Pérez Alcázar² and J.F. Marco^{1,*}

¹Instituto de Química Física Blas Cabrera, CSIC, c/ Serrano 119, Madrid, España

²Departamento de Física, Universidad del Valle, Cali, Colombia

⁺Deceased (This article collects a part of the Ph.D. work of VFRS, who unexpectedly died during the preparation of his Ph.D. manuscript)

^{*}jfmarco@iqf.csic.es

Four different compositions of Fermanal steels, covering high and low manganese content (austenitic and ferritic alloys) and with or without copper, as a minor alloying element, were selected to evaluate the influence of the manganese content and that of copper on their corrosion behavior. For this purpose, alloy samples were submitted to a SO₂-polluted atmosphere under humid/dry cycles exposure. The selected aluminum concentration is within the range reported to be necessary for assuring good corrosion resistance. The study was carried out using X-ray photoelectron (XPS), Auger electron (AES, + Ar⁺-depth profiling), and ⁵⁷Fe-Mössbauer spectroscopies, X-ray diffraction (XRD), and Scanning Electron Microscopy (SEM). The characterization of the native oxide film formed after exposure of the freshly-polished alloy surfaces to the laboratory atmosphere showed that the films contain Al³⁺, Mn²⁺/Mn³⁺, and Fe³⁺. The aluminum and manganese concentrations in the native oxide layer were always higher than those of the base alloy, whereas the iron concentration decreased with respect to that of the alloy. Under exposure to the SO₂-polluted atmospheres, the initial corrosion rate of the alloy strongly depends on the nature and thickness of this naturally formed native oxide film. The thicker film formed on the austenitic samples can be explained because austenitic alloys have a major abundance of manganese, which is more reactive towards atmospheric oxygen. The very low corrosion rate shown by these alloys, as compared with that observed in pure iron and weathering steel, must be related to the formation of corrosion products constituted by aluminum and manganese compounds (Al₂O₃, MnSO₄). These compounds form a uniform layer able to block the access of the acid electrolyte to the metallic surface. The austenitic sample micro alloyed with copper presents the lowest corrosion rate. This can be attributed to the cooperative effect of higher concentrations of amorphous and/or finely divided Fe-oxyhydroxides with the presence of Mn/Al-corrosion compounds.

ICAME-T04-P17

Estimation of Hyperfine Interactions in Mössbauer Spectra with Multiple Components

Ryota Moriguchi^{1*}, Satoshi Tsutsui^{2,3}, Shun Katakami⁴, Kenji Nagata⁵, Masaichiro Mizumaki⁶, and Masato Okada⁴

¹Graduate School of Science, The University of Tokyo, Tokyo, Japan

²Japan Synchrotron Radiation Research Institute (JASRI), SPring-8, Hyogo, Japan

³Institute of Quantum Beam Science, Graduate School of Science and Engineering, Ibaraki University, Ibaraki, Japan

⁴Graduate School of Frontier Sciences, The University of Tokyo, Tokyo, Japan

⁵Center for Basic Research on Materials, National Institute for Materials Science (NIMS), Tsukuba, Japan

⁶Faculty of Science, Kumamoto University, Kumamoto, Japan

*moriguchi-ryota896@g.ecc.u-tokyo.ac.jp

We previously developed a Bayesian inference-based quantitative analysis method for hyperfine interactions in single-component ^{57}Fe Mössbauer spectra and demonstrated its effectiveness [1]. However, actual samples frequently produce multi-component spectra reflecting various electronic states at Fe sites in materials. To address this, we have extended our Bayesian analytical approach to accommodate more complex sample systems comprising multiple spectral components.

Our method utilizes Bayesian inference to simultaneously and data-driven estimate the number of components as well as the Mössbauer parameters for each component. The optimal combination of hyperfine interactions and the number of components is objectively selected based on Bayesian free energy comparisons among candidates.

To validate our method, we have analysed simulated Mössbauer spectral data of magnetite (Fe_3O_4), generated using Mössbauer parameters reported in [2], and evaluated the accuracy of our analytical approach. Figure 1 illustrates an example of the fitting results. In this presentation, we report the application of Bayesian inference to the spectral analyses of Mössbauer spectra, those of magnetite above and below the Verwey transition temperature, for example.

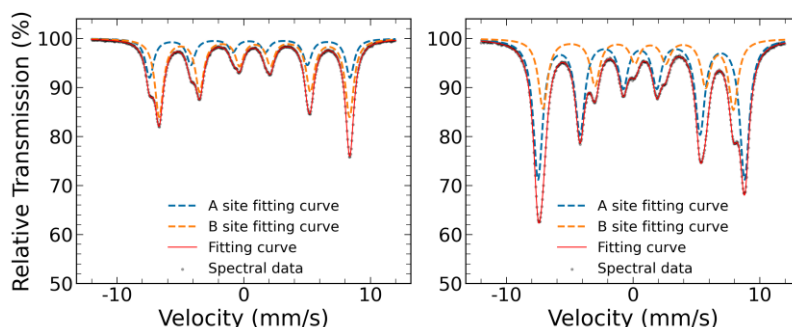


Figure 1. ^{57}Fe Mössbauer spectra of Fe_3O_4 simulated with the parameters reported in Ref. 2 and fitting curves with the Bayesian inference. The left (right) panel is the spectrum above (below) the Verwey transition temperature.

[1] R. Moriguchi *et al.*, *J. Phys. Soc. Jpn.* **91** (2022) 104002.

[2] A. Ito *et al.*, *J. Phys. Soc. Jpn.* **18** (1963) 1465.

Magnetic and Structural Insights Into the Hexagonal Polymorph of CuFeO₂ Delafossite

Karolina Siedliska^{1*}, Tomasz Pikula¹, Łukasz Gondek², Kamila Komędera^{2,3}

¹Lublin University of Technology, Lublin, Poland

²AGH University of Krakow, Kraków, Poland

³University of Zagreb, Zagreb, Croatia

*k.siedliska@pollub.pl

Delafossites are binary oxides with the general formula ABO₂, where A is a monovalent cation (e.g., Cu, Ag) and B is a trivalent metal ion (e.g., Al, Co, Fe). The parent compound, CuFeO₂, crystallizes in two polymorphs: rhombohedral (3*R*, space group *R*-3*m*) and hexagonal (2*H*, space group *P*6/*mmc*), which differ in the stacking orientation of B³⁺O₆ octahedra and A⁺ layers. While the 3*R* polymorph has a three-layer repeat along the *c*-axis, the 2*H* form features alternating A⁺ layers rotated by 180°, resulting in a two-layer sequence. The stacking sequence significantly influences physical properties, and although the 3*R* form is kinetically favored, the 2*H* polymorph is difficult to synthesize and often appears as a transient phase. CuFeO₂ is of interest due to its unique magnetic behavior, with the 3*R* polymorph exhibiting frustrated triangular lattice magnetism and two successive phase transitions near 14 K and 11 K, accompanied by a structural transition to monoclinic symmetry. In contrast, the magnetic properties of the rare 2*H*-CuFeO₂ polymorph remain still underexplored. This study presents a low-temperature hydrothermal synthesis of 2*H*-CuFeO₂ and investigates its structural and magnetic properties via XRD and Mössbauer spectroscopy, revealing distinct features compared to the well-known 3*R* form.

XRD analysis (12–280 K) showed that the sample contains mainly hexagonal 2*H*-CuFeO₂ (78.1%) with minor trigonal 3*R* phase (18.3%) and trace Fe₂O₃ (3.6%). Both phases exhibit typical temperature-dependent changes in *a*-lattice parameters, but their *c*-lattice behaviors differ. The 3*R* phase shows almost no change in *c* with a slight anomaly near 15–16 K, likely due to magnetic ordering. In contrast, the 2*H* phase shows a broad maximum in *c* between 50–100 K and a similar anomaly at low temperatures, indicating complex anisotropic lattice dynamics. Low-temperature Mössbauer effect measurements provided insights into the hyperfine interactions of 2*H*-CuFeO₂, revealing behavior distinct from the well-known 3*R* polymorph. Below 20 K, the spectra show complex shapes, indicating the presence of spin density waves and magnetic relaxations. Notably, below 11 K, a broad distribution of hyperfine magnetic fields emerges, which progressively narrows with decreasing temperature, suggesting gradual changes in the magnetic ordering type.

This work was supported by the grant from the framework of the pro-quality program of Lublin University of Technology, “Grants for Grants” (Grant no. 9/GnG/2023).

Synchrotron-based In-situ Mössbauer Study of the Red-Ox Cycling of Iron and Iron Oxides for Energy Applications

Jonas Spielmann^{1*}, Lukas Braun², Sergey Yaroslavtsev,³ Nils Thönissen¹, Jianing Bao¹, Dmitry Doronkin², Jan-Dierk Grunwaldt² and Ulrike I. Kramm¹

¹Technical University of Darmstadt, Darmstadt, Germany

²Karlsruhe Institute of Technology, Karlsruhe, Germany

³European Synchrotron Research Facility, Grenoble, France

*jonas.spielmann@tu-darmstadt.de

Iron is a promising candidate as a carrier for renewable energy, e.g., by retrofitting existing coal-fired power plants.[1] It is non-toxic, abundant, and has low safety concerns. Release of energy is achieved by the oxidation of the iron powder. Charging the carrier involves the subsequent reduction of iron oxide using green H₂.

In a previous work [2], we investigated how the oxidation behavior of iron powders differs from the well-understood slab oxidation. We thereby found that the mass gain of solid spherical iron particles also followed a parabolic rate law, but considering their size distribution and shape during modeling is crucial. In a second work [3], we investigated the reduction behavior of a porous iron oxide powder by in-situ SMS, QEXAFS, and XRD. Each of the techniques contributed unique information, complementing each other and enabling a more complete understanding of the full process. SMS thereby showed an edge in identifying iron phases [3].

The overall feasibility of using iron as an energy carrier in a circular system and the cyclability of the iron powder (repeated charge–discharge cycles) were investigated by TGA, SEM, and post-mortem XRD.[4,5] It becomes apparent that repeated oxidation and reduction of solid-state particles leads to a pronounced change in particle morphology, which impacts their reaction characteristics. For example, induced by the cycling, particles become more porous resulting in an increase in reactive surface. This improves the speed of the reactions and the mass transport of reactive gases and water in and out of the particle. Missing in these studies, however, is the use of techniques to resolve iron phases during the reactions.

Thus, we followed iron's oxidation and reduction behavior at several temperatures under isothermal conditions for several cycles in synthetic air for oxidation and forming gas for the reduction by synchrotron-based Mössbauer spectroscopy in a capillary tube reactor. Using partially enriched iron oxide powder, we achieved a time resolution of 60 s while still being able to unambiguously distinguish between the different iron phases present during the oxidation and reduction reactions. We will present our approach to data analysis. A mechanistic model describing the processes involved in oxidation and reduction reactions is derived from these learnings. Our insights clearly prove the importance of synchrotron-based Mössbauer spectroscopy for the characterization of iron (oxide) powders as energy storage materials.

[1] P. Debiagi et al., *Renew. Sustain. Energy Rev.* **165** (2022) 112579.

[2] J. Spielmann & D. Braig et al., *Phys. Chem. Chem. Phys.* **26** (2024) 13049.

[3] L. Braun & J. Spielmann et al., *ChemSusChem* (2024) e202401045.

[4] A. Sepman et al., *Combustion and Flame* **259** (2024) 113137.

[5] C. Kuhn et al., *Proc. Combust. Inst.* **40** (2024) 105207.

ICAME-T04-P20

Effects of Iron Introduction to the Silica Supported Nickel Catalysts on the Formation of NiFe-based Nanoparticles

Karolina Karpińska-Wlizło¹, Zbigniew Surowiec^{2*}, Wojciech Gac¹

¹ Faculty of Chemistry, Maria Curie -Skłodowska University, Lublin, Poland

² Institute of Physics, Maria Curie -Skłodowska University, Lublin, Poland

*zbigniew.surowiec@mail.umcs.pl

Nanostructured nickel-iron materials are of widespread interest due to their unique mechanical, structural, magnetic, surface, and catalytic properties. Particularly interesting effects of the presence of iron can appear in the catalysts containing bimetallic NiFe nanoparticles used in numerous catalytic processes. The CO₂ hydrogenation reaction is an interesting proposal for the utilisation of waste CO₂ using green hydrogen for the production of valuable chemicals and energy carriers. The possibility of improving the activity of nickel catalysts for the low-temperature methanation of CO₂ by introducing small amounts of an iron modifier has been indicated in the literature. However, the reasons for this effect have not been fully elucidated.

The aim of the studies was to investigate the influence of iron addition on the formation of bimetallic NiFe nanoparticles on the silica support and their physicochemical properties. A series of silica-supported catalysts was prepared with a nickel content of 10 wt.%, containing different amounts of iron, from 0 to 10 wt.%, by the application of the impregnation method. The catalysts were investigated by the application of different experimental methods, including XRD, temperature-programmed reduction and hydrogen desorption, as well as Mössbauer spectroscopy. It was found that the introduction of iron to the nickel catalysts led to the formation of small NiFe-based oxide nanoparticles. Their reduction facilitated the formation of the bimetallic nanostructured objects of different structural and surface properties. It was demonstrated that the state of iron was related to the composition of the catalysts.

[1] N. Ullah, F. Jerome, K. Vigier, *Mol. Catal.* **529** (2022) 112558.

[2] X. Xu, F. Song, X. Hu, *Nature Commun.* **7** (2016) 12324.

[3] K. Tomishige, D. Li, M. Tamura, Y. Nakagawa, *Catal. Sci. Technol.* **7** (2017) 3952

Structural and Magnetic Studies of $\text{Co}_x(\text{Cr,Fe,Mn,Ni})_{3-x}\text{O}_4$ High-entropy Spinel Oxides

M. Szymczak^{1*}, K. Berent², M. Nowakowska³, J. Dąbrowa³, M. Reissner⁴,
M. Sikora⁵, J. Cieślak¹

¹ Faculty of Physics and Applied Computer Science, AGH University of Krakow, Poland

² Academic Center for Materials and Nanotechnology, AGH University of Krakow, Poland

³ Faculty of Materials Science and Ceramics, AGH University of Krakow, Poland

⁴ Institute of Solid State Physics, TU Wien, Wien, Austria

⁵ National Synchrotron Radiation Centre SOLARIS, Jagiellonian University, Poland

*szymczak@agh.edu.pl

Over the last years, high-entropy oxides (HEOx) [1] have gained significant interest as a strategy for designing functional materials. The core of this concept is introducing multiple (usually, at least 5) cations to the same sublattice, most often in the near-equimolar ratio. The intent is to trigger synergistic effects rooted in the complex interactions between the elements, beyond the regular rule-of-mixtures, to obtain properties unavailable to conventional materials. The reports show the potential of HEOx for application in several fields, such as catalysis or energy conversion (Li-ion, Solid Oxide Fuel Cells), as well as distinctive magnetic behavior. Yet, what hinders their effective design is the limited understanding of the exact structure of HEOx and the mechanisms underlying the observed characteristics [2]. Spinel-structured oxides provide an exceptionally vast space for exploiting the high-entropy approach. Due to their two non-equivalent cationic sublattices, they allow for significant property modifications even in conventional systems. Yet, the very same feature makes the description and understanding of these systems even more complex.

In this work, we begin systematic studies of the composition-structure-properties relationship in this group of HEOx. Starting with the first high-entropy spinel, $(\text{Co,Cr,Fe,Mn,Ni})_3\text{O}_4$ [3], we vary the Co content, obtaining a $\text{Co}_x(\text{Cr,Fe,Mn,Ni})_{3-x}\text{O}_4$ series ($x = 0-2$). We employ Mössbauer spectroscopy for structural analysis at room temperature and below, to access the multicomponent system through an element-selective probe. We use X-ray diffraction (XRD) with Rietveld analysis and scanning electron microscopy (SEM-EDS) to identify the symmetry of the systems, lattice parameters, and solubility limit of Co. We analyze the magnetic properties and their evolution with temperature through vibrating sample magnetometry. The increase of Co content leads to a lowering of the lattice constant. Over the solubility limit, segregation of Co and Ni is observed. The higher dopant concentration lowers the temperature of the transition from a magnetic to a paramagnetic state, while the dependence of the effective magnetic moment per atom on x exhibits a maximum ($x \approx 0.8$). The Mössbauer spectra exhibit features reflecting the highly distorted lattice of the HEOx, such as the wide distribution of quadrupole splitting values. They also illustrate the transition to a paramagnetic state, consistent with the global VSM measurements. Overall, our studies provide extensive analysis of the $\text{Co}_x(\text{Cr,Fe,Mn,Ni})_{3-x}\text{O}_4$ system and showcase the effectiveness of the applied methodology in the research in high-entropy oxides.

[1] C.M. Rost, et al., *Nature Communications* **6** (2015).

[2] A. Sarkar, et al., *Dalton Transactions* **50** (2021).

[3] J. Dąbrowa, et al., *Materials Letters* **216** (2018).

Research project partly supported by the program „Excellence initiative – research university” for the AGH University of Krakow and the Polish National Science Center (NCN) under project no. UMO-2022/45/B/ST8/.

ICAME-T04-P22

Synthesis, Mössbauer Study, and Catalytic Test of La-Sr-Fe Perovskite-related Materials

Nikolay Velinov^{1*}, Tanya Petrova¹, Katerina Tumbalova², Ralitsa Velinova², Georgi Ivanov², Hristo Kolev¹, Daniela Kovahceva², Anton Naydenov²

¹Institute of Catalysis, Bulgarian Academy of Sciences, Sofia, Bulgaria

² Institute of General and Inorganic Chemistry, Bulgarian Academy of Sciences, Sofia, Bulgaria

* nikivelinov@abv.bg

Materials with a perovskite structure (ABO_3) are among the most promising oxide catalytic materials for the catalytic combustion of volatile organic compounds (VOCs) due to their unique structure and properties. The ideal perovskite structure is characterized by cubic symmetry, where the A atoms are surrounded by 12 oxygen atoms and the B atoms by 6 oxygen atoms. Studies have shown that the catalytic efficiency of ABO_3 mainly depends on the B-cation, while the A-cation primarily plays a role in stabilizing the crystal structure. However, if the A-cation is replaced by another metal ion, the oxidation state of the B-site cation, oxygen vacancies, and cation defect density can change, indirectly affecting the catalytic combustion efficiency. It is possible to introduce different ions by partial or simultaneous substitution of A- and B-cations to adjust the oxidation state of B-cations, thereby influencing the catalytic properties of ABO_3 . From the perspective of searching for materials with the potential to modify and improve oxygen-ion transport properties in the crystal lattice, materials with layered perovskite structures are of particular interest. These include the Ruddlesden-Popper (R-P) phases, which are described by the general formula $\text{A}_{n+1}\text{B}_n\text{O}_{3n+1}$, where A is an alkaline, alkaline earth, or lanthanoid element, and B is an octahedrally coordinated cation. The structure consists of layers with a perovskite structure separated by layers with a NaCl-type structure. The value of n determines the thickness of the perovskite layer and corresponds to the number of BO_6 octahedra along the c-axis. Thus, the perovskite ABO_3 structure corresponds to the R-P phase with $n = \infty$, while A_2BO_4 (R-P, $n = 1$) is also known as the K_2NiF_4 -type structure. The present work aims to obtain La-Sr-Fe perovskite-related materials with different La:Sr ratios and to study their structure and catalytic behavior in the oxidation of VOCs.

Materials with nominal compositions $\text{La}_{1-x}\text{Sr}_x\text{FeO}_4$, where $x = 0.5, 1$, and 1.5 , were prepared using a sol-gel auto-combustion technique with the corresponding metal nitrates and citric acid as complexing/fuel agents. Structural characterization of the materials was performed using X-ray diffraction, Mössbauer spectroscopy, X-ray photoelectron spectroscopy, and nitrogen physisorption. X-ray diffraction confirmed the formation of single- and double-layer R-P phases, along with additional phases such as LaFeO_3 , La_2O_3 , and SrCO_3 . The Mössbauer spectrum of the sample with $x = 1.5$ consists of a singlet with $\delta = 0.04$ mm/s and a doublet with $\delta = 0.17$ mm/s and $\Delta = 0.51$ mm/s, proving the presence of Fe^{4+} in the Sr-rich sample. Catalytic tests of the synthesized materials were carried out in the complete oxidation of volatile organic compounds such as propane and butane. A correlation between the presence of Fe^{4+} in the perovskite-related catalysts and catalytic activity was established.

Acknowledgment: This work was supported by the Bulgarian Science Fund (Contract No KII-06-H89/5).

ICAME-T04-P23

Mössbauer Study of the Influence of Cold Plastic Deformation and Thermal Impact on Structural Transformations of Cast Duplex Steel cf8

Gaukhar Yeshmanova^{1*}, Mikhail Vereshchak¹, Irina Manakova¹,
Zhandos Tleubergenov¹

¹Institute of Nuclear Physics, Ibragimov str. 1, 050032 Almaty, Kazakhstan

*g.yeshmanova@inp.kz

A considerable number of works are devoted to the study of structural changes and the volume fraction of emissions during martensitic-austenitic transformation in austenitic steel by deformation, thermal, and radiation effects using the Mössbauer effect. Since the processes of identification of the patterns of martensitic transformations, as well as residual austenite stabilization in steels, are of considerable practical importance for predicting the long-term properties of steel. Mössbauer spectroscopy in the transmission geometry (MS) mode and in the electron channel backscattering mode (CEMS), and X-ray diffraction (XRD) have been used to study the austenitic-martensitic transformation in duplex steel CF8 under cold plastic deformation ($\varepsilon = 20\text{--}95\%$) and the kinetics of the reverse martensitic-austenitic transformation under thermal effect ($300\text{--}850\text{ }^{\circ}\text{C}$).

The dynamics of changes in the relative intensity of the MS spectrum of α' -martensite indicated the presence of a certain value of the deformation degree (in our case $\varepsilon \sim 10\%$), above which the process of α' -martensite formation can be followed by the MS method. After rolling the sample with $\varepsilon \geq 20\%$, the MS spectra were superpositions of two partial subspectra. In addition to the paramagnetic doublet, a magnetic sextet was observed, which corresponded to α' -martensite. During the growth of the deformation degree, the relative intensity of the sextet increased and reached about 88% at $\varepsilon = 95\%$, which was accompanied by a decrease in the content of γ -austenite. From the comparative analysis of the MS and CEMS spectra, it was evident that the formation of α' -martensite during plastic deformation occurred most intensively in the near-surface layers of steel, spreading in depth with the growth of the deformation degree.

The X-ray diffraction pattern of the sample before deformation was represented by a single phase with an *fcc* lattice corresponding to γ -austenite. The sample subjected to deformation $\varepsilon = 40\%$ showed the presence of α' -martensite in the reflections $(110)_{\alpha}$, $(200)_{\alpha}$ and $(211)_{\alpha}$. At high deformation degrees, this phase was particularly clearly visible; γ -austenite showed only the traces in the reflection $(220)_{\gamma}$. The phase composition, estimated by the intensities of main α' - and γ -phases, suggests that the martensite content reached its maximum value of 93 % at a deformation of $\sim 95\%$.

MS spectra of the samples deformed at 55 % after annealing at $300\text{--}850\text{ }^{\circ}\text{C}$ show that the relative intensity of the γ -austenite describing doublet increased during the rise of the annealing temperature. The isomer shift of the doublet remained constant, indicating that the electronic structure of austenite was unchanged. The steel sample before annealing had a two-phase structure containing α' -martensite (73 %) and residual γ -austenite (27 %); and the restoration of the original steel structure was completed at $850\text{ }^{\circ}\text{C}$.

The work was carried out under the support of the Ministry of Science and Higher Education of the Republic of Kazakhstan (Project AP19679693).

Mössbauer and X-ray Diffraction Studies of the Ion-induced Effects on Nb-Zr alloy

Mikhail Vereshchak¹, Irina Manakova¹, Gaukhar Yeshmanova^{1*},
Zhandos Tleubergenov¹, Adilkhan Shokanov²

¹Institute of Nuclear Physics, Ibragimov str. 1, 050032 Almaty, Kazakhstan

²Abai Kazakh National Pedagogical University, 050010 Almaty, Kazakhstan

*g.yeshmanova@inp.kz

Development of structural materials for nuclear power engineering is a complex scientific and technical task. The main requirement for such materials is radiation resistance, closely related to their mechanical properties. In our previous works [1,2], it was shown that ion implantation in charged particle accelerators is a convenient method for studying the radiation resistance of materials and a good simulator of neutron irradiation. Niobium alloys are characterized by good technological properties: relatively low density, small cross-section for the capture of thermal neutrons, and good resistance in contact with liquid metal coolants. Almost all niobium alloys have high hardness and electrical conductivity. These alloys are widely used as high-temperature fuel elements. In addition, they have good resistance to mechanical and radiation damage.

The aim of this work was a detailed study of the radiation-induced processes in the Nb-1.8Zr alloy implanted with ⁵⁷Fe ions. The elemental composition of the alloy, selected for the study, belongs to the poorly studied niobium part of the diagram of the Nb-Zr binary system. The samples for the study were prepared from 106 µm thick Nb-1.8Zr alloy plates using polishing and homogenizing annealing. Implantation of high-energy ⁵⁷Fe ions was carried out using the most optimal modes ($1 \cdot 10^{17} \text{ cm}^{-2}$ fluence, 0.2 MeV energy, and 100 nA current) at the UKP-2-1 heavy ion accelerator of the Institute of Nuclear Physics (Almaty, Kazakhstan).

Using the SRIM-2013 program, the projected range length of ions was determined to be 70 nm, which is comparable to the depth of the yield of conversion electrons from the irradiated layer. Ions of such energy have a small sputtering coefficient and most effectively form an irradiated layer for the study by the Mössbauer spectroscopy method on ⁵⁷Fe nuclei in the electron backscattering geometry. X-ray diffraction was also used to study the implantation effect on the alloy structure. Successive isochronous two-hour annealings were carried out in a vacuum furnace (vacuum $1 \cdot 10^{-6} \text{ mm Hg}$) at a temperature from 400 °C to 1000 °C with a step of 100 °C. The alloy structure was studied after each annealing. X-ray diffraction studies were carried out on a Bruker D8 diffractometer with a Cu-Kα emitter in the Bragg-Brentano geometry. The phases were identified using an ASTM and JCPDS card index. The Mössbauer studies were carried out on an MS-1104Em spectrometer. The Mössbauer spectra were processed by the model decoding method using the SpectrRelax program. The phase composition of the Nb-1.8Zr alloy was determined after implantation and at each stage of thermal annealing. The total number of atoms, the concentration of ⁵⁷Fe ions in the irradiated layer, and the distribution of the implant by phases were calculated.

This research was funded by the Ministry of the Republic of Kazakhstan. Project BR 23891530, Development of integrated scientific research in nuclear and radiation physics based on Kazakhstan's accelerator complexes.

[1] M. Vereshchak et al., *Materials* **16** (2023) 10.

[2] M Vereshchak et al., *J. Phys: Conf. Series* **2984** (2025) 012001.

ICAME-T05-P1

Mössbauer Spectroscopy as a Tool for Exploring the Effect of β -carotene on Red Blood Cells Oxygen Binding Properties

Joanna Fiedor^{1*}, Aleksander Siniarski^{2,3}, Grzegorz Gajos^{2,3}, Nika Spiridis⁴,
Květoslava Burda¹

¹AGH University of Krakow, Kraków, Poland

²Jagiellonian University, Medical College, Kraków, Poland

³The John Paul II Hospital, Kraków, Poland

⁴Jerzy Haber Institute of Catalysis and Surface Chemistry, Polish Academy of Sciences,
Kraków, Poland

*fiedor@agh.edu.pl

Carotenoids are a structurally and functionally very diverse group of natural pigments of isoprenoid type. They are important dietary compounds related to human health [1]. β -carotene is one out of ~30 carotenoids found in human blood samples. It is known to act as an efficient antioxidant [2,3] and modulator of the physicochemical properties of membranes [3,4]. It was suggested to act as an inhibitor of haemoglobin oxidation reactions induced by exogenous radical generators [5,6].

The objective of the present study was to investigate the effect of β -carotene on red blood cells, in particular on the hemoglobin-oxygen affinity. Blood samples were obtained from healthy donors. Erythrocytes were isolated, purified, and subjected to β -carotene treatment in concentrations ranging from physiological up to 500 μ M. To monitor the response of red blood cells to β -carotene presence, UV-VIS absorption and Mössbauer spectroscopies were applied. The results indicate that even at concentrations slightly above the physiological level β -carotene affects the molecular parameters of hem-iron and its ability of efficient oxygen binding and releasing.

Research project partly supported by the programme “Excellence initiative – research University” for the AGH University of Krakow and the National Science Centre (grants 2019/03/X/NZ7/01265 and 2019/33/B/NZ7/02724).

- [1] J. Fiedor and K. Burda, *Nutrients* **6** (2014)466.
- [2] T. Bohn et al., *Nutrition Research Reviews* **34** (2021) 276.
- [3] J. Fiedor et al., *Antioxidants* **10** (2021) 451.
- [4] J. Fiedor et al., *Acta Physica Polonica A* **139** (2021) 283.
- [5] S.T. Omaye et al., *Fundamental and Applied Toxicology* **40** (1997) 163.
- [6] R.C. Chist et al., *Life Sciences* **99** (2014) 52.

pH Dependent Low-frequency Modes in an Electron Transport Protein

Lukas Knauer^{1*}, Xenia Mechler¹, Marco A. M. Tummeley¹, Maren Hoock¹, Konstantin Gröpl¹, Paul Hausbrandt¹, Tim Hochdörffer¹, Juliusz Wolny¹, Bertha Martins², Serguy Yaroslavtsev², Dimitrios Bessas², Aleksandr Chumakov², Deepak Prajapat⁴, Ilya Sergeev⁴, Antonio J. Pierik¹, Volker Schünemann¹

¹University of Kaiserslautern-Landau, Kaiserslautern, Germany

²Humbolt-Universität zu Berlin, Berlin, Germany

³European Synchrotron Radiation Facility, Grenoble, France

⁴Deutsches Elektronen-Synchrotron, Hamburg, Germany

*lknauer@rptu.de

Iron sulfur [Fe-S] clusters play an important role in the essential processes of life such as photosynthesis, cellular respiration, and nitrogen fixation. Among other functions, they are involved in electron transfer (ET). Well-studied examples are ferredoxins, which harbour a [2Fe-2S] cluster bound via four cysteines. The protein Apd1 has an unusual [2Fe-2S] cluster, which is bound to the protein matrix via two cysteines and two histidines (Fig. 1a) [1]. This so-called bishistidinyl-coordination was verified by mutation studies and spectroscopic investigations, including Mössbauer spectroscopy. Moreover, it was shown that the histidines are protonated at low pH values and deprotonated at high pH values. This observation suggests that Apd1, which is necessary for cell survival in yeast in the presence of redox mediators such as gallobenzophenone or pyrogallol, is engaged in proton-coupled electron transfer (PCET). To elucidate the influence of the protonation state on the electronic and vibrational properties of the histidine-coordinated iron, we have performed nuclear forward scattering (NFS) and nuclear inelastic scattering (NIS) at different pH values. In addition, using the new high-resolution monochromator (Spectrograph) at ID14, ESRF, NIS data with an energy resolution of 0.12 meV have been measured that clearly show the influence of protonation on the low-energy protein modes $< 80 \text{ cm}^{-1}$. Further, we have measured an Apd1 double mutant with a ferredoxin-like [2Fe-2S] cluster coordination (Fig. 1b) and observed significant differences in the low-frequency mode region compared to the native protein.

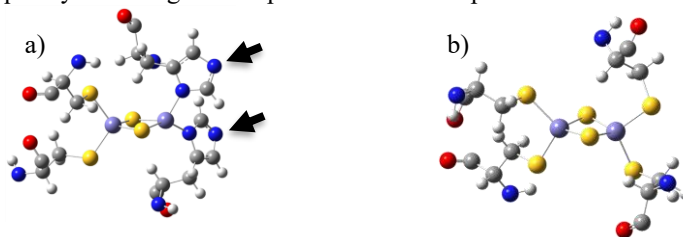


Figure 1. a) Coordination of the [2Fe-2S] cluster in Apd1. The arrows mark the protonation sites of the histidines. b) Coordination of the ferredoxin-like [2Fe-2S] cluster in the Apd1 double mutant.

[1] K. Stegmaier et al., *J. Am. Chem. Soc.*, **141** (2019) 5753-5765.

ICAME-T05-P3

A [2Fe-2S] Cluster in a Rieske-Dioxygenase-like Protein of *Aspergillus fumigatus*

Lukas Knauer¹, Simon Unik¹, Antonio J. Pierik¹, Volker Schünemann¹

¹University of Kaiserslautern-Landau, 67663 Kaiserslautern, Germany

*lknauer@rptu.de

Iron sulfur [Fe-S] clusters play an important role in the essential processes of life, such as photosynthesis, cellular respiration, and nitrogen fixation. Among other functions, they are involved in electron transfer (ET). Well-studied examples are ferredoxins, which harbour a [2Fe-2S] cluster bound via four cysteines. The Rieske protein is the best-known example of a [2Fe-2S] cluster that is not purely cysteine-bound. One of the Fe atoms is bound via Histidines to the protein matrix. The Histidines are protonated at low pH values and deprotonated at high pH values. This special coordination, also known as bishistidinyll-coordination, is crucial for proton-coupled electron transfer (PCET) [1].

In oxygenases, molecular oxygen is integrated into biochemical substrates. In Rieske-Dioxygenases (RDOs), Rieske-like [2Fe-2S] clusters play a decisive role as electron carriers. The actual reaction takes place on a mononuclear Fe atom [2]. We were able to identify such a coordinated cluster in a Rieske-Dioxygenase-like protein from *Aspergillus fumigatus* using spectroscopic measurements, including Mössbauer spectroscopy (Fig. 1). We carried out Mössbauer measurements with an external magnetic field to characterise the electrical properties of the cluster in more detail.

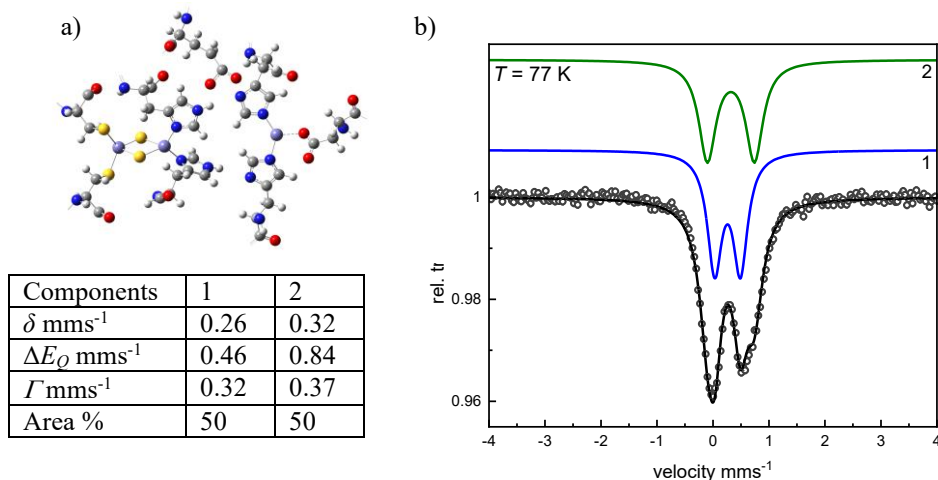


Figure 1: a) AlphaFold structural model of the [2Fe-2S] cluster and the mononuclear Fe with its ligands and an aspartate in between. b) Mössbauer spectra of the Oxygenase-like protein of *Aspergillus fumigatus* at 77 K and the corresponding Mössbauer parameters.

[1] A. Alberts et al., *J. Am. Chem. Soc.*, **136**, **10** (2014) 3946-3954.

[2] M. Quareshy et al. *J. Biol. Chem.*, **296** (2021) 100038

ICAME-T05-P4

Fe²⁺ Vacancies in Zn Doped Iron Oxide Magnetic Nanoparticles

José S. Garitaonandia¹, David Merida², Idoia Castellanos-Rubio³, Daniela Iglesias-Rojas³, Maite Insausti³, Fernando Plazaola^{2*}

¹Fisika Aplikatua II saila, Zientzia eta Teknologia Fakultatea, UPV/EHU, 48940 Leioa, Spain

²Elektrizitatea eta Elektronika saila, Zientzia eta Teknologia Fakultatea, UPV/EHU, 48940 Leioa, Spain

³Kimika Organikoa eta ez-organikoa saila, Zientzia eta Teknologia Fakultatea, UPV/EHU, 48940 Leioa, Spain

*fernando.plazaola@ehu.eus

The effectiveness of magnetic hyperthermia therapies depends on the heating capacity or specific absorption rate of magnetic nanoparticles (MNPs) in the presence of an alternating magnetic field [1]. Therefore, it is necessary to optimize the physical properties of the nanoparticles: the most widely used are iron oxide MNPs due to their biocompatibility. The introduction of zinc into the spinel structure of magnetite nanoparticles has proven to be an effective strategy for optimizing MNP properties [2]. However, for this to occur, the zinc ion must be present in the desired stoichiometry and occupy the appropriate sublattice, which critically depends on the synthesis method.

In this work, Zn-doped magnetite nanoparticles are studied based on the thermolysis of two types of organometallic precursors: (i) a mixture of two monometallic oleates (FeOl+ZnOl) and (ii) a bimetallic oleate of iron and zinc (Fe_{3-y}Zn_yOl) [3]. The distribution of the Fe center and vacancies within the ferrite lattice has been examined in detail using Mössbauer spectroscopy, which allowed a determination of the stoichiometry in each sample, highly consistent with lattice parameters estimated by Rietveld refinement of X-ray powder diffraction patterns.

In addition, the methodology used to determine the vacancy concentration within the ferrite lattice in the studied nonstoichiometric Zn-doped iron oxide MNPs indicates that in samples with similar Zn content.

This work was supported by institutional funding from the Basque Government under IT-1500-22, GU_IT1226-19, ELKARTEK20/06 projects, and from the Spanish Ministry of Economy and Competitiveness under MAT2019-106845RB-100 project.

[1] B. Kozissnik et al., *Int. J. Hyperthermia* **29** (2013) 706.

[2] T. Zargar et al., *Ceram. Int.* **43** (2017) 5794.

[3] I. Castellanos-Rubio et al., *Chem. Mater.* **33** (2021) 3139.

ICAME-T06-P1

⁵⁷Fe Mössbauer Spectroscopy of Selected Serpentine-Related Nephrite Samples

Dariusz Malczewski¹, Maria Dziurawicz^{1*}, Agnieszka Grabias²

¹University of Silesia, Institute of Earth Sciences, 41-200 Sosnowiec, Poland

²Łukasiewicz Research Network - Institute of Microelectronics and Photonics, 02-668 Warszawa, Poland

*maria.dziurawicz@us.edu.pl

The poster presents the preliminary results of ⁵⁷Fe Mössbauer spectroscopy of serpentinite-related nephrite (ortho-nephrite, nephrite jade) samples collected from deposits in Jordanów and Nasławice (Poland), and Ospa, East Sayan (Russia) [1]. Nephrite, an almost monomineral rock, is made of full-grained amphiboles: actinolite $\text{Ca}_2(\text{Mg}, \text{Fe}^{2+})_5[\text{Si}_8\text{O}_{22}](\text{OH})_2$ and tremolite $\text{Ca}_2\text{Mg}_5[\text{Si}_8\text{O}_{22}](\text{OH})_2$. Secondary minerals in the nephrites include: magnetite, chromite, diopside, grossular, graphite, apatite, rutile, vesuvianite, datolite, fuschite, antigorite, and chrysotile [2].

The practical and ornamental use of nephrite jade by humans dates back to at least the early Neolithic. Chinese culture and artwork have featured jade since its earliest inception, and jade carving is particularly well-developed in East Asia. From antiquity and even into the present day, items made of nephrite jade are prized as gifts and stores of value.

A primary goal of this research was to ascertain whether the observed differences in the ⁵⁷Fe Mössbauer spectra and derived hyperfine parameters of the samples studied could be used to determine the geographical origin of nephrite.

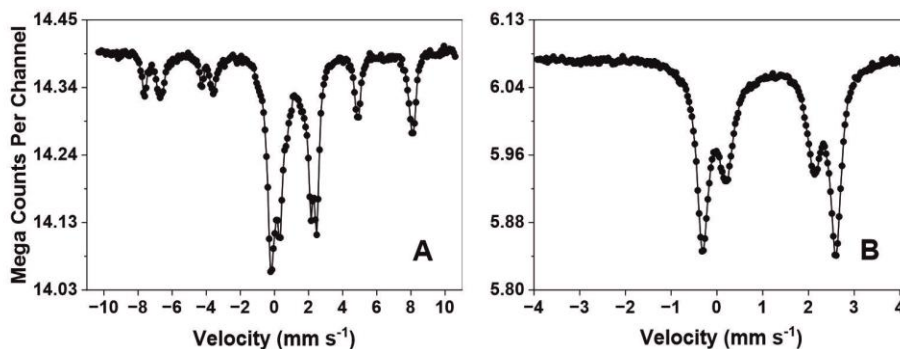


Figure 1. Experimental ⁵⁷Fe Mössbauer spectra of (A) Nephrite from Naslawice (NS2), and (B) Nephrite from East Sayan (SB2).

Acknowledgements. This work was supported by the National Science Centre of Poland; grant no. 2018/29/B/ST10/01495.

[1] D. Malczewski et al., *Gems Gemol.* **57** (2022) 196-213.

[2] G. Gil, *Geol. Q.* **57** (2013) 395-404.

ICAME-T06-P2

Utilization of Synchrotron Mössbauer Radiation for Single Particle Analysis of Luna 24 Samples

R. Groß, J. Pawlak, K. Tran, E. Bonato, M. Blumers, I. Kuppenko, X. Li, H. Gaber, S. Rajnak, J. Helbert, A. Chumakov, C. Hamann, A. Airo, J. Feige, Sergey Yaroslavtsev, Dimitrios Bessas, Wolfgang Schöner, Aurélie Van den Neucker, F. Renz

Leibniz University Hannover, Institute for Coordination Chemistry, Germany

*rene.gieseler@acd.uni-hannover.de

To broaden our understanding of extraterrestrial processes, space agencies globally are exploring innovative analytical tools. The instruments used in space missions must meet stringent requirements for volume, mass, power consumption, radiation resistance, and data transmission, limiting the applicability of some analytical tools for in situ use. However, the ability to return samples to Earth provides an opportunity to leverage advanced analytical methods not feasible on space missions. This study presents an advanced analysis of the Luna 24 sample using the Synchrotron Mössbauer Source (SMS) at the European Synchrotron Radiation Facility (ESRF) in Grenoble, France.

The Luna 24 sample was collected during the Soviet Luna 24 mission, the last mission of the Luna program, in August 1976. It involved the successful return of lunar soil from the Moon's Mare Crisium region. This soil is known to contain a variety of minerals, including ilmenite, pyroxenes, olivine, and iron-rich glass. Traditional Mössbauer spectroscopy, typically employed with centimeter-scale beam sizes, can also be used in situ, as demonstrated by the MIMOS II spectrometer on the Mars rover in 2004. However, the beam size typically limits examinations to bulk samples or powders, making it challenging to analyze single particles and complicating the differentiation of individual compounds within complex powder compositions.

In contrast, SMS enables a reduction of beam size to sub-micron levels, facilitating the analysis of single particles—an unprecedented achievement for extraterrestrial sample analysis at the synchrotron that allows for the resolution of more complex compounds. Our current analysis of the Luna 24 sample benefits from this enhanced resolution, leading to improved spectral evaluation and greater precision in phase assignment and mineralogical composition assessment.

Furthermore, by comparing our results with those from conventional Mössbauer spectroscopy performed at the lab, we underscore the advantages of synchrotron-based techniques in effectively resolving complex compositional spectra. This research not only demonstrates the feasibility and superior resolution afforded by synchrotron techniques but also highlights the potential of synchrotron-based Mössbauer spectroscopy for future space missions. Ultimately, this study not only validates the effectiveness of the SMS in extraterrestrial sample analysis but also lays the groundwork for future research into the oxidation states and phase compositions of materials from beyond Earth.

ICAME-T06-P3

Mössbauer Spectroscopy and Magnetization Measurements of Fe-Ni-Co Alloys from Some Meteorites

M.V. Goryunov¹, I. Felner², G. Leitus³, A.V. Chukin¹, S.P. Naumov^{1,4}, G. Varga⁵,
Z. Dankházi⁵, E. Kuzmann^{5*}, Z. Homonnay⁵, M.I. Oshtrakh¹

¹Ural Federal University, Ekaterinburg, 620002, Russian Federation

²The Hebrew University, Jerusalem, 91904 Israel

³Weizmann Institute of Science, Rehovot, Israel

⁴M.N. Mikheev Institute of Metal Physics UB RAS, Ekaterinburg, Russian Federation

⁵Eötvös Loránd University, Budapest, Hungary

*erno.kuzmann@ttk.elte.hu

The Fe-Ni-Co alloys in meteorites have a very complex structure due to (i) slow cooling from high temperatures and, in some cases, due to (ii) reheating within metamorphic processes or after shock effects in space. The samples of Fe-Ni-Co alloys from four iron meteorites (Kayakent IIIAB, Campo del Cielo IAB-MG, Gebel Kamil ung, and Trenton IIIAB) and one stony-iron meteorite (Omolon PMG) were studied by scanning electron microscopy (SEM) with energy dispersive spectroscopy (EDS), X-ray diffraction (XRD), magnetization measurements, and Mössbauer spectroscopy. SEM with EDS demonstrated variations in Ni concentrations even within one metal phase, e.g., the α -Fe(Ni, Co) phase. The presence of the main α -Fe(Ni, Co) phase and minor γ -Fe(Ni, Co) phase, and in some cases, small contents of iron-nickel phosphides (Fe, Ni)₃P were indicated by XRD in these meteorites. Saturation magnetic moments at ~300 K were slightly different: 175 emu/g (Kayakent IIIAB), ~192 emu/g (Gebel Kamil ung), 235 emu/g (Trenton IIIAB), 238 emu/g (Omolon), and 241 emu/g (Campo del Cielo IAB-MG). The Mössbauer spectra of Fe-Ni-Co alloys from these meteorites are asymmetric six-line patterns that were well fitted using different numbers of magnetic sextets assigned to the corresponding phases (Fig. 1). Additional minor components were associated with the paramagnetic γ -Fe(Ni, Co) phase and (Fe, Ni)₃P. The presence of several sextets with different H_{eff} values associated with one magnetic phase, e.g., the α -Fe(Ni, Co) phase, was related to the variation of Ni concentrations in this phase.

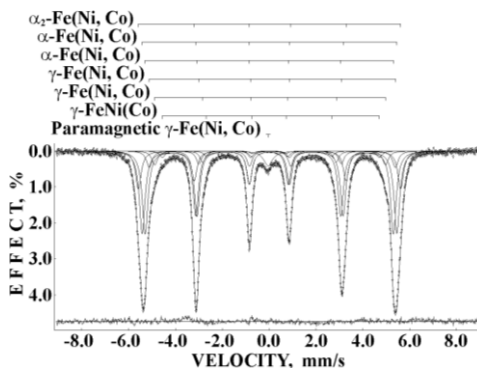


Figure 1. Mössbauer spectrum of Gebel Kamil ung iron meteorite. Indicated components are the result of the best fit. The differential spectrum is shown on the bottom. $T = 295$ K.

This work was supported by the Ministry of Science and Higher Education of the Russian Federation, project № FEUZ-2023-0013. M.I.O., M.V.G., and S.P.N. gratefully acknowledge the Ural Federal University Program of Development within the Priority-2030 Program (research funding from the Ministry of Science and Higher Education of the Russian Federation). This work was carried out within the Agreement of Cooperation between the Ural Federal University (Ekaterinburg) and the Eötvös Loránd University (Budapest).

ICAME-T06-P4

Mössbauer Spectroscopy, X-Ray Diffraction and Magnetization Study of Tamdakht H5 and Annama H5 Ordinary Chondrites

E.V. Petrova¹, M.V. Goryunov¹, A.V. Chukin¹, A.A. Maksimova², G. Leitus³, I. Felner⁴, G. Varga⁵, Z. Dankházi⁵, M. Gritsevich⁶, E. Kuzmann^{5*}, Z. Homonnay⁵, T. Kohout⁷, M.I. Oshtrakh¹

¹Ural Federal University, Ekaterinburg, 620002, Russian Federation

²University of South Carolina, Columbia, South Carolina 29208, USA

³Weizmann Institute of Science, Rehovot, Israel

⁴The Hebrew University, Jerusalem, 91904 Israel

⁵Eötvös Loránd University, Budapest, Hungary

⁶University of Helsinki, Helsinki, Finland

⁷Aalto University, Espoo, Finland

*erno.kuzmann@ttk.elte.hu

The iron-bearing phases and crystals in the bulk interiors of the Tamdakht H5 and Annama H5 ordinary chondrites were studied by optical microscopy, scanning electron microscopy with energy dispersive spectroscopy, X-ray diffraction (XRD), magnetization measurements, and Mössbauer spectroscopy. The main iron-bearing phases/crystals such as olivine, orthopyroxene, clinopyroxene, troilite, chromite, and hercynite, as well as Fe-Ni-Co alloy with the α_2 -Fe(Ni, Co), α -Fe(Ni, Co), and γ -Fe(Ni, Co) phases were identified in both meteorites. XRD showed some similarities and differences in the bulk interior compositions from Tamdakht H5 and Annama H5, with a high content of Fe-Ni-Co alloy (7.5 wt.%) in both ordinary chondrites. Saturation magnetic moments at 5 K for the bulk interiors from Tamdakht H5 and Annama H5 were 49.9 emu/g and 38.9 emu/g, respectively. The Mössbauer spectra of the bulk interiors from both meteorites were fitted well with estimation of the Mössbauer parameters for all spectral components with their relation to the corresponding iron-bearing phases and crystals (Figure 1). These results showed a significantly higher total relative areas of the spectral components associated with Fe-Ni-Co alloy (53.2% and 52.2% for Tamdakht H5 and Annama H5, respectively), which was unusual for H ordinary chondrites.

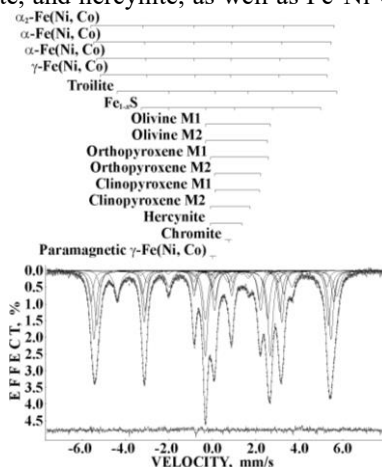


Figure 1. Mössbauer spectrum of Tamdakht H5 ordinary chondrite. Indicated components are the result of the best fit. The differential spectrum is shown on the bottom. $T=295$ K.

This work was supported by the Ministry of Science and Higher Education of the Russian Federation, project № FEUZ-2023-0013. M.I.O., E.V.P., and M.V.G. gratefully acknowledge the Ural Federal University Program of Development within the Priority-2030 Program (research funding from the Ministry of Science and Higher Education of the Russian Federation). This work was carried out within the Agreement of Cooperation between the Ural Federal University (Ekaterinburg) and the Eötvös Loránd University (Budapest).

ICAME-T06-P5

Studying Phosphorous Containing Vivianite $\text{Fe}_3(\text{PO}_4)_2 \cdot 8\text{H}_2\text{O}$ Extracted from Wastewater

Johan Lindén^{1*}, Lobna Amin^{2,3}, Fredrik Lindroos¹, Raed A. Al-Juboori^{2,4}, Anna Mikola², Eeva-Leena Rautama⁵, and Mathieu Spérandio³

¹Åbo Akademi University/Faculty of Science and Engineering/Physics, Turku, Finland

²Aalto University, Department of Built Environment, Espoo, Finland

³TBI, Université de Toulouse, CNRS, INRAE, INSA, Toulouse, France

⁴NYUAD Water Research Center, New York University – Abu Dhabi Campus, UAE

⁵Aalto University, Department of Chemistry and Materials Science, Espoo, Finland

*jlinden@abo.fi

Phosphorus is a natural resource obtained by mining and is an important element for agricultural fertilizers. Sources of phosphorus ores are globally limited and subject to increasing demands. Therefore, recycling phosphorus from wastewater is desirable both from an environmental and an economic perspective. It has been suggested that recovery of phosphorus could be achieved by mineralizing it using iron to vivianite $\text{Fe}_3(\text{PO}_4)_2 \cdot 8\text{H}_2\text{O}$. [1]

Apart from vivianite formation, there are competing reactions occurring in the wastewater treatment plants (WWTP), leading to the formation of other iron-based compounds. We have studied dried sludge samples obtained from various stages of the treatment process at Viikinmäki WWTP in Finland, in order to quantify the occurrence of vivianite. ^{57}Fe Mössbauer spectroscopy was one of the main tools, along with chemical analyses and X-ray diffraction. [2]

Room temperature Mössbauer spectra reveal the characteristic quadrupole doublets of high-spin Fe^{2+} in vivianite. A part of the iron atoms of vivianite oxidise to Fe^{3+} , giving rise to small doublets strongly overlapping with other non-phosphorus iron compounds. Some of the samples were measured at 5.6 K to study magnetically ordered vivianite ($T_N \approx 12$ K).

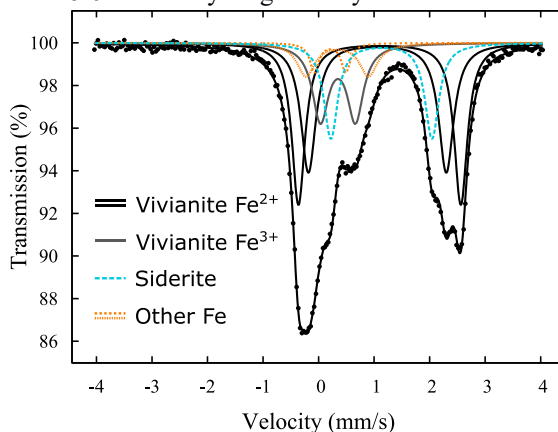


Figure 1. Room-temperature spectrum of wastewater sludge containing vivianite. Components due to divalent (trivalent) vivianite are indicated in black (gray), while other Fe-containing phases are drawn with a dashed line.

[1] P. Wilfert et al., *Water Research* **144** (2018) 312.

[2] L. Amin et al., *Science of the Total Environment* **912** (2024) 169520.

Tungsten-modified Iron Oxides as Nanocatalysts for Degradation of a Painkiller, Acetaminophen by Activating Peroxymonosulfate

Aebin Sin², Libor Machala^{1*}, Petr Novák¹, Changseok Han²

¹Department of Experimental Physics, Faculty of Science, Palacký University Olomouc, Olomouc, Czech Republic

²Department of Environmental and Polymer Engineering, Graduate School of INHA University, Incheon, Republic of Korea

*libor.machala@upol.cz

Acetaminophen (APAP) is a well-known type of over-the-counter painkiller and is frequently found in surface waterbodies, causing hepatotoxicity and skin irritation. Due to its persistence and chronic effects on the environment, innovative solutions must be provided to decompose APAP effectively [1]. Nanocatalysts based on tungsten-modified iron oxides (TF) were successfully synthesized by using a combustion method and thoroughly characterized using SEM, TEM, XRD, XPS, porosimetry analysis, ⁵⁷Fe Mossbauer spectroscopy, VSM magnetometry, and EPR. A series of samples with various relative contents of tungsten was prepared. The role of polyvinyl alcohol (PVA), which has been added to the reaction system during the synthesis, was investigated. Particularly, as confirmed by ⁵⁷Fe Mössbauer spectroscopy and XRD, by adding PVA, the syntheses resulted in magnetic γ -Fe₂O₃ nanoparticles instead of hematite. The enhanced magnetism of the TF nanocatalysts was confirmed by magnetometry as well and allowed an effective post-processing magnetic separation and recycling of the nanocatalysts.

The catalytic activities of the TF samples for APAP degradation by activating peroxymonosulfate (PMS) were evaluated under various conditions. Under optimal conditions, the sample TF 2.0 (the molar ratio of Fe precursor to W was 2.0 during the synthesis) showed the highest APAP degradation of 95 % removal with a catalyst loading of 2.0 g/L, initial APAP concentration of 5 mg/L, PMS of 6.5 mM, and pH ~2.15 at room temperature. The catalysts also showed chemical and mechanical stability, achieving 100 % degradation of 1 mg/L APAP during reusability tests with three consecutive experiments. These results show that TFs can effectively degrade persistent contaminants of emerging concern in water, offering an impactful contribution to wastewater treatment to protect human health and the ecosystem.

The authors gratefully acknowledge funding support by the grant No. 25-17807J provided by the Grant Agency of the Czech Republic and the National Research Foundation of Korea (NRF) grant funded by the Korean government (MSIT) (No RS-2025-00461931).

[1] A. Sin et al., *Science of the Total Environment* **951** (2024) 175472.

ICAME-T06-P7

Spin States of Ferrous and Ferric Irons in Peridotite Glass to Megabar Pressure: Implications for Dense Iron-Rich Silicate Melt at the Base of the Mantle

Izumi Mashino^{1*}, Takashi Yoshino¹, Takaya Mitsui², Kosuke Fujiwara², Sayako Inoue³, Takeshi Sakai³

¹Institute for Planetary Materials, Okayama University, 827 Yamada, Misasa, Tottori, Japan

²Synchrotron Radiation Research Center, Kansai Institute for Photon Science, National Institutes for Quantum Science and Technology, Sayo, Hyogo, Japan

³Geodynamics Research Center, Ehime University, 2-5 Bunkyo-cho, Matsuyama, Ehime, Japan

*izumi.mashino@okayama-u.ac.jp

The presence of dense silicate melts is thought to be one of the causes of the seismic anomalies observed at the base of the Earth's mantle, such as ultra-low velocity zones (ULVZs); however, the stability of the silicate melts under the lower-mantle conditions has not yet been completely understood. Previous melting experiments on peridotite and olivine components showed that the iron partitioning coefficient between solid and melt decreases at 60–80 GPa [1,2]. These studies argued that the decrease of the coefficient may be related to a spin transition of iron in melts or a sudden change in Al-Fe incorporation mechanisms in the crystal. In contrast, another study of melting experiments on chondritic composition did not observe any decrease in the iron partitioning coefficient [3]. To address these origins of discrepancy, knowledge of the spin transition and structural change of silicate melts is needed.

In this study, we have conducted high-pressure electrical conductivity and Mössbauer spectroscopic measurements of peridotite glass as an analogue of silicate melts in the deep mantle. We observed the shoulder feature in the Mössbauer spectra above 60 GPa due to the emergence of the new Fe²⁺ component, which could be associated with the change of the iron partitioning coefficient observed in previous melting experiments [1,2]. The change in the trend of the electrical conductivity profile has been observed at around ~83 GPa, suggesting an increase in the relative abundance of the new Fe²⁺ component. The pressure dependence of hyperfine parameters indicates that the spin transitions of both Fe²⁺ and Fe³⁺ occur above 100 GPa, which is likely related to the structural change of the glass. Because the radii of Fe²⁺ and Fe³⁺ ions become smaller due to the spin state changes, the glass becomes more compact above 100 GPa, which is much lower pressure than the pressure conditions of the ULVZs (~130 GPa) as well as the core-mantle boundary (~134 GPa). Our results suggest that the spin state changes lead to denser and more stable melts at the base of the mantle, and the presence of the silicate melts can be the cause of the ULVZs.

[1] R. Nomura *et al.*, *Nature* **473** (2011) 7346.

[2] S. Tateno *et al.*, *Journal of Geophysical Research: Solid Earth* **119** (2014) 6.

[3] D. Andrault *et al.*, *Nature* **487** (2012) 7407.

ICAME-T06-P8

High-Pressure Mössbauer, Raman, and Infrared Spectroscopic Studies of Breunnerite Across the Spin Transition of Iron

Izumi Mashino^{1*}, Shigeru Yamashita¹, Takaya Mitsui², Kosuke Fujiwara²

¹Institute for Planetary Materials, Okayama University, 827 Yamada, Misasa, Tottori, Japan

²Synchrotron Radiation Research Center, Kansai Institute for Photon Science, National Institutes for Quantum Science and Technology, Sayo, Hyogo, Japan

*izumi.mashino@okayama-u.ac.jp

Carbonates are regarded as the host phases to supply carbon into the Earth's deep interior through subducting slabs because of their wide stability under high-pressure and -temperature [1,2]. In particular, breunnerite, Fe-bearing MgCO_3 with a Mg/Fe ratio of 90/10 to 70/30, has a plausible mantle carbonate composition. Therefore, investigating the high-pressure behaviour of breunnerite contributes to understanding the deep carbon cycle of the Earth.

In this study, we have conducted high-pressure Mössbauer, Raman, and infrared spectroscopic measurements of breunnerite up to 70 GPa. The solid solution of $\text{MgCO}_3\text{-FeCO}_3$ undergoes a pressure-induced high-spin (HS) to low-spin (LS) transition of octahedral Fe^{2+} . The obtained high-pressure spectra can be fitted by one doublet up to ~47 GPa and one singlet at pressures higher than 49 GPa. The spectra at 47.6 GPa with the compression path can be analysed into one doublet and one singlet. The CS and QS values of the doublet are 0.9–1.2 mm/s and 1.9–2.1 mm/s, which should correspond to the HS state of Fe^{2+} in an octahedral site. The CS values of the singlet are 0.4–0.8 mm/s, which corresponds to the LS state of Fe^{2+} in an octahedral site. The abundance ratio of the doublet decreases and that of the singlet increases within the pressure range of 47–49 GPa, also indicating that breunnerite undergoes the HS-LS transition at 47–49 GPa. The CS and QS values of HS Fe^{2+} in breunnerite (Fe-bearing MgCO_3) are slightly smaller than the values of siderite (Mg-bearing FeCO_3) [3], suggesting the shorter Fe-O distance and the lower distortion of FeO_6 octahedra. The CS value of LS Fe^{2+} in breunnerite is almost the same as that in siderite within the margin of error. The Fe-O distance is almost identical to Mg-O after the spin transition, resulting in similar CS values of LS Fe^{2+} between breunnerite and siderite. The spin transition in the $\text{MgCO}_3\text{-FeCO}_3$ solid solution has been identified by a discontinuous change in the peak position of internal vibrations of the CO_3^{2-} groups of A_{1g} symmetric stretch (ν_1), which is attributed to the increase of the C-O distance across the spin transition [4,5]. We also observe the discontinuous decrease in the ν_1 mode at 45–50 GPa in the high-pressure Raman spectra. In the obtained IR spectra, we found the peaks at around 2850 cm^{-1} , which can be interpreted as the asymmetric stretching $2\nu_3$ mode. The peak position of the $2\nu_3$ mode increases linearly up to 45 GPa and then shifts slightly towards higher wavenumber above 49 GPa. The shift to higher wavenumber may result from the decrease in the distance between neighboring oxygen atoms. Our study also supports that the compositional effect on the spin transition pressure in $(\text{Mg,Fe})\text{CO}_3$ is less sensitive than that of $(\text{Mg,Fe})\text{O}$ because of the weaker Fe-Fe interactions in $(\text{Mg,Fe})\text{CO}_3$.

[1] M. Isshiki et al., *Nature* **427** (2004) 6969.

[2] V. Cerantola et al., *Nature Communications* **8** (2017) 1.

[3] I. Mashino et al., *Physics and Chemistry of Minerals* **51** (2024) 2.

[4] G. Farfan et al., *American Mineralogist* **97** (2012) 8-9.

[5] V. Cerantola et al., *American Mineralogist* **100** (2015) 11-12.

ICAME-T06-P9

Weathering of Granite and Its Relationship to the Content of Natural Radionuclides in the Rock

Akio Nakanishi^{1*}

¹Department of Physics, Shiga University of Medical Science, Shiga 520-2192, Japan

*nakanisi@belle.shiga-med.ac.jp

Granite is known to have a higher content of natural radionuclides than other plutonic rocks. As granite weathers, its color changes from whitish to reddish. This indicates that as weathering progresses, the iron contained in the rock becomes oxidized, and the amount of trivalent iron increases. Mössbauer spectroscopy has been extensively applied to minerals for characterizing oxidation states of iron atoms [1]. From the Mössbauer spectrum, the content of trivalent iron was estimated. As weathering progresses, it is thought that the natural radionuclides contained in the granite will also leak into the environment. The flow of radionuclides is believed to have a significant impact on the surrounding environment. In order to gain insight into the process of radionuclides flowing out, this study investigated the relationship between the content of radionuclides and trivalent iron in granite.

Several samples of granite with different degrees of weathering from the same locality were collected and washed in water. After drying, they were crushed. The Mossbauer spectra were obtained using a conventional constant acceleration spectrometer in a transmission geometry at room temperature. A ^{57}Co radioactive source in Rh matrix was used with a krypton-carbon dioxide proportional counter as γ -ray detector. Velocity calibration was carried out with a natural Fe foil. The Mössbauer absorber was prepared from the powdered sample, which passed through a 200-mesh sieve. The typical spectrum is shown in Fig.1. Ferric and Ferrous doublets were observed. The content of trivalent iron was evaluated from the area ratio of doublets.

Granite contains the radioactive nuclides ^{238}U and ^{232}Th , each forming a decay series. Crushed samples were packed in plastic containers and left for several months in order to reach the radioactive equilibrium. The radioactive measurements of samples were carried out with a high-purity germanium detector. The sample was placed on the end cap of the detector, and they were enclosed with lead blocks to reduce the background, which was contributed by cosmic rays and radioactive nuclides in surrounding materials. The contents of both the U and Th series were estimated from peak-area counts of γ -ray. The relationship between the content of radionuclides and trivalent iron in granite will be discussed.

[1] P.A. Bland *et al.*, *Hyperfine Interactions* **142** (2002) 481.

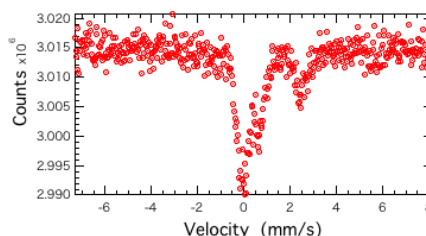


Figure 1. Mössbauer spectrum of granite.

ICAME-T07-P1

Lattice Dynamics of Ultrathin Fe Films on GaAs(001)

Sagar Bisoyi^{1,2,*}, Małgorzata Sternik³, Jochen Kalt^{1,2}, Rabee Najeeb^{1,2}, Ilya Sergeev⁴,
Sergey Yaroslavtsev⁵, Aleksandr I. Chumakov⁵, Przemysław Piekarczyk³, Tilo
Baumbach^{1,2} and Svetoslav Stankov^{1,2}

¹Laboratory for Applications of Synchrotron Radiation, Karlsruhe Institute of Technology,
Karlsruhe, Germany

²Institute for Photon Science and Synchrotron Radiation, Karlsruhe Institute of Technology,
Karlsruhe, Germany

³Institute of Nuclear Physics, Polish Academy of Sciences, Kraków, Poland

⁴Deutsches Elektronen-Synchrotron DESY, Hamburg, Germany

⁵ESRF-The European Synchrotron, Grenoble, France

*sagar.bisoyi@kit.edu

The confinement of atoms at surfaces and interfaces significantly alters lattice dynamics of thin films and nanostructures. At the nanoscale, phonon behavior is modified compared to the bulk counterparts, influencing their interactions with electrons and magnons [1, 2]. These changes are critical for understanding the properties of low-dimensional materials and their potential applications in advanced nanotechnologies. Therefore, investigating the lattice dynamics of ultrathin films is essential for tailoring their properties for specific applications spanning thermoelectrics, thermal management of micro- and nanoelectronics, spintronics, and superconductivity.

Here, we present a combined experimental and *ab initio* calculations study of lattice dynamics in both uncovered (*in situ*) and Si-capped (*ex situ*) ultrathin Fe(001) films epitaxially grown on the GaAs(001) surface. Crystallographic orientation, local atomic coordination, and magnetic ordering were systematically characterized by reflection high-energy electron diffraction (RHEED), X-ray absorption spectroscopy (XAS), and nuclear forward scattering (NFS), respectively.

The phonon density of states (PDOS) of the ultrathin Fe films was obtained at room temperature by nuclear inelastic scattering [3, 4]. The experimental data are in excellent agreement with the *ab initio* calculated PDOS, unveiling the presence of surface- and interface-specific PDOS in the uncovered Fe films. The Si capping suppresses the surface PDOS and leads to the formation of a thin non-stoichiometric FeSi layer.

This work is financially supported by the Federal Ministry of Education and Research BMBF (05K22VK2).

[1] D. Bozyigit et al., *Nature* **531** (2016) 618.

[2] R. Pradip et al., *Nanoscale* **11** (2019) 10968.

[3] M. Seto et al., *Phys. Rev. Lett.* **74** (1995) 3828.

[4] W. Sturhahn et al., *Phys. Rev. Lett.* **74** (1995) 3832.

ICAME-T07-P2

Molecular Modes of a Trapped Light-Induced Excited Spin State in an Iron-Containing Molecular Switch

Konstantin Gröpl^{1*}, Tim Hunsicker¹, Juliusz A. Wolny¹, Marco A. M. Tummeley¹, Maren H. Hooch¹, Paul Hausbrandt¹, Lukas Knauer¹, Xenia Mechler¹, Tim Hochdörffer¹, Vivien Christl¹, Deepak Prajapat², Ilya Sergeev², Volker Schünemann¹

¹University of Kaiserslautern-Landau, Kaiserslautern, Germany

²Deutsches Elektronen-Synchrotron, Hamburg, Germany

*konstantin.groep1@rptu.de

Iron(II)-containing spin crossover (SCO) complexes can be reversibly switched between a low-spin (LS; $S = 0$) state and a high-spin (HS; $S = 2$) state. Switching between the two states can be performed, e.g., via temperature changes. In some SCO complexes, it is also possible to induce an excited spin state trapping (LIESST) effect by irradiating green light to switch from the LS to the HS state. This makes these complexes predestined for optical data processing and data storage [1].

To study the LIESST state of the SCO complex $\text{Fe}(\text{PM-BiA})_2(\text{NCS})_2$ (Fig. 1) with nuclear forward scattering (NFS) and nuclear inelastic scattering (NIS) at P01, PETRA III, DESY, it was necessary to modify a sample rod of a He-bath cryostat for illumination (Fig. 2). The light passes through four fibers mounted in the variable temperature insert (VTI) to the sample, which is located between two transparent foils. With this setup, we could stabilize the LIESST state of $\text{Fe}(\text{PM-BiA})_2(\text{NCS})_2$ at a sample temperature of 25K (Fig. 3).

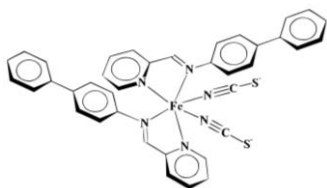


Figure 1. Schematic representation of $\text{Fe}(\text{PM-BiA})_2(\text{NCS})_2$ [2]



Figure 2. Sample between foils (white) in sample mount and optical fibers

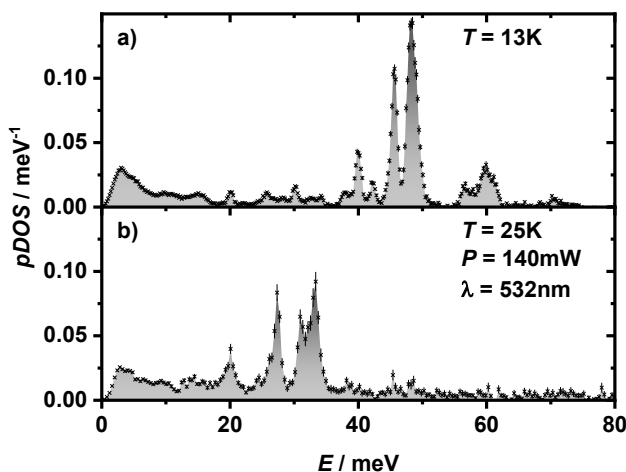


Figure 3. pDOS of $\text{Fe}(\text{PM-BiA})_2(\text{NCS})_2$ at 13K without illumination (a) and at 25K while illumination (b)

[1] P. Gülich, *Chemical Society Reviews* **29** (2000) 419.

[2] J.-F. Létard, *Inorganic Chemistry* **37** (1998) 4432.

ICAME-T07-P3

Nuclear Inelastic Scattering of a Molecular Crystal at 10 K

Marco A. M. Tummeley^{1*}, Juliusz A. Wolny¹, Konstantin Gröpl¹, Hannah Akhtar¹,
Tim Hochdörffer¹, Tim Hunsicker¹, Deepak Prajapat², Ilya Sergeev²,
Volker Schünemann¹

¹University of Kaiserslautern-Landau, Kaiserslautern, Germany

²Deutsches Elektronen Synchrotron, Hamburg, Germany

*marco.tummeley@physik.rptu.de

Crystals of the complex $[\text{Fe}(\text{b}(\text{bdpa}))](\text{PF}_6)_2$, with $(\text{b}(\text{bdpa})) = \text{N}, \text{N}'\text{-bis}(\text{benzyl})\text{-N}, \text{N}'\text{-bis}(2\text{-pyridylmethyl})\text{-6,6'}\text{-bis}(\text{aminomethyl})\text{-2,2'}\text{-bipyridine}$, have unit cells containing two crystallographically independent molecular sites. One molecule remains in its low spin state, which is temperature-independent. The other site is occupied in a dynamic, disordered structure. Mössbauer spectroscopy and susceptibility measurements indicate 0.25 molar fraction of the high spin state in the whole temperature range, although the complex displays spin equilibrium in solution [1]. The described phenomenon in the solid state implies, to the best of our knowledge, a previously unreported case of frozen spin crossover. We have investigated a single crystal of this system with nuclear inelastic scattering (NIS). The crystal was placed in a helium bath cryostat at the beamline P01, PETRA III, DESY Hamburg. Orientation-dependent ^{57}Fe NIS experiments have been performed at 10 K. Due to rotation from 0° to 90° with increments of 30° along the smallest axis of the crystal, the vibrational patterns change significantly due to the different phonon propagation in the crystal [2].

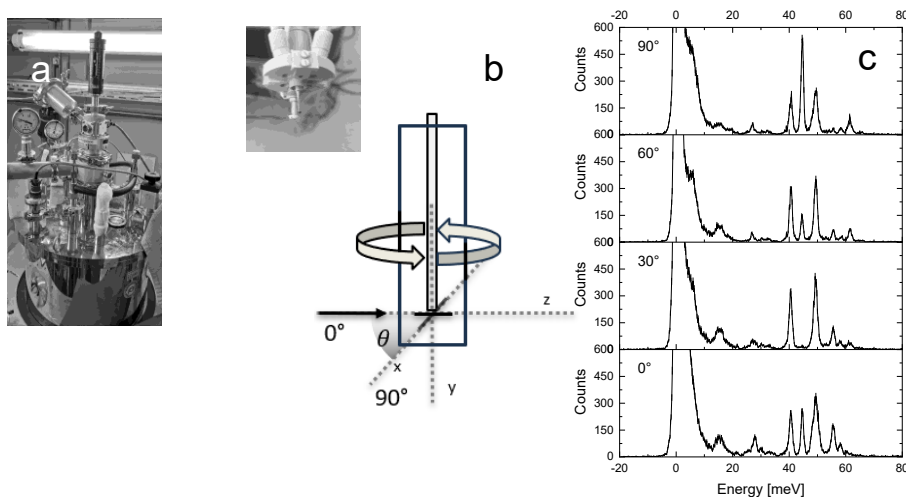


Figure 1. a) LHe-cryostat at P01, PETRA III, DESY. b) Mounted crystal and scheme of the mounting orientation of the crystal inside the cryostat. At 0° the longest side of the crystal is aligned with the incoming synchrotron beam. It is perpendicular to the beam after a rotation of 90° around the y-axis. c) Orientation dependent NIS data of the $^{57}\text{Fe}(\text{b}(\text{bdpa}))(\text{PF}_6)_2$ single crystal in increments of 30° up to 90° .

[1] C. Brady, *Inorg. Chem.* **43** (2004) 4289-4299.

[2] V.G. Kohn, *Phys. Rev. B* **58** (1998) 8437.

ICAME-T07-P4

Nuclear Inelastic Scattering Displays the Effects of Elastic Interactions in Spin Crossover Materials

J.A. Wolny^{1*}, A.I. Chumakov², K. Gröpl¹, M. Hooek¹, D. Prajapat³, I. Sergeev³,
M. Tummeley¹, V. Schünemann¹

¹University of Kaiserslautern-Landau, Kaiserslautern, Germany

²ESRF, Grenoble, France

³DESY, Hamburg, Germany

*wolny@rptu.de

Elastic interactions are at the heart of the spin crossover (SCO) phenomenon [1]. They occur when a local spin transition takes place, leading to the creation of a defect in the matrix of the other spin. The associated structural and spectroscopic effects are quite difficult to observe because the effects of elastic stretching are caused by minority molecules. One strategy to overcome this problem is to use isotope-sensitive inelastic nuclear scattering for systems in which the HS Fe(II) centers are replaced by the structurally analogous Zn(II). Thus, the observation of the LS signals in the Zn(II) matrix can reveal the vibrational properties of the elastically distorted LS-Fe(II) molecules.

In this presentation, we show the results of such studies for 3D, 1D, and mononuclear SCO Fe(II) complexes. Using density functional theory (DFT) calculations, it is shown that dilution in the Zn(II) matrix shifts the Fe-N stretching vibrations towards lower frequencies, with the effect ranging from 40 cm⁻¹ for the 3D/1D [2] systems down to 10 cm⁻¹ for molecular crystals.

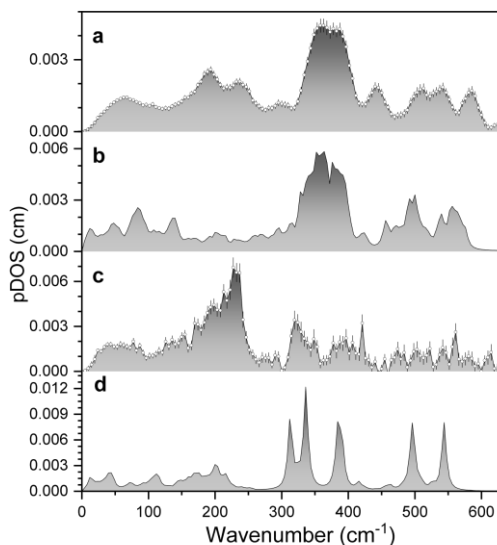


Figure 1. Experimentally derived (a) and DFT calculated (b) pDOS of low-spin Fe[pyz(Pt(CN)₄)] (b) and for Zn_{0.9}Fe_{0.1}[pyz(Pt(CN)₄)] (c) and (d), respectively. The large peaks observed in the experimental pDOS of Zn_{0.9}Fe_{0.1}[pyz(Pt(CN)₄)] are due to a high-spin isomer.

[1] G. Molnar et al., *Ann. Phys. (Berlin)* **531** (2019) 1900076.

[2] T. Hochdörffer et al., *Dalton Trans* **48** (2019) 15625.

ICAME-T08-P1

Parabolic Test Flight for the MIMOS II – Mössbauer Instrument

Blumers Mathias^{1*}, Harald Gaber^{1*}, Franz Renz²

¹Johannes Gutenberg University, Mainz, Germany

²Institution of Coordination Chemistry, Leibniz University Hannover

*mblumers@uni-mainz.de, harald.gaber@uni-mainz.de

Despite the high quality of the Mössbauer spectra from Mars, the calibration spectra of the MER-rovers SPIRIT and OPPORTUNITY recorded with the miniaturized Mössbauer Spectrometer MIMOS II during the cruise phase under zero gravity did show distortions, respectively, spectra of poor quality. A gravity dependent feedback behavior of the drive control unit under zero-gravity could be the reason. For evaluating the associated risk for the subsequent PHOBOS-GRUNT mission, and probably for taking counteractive measures, a parabolic test flight has been performed. Altogether, both the signals of the drive control and the Mössbauer spectra show that MIMOS II is working well under gravitational or acceleration conditions of $1 - 3 \cdot 10^{-1} \text{ m/s}^2$ (as with mounted sensor head) as well as $1 - 3 \cdot 10^{-3} \text{ m/s}^2$ (as with free floating sensor head).



Fig. 1. A300 during ESA 'ZERO-G' flight



Fig. 2. Experimental set-up with floating device

ICAME-T08-P2

NEXUS - New Developments in Evaluating Nuclear Resonant Scattering Experiments

Lars Bocklage^{1*}

¹ Deutsches Elektronen-Synchrotron DESY, Hamburg, Germany

*lars.bocklage@desy.de

Data evaluation and scientific software for Mössbauer science have a long tradition, and dedicated software tools have been developed. However, fitting of large data sets in parallel or evaluating complex experiments with several optical components and samples in the beam path, as found in modern synchrotron experiments, e.g., in nuclear quantum optics, is limited. NEXUS – the Nuclear Elastic X-ray scattering Universal Software [1] is a modern software package for flexible simulation and fitting of various types of Mössbauer spectra and nuclear resonant scattering data in various geometries, like transmission and reflection.

Nexus is an extension for Python and, therefore, easy to use. It offers high flexibility to combine various objects in the beam path with arbitrary sample structures and calculates the complete electronic and nuclear response of the experiment. It is fully integrable into Python workflows, including experiment and sample design, data plotting, data evaluation, simulation, and fitting. Nexus offers dedicated fit algorithms to simulate modern types of Mössbauer or nuclear resonant scattering experiments, with special emphasis on combined fitting of multiple measurements and experiments, as well as for automatized parameter optimization for experiment design or setups.

We will present latest applications of NEXUS to recent experiments, like the evaluation of a nuclear frequency comb for quantum memory applications [2], and show newest developments of the NEXUS software package, which include advanced data presentation, improved support for fitting Mössbauer spectra, an extended theory module and fit capabilities with new error calculations methods and log-likelihood estimators, and optimized calculation methods for special hyperfine arrangements. In addition, the software support has been improved via jupyter notebook examples for users, an extended continuous integration and delivery (CI/CD), unit testing, as well as support for Windows, Linux, and macOS.

[1] L. Bocklage, *Zenodo*, doi:10.5281/zenodo.7716207.

[2] S. Velten, L. Bocklage, et al. *Sci. Adv.* **10**, eadn9825 (2024).

ICAME-T08-P3

Three-Dimensional Mössbauer Microscope Using Synchrotron Mössbauer Source

Kosuke Fujiwara^{1*}, Takaya Mitsui¹, Noboru Hasegawa², Yasuhiro Kobayashi³, Mibu⁴, Ryo Masuda⁵, Makoto Seto³

¹National Institutes for Quantum Science and Technology, Sayo, Hyogo, Japan

²National Institute for Quantum Science and Technology, Kizugawa, Kyoto, Japan

³Institute for Integrated Radiation and Nuclear Science, Kyoto University, Kumatori, Osaka, Japan

⁴Graduate School of Engineering, Nagoya Institute of Technology, Nagoya, Japan

⁵Graduate School of Science and Technology, Hirosaki University, Aomori, Hirosaki, Japan

*fujiwara.kosuke@qst.go.jp

Understanding the chemical state of iron compounds and their three-dimensional (3D) distribution near the surface is crucial for advancing steel science. ⁵⁷Fe Mössbauer spectroscopy is one of the most effective tools for chemical analysis of iron. In particular, CEMS typically provides a surface sensitivity of approximately 100 nm, corresponding to the escape depth of the conversion electrons. This sensitivity can be enhanced by analyzing the electron energy using a method known as depth-selective CEMS (DCEMS) [1].

Furthermore, DCEMS can enable 3D analysis by scanning the sample surface with a focused probe beam, making it sensitive to both depth and lateral position. However, the non-directional nature of γ -rays emitted from traditional radioactive isotopic sources poses challenges for achieving a small γ -ray probe with sufficient photon flux for practical 3D surface analysis. We developed an "iron microscope" using a highly brilliant synchrotron Mössbauer source (SMS), beam-focusing mirrors, a precision stage, a gas-flow proportional counter, and multiple multichannel scalers (MCS). This system was successfully applied to 3D chemical state analysis near the surface of a laser-ablated ⁵⁷Fe foil [2].

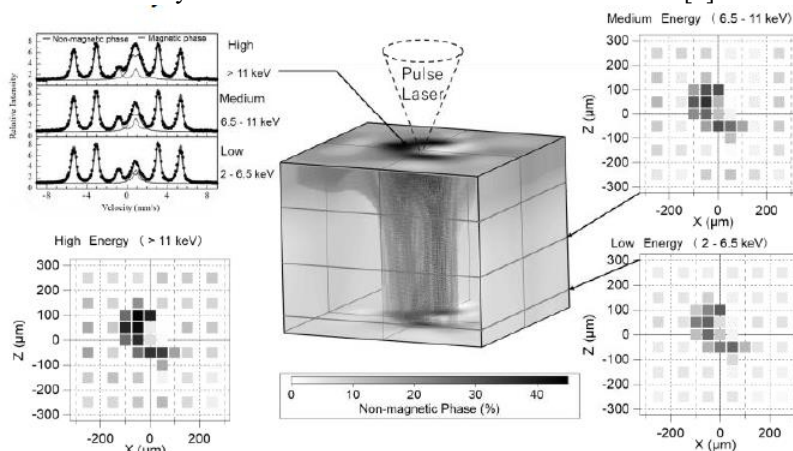


Figure 1. DCEMS spectra measured near the laser irradiation center [$X = -100 \mu\text{m}$, $Z = 100 \mu\text{m}$] and mapping diagram of the area ratio for the nonmagnetic phase determined by DCEMS spectra with energy discrimination measurement in High, Medium, and Low regions. And the 3-D distribution of the nonmagnetic phase.

[1] K. Nomura et al., *Spectroc. Acta B: Atom. Spectr.* **59**(2004), 1259.

[2] K. Fujiwara et al., *Appl. Phys. Exp.* **17**(2024) 082002.

ICAME-T08-P4

In-beam Mössbauer Spectroscopy Using the Neutron Capture Reaction of ^{56}Fe

M. Yoshida¹, S. Kimoto¹, Y. Kobayashi^{1,2,3*}, M. K. Kubo², M. Mihara⁴, W. Sato⁵, J. Miyazaki⁶, Y. Watanabe¹, J. Nakamura¹, I-Huan Chiu⁷, T. Osawa⁷

¹Dept. Fundamental Sci. Eng., Univ. Electro-Commun., Chofu, Tokyo, Japan

²Div. Arts Sci., Int. Christ. Univ., Mitaka, Tokyo, Japan

³RIKEN Nishina Center, Wako, Saitama, Japan

⁴Grad. Sch. Sci., Osaka Univ., Toyonaka, Osaka, Japan

⁵Inst. Sci. Eng., Kanazawa Univ., Kanazawa, Ishikawa, Japan

⁶Sch. Eng., Tokyo Denki Univ., Adachi, Tokyo, Japan

⁷Mater. Sci. Res. Center, JAEA, Tokai, Ibaraki, Japan

*yoshio.kobayashi@uec.ac.jp

The chemical effects of hot atoms produced after neutron capture reactions have been studied in radiochemistry [1]. The hot atoms with high excitation energies were known to create unusual and exotic chemical species different from ordinary chemical reactions. The chemical behavior of hot atoms in the gas and liquid phases has been elucidated, but their effects in solids are not yet fully understood. The chemical behavior of excited atoms in solids is important for understanding the effects of radiation on materials used in nuclear facilities. *In-situ* characterization of the excited atoms can be realized by means of in-beam Mössbauer spectroscopy, in which we detect Mössbauer γ rays emitted right after their neutron capture reactions by a transducer-driven detector.

The experiments were carried out at the prompt γ -ray analysis port (PGA) installed at the thermal neutron beamline of the JRR-3 research reactor in Japan Atomic Energy Agency (JAEA). Samples of stainless steel and α -Fe were used. The neutron flux at the PGA port was $1.8 \times 10^8 \text{ cm}^{-2}\cdot\text{s}^{-1}$. Mössbauer spectra were obtained at room temperature by measuring internal conversion electrons emitted via the Mössbauer effect using a parallel-plate avalanche counter [2].

The Mössbauer spectrum of ^{57}Fe in stainless steel under thermal neutron irradiation is shown in Figure 1. When the obtained spectrum was analyzed using a single absorption line, the linewidth was approximately 50% broader compared to conventional stainless steel. This broadening was considered to result from lattice defects induced by neutron irradiation. A more comprehensive discussion will be conducted with the results for α -Fe.

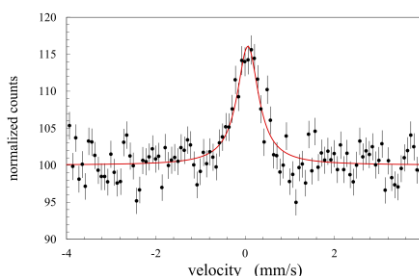


Figure 1. Mössbauer spectrum of ^{57}Fe in stainless steel under thermal neutron irradiation.

[1] T. Tominaga, E. Tachikawa, *Modern Hot Atom Chemistry and Its Applications*, Springer (1981).

[2] M. K. Kubo et al., *AIP Conf. Proc.*, **765**, (2005) 348.

ICAME-T08-P5

Progress in Gamma Ray Doppler Energy Modulation for Mössbauer Spectroscopy

Petr Novák^{1*}, Aleš Stejskal¹, Vít Procházka¹

¹Department of Experimental Physics, Faculty of Science, Palacký University Olomouc, 17. listopadu 12, 77900 Olomouc, Czech Republic

*petr.novak@upol.cz

Precise modulation of gamma radiation is essential for measuring Mössbauer spectra. Significant progress has been made in this area, particularly with the development of a transducer that enables movement with a scintillation detector [1], alongside an auto-tuning procedure to ensure linear movement [2]. This advancement allows the gamma radiation source to remain static while the absorber is moved.

This implementation offers a wide range of possibilities, such as the simultaneous measurement of Mössbauer spectra of multiple different samples using a single radiation source [3]. Alternatively, a resonance detector can be used to measure resonance spectra of a static absorber, which can be placed, for instance, in a cryostat. Moreover, by using a resonance detector and adjusting the apparatus configuration, it is possible to obtain the Lamb-Mössbauer factor of the studied absorber [4,5].

This work will present three key studies describing the concept of the system. The first study describes the parameters of the movement device, the second shows the principle of the autotuning procedure, and the third outlines the control system and its capabilities. Subsequently, several applications of this improvement will be presented, based on numerous other publications.

- [1] P. Novák et al., *Nucl. Instruments Methods Phys. Res. Sect. A Accel. Spectrometers, Detect. Assoc. Equip.* **1031** (2022) 166573.
- [2] V. Procházka et al., *Nucl. Instruments Methods Phys. Res. Sect. B Beam Interact. with Mater. Atoms* **483** (2020) 55.
- [3] A. Stejskal et al., *J. Int. Meas. Confed.* **215** (2022) 112850.
- [4] V. Procházka et al., *Phys. Lett. Sect. A Gen. At. Solid State Phys.* **442** (2022) 128195.
- [5] P. Novák et al., *Chem. Pap.* **77** (2023) 7283.

ICAME-T08-P6

2D Backscattering Mössbauer Measurements with MIMOS II

J. Pawlak^{1*}, T. Sindelar¹, M. S. Kilic¹, M. Beyki^{1,2}, R. Patzke², and F. Renz¹

¹Institute of Coordination Chemistry, Leibniz University Hanover, Callinstraße 9, D-30167 Hanover, Germany

²Faculty I – Electrical Engineering and Information Technology, Hanover University of Applied Sciences and Arts, Ricklinger Stadtweg 120, D-30459 Hanover, Germany

*justus.pawlak@acd.uni-hannover.de

The miniaturised Mössbauer spectrometer (MIMOS II), originally developed by Göstar Klingelhöfer [1], is being further developed by the Renz group at the Leibniz University Hanover in collaboration with the Hanover University of Applied Sciences and Arts. The former MIMOS II processing unit can no longer be manufactured because the necessary components are no longer available. Building on our previous work, which introduced a new processing unit with Arduino-based two-dimensional (2D) data acquisition [2] that allowed the operation of the MIMOS hardware (including the drive and a detector) [3], we have now further developed the hardware and software. This further development makes it possible to operate the entire MIMOS II sensor head with four reflection detectors and one transmission detector simultaneously.

2D data processing simplifies data acquisition without the need for predetermined thresholds. Therefore, the energy of each photon is determined and stored together with the velocity of the drive, allowing the selection of relevant regions for the Mössbauer spectrum after the measurement. [2] With this approach, it is now possible to simultaneously measure 6.4 keV and 14.4 keV signals of iron-57 for the four reflection detectors of the MIMOS sensor head. This is in contrast to the old processing unit, where it was only possible to measure either 6.4 keV or 14.4 keV separately for the detectors. Simultaneous measurement of both energies was only possible by adding the counts from the energy ranges of two detectors, which posed a problem if, for example, one detector produced noise.

[1] G. Klingelhöfer et al., *Planetary and Space Science*, **44** (1996) 1277-1288.

[2] M. Jahns et al., *Nucl. Inst. Methods Phys. Res. A*, **1031** (2022) 166529.

[3] J. Pawlak et al., *Interactions*, **244** (2023) 20.

ICAME-T08-P7

Fourier Analysis of γ -Ray Intensity Signals Modulated by an Ultrasonically Vibrating Mössbauer Absorber

Vlastimil Vrba^{1*}, Michal Hausner¹, Aleš Stejskal¹ and Vít Procházka¹

¹Department of Experimental Physics, Faculty of Science, Palacký University Olomouc,
17. listopadu 1192/12, 779 00 Olomouc, Czech Republic

*vlastimil.vrba@upol.cz

The time profile of γ -ray intensity can be effectively modified through interactions with a vibrating resonant absorber. The shape of the resulting intensity waveform can be precisely controlled by selecting an appropriate absorber motion profile. Such γ -photon manipulation is achievable in time-coincidence Mössbauer setups utilizing a periodic absorber motion at ultrasonic frequencies. In this work, we demonstrate a theoretical approach to describing this phenomenon based on the application of Fourier analysis. A formal connection between the Fourier coefficients of the intensity signals and the Fourier coefficients of the absorber motion exponential can be established. The relation between the absorber vibrations and the characteristics of the γ -ray intensity signals can thus be analyzed in the frequency domain using a discrete set of coefficients. This can be applied to examine and optimize the time dependence of the γ -photon detection rates. The method is demonstrated on ultrasonically modified time histograms of the 14.4 keV γ -photon detections, where the starting signal is synchronized with the ^{57}Fe absorber vibrations. Results for selected types of the resonant absorber motion are presented. The method can be applied to essentially any experimentally feasible motion profile, offering a promising optimization tool for working with the periodic γ -ray waveforms, e.g., in nuclear quantum optics and metrology.

Synchrotron-Radiation-Based Mössbauer Spectroscopy of ^{99}Ru Nuclei

Mio Yoshida^{1*}, Ryo Masuda², Nobumoto Nagasawa³, Satoshi Tsutsui^{3,4},

Jin Nakamura¹, Yoshio Kobayashi^{1,5,6}

¹Dept. Fundamental Sci. Eng., Univ. Electro-Commun., Chofu, Tokyo, Japan

²Grad. Sch. Sci. Tech., Hirosaki Univ., Hirosaki, Aomori, Japan

³Japan Synchro. Radia. Res. Inst. (JASRI), SPring-8, Sayo, Hyogo, Japan

⁴Inst. Quant. Beam Sci., Grad. Sch. Sci. Eng., Ibaraki Univ., Hitachi, Ibaraki, Japan

⁵Div. Arts Sci., Int. Christ. Univ., Mitaka, Tokyo, Japan

⁶RIKEN Nishina Center, Wako, Saitama, Japan

*y2343013@edu.cc.uec.ac.jp

Ruthenium is one of the elements used in many functional materials such as catalysts and solar cells, and it exhibits a wide variety of oxidation states from -2 to $+8$. Mössbauer spectroscopy is an important tool to obtain information about the valence states and coordination environment of Ru in these materials [1], but there are not many studies of ^{99}Ru Mössbauer spectroscopy because there are some experimental difficulties, such as the preparation of a short half-lived ^{99}Rh source ($T_{1/2} = 16.1$ d) in a cyclotron. Recently, the establishment of synchrotron-radiation-based Mössbauer spectroscopy [2] has made it possible to perform Mössbauer measurements using synchrotron-radiation sources of various nuclei such as ^{61}Ni [3], ^{149}Sm [4], and ^{193}Ir [5], which had conventionally been performed using radioactive sources. In this study, synchrotron-radiation-based Mössbauer spectroscopy was applied to measure the ^{99}Ru Mössbauer spectra of some Ru metal, RuO_2 , and Na_2RuO_3 .

The experiments were performed at BL35XU in SPring8. Figure 1 shows the ^{99}Ru Mössbauer spectrum of natural abundance of Ru metal (23.1 mg) obtained at 7 K using synchrotron radiation-based Mössbauer spectroscopy. The spectrum could be fitted by a single line with a linewidth (FWHM) of $0.34(2)$ mm/s. The peak height of the resonance absorption was 2.1%, about 1.7 times that obtained using a conventional ^{99}Rh source. ^{99}Ru Mössbauer spectra of the Ru compounds and lifetime of the ^{99}Ru first excited state ($E_\gamma = 89.7$ keV) will be discussed.

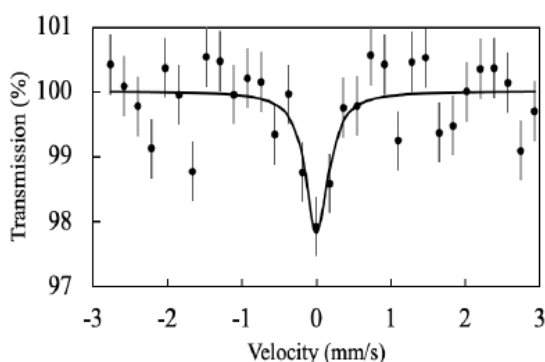


Figure 1. ^{99}Ru Mössbauer spectrum of Ru metal using synchrotron-radiation technique at 7 K.

- [1] Y. Kobayashi *et al.*, *Hyp. Int.* **217** (2010) 012023.
- [2] M. Seto *et al.*, *Phys. Rev. Lett.* **102** (2009) 217602.
- [3] R. Masuda *et al.*, *Sci. Rep.* **6** (2016) 27053.
- [4] S. Tsutsui *et al.*, *J. Phys. Soc. Jpn.* **85** (2016) 083704.
- [5] S. Tsutsui *et al.*, *J. Phys. Soc. Jpn.* **90** (2021) 083701.

Abstracts of Poster Contributions



HYPERFINE Posters

HYPERFINE-T01-P1

ASCII: The Ultra-Low Energy Ion Implantation of Radioisotopes for Surface Characterization at ISOLDE-CERN

Nicole Pereira De Lima^{1,3*}, Juliana Schell^{1,2}, Artur Carbonari³, Bruno Correa³,
Levy Scalise³, Koen Van Stiphout⁴, Carl Friedrich Jarschke⁵,

Hannes Gürlich⁶, Felix Junge⁷, Hans Hofsäss⁷

¹European Organization for Nuclear Research, CERN, Switzerland

²Universität Duisburg-Essen, UDE, Germany

³Instituto de Pesquisas Energéticas e Nucleares, IPEN, Brazil

⁴KU Leuven, Belgium

⁵Karlsruhe Institute of Technology, Germany

⁶Technische Universität Dresden, TU Dresden, Germany

⁷Georg-August-Universität Göttingen, Universität Göttingen, Germany

*nicole.pereira.de.lima@cern.ch

Over the past four decades, the Apparatus for Surface Physics and Interfaces at CERN (ASPIC) has been an ultra-high vacuum ($\text{UHV} \leq 10^{-8}$ mbar) setup installed in the ISOLDE experimental hall. It was dedicated to the study of metallic surfaces [1], the magnetic behaviour of thin films [2], an interface evolution [3], among other systems, employing radioactive isotopes, and a variety of surface and thin film fabrication and modification techniques [4].

Recently, the installation has been upgraded with the creation of a brand-new UHV chamber known as the ASPIC's Ion Implantation Chamber (ASCII) [5]. Thus, the ASCII chamber's purpose is to implant radioactive ions at various energies, including ultra-low (> 20 eV) values.

This allows for the implantation of several probes, including (^{111}mCd , $^{204\text{m}}\text{Pb}$) in two-dimensional materials (graphene, MoS_2), (multi)ferroic materials, nanoparticles, and topological insulators [5, 6]. Similar to the initial ASPIC chamber, it is kept at an extremely high vacuum of $\leq 10^{-9}$ mbar. The chamber was successfully tested at the University of Göttingen for implanting ^{111}Ag , including the beam sweep.

Currently, the setup is being finished at ISOLDE to become operational. Once the commissioning finishes, the setup will be available for the wide community of collaborators. In particular, ASCII will play an important role in nuclear-condensed matter physics for the local study of surfaces and interfaces.

[1] E. Hunger, H. Haas, *Surf. Sci.* **234**(3) (1990) 273-286.

[2] K. Potzger et al., *J. Phys. G: Nucl. Part. Phys.*, **6** (2017).

[3] H. Bertschat et al., *Hyperfine Interact.* **129** (2000) 475-492.

[4] K. Van Stiphout et al., *Cryst.* (2022).

[5] K. Van Stiphout, J. Schell, *Tech. rep.*, CERN, Geneva (2023).

[6] K. Van Stiphout, H. Hofsäss, *Tech. rep.*, CERN, Geneva (2020).

Nuclear Quadrupole Interaction of ^{58}Cu in Si Studied by β -NMR spectroscopy

M. Mihara^{1*}, M. Tanaka^{1,a}, Y. Tanaka¹, H. Du¹, T. Sugihara¹, K. Ohnishi¹, S. Yagi¹,
Y. Ishibashi^{2,b}, Y. Abe², H. Ueno², K. Yamada², T. Fujimura³, M. Fukuda¹, T. Hori¹,
Y. Ichikawa^{2,a}, K. Imamura⁴, T. Izumikawa⁵, K. Matsukawa⁶, K. Matsuta¹,
T. Minamisono¹, S. Momota⁷, T. Moriguchi⁸, D. Nagae^{8,c}, T. Nagatomo²,
S. Nakamura¹, D. Nishimura⁹, T. Ohtsubo⁵, A. Ozawa⁸, K. Shirai^{3,d}, T. Suzuki¹⁰,
M. Takechi^{5,c}, T. Yamaguchi¹⁰, R. Yanagihara¹

¹The Univ. Osaka, Toyonaka, Japan, ²RIKEN, Wako, Japan, ³The Univ. Osaka, SANKEN, Ibaraki, Japan, ⁴Meiji Univ., Tokyo, Japan, ⁵Niigata Univ., Niigata, Japan, ⁶SUMUCO Co., Saga, Japan, ⁷Kochi Univ. Technology, Kami, Japan, ⁸Univ. Tsukuba, Tsukuba, Japan, ⁹Tokyo City Univ., Tokyo, Japan, ¹⁰Saitama Univ., Saitama, Japan

*mihara@phys.sci.osaka-u.ac.jp

Cu impurities in Si devices are known as serious contaminants because of their unique feature of the fastest diffusivity among transition metal impurities. Short-lived β emitter ^{58}Cu ($I^\pi = 1^+$, $T_{1/2} = 3.2$ s) is an attractive β -NMR probe nucleus that can possibly provide valuable information on the behavior of Cu impurities in Si, such as the lattice site or the formation of Cu-dopant complex related to the gettering technique [1], as well as the fast diffusion property.

In this paper, we report the result on the nuclear quadrupole splitting ν_Q of ^{58}Cu implanted into Si measured to probe the electric field gradient at the Cu site by means of the β -NMR technique.

The experiment was performed at RI Beam Factory operated by RIKEN Nishina Center and CNS, University of Tokyo. A spin polarized ^{58}Cu beam was provided by the RIKEN Projectile Fragment Separator (RIPS) with an energy of ~ 35 MeV/nucleon, which was implanted into a single crystal Si sample with the crystal c axis set parallel to the external magnetic field $B_0 = 0.93$ T. Since in the case of ^{58}Cu with nuclear spin $I = 1$ the quadrupole interaction generates a splitting into two NMR lines with frequencies of $\nu \pm \nu_Q/2$ under a strong magnetic field, the resonance was searched as a function of ν_Q by applying multi RF pulses. Figure 1 shows a ν_Q spectrum measured at room temperature, suggesting the presence of a resonance around $\nu_Q = 2.5$ MHz. While the β -ray emission channeling experiment by Wahl et al. had shown that Cu ions implanted in Si occupy positions slightly displaced from the substitutional lattice site [2], the present result suggesting the possibility of a quadrupole splitting may support this picture.

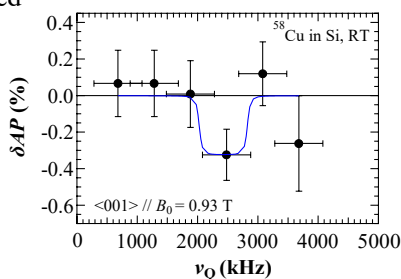


Figure 1. ν_Q spectrum of ^{58}Cu in Si.

Present address: ^aKyushu Univ., Fukuoka, Japan,

^bAEC Co., Chiba, Japan, ^cSaitama Univ., Saitama, Japan, ^dVietnam-Japan Univ., Hanoi, Vietnam, ^eGSI, Darmstadt, Germany

[1] K. Shirai et al., *Jpn. J. Appl. Phys.* **44** (2005) 7760.

[2] U. Wahl et al., *Phys. Rev. Lett.* **84** (2000) 1495.

HYPERFINE-T01-P3

The New Ion Implantation Chamber in the GLM Area of ISOLDE

Ian Chang Jie Yap^{1*}, Juliana Schell^{1,2}, Thien Thanh Dang¹, Ulrich Vetter³,
Matthias Nagl³, Hans-Christian Hofsäss⁴, Doru Constantin Lupascu¹

¹Institution for Material Science and Center for Nanointegration Duisburg-Essen (CENIDE),
University of Duisburg-Essen, 45141 Essen, Germany

²European Organization for Nuclear Research (CERN), CH-1211 Geneva, Switzerland

³Nagl & Vetter GmbH, Hans-Adolf-Krebs-Weg 1, 37077 Göttingen, Germany

⁴II. Physikalisches Institut, Georg-August-Universität Göttingen, Friedrich-Hund-Platz 1,
37077 Göttingen, Germany

*ian.chang.jie.yap@uni-due.de

The General Low Mass (GLM) beamline of ISOLDE is dedicated to collecting and handling radioactive isotopes and is frequently used by various groups, including the local solid-state physics group at ISOLDE.

There is an initiative to upgrade the ion implantation facilities. It includes the 1) introduction of two sub-chambers (the implantation and the sample loading/unloading part), connected by a DN200 gate valve and each evacuated by an individual turbo pump (HiPace 700 and 1200, respectively), and 2) computer-controlled stepper motors that a) include the transfer of the sample between the two sub-chambers, and b) allows for adjustment of the collimator in the implantation sub-chamber that allows for optimization of the incoming radioactive ion-beam.

The advantages of the new ion implantation chamber are 1) the introduction of the load-lock mechanism between the two sub-chambers ensures that the implantation sub-chamber is kept at operational pressure ($< 10^{-6}$ mbar) and not vented for rapid sample change and implantation (for more frequent implantations), 2) user-friendliness, in which the automation afforded by the motors decrease the risk of user error, 3) safety, inbuilt in both hardware and software, in which minimization of mechanical contact between the GLM users and the new ion implantation chambers will lead to radiological exposition reduction.

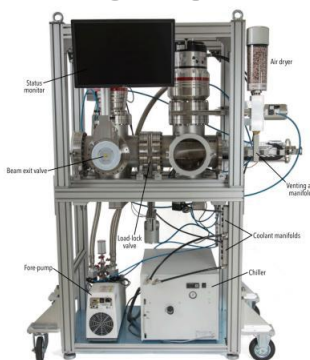


Figure 1. A photo of the new implantation chamber for the GLM area of ISOLDE [1]

[1] Matthias Nagl, PhD thesis (2014), Chapter 10.

HYPERFINE-T03-P1

TDPAC in Molybdenum Oxide Complexes Revisited

Anastasia Burimova^{1*}, Katiusse Soares Souza¹, Rajendra Narain Saxena¹,
Artur Wilson Carbonari¹

¹Nuclear and Energy Research Institute, IPEN-CNEN/SP, São Paulo, Brazil

* anstburimova@gmail.com

Time Differential Perturbed Angular Correlation (TDPAC) spectroscopy, utilizing Mo-99 and In-111 probe parents, has been extensively applied to investigate local effects and defects in molybdenum oxides (MoO_x) [1, 2]. However, the preparation techniques and pre-measurement treatments of samples, which induce probe incorporation, may significantly influence their stoichiometry and structural characteristics. Furthermore, due to the layered nature of MoO₃, probe atoms can occupy interstitial sites [3], complicating the interpretation of hyperfine data. In this study, we present a new series of TDPAC measurements obtained for nominal MoO₃ samples using an In generator that allows tracing probe diffusion. We critically summarize and discuss alternative interpretations of these new data sets, supporting our analysis by comparisons with complementary TDPAC experiments involving Mo-based chelates.

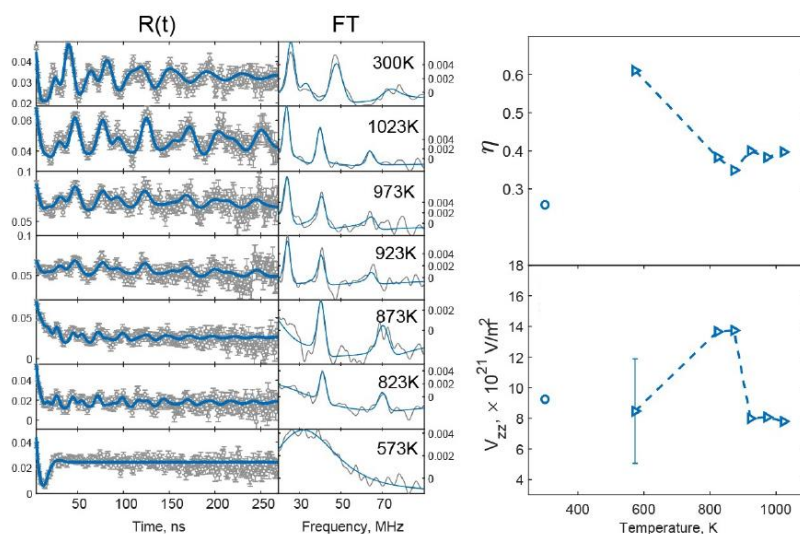


Figure 1. TDPAC $R(t)$ of nominal α -MoO₃ collected at different temperatures with radioactive ¹¹¹In tracer and their Fourier Transforms (left), evolution of hyperfine parameters on heating (right). The RT data was obtained after cooling (°).

- [1] T. Butz et al., *Hyperfine Interact.* **15/16** (1983) 915.
- [2] F. G. Requejo et al., *Physica Status Solidi* **116** (1989) 503.
- [3] A. M. Gerami et al., *Phys. Rev. Mater.* **7** (2023) 033603.

HYPERFINE-T03-P2

Potassium Loading Density Dependence of Hyperfine Coupling in Na-K Alloy Clusters in Zeolite Low-Silica X

Mutsuo Igarashi^{1*}, Tadashi Shimizu², Atsushi Goto², Kentaro Hashi²,
Keiko Yamamichi¹, Takehito Nakano^{3**}

¹National Institute of Technology, Gunma College, Maebashi, Gunma 371-8530, Japan

²National Institute for Materials Science, Tsukuba, Ibaraki 305-0003, Japan

³Institute of Quantum Beam Science, Graduate School of Science and Engineering,
Ibaraki University, Mito, Ibaraki 310-8512, Japan

* igarashi@gunma-ct.ac.jp

** takehito.nakano.phys@vc.ibaraki.ac.jp

Zeolite low-silica X (LSX) is a type of aluminosilicate. Within its crystal structure, there are periodic spaces called cages, which can be loaded with external atoms. When alkali atoms are loaded under appropriate conditions, they exhibit unique behaviours on electromagnetic properties such as magnetic orders, insulator-metal transitions, and so on [1]. Since, as can be easily imagined, electrons of loaded atoms in s-orbitals form clusters, which are said to behave as pseudo-atoms [2], microscopic configurations of atoms have direct influences on such electromagnetic properties. However, there has never been enough information about them because of the complexity of the configurations of atoms in cages, where there are many crystallographically equivalent sites with low occupancy. In such a situation, hyperfine coupling has the possibilities of giving basic information.

When the Na-K type LSX is loaded with external K atoms, a ferrimagnetic transition occurs for a loading level of less saturation state with metallic property [3]. The features of ²³Na and ²⁷Al NMR spectra have been reported for the saturated loading level [4]. In the case of ²³Na, two separate peaks appear, and both show shifts that are proportional to the magnetic susceptibility. This fact indicates the existence of several atomic sites with different hyperfine coupling with the magnetic moment. In the case of ²⁷Al, no independent peaks are observed, but the tail of the spectrum shifts in proportion to the magnetic susceptibility. Since the shift of ²³Na is small in the sample with a low loading level [5], it is expected that the electron cloud transfigures with following the loading level.

According to the above, we extend the measurement condition of the loading level between the above two cases. We will present the results of such an extension.

[1] T. Nakano and Y. Nozue, *Adv. Phys.: X* **2** (2017) 254.

[2] R. Arita et al., *Phys. Rev. B* **69** (2004) 195106.

[3] D. T. Hanh et al., *J. Phys. Chem. Solids* **71** (2010) 677.

[4] M. Igarashi et al., *Dalton Trans.* **53** (2024) 9838.

[5] M. Igarashi et al., *J. Magn. Magn. Mater.* **310** (2007) e307.

Liquid-State β -NMR Spectroscopy of Short-lived Boron and Nitrogen Isotopes and Precise Nuclear Magnetic Moments

M. Mihara^{1*}, Y. Kimura¹, Y. Otani¹, H. Takahashi², R. Wakabayashi¹, M. Amitani², S. Chen¹, M. Fukuda¹, C. Fukushima², M. Fukutome¹, A. Gladkov³, S. Ishitani¹, T. Izumikawa⁴, A. Kitagawa⁵, K. Matsuta¹, T. Minamisono¹, R. Miyahara¹, S. Momota⁶, T. Nagatomo³, Y. Nakamura², H. Nishibata^{3,a}, D. Nishimura², N. Noguchi⁴, M. Ogose⁴, T. Ohtsubo⁴, N. Okimoto¹, A. Ozawa⁷, S. Sato⁵, T. Sugisaki¹, R. Taguchi¹, G. Takayama¹, M. Tanaka⁸, K. Watanabe¹

¹The Univ., Osaka, Toyonaka, Japan, ²Tokyo City Univ., Tokyo, Japan, ³RIKEN, Wako, Japan, ⁴Niigata Univ., Niigata, Japan, ⁵QST, Chiba, Japan, ⁶Kochi Univ. Technology, Kami, Japan, ⁷Univ., Tsukuba, Tsukuba, Japan, ⁸Kyushu Univ., Fukuoka, Japan

*mihara@phys.sci.osaka-u.ac.jp

Liquid-state nuclear magnetic resonance (NMR) spectroscopy has been used as a powerful tool for probing the structure of molecules and their dynamics because of the narrow line width of the spectrum and its advantage in the NMR detection. On the other hand, the β -ray-detected NMR (β -NMR) spectroscopy using unstable nuclei has been used almost exclusively for the measurement of solid samples so far, but recently liquid samples are being used for application to biochemical research [1-3]. In this paper, we report results on the β -NMR spectroscopy of short-lived boron and nitrogen isotopes ^{12}B ($I = 1$, $T_{1/2} = 20$ ms), ^{12}N ($I = 1$, $T_{1/2} = 11$ ms) and ^{17}N ($I = 1/2$, $T_{1/2} = 4.2$ s) implanted into several liquid samples.

The experiments were performed at the facility of the Heavy Ion Medical Accelerator in Chiba (HIMAC) in the Institute for Quantum Medical Science. Typical β -NMR spectra are shown in Figure 1. The resonance line of ^{12}B in H_2O appears to be shifted by 20-30 ppm from that of B(OH)_3 solution. For ^{17}N , a doublet in KCN solution was observed, and the frequencies seem different from those in H_2O . By analogy with ^{15}N -NMR the doublet was assigned to C^{17}N^- ions and HC^{17}N molecules. These results lead to identify chemical species formed by ^{12}B and ^{17}N ions injected into H_2O by using B(OH)_3 and KCN solutions as reference samples, respectively, or to determine the nuclear magnetic moments within 10 ppm-order accuracy using correct magnetic shielding factors. In addition, by measuring the spectra of nitrogen isotopes ^{12}N and ^{17}N in the same liquid sample, the ratio of the magnetic moments of the two isotopes could be precisely determined. The results of the spin-lattice relaxation times will be also presented.

^aPresent address; University of Teacher Education of Fukuoka, Munakata, Japan

[1] R.D. Harding et al., *Phys. Rev. X* **10** (2020) 041061.

[2] R.M.L. McFadden et al., *Angew. Chem. Int. Ed.* **61** (2022) e202207137.

[3] M. Mihara et al., *Hyperfine Interact.* **242** (2021) 49.

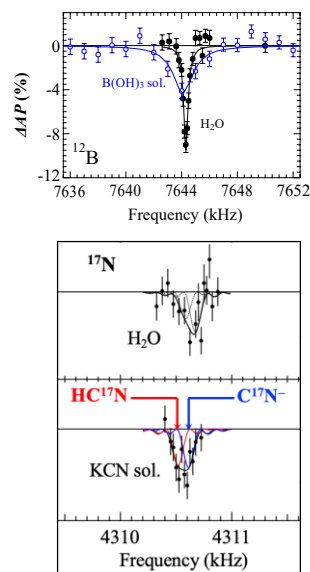


Figure 1. Typical liquid-state β -NMR spectra of B and N radioisotopes.

HYPERFINE-T03-P4

Local Probing of Structural Phase Transitions in Ferroelectric $\text{Li}_2\text{AB}_2\text{O}_7$ Layered Perovskites

A. Cesário^{1*}, P. Rocha-Rodrigues¹, R. P. Moreira¹, P. N. Lekshmi¹,
J. G. Correia², L. V. C. Assali³, H. M. Petrilli³, J. P. Araújo¹, A. M. L. Lopes¹

¹IFIMUP, Departamento de Física e Astronomia da Faculdade de Ciências da Universidade do Porto, Rua do Campo Alegre, 687, 4169-007 Porto, Portugal

²C2TN, Centro de Ciências e Tecnologias Nucleares, Universidade de Lisboa, Estrada Nacional 10, 2695-066 Bobadela LRS, Portugal

³Instituto de Física, Universidade de São Paulo, CP 66318, 05315-970, São Paulo-SP, Brazil

*antonio.duarte.neves.cesario@cern.ch

Naturally layered perovskites have become an impressive playground for the birth of novel multifunctional devices due to its great electronic tunability, aiming at innovative alternatives for improved energy storage devices and electronics. In particular, the search for room temperature ferroelectrics (FE) has seen a boost in research focused on these structures. However, an accurate structural characterization at a microscopic scale can be notably difficult to establish by conventional scattering experiments [1], leading to conflicting reports in the literature.

Our case study is the $n = 2$ pseudo Ruddlesden Popper (pRP) $\text{Li}_2\text{AB}_2\text{O}_7$ family ($A = \text{Ca/Sr}$, $B = \text{Nb/Ta}$), an interesting family exhibiting anti-FE and weak-FE where the structural phases are not yet fully understood with temperature and are highly dependent on the chosen cations for the A - and B -sites [2,3]. Perturbed Angular Correlation (PAC) Spectroscopy measurements conducted at CERN/ISOLDE using $^{111\text{m}}\text{Cd}$ radio-isotopes can probe the Electric Field Gradients at the Li and Sr lattice sites to distinguish between the various structural phases that have been proposed up to now.

Ab-initio Density Functional Theory (DFT) calculations can establish the local effects that reproduce our measurements, granting us the fundamental understanding required to design new and optimal multifunctional materials.

[1] P. Rocha-Rodrigues et al. *Phys. Rev. B* **109** (2024) 224101.

[2] R. Uppuluri et al., *Chem. Mater.* **31** (2019) 4418–4425.

[3] T. Nagai et al., *Chem. Mater.* **31** (2019) 6257–6261.

HYPERFINE-T03-P5

CDW Transitions in Spinel-type $\text{Cu}(\text{Ir}_{1-x}\text{V}_x)_2\text{S}_4$ Studied by ^{63}Cu NMR

Haruo Niki^{1*}, Mamoru Yogi¹, Kaori Niki², Takahiro Maehira¹,
Masato Hedo¹, Takao Nakama¹, Shuji Ebisu³, Shoichi Nagata³

¹Department of Physics, Faculty of Science, University of the Ryukyus, Nishihara,
Okinawa 903-0213, Japan

²Advanced Integration Science, Chiba University, Chiba, Chiba 263-8522, Japan

³Muroran Institute of Materials Research, Muroran, Hokkaido 980-8577, Japan

*niki@sci.u-ryukyu.ac.jp

The spinel CuV_2S_4 exhibits two-step anomalies at about 92 K (T_{t1}) and 56 K (T_{t2}), indicating the charge-density-wave (CDW) state. To investigate the CDW state on V rich side in $\text{Cu}(\text{Ir}_{1-x}\text{V}_x)_2\text{S}_4$ microscopic level, the Knight shift and spin-lattice relaxation time (T_1) of ^{63}Cu NMR were measured for powdered samples of $\text{Cu}(\text{Ir}_{1-x}\text{V}_x)_2\text{S}_4$ ($x = 1.00, 0.98$, and 0.95) at temperatures between 4.2 K and 300 K.

The temperature dependence of the Knight shift of ^{63}Cu NMR in CuV_2S_4 corresponds to that of the magnetic susceptibility, and the Knight shift indicates a hysteresis at the phase transition at T_{t2} . The temperature dependence of $1/T_1T$ of ^{63}Cu NMR in CuV_2S_4 follows the Korringa law, with an enhancement observed around T_{t1} .

For $x = 0.98$ and 0.95 in $\text{Cu}(\text{Ir}_{1-x}\text{V}_x)_2\text{S}_4$, the temperature dependence of the Knight shift also corresponds to that of their respective magnetic susceptibilities. Furthermore, the temperature dependence of $1/T_1T$ follows the Korringa law and shows an enhancement of around 130 K for each composition.

[1] Y. Kawashima, et al., *Physica B* **387** (2007) 208.

[2] H. Niki, et al., *J. Phys.: Conf. Ser.* **391** (2012) 012101.

HYPERFINE-T04-P1

μ^+ SR Study on N-type Ferrimagnetism of Na-K Alloy Clusters in Zeolite Low-Silica X

Takehito Nakano^{1*}, Jun Matsumoto², Isao Watanabe³

¹ Institute of Quantum Beam Science, Ibaraki University, Mito, Ibaraki 310-8512, Japan

²Department of Physics, Osaka University, Toyonaka, Osaka 560-0043, Japan

³RIKEN Nishina Center, Wako, Saitama 351-0198, Japan

*takehito.nakano.phys@vc.ibaraki.ac.jp

Porous zeolite crystals allow us to fabricate new electronic states in their periodic nanospaces by loading guest alkali atoms. Various magnetic orders, insulator-metal transitions, etc., have been found in these systems, depending on the host crystal structures, the guest alkali species, and the loading densities [1-4]. In zeolite low-silica X (LSX), β -cages with an inner diameter of ~ 0.7 nm and supercages with that of ~ 1.3 nm are arranged in a double diamond structure. When LSX, which contains both Na and K cations ($\text{Na}_4\text{K}_8\text{Al}_{12}\text{Si}_{12}\text{O}_{48}$), is loaded with guest K atoms, N-type ferrimagnetic order occurs [1]. This is interesting because of the magnetic order induced by s-electrons in the nanospace. The Na-K alloy clusters formed in the β -cages and supercages, respectively, are thought to be responsible for the magnetic sublattice [1,3]. In this study, we investigate the ferrimagnetic properties of Na-K alloy clusters in LSX by muon spin rotation/relaxation (μ SR) technique.

Figure 1 (a) shows the temperature dependence of the magnetization of Na-K alloy clusters in LSX at 10 Oe. The average number of guest K atoms is 7.7 per unit. Typical behaviour of the N-type ferrimagnetism is seen with the Curie temperature T_C of ~ 13 K and the compensation temperature of ~ 5.5 K. Figure 1 (b) shows the zero-field (ZF) μ SR spectra of the same sample measured at the RIKEN RAL Muon Facility. Below T_C , muon spin relaxation and rotation signals are clearly observed. This clearly indicates the spontaneous development of an internal magnetic field associated with magnetic order. The magnetism of this system will be discussed in terms of the local magnetic field distribution.

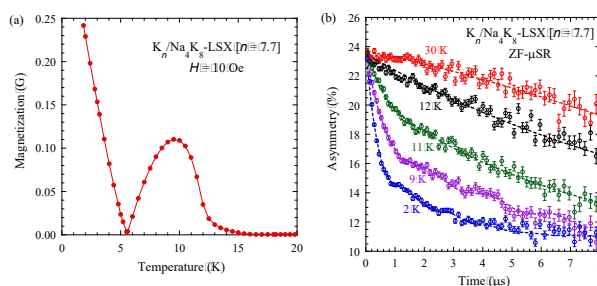


Figure 1. (a) Magnetization and (b) ZF- μ SR spectra of Na-K alloy clusters in zeolite LSX.

- [1] T. Nakano, Y. Nozue, *Adv. Phys.: X* **2** (2017) 254.
- [2] L. M. Kien et al., *Interactions* **245** (2024) 29.
- [3] T. Nakano, S. Harashima, *Interactions* **245** (2024) 59.
- [4] M. Hiraishi et al., *Interactions* **245** (2024) 104.

HYPERFINE-T04-P2

Muon Knight Shift and Electron Spin Resonance Studies on Metallic State of Rb-Loaded Sodalite

Takehito Nakano^{1*}, Masatoshi Hiraishi^{1,2}, Kaito Utsuno¹, Yuko Ishida³
Kazuki Ohishi⁴, Kenji M. Kojima^{5,6}

¹Institute of Quantum Beam Science, Ibaraki University, Mito, Ibaraki 310-8512, Japan

²Muon Science Laboratory, IMSS, KEK, Tsukuba, Ibaraki 305-0801, Japan

³Department of Physics, Osaka University, Toyonaka, Osaka 560-0043, Japan

⁴Neutron Science and Technology Center, CROSS, Tokai, Ibaraki 319-1106, Japan

⁵TRIUMF, British Columbia, V6T 2A3, Vancouver, Canada

⁶The University of British Columbia, V6T 1Z4, Vancouver, Canada

*takehito.nakano.phys@vc.ibaraki.ac.jp

Porous zeolite crystals allow us to fabricate new electronic states in their periodic nanospaces by loading guest alkali atoms. Various magnetic orders, insulator-metal transitions, etc., have been found in these systems, depending on the host crystal structures and the guest alkali species [1-4]. In sodalite, a type of zeolite, β -cages with an inner diameter of ~ 0.7 nm are arranged in a bcc structure. Each cage can accommodate an A_4^{3+} cluster where one s-electron is shared by four alkali cations (A^+ s). Na, K, and K-Rb alloy clusters in sodalite show antiferromagnetic order with the Mott insulating state, while Rb clusters show a non-magnetic metallic state [5]. This is understood to be the Mott transition associated with bandwidth expansion [5]. In this study, we investigate the metallic state of the Rb-loaded sodalite using high transverse field (TF) muon spin rotation (μ SR) and electron spin resonance (ESR) measurements. The former was performed at TRIUMF using the NuTime spectrometer. The latter was performed with conventional equipment using X-band frequency (9.7 GHz).

The muon frequency shift was estimated from TF- μ SR spectra at 60 kOe, with the Rb-loaded sample showing a negative shift relative to the non-loaded sample. The shift was nearly constant in the temperature range of 50 to 300 K and was about 5 ppm. The cause of the negative value is not clear, but it is thought to be a muon site that senses electron spin polarization in the opposite direction. The absolute value of the shift is about 8% of that of bulk Rb metal, 66(5) ppm [6]. Since the relative shift from the non-loaded sample can be regarded as the Knight shift, the density of states (DOS) at the Fermi energy of the Rb-loaded sample is about 8% of that of bulk Rb metal. The ESR line width increased linearly with increasing temperature above 50 K. This is consistent with the well-known Elliot mechanism of spin-lattice relaxation in metals [7]. These results suggest that Rb-loaded sodalite is a normal metal with a small DOS at the Fermi energy.

[1] T. Nakano, Y. Nozue, *Adv. Phys.: X* **2** (2017) 254.

[2] L. M. Kien et al., *Interactions* **245** (2024) 29.

[3] T. Nakano, S. Harashima, *Interactions* **245** (2024) 59.

[4] M. Hiraishi et al., *Interactions* **245** (2024) 104.

[5] T. Nakano et al., *Dalton Trans.* **53** (2024) 7358.

[6] A. Schenck, *Helv. Phys. Acta* **54** (1981) 471.

[7] R. J. Elliot, *Phys. Rev.* **96** (1954) 266.

HYPERFINE-T04-P3

Muon Dose Estimation in Brain Tumor and Soft Tissue

Anup Shrestha¹, Amba Datt Pant^{2,3*}, Surendra Bahadur Chand⁴, Anjan Dahal¹, Hari Shankar Mallik¹, Hiromi Sakai⁵, Akihiro Koda^{2,3}, Burkhard Geil⁶, Katsuhiko Ishida^{2,3}, Koichiro Shimomura^{2,3}

¹Central Department of Physics, Tribhuvan University, Kathmandu, Nepal

²Institute of Materials Structure Science, KEK, 1-1 Oho, Tsukuba, Ibaraki 305-0801, Japan

³Muon Section, Materials and Life Science Division, J-PARC center, 2-4 Shirane Shirakata, Tokai-mura, Naka-gun, Ibaraki 319-1195, Japan

⁴Department of Radiation Oncology, BPKM Cancer Hospital, Bharatpur-7, Nepal

⁵Department of Chemistry, Nara Medical University, Kashihara 634-8521, Japan

⁶Institut für Physikalische Chemie, Universität Göttingen, Tammannstrasse 6, 37077 Göttingen, Germany

*pant@post.kek.jp

Detection of low oxygenation in tissue (hypoxia) plays an important role in diagnosing and managing cancer treatment [1,2]. Since a noninvasive method is needed to detect hypoxia [3], we propose a noninvasive muon method [4,5] to estimate the spatial distribution of molecular oxygen (O₂) in the tissue (especially in tumor). The sensitivity of the proposed muon method was tested by detecting low O₂ in dilute protein solutions [4,5]. In order to support the muon experiment for further muon study in tumor and application to cancer research, we perform a Monte Carlo simulation using PHITS code [6] to estimate the muon stopping range, depth distribution, and the muon dose at different hypoxic states in two selected tumors (tumor in brain and soft tissue). The simulation shows that less energy of muon beam with respect to that of the proton beam is required to achieve the Braggs peak at same depth in the tumor. From the O₂ dependent simulation, the high energy of muon beam is required with decreasing the O₂ concentration in the tumor. In the program, the details of muon dose distribution using both polarities of muons in the brain tumor and soft tissues will be discussed.

[1] J. M. Brown, W. R. Wilson, *Nat. Rev. Cancer* **4** (2004) 437–447.

[2] P. Vaupel, L. Harrison, *Oncologist* **9** (2004) 4-9.

[3] J. P. B. O’Conner et. al., *Cancer Res.* **76**(4) (2016) 787-795.

[4] A. D. Pant et. al., *Nucl. Instrum. Methods Phys. Res. A* **1011** (2021) 165561.

[5] A. D. Pant et. al., *J. Phys. Conf. Ser.* **551**(1) (2014) 012043.

[6] T. Sato, et. al., *J. Nucl. Sci. Technol.* **55** (2018) 684-690.

HYPERFINE-T04-P4

Magnetic Transitions and Spin Freezing in the Correlated Electron System ErVO_3 Probed by Muon Spin Rotation and Relaxation (μSR)

E. Sadrollahi^{1*}, A. Mistonov¹, S. Mishra¹, F. J. Litterst², S. Seiro³,
T. Ritschel¹, J. Geck¹

¹Institut für Festkörper- und Materialphysik, Technische Universität Dresden, 01069
Dresden, Germany

²Institut für Physik der Kondensierten Materie, Technische Universität Braunschweig,
38106 Braunschweig, Germany

³Institut für Festkörperforschung, IFW Dresden, 01069 Dresden, Germany

*elaheh.sadrollahi@tu-dresden.de

The perovskite-type vanadium oxide ErVO_3 , characterized by Jahn-Teller active t_{2g} electrons at the vanadium site, represents a prototypical correlated electron system with active orbital degrees of freedom [1–3]. The compound exhibits a complex interplay between spin, orbital, and lattice interactions, resulting in a sequence of magnetic and orbital transitions.

In this study, we present results from muon spin rotation (μSR) measurements on single crystals of ErVO_3 , complemented by magnetic susceptibility, specific heat, and neutron diffraction experiments. These measurements reveal orbital ordering and orbital-flipping transitions, as well as spin ordering and spin reorientation phenomena. Our single-crystal X-ray diffraction data further indicate a structural phase transition associated with the orbital and magnetic ordering. Notably, μSR detects these magnetic transitions and additionally reveals spin freezing in approximately 20% of the sample volume below 3 K.

[1] P. Telang et al., *J. Cryst. Growth* **507** (2019) 406–412

[2] P. Bordet et al., *J. Solid State Chem.* **106** (1993) 253

[3] M. Reehuis et al., *Phys. Rev. B* **73** (2006) 094440

HYPERFINE-T04-P5

Muon Precision Measurement with Penning Trap at J-PARC

Koichiro Shimomura^{1,2}, Yukinori Nagatani^{1,2}, Takayuki Yamazaki^{1,2},
Patrick Strasser^{1,2}, Shoichiro Nishimura^{1,2}, Ken-ichi Sasaki^{1,2}, Masatoshi Hiraishi^{1,2},
Amba Dat Pant^{1,2}, Hiroto Kokubo³, Hiromi Inuma³, Taihei Adachi⁴,
Makiko Nio⁴, Hirotaka Okabe⁵, Takashi Higuchi⁶

¹High Energy Accelerator Research Organization (KEK), Tsukuba, Ibaraki, Japan

²J-PARC Center, Tokai, Ibaraki, Japan

³Graduate School of Science and Engineering, Ibaraki University, Mito, Ibaraki, Japan

⁴RIKEN Nishina Center for Accelerator-Based Science, Wako, Saitama, Japan

⁵Institute for Materials Research (IMR), Tohoku University, Sendai, Miyagi, Japan

⁶Institute for Integrated Radiation and Nuclear Science, Kyoto University, Kumatori, Osaka, Japan

*ksimomu@post.kek.jp

Muon precision measurements constitute a powerful probe in the search for new physics beyond the Standard Model of particle physics. A prominent example is the measurement of the muon anomalous magnetic moment ($g - 2$), which exhibits a 4.2σ discrepancy between theoretical predictions and experimental results. This deviation is regarded as a potential indication of new physics [1]. In previous precision measurements, muons were either in an accelerated state or in a muonium state.

In this study, a novel method is proposed to precisely measure slow free muons by confining them in an electromagnetic field utilizing the Penning trap technique. This represents the first application of a Penning trap to particles with lifetimes as short as that of muons ($2.2 \mu\text{s}$). The experiment will be conducted using the high-intensity pulsed muon beam at J-PARC H-Line [2]. The ultimate goal is to measure the muon mass and magnetic moment with a precision of 1 ppb and the muon lifetime with a precision of 1 ppm.

A schematic representation of the experimental setup is provided in Figure 1. Muons are initially injected into a degrader or an ultra-slow muon-producing target within a 3 T superconducting magnet to decelerate them. The resulting slow or ultra-slow muons are subsequently transported to the trap region via an electric field. During transport, an RF magnetic field is applied to rotate their spin direction by $\pi/2$, aligning it perpendicular to the magnetic field to facilitate the observation of Larmor precession. The muon spins and positions are precisely controlled by the electromagnetic field, and their oscillation frequencies are measured using upper and lower detectors via the detection of decay electrons or positrons.

At present, the development of electrodes, which are integral to the trap, as well as detectors for measuring rapid spin precession, is underway. The current status of these developments will be reported.

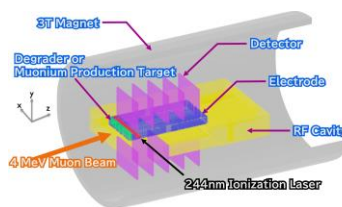


Figure 1. Schematic view of the muon trap experiment.

[1] B. Abi, et al., *Phys. Rev. Lett.* **126** (2021) 141801.

[2] T. Yamazaki, et al., *EPJ Web Conf.* **282** (2023) 01016.

HYPERFINE-T06-P1

Synthesis and TDPAC Characterization of Rare-Earth Manganites

Nicole Pereira de Lima^{1*}, Anastasia Burimova¹, Juliana Schell^{2,3}, Artur Wilson Carbonari¹

¹Instituto de Pesquisas Energeticas e Nucleares (IPEN - CNEN/SP), Sao Paulo, Brazil

²European Organization for Nuclear Research (CERN), Geneva, Switzerland

³University Duisburg-Essen (UDE), Essen, Germany

The perovskite family RMnO_3 (where R is a rare-earth element such as Ho, Tb, or La) has garnered significant attention within the solid-state physics community due to its diverse physical properties, including ferroelectricity, high-temperature superconductivity, and colossal magnetoresistance [1,2]. These characteristics make RMnO_3 compounds particularly relevant for various technological applications such as spintronics, data storage, and sensors [3]. Beyond these applied perspectives, RMnO_3 compounds, especially the rare-earth manganites, are of great interest for fundamental research. This fascination is primarily due to their spin-charge-orbital coupled systems, where a strong interaction between ferroelectricity and magnetism offers a rich field for investigation [4]. Among the different structural phases of these compounds, rare-earth manganites like HoMnO_3 can exist in both hexagonal and orthorhombic forms [5]. The formation of these phases is influenced by the ionic radius of the rare-earth element and the specific synthesis route employed. Hexagonal structures (space group $P63cm$) naturally occur in certain elements like Ho, Y, and Er, but orthorhombic phases (space group $Pbnm$) can also form under particular conditions [6]. Our experimental approach includes synthesizing HoMnO_3 using the sol-gel method, a low-cost and efficient process that has been adapted from the literature [7]. While various synthesis techniques like the solid-state method, citrate combustion, and Pechini method have been employed for perovskites, sol-gel synthesis remains under-explored for RMnO_3 compounds, particularly for rare-earth manganites like HoMnO_3 . This limitation makes our investigation of the sol-gel method particularly valuable. In addition to synthesis, we employ hyperfine interaction techniques, specifically Time-Differential Perturbed Angular Correlation (TDPAC), to probe the local magnetic and electric environments of the material [8]. These techniques allow us to gain insight into the coupling between ferroelectricity and magnetism at the atomic scale. Probes such as ^{111}In and ^{111m}Cd are incorporated during synthesis or implanted at the ISOLDE/CERN facility to enable these measurements. This study explores a synthesis method for the hexagonal HoMnO_3 phase. The crystallographic structure of the sample is analyzed using X-ray diffraction, followed by the ^{111m}Cd implantation process. TDPAC measurements are conducted, followed by a discussion on ferroelectricity and magnetism. The results seek to elucidate phase-specific behaviors, facilitating further research on complex compounds and their doped variants, where phase stability is essential for optimizing multiferroic properties.

[1] A. Munoz, *J. Alloys Compd.* **323** (2001).

[2] N. Hur, *Phys. Rev. B* **79** (2009).

[3] V. Hreb, *10th International Conference Nanomaterials* (2020).

[4] H. Brinks, *J. Solid State Chem.* **129** (1997).

[5] H. T. Wang, *Phys. Lett.* **28** (2011).

[6] W. Prellier, *J. Phys.: Condens. Matter* **17** (2005).

[7] K. Uusi-Esko, *Mater. Chem. Phys.* **112** (2008).

[8] G. Darriba, *Phys. Rev. B* **79** (2009).

HYPERFINE-T06-P2

Initial TDPAC Investigations on Calcium Metavanadate

Anderson S. Pereira^{1*}, Renata Maziviero^{2,3}, Arnaldo A. Miranda Filho¹, Juliana H. Schell^{4,5}, Artur W. Carbonari¹, Anastasia Burimova¹

¹ Instituto de Pesquisas Energéticas e Nucleares, IPEN, São Paulo, Brazil

² Instituto Federal de Educação, Ciência e Tecnologia de São Paulo, Campus São Paulo, São Paulo, Brazil

³ Universidade de São Paulo, Instituto de Química, São Paulo, Brazil

⁴ European Organization for Nuclear Research (CERN), CH-1211 Geneva, Switzerland

⁵ Institute for Materials Science and Center for Nanointegration Duisburg-Essen (CENIDE), University of Duisburg-Essen, 45141 Essen, Germany

*s.anderson@usp.br

In this study, we present for the first time the application of Time Differential Perturbed Angular Correlation (TDPAC, or PAC) spectroscopy to assess its suitability for investigating ion (de)intercalation in calcium metavanadate (CaV_2O_6). Samples were synthesized using both the standard Pechini method and a hydrothermal route, and characterized by X-ray diffraction (XRD) before and after PAC measurements to monitor structural modifications and detect potential contamination by calcium pyrovanadate ($\text{Ca}_2\text{V}_2\text{O}_7$). The inherent inter-contamination of CaV_2O_6 and $\text{Ca}_2\text{V}_2\text{O}_7$ — a common challenge in vanadate synthesis — complicates PAC data interpretation. By comparing results obtained with different probe parents (In-111 and Cd-111m) across various vanadate samples, we tentatively correlate an interaction with a hyperfine frequency near 60 MHz to Cd substituting for Ca in CaV_2O_6 . Although further studies are needed to confirm this association, our preliminary findings support the potential of PAC spectroscopy as a tool for future investigations of ion (de)intercalation in divalent metal metavanadates.

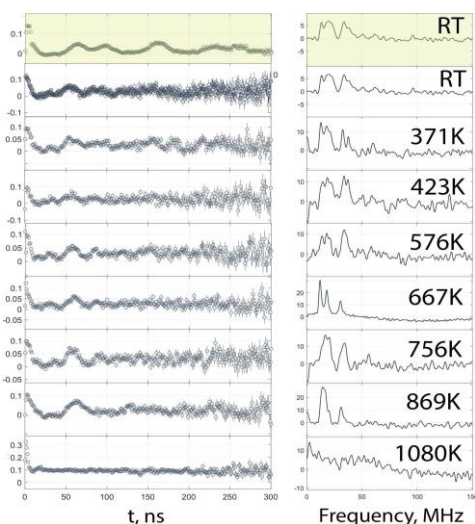


Figure 1. TDPAC $R(t)$ functions (left) and their Fourier Transform collected for nominal CaV_2O_6 . Highlighted data corresponds to In-111 probe parent, other data was obtained with Cd-111m.

HYPERFINE-T06-P3

Ab-initio Study on CsNdNb₂O₇ and CsLaNb₂O₇ Dion-Jacobson Perovskites

Pedro A. Sousa^{1*}, Helena M. Petrilli², P. N. Lekshmi¹, António N. Cesário¹,
P. Rocha Rodrigues¹, Lucy Assali², E. Lora da Silva¹, S. S. M. Santos³,
J. G. Correia⁴, J. P. Araújo¹ and A. M. L. Lopes¹

¹IFIMUP, Faculdade de Ciências da Universidade do Porto, Portugal

²Instituto de Física da Universidade de São Paulo, São Paulo, Brazil

³Instituto Federal de Educação, Ciência e Tecnologia de Rondônia, Campus Colorado, Brazil

⁴C2TN, Centro de Ciências e Tecnologias Nucleares, Universidade de Lisboa, Portugal

*up201704307@edu.fc.up.pt

In the pursuit of novel and highly efficient multiferroic materials, significant exploration over the past decades has revealed a class of compounds capable of exhibiting coupled electric and magnetic order parameters. Such materials hold promise for enabling the electrical manipulation of magnetic degrees of freedom, offering numerous potential applications in magnetoelectric devices. Our research group focuses on naturally layered perovskite derivatives—specifically Ruddlesden–Popper and Dion–Jacobson (DJ) phases—where alternating perovskite slabs and interleaving rock-salt layers introduce rich structural flexibility. Among these, DJ compounds present particularly complex structural pathways: rotations and tilts of corner-sharing oxygen octahedra that directly influence the magnitude and orientation of ferroelectric polarization.

To probe these subtle distortions, which often elude conventional X-ray diffraction (XRD), we combine local-probe Perturbed Angular Correlation (PAC) spectroscopy—with its heightened sensitivity to electric-field gradients (EFG) at the probe nucleus—with first-principles Density Functional Theory (DFT) simulations. We investigate CsNdNb₂O₇ [1, 2] and its non-magnetic analog CsLaNb₂O₇, explicitly treating Nd 4f electrons at the semi-core level rather than frozen in the core as in earlier studies. By systematically varying Hubbard U parameters and exploring multiple magnetic configurations, we compute EFG tensors variation with such models. This DFT approach provides comprehensive insights into the interplay of electron correlation, magnetism, and ferroelectricity in DJ perovskites, and paves the way for the targeted design of layered multiferroics with optimized functional properties.

[1] T. Zhu et al., *Chem. Mater.* **32** 10 (2020) 4340–4346.

[2] N.A. Benedek *Inorg. Chem.* **53** 7 (2014) 3769–3777.

Acknowledgments This work was financially supported by the FCT under the project CERN/FIS-TEC/0003/2021 (DOI: 10.54499/CERN/FIS-TEC/0003/2021) and the PhD grant PRT/BD/154996/2023. Additional support was provided by the EURO-LABS network through the IS730 and IS738 proposals, by the German Federal Ministry of Education and Research (BMBF) through grant 05K22PGA, and by the Brazilian agencies CNPQ and FAPESP under the project 2022/10095- 8. The authors also acknowledge support from FCT through the projects LA/P/0095/2020, UIDB/04968/2025, and UIDP/04968/2025, as well as the Institute of Physics for Advanced Materials, Nanotechnology and Photonics (IFIMUP)/

HYPERFINE-T07-P1

Diffusion of Interstitial Impurities ^{12}B and ^{12}N in fcc Metals Cu and Al

K. Matsuta^{1*}, M. Mihara², M. Fukuda², T. Minamisono³, and Y. Nojiri⁴

¹None, Osaka, Japan

²Department of Physics, Osaka Univ., Toyonaka, Osaka 560-0043, Japan

³None, Kyoto, Japan

⁴None, Tokyo, Japan

*matralf142c@gmail.com

Crystal sites of impurities are important knowledge to study the behaviour of impurities in materials. The implantation sites of ^{12}B , ^{12}N , and ^8Li into Cu and Al crystals were investigated by the Lockheed, Osaka, and Marburg groups [1-7] using van de Graaff accelerators, by β -NMR technique. From these linewidth analyses, ^{12}B and ^{12}N were found to be in (Octahedral or tetrahedral) interstitial sites, while ^8Li was found to be in a substitutional site. In these papers, lattice expansion due to impurity ions as well as implantation sites were studied through the linewidths of NMR spectra.

We revisit this longstanding issue. From the motional narrowing of the NMR spectra, the jumping rate can also be determined. From the temperature dependence of the jumping rate, we can determine the activation energy at which impurities migrate to adjacent sites. As an example, Figure 1 (Arrhenius plot) shows the jump rate as a function of the inverse of temperature for ^{12}N impurity in Cu. From the slope of the plot, the activation energy was determined to be 0.2 eV.

Crystal sites, lattice rearrangements, and diffusion or jump, and the relation between these phenomena and the ion size of the impurities will be discussed in this report.

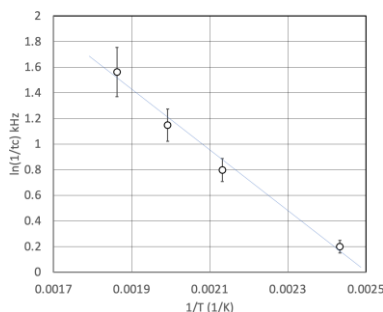


Figure 1. Jump rate as a function of the inverse of temperature for ^{12}N impurity in Cu.

- [1] R. E. McDonald, T. K. McNab, *Phys. Rev.* **B13** (1976) 34.
- [2] R. E. McDonald, T.K. McNab, *Phys. Lett.* **63A** (1977) 177.
- [3] T. K. McNab et al., *Phys. Rev.* **B18** (1978) 92.
- [4] T. Minamisono et al., *Phys. Lett.* **94A** (1983) 312- 316.
- [5] E. Jaeger et al., *Z. Phys.* **B86** (1992) 389.
- [6] F. Ohsumi et al., *Hyperfine Interact.* **120/121** (1999) 419-422.
- [7] K. Matsuta et al., *Hyperfine Interact.* **136/137** (2001) 503-507.

HYPERFINE-T07-P2

***Ab Initio* Study of Temperature Dependence of Structural, Electronic, and Hyperfine Properties at Pure and Cd-doped (001) Cu Surface**

Germán N. Darriba,¹ Ricardo J. Faccio,² and Mario Rentería^{1*}

¹Departamento de Física and Instituto de Física La Plata (IFLP, CCT La Plata, CONICET-UNLP), Facultad de Ciencias Exactas, Universidad Nacional de La Plata, CC 67, 1900 La Plata, Argentina

²Crystallography, Solid State and Materials Laboratory (Cryssmat-Lab), DETEMA, Facultad de Química, Universidad de la República, Uruguay y Centro NanoMat, Polo Tecnológico de Pando, Facultad de Química, Universidad de la República, Uruguay

*renteria@fisica.unlp.edu.ar

In this work, we present a complete *ab initio*/DFT study of structural, electronic, and hyperfine properties of pure and Cd-doped (001) Cu surface. We studied the structural and electronic changes produced by the generation of the surface itself and by the inclusion of the Cd impurity.

As a first step, we performed a complete optimization of all atomic positions in the supercell of the pure system. For the doped ones, a Cd atom replaced a Cu atom at the different inequivalent Cu sites (depths) of this pure optimized surface, followed by a new complete optimization. The appearance of a nonvanishing surface electric field gradient is a property of the broken symmetry at the copper surface since probe atoms placed substitutionally inside the Cu bulk are not exposed to any electric field gradient because of the cubic lattice structure. In this sense, we show that the EFG becomes practically null at a depth of 5 Cu monolayers from the (001) surface.

The magnitude, symmetry, and orientation of the electric-field gradient (EFG) tensor were studied using experimental lattice parameters of Cu fcc structure as a function of temperature. For Cd-doped (001) Cu surface, the predicted EFGs are compared with those observed in Time-Differential Perturbed γ - γ Angular Correlation (TDPAC) experiments with $^{111}\text{In}(\text{EC} \rightarrow ^{111}\text{Cd})$ ions deposited onto the (001) Cu surface, performed in the 77-570 K temperature range [1]. This combined approach enables us to study in detail the linear dependence of the surface EFG as a function of T that was experimentally determined.

[1] T. Klas et al., *Phys. Rev. Lett.* **57** (1986) 1068.

HYPERFINE-T07-P3

Local Impact of Cd Substitution in h -YMnO₃ Explored with *Ab Initio* Calculations

L. Scalise^{*1}, E. Lora da Silva², A. Mokhles Gerami³, A. Muhammad²,
A. Burimova¹, A. W. Carbonari¹

¹ Instituto de Pesquisas Energéticas e Nucleares (IPEN), São Paulo, Brazil

² IFIMUP, Departamento de Física e Astronomia da Faculdade de Ciências, Universidade do Porto, Porto, Portugal

³ School of Particles and Accelerators, Institute for Research in Fundamental Sciences (IPM), Tehran, Iran

*levyscalise@gmail.com

Aliovalent doping is a powerful strategy for tuning the multifunctional properties of hexagonal manganites, which are of great interest for applications in multiferroics, sensors, and spintronic devices. In this work, we extend the range of dopants for hexagonal YMnO₃ (h -YMO) by investigating Cd-doped h -YMO, considering the possibilities of Cd²⁺ substituting Mn³⁺ and Y³⁺ sites. Using density functional theory (DFT) calculations, we explore the local structural relaxations induced by Cd incorporation, analyze the resulting changes in the charge density distribution, and evaluate how these modifications influence hyperfine interactions. Our computational results are directly compared with the experimental findings of Mendonça et al., as well as with findings for similar manganites [1,2].

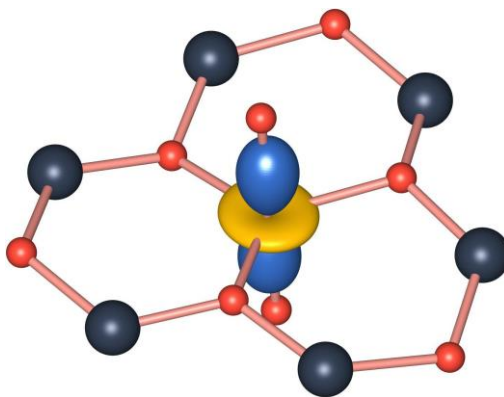


Figure 1. Visualization of the electric field gradient tensor at the Cd Site Substituting Mn in Hexagonal YMnO₃, as calculated with the VASP package.

- [1] T. M. Mendonça et al., *Hyperfine Interact.* **197** (2010) 83.
- [2] J. N. S. Gonçalves, "Measurement and Modeling of Hyperfine Properties in Ferroic Materials" *Doctoral Thesis* (2011).
- [3] W. Sato et al., *Phys. Rev. B* **100** (2019) 184111.
- [4] Lopes et al., *Phys. Rev. B* **73**(2006) 100408.

HYPERFINE-T08-P1

^{14}N NQR Spectrum of Nitrourea

Nadia Singh^{1*}, David Stephenson¹

¹Department of Chemistry, The University of the West Indies, St. Augustine, Trinidad and Tobago

*nadia.singh@uwi.edu; nadiabeepath@hotmail.com

The ^{14}N nuclear quadrupole resonance (NQR) spectrum of nitrourea has been recorded using Cross Relaxation Double Resonance [1]. Nitrourea is an important reagent and intermediate in many organic chemical reactions and has applications in the preparation of medicines, explosives, foaming reagents, and many additives [2]. It has three distinct nitrogen atoms in its chemical structure. One nitrogen atom belongs to the nitro group, while the other two are part of the urea moiety (carbamide). The ^{14}N NQR experimental quadrupole coupling constants (QCCs) and asymmetry parameters (η) of nitrourea have been compared to its calculated ab-initio values [3], and the orientation of the principal electric field gradient (EFG) axes for each nitrogen atom has been assigned. The nitrogen atom of the nitro group has the lowest calculated QCC and, by extension, the lowest q_{zz} EFG component, while the amide nitrogen attached to the nitro group has the largest QCC and asymmetry parameter. The asymmetry parameters and QCCs for the amide nitrogen atoms indicate the presence of intermolecular hydrogen bonding in the molecule.

[1] D. Stephenson, J. A. S. Smith, *Proc. R. Soc. Lond.*, A **416**, (1988)149.

[2] ChemBK.com, (2015, 2023) *NITROUREA*. <https://www.chembk.com/en/chem/NITROUREA> (Accessed: 31 March 2025).

[3] J. Baker, et al., PQS version 3.3, Parallel Quantum Solutions, P. O. Box 293, Fayetteville, Arkansas 72702-0293, U.S.A. www.pqs-chem.com 4.

HYPERFINE-T08-P2

^{14}N NQR Spectrum of Albendazole

Nadia Singh^{1*}, David Stephenson¹

¹Department of Chemistry, The University of the West Indies, St. Augustine,
Trinidad and Tobago

*nadia.singh@uwi.edu; nadiabeepath@hotmail.com

The ^{14}N nuclear quadrupole resonance (NQR) spectrum (Figure 1) of albendazole has been recorded using cross relaxation double resonance [1]. Albendazole is a broad spectrum anthelmintic benzimidazole with urethane and propyl sulfide substituents and is mainly used in the treatment of parenchymal neurocysticercosis and other helminth (parasitic worm) infections [2, 3]. Benzimidazoles are heterocyclic aromatic organic compounds comprising fused rings of benzene and imidazole and have two distinct nitrogen atoms. Albendazole has two stable polymorphs [3]. Form I has three distinct nitrogen atoms, while Form II has two distinct nitrogen atoms since the nitrogen atoms on the bicyclic ring are equivalent. Ab initio calculations have been done to support the assignment of the ^{14}N NQR experimental frequencies, quadrupole coupling constants (QCCs), and asymmetry parameters to their respective nitrogen atoms in albendazole [3]. Significant differences in the expected QCCs, asymmetry parameters, and ^{14}N NQR frequencies for both polymorphs permit the confirmation of the structure and, subsequently, authentication of the compound in the solid state.

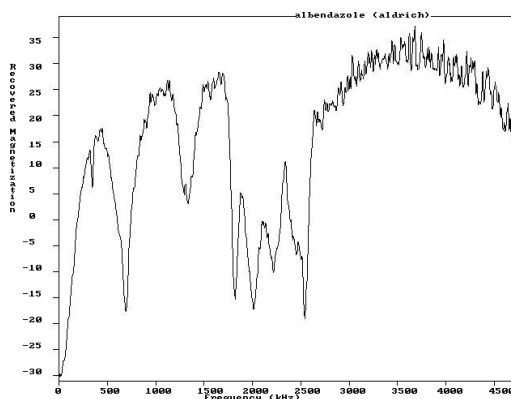
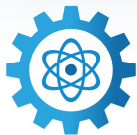


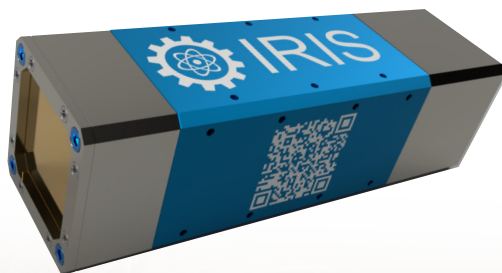
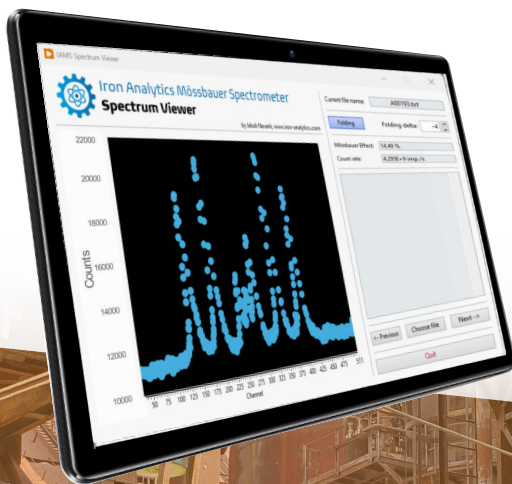
Figure 1. ^{14}N NQR Spectrum of Albendazole.

- [1] D. Stephenson, J. A. S. Smith, *Proc. R. Soc. Lond.*, A **416** (1988)149.
- [2] DrugBank Online, (2025) *Albendazole: Uses, Interactions, Mechanism of Action*. <https://go.drugbank.com/drugs/DB00518> (Accessed: 31 March 2025).
- [3] M. B. Pranzo et al., *J. Pharm. Sci.* **99** (2010) 3731. doi: 10.1002/jps.22072.
- [4] J. Baker et al., PQS version 3.3, Parallel Quantum Solutions, P. O. Box 293, Fayetteville, Arkansas 72702-0293, U.S.A. www.pqs-chem.com 4.

RESEARCH

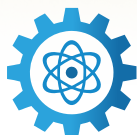


Iron Analytics

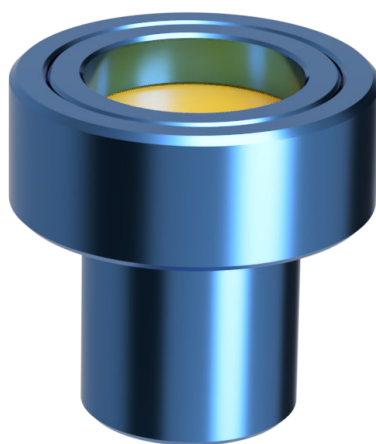
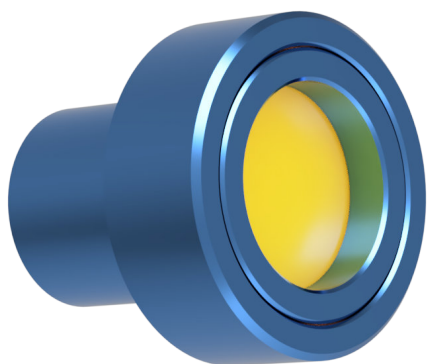


INDUSTRY

SOURCES



Iron Analytics



^{57}Co MÖSSBAUER SOURCES

Iron Analytics is addressing the global crisis related to the shortage of Mössbauer sources. We are currently working on the design and certification of a new ^{57}Co source.

If you are interested in ^{57}Co sources, please let us know your expected needs. As a thank you, we will provide you with the email updates and exclusive priority for your orders.

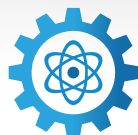
MEET US AT THE CONFERENCE
OR USE THE QR CODE
FOR ONLINE SURVEY:



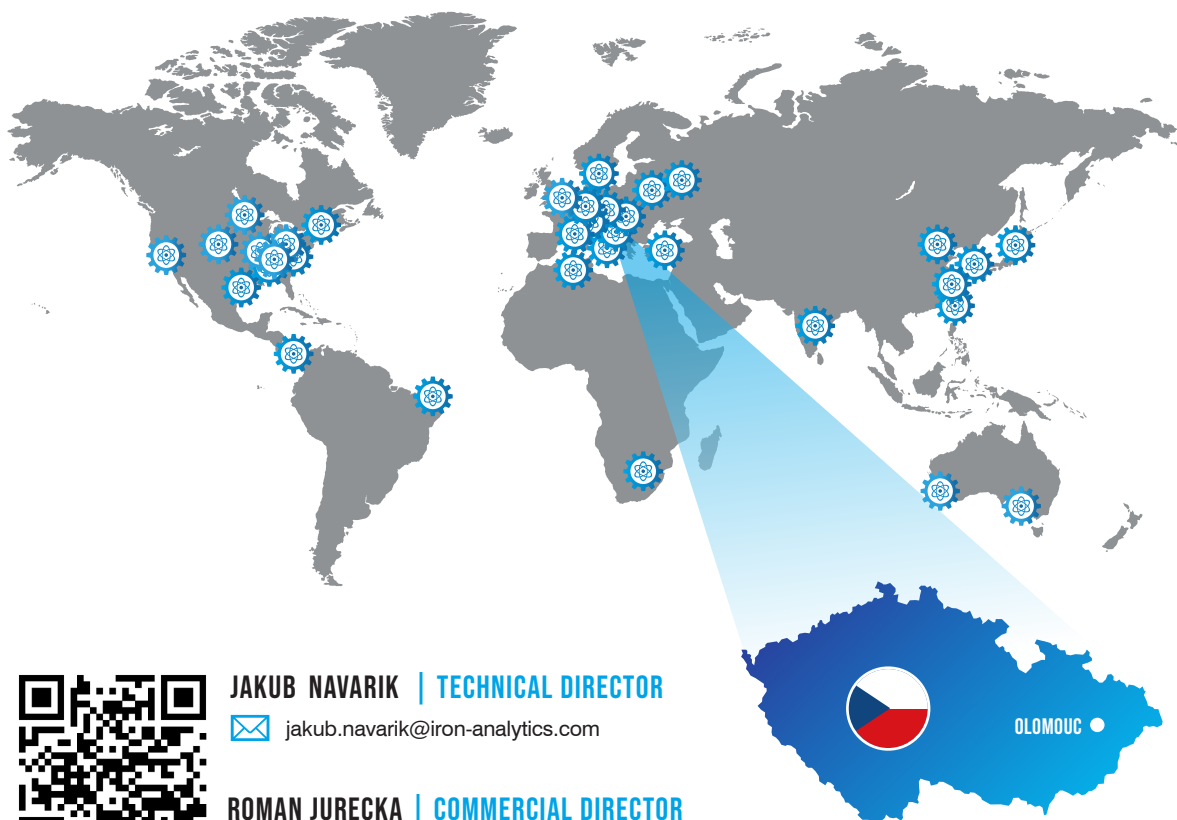
EXPECTED AVAILABILITY: END OF 2025

WORLDWIDE USED TOOLS FROM THE HEARTH OF EUROPE

Iron Analytics Company builds on more than 30 years of experience in Mössbauer spectroscopy research and design based on Palacký University Olomouc. Mössbauer spectrometers, designed and manufactured in Olomouc, originally labeled as MS96, are used in more than 50 academic and industrial research laboratories worldwide for the analysis of nanomaterials, pharmaceuticals, iron and steel products, biological samples, ferrites, minerals, archaeological samples, and others. Iron Analytics is challenging the potential of Mössbauer spectroscopy for new industrial applications as well as for space research.



Iron Analytics



JAKUB NAVARIK | TECHNICAL DIRECTOR

✉ jakub.navarik@iron-analytics.com

ROMAN JURECKA | COMMERCIAL DIRECTOR

✉ roman.jurecka@iron-analytics.com

STRATEGIC PARTNERS:



Palacký University
Olomouc



CATRIN
Czech Advanced
Technology and Research
Institute



Lake Shore
CRYOTRONICS



Iron Analytics Products developed in cooperation
with Palacký University Olomouc

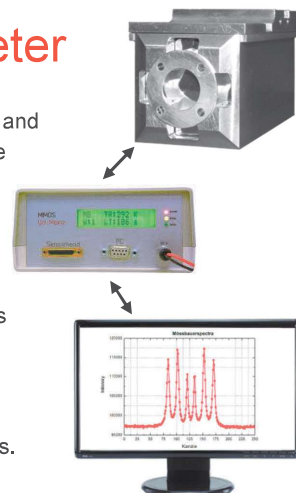
Miniaturized Mössbauer-Spectrometer

Due to its miniaturization and backscattering geometry, **MIMOS II** is portable and used in a wide range of Fe-Mössbauer applications, especially where sample preparation is not possible (**non-destructive measurement**).
MIMOS II works over a wide temperature range (-120°C to +40°C).

This performance combined with its low power consumption enables MIMOS II to be used in a wide variety of applications. In the field, power can be supplied by battery or solar cell arrays. No additional human intervention is required. The system operates autonomously without a time limitation.

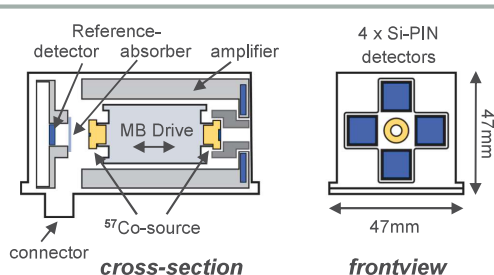
MIMOS II can also be used for transmission measurements.

Size and shape of the transmission detectors are optimized for different applications. The system can be easily adapted to experimental requirements. Transmission and backscattering mode are performed simultaneously.



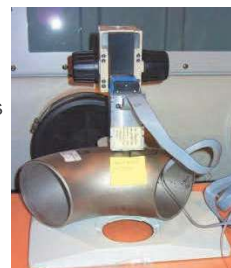
Technical information

- Power consumption: < 4 W at 12 V optional power supply by battery
- Interface: serial RS 232 / RS 422 USB / Bluetooth data transfer (optional)
- Data storage in internal memory with power-independent backup
- Internal reference channel: simultaneous calibration measurement
- 2 temperature sensors for temperature dependent investigations
- Simultaneous measurement of 14.4 keV γ -rays and 6.4 keV Fe-X-rays
- Additional transmission detector available



Industrial applications

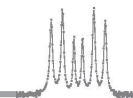
- In-situ monitoring of reaction educts and products to optimize the production process and output of iron and iron carbide
- Measurement of the sigma-phase by evaluating the ferrite-phase
- Absolute content of Martensite / Austenite phases by analysis of Mössbauer-spectra



MIMOS II: compact, mobile, power-efficient, easy to use, non-destructive measurement

- In-situ quality inspection of parts, even in hard-to reach places (e.g. on ground, in water and other remote places)
- remote access to MIMOS II
- Fast operational readiness even in special applications and configurations
- Power by battery, solar panel or other sources
- Backscattering & transmission mode (possible)

Contact: Prof. Dr. Dr. h.c. Franz Renz, Leibniz University Hannover, Institut für Koordinationschemie
E-Mail: mimos@acd.uni-hannover.de Phone: +49 179 9462053

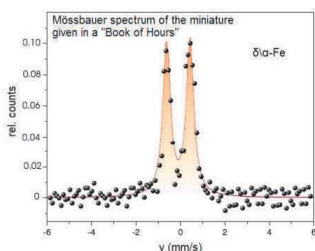


Application in Archaeology

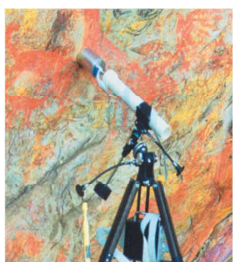
Material analysis & preservation of art treasures
No sample preparation

→ **Non-destructive measurement**

- Determination of pigment compositions in paintings and pottery



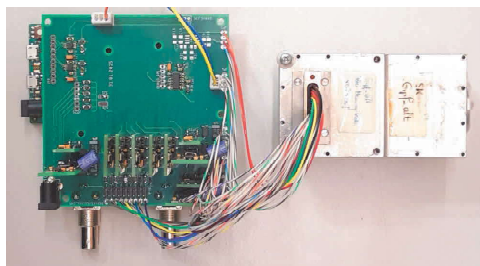
- Depth-selective analysis of surface layers (~ μm range)



- Analysis of iron-phases, and identification of origin of phases (e.g. pigments), and history of Fe-compounds and therefore artifacts, paintings, etc.
- Identification of possible correlations or connections between different artifacts

Arduino Technology

State of the art technology for electronic board



2-D data processing

Simultaneous recording of each detected energy pulse and actual velocity value over a wide range of energy (4 - 140 keV)

- Optimized data processing → higher count rate
- Simultaneous measurement of 6.4 and 14.4 keV Mössbauer-spectra
- No thresholds setting
- 1024 channels → higher resolution
- Simultaneous data processing of 5x detectors

Hardware

Digital data analysis and processing

- Reduced electronic hardware
- Small, cost-effective
- Power supply: USB/+5 V
- Compatible with other Moessbauer systems (e.g. WissEl)

Key sentences

- No sample preparation, non-destructive measurements, mobile & miniaturized, fast operational readiness
- Portable Mössbauer spectroscopy: field and exotic other places (e.g. museums). Acquisition time per spectrum between some minutes and several hours depending on experiment conditions
- The system can operate autonomously for several weeks

Contact: Dr. Mathias Blumers, Johannes Gutenberg-University Mainz, Germany
E-Mail: mimos@acd.uni-hannover.de Phone: +49 170 6708528





Serdecznie zapraszamy do udziału w **Ogólnopolskim Seminarium Spektroskopii Mössbauerowskiej (OSSM 2026)**, które odbędzie się w 2026 roku. OSSM to cykliczne wydarzenie integrujące środowisko naukowców, doktorantów oraz studentów zajmujących się spektroskopią Mössbauera i jej zastosowaniami w badaniach materiałowych, chemicznych oraz biologicznych. Więcej informacji oraz szczegóły dotyczące miejsca OSSM 2026 zostaną wkrótce opublikowane na stronie wydarzenia. Organizatorem konferencji jest Katedra Fizyki Politechniki Częstochowskiej.



We warmly invite you to participate in the **All-Polish Mössbauer Spectroscopy Seminar (OSSM 2026)**, which will be held in 2026. OSSM is a periodic event integrating researchers, PhD students, and undergraduate students working with Mössbauer spectroscopy and its applications in materials science, chemistry, and biology. More details regarding the venue of OSSM 2026 will be announced soon on the event website. The conference is organized by the Physic Department Czestochowa University of Technology.



ICAME 39 & HYPERFINE, Argonne, Chicago, IL, USA

Welcome to ICAME & HYPERFINE 2027 at Argonne National Laboratory, in Illinois, USA.

We are happy to invite all of you to participate in the 39th International Conference on the Applications of the Mössbauer Effect, ICAME, and the International Conference on Hyperfine Interactions and Their Applications, HYPERFINE, which will be held at Argonne National Laboratory, Illinois, USA, between September 5-10, 2027.

United States played a major role in developing Mössbauer Spectroscopy since 1959 with the discovery of Mössbauer Effect in ^{57}Fe , and held the first major workshops in 1960 and 1961. Yet, no ICAME meeting was ever held in the United States. Also, pioneering work on exciting Mössbauer resonance with synchrotron radiation was done and reached its zenith with the construction of Advanced Photon Source with multiple beamlines having nuclear resonance facilities.

The conference will be hosted by Argonne National Laboratory at the Argonne site, which is 35 miles southwest of Chicago city center. There is a 160 room Guest House inside the laboratory and there are many alternative hotels nearby.

The conference will be organized by 3 Mössbauer scientists, Dr. Ercan Alp of Argonne National Laboratory, Dr. Raphael Hermann of Oak Ridge National Laboratory and Prof. Brent Fultz of California Institute of Technology. There are more than 3 dozens of active Mössbauer research laboratories in the National Laboratory and Universities. The USA Mössbauer Community is active with biannual national meetings, and frequent workshops on applications of synchrotron radiation.

The scientific program of both conferences will cover the traditional topics of the previous ICAME and HYPERFINE events with some emphasis on synchrotron radiation. We are planning a common book of abstracts, a joint welcome session and coffee breaks, plenary sessions as well as parallel sessions, tutorials on both Mössbauer and hyperfine topics, and joint social events like a boat tour in Chicago River and Lake Michigan. We warmly invite all the Mössbauer and Hyperfine community and look forward to seeing you in Chicago.



38th International Conference
on the Applications of the Mössbauer Effect, ICAME,
and the International Conference on Hyperfine Interactions
and Their Applications, HYPERFINE



"The project is co-financed from the state budget, granted by the Polish Minister of Science under the Excellent Science II Program."

"Projekt dofinansowany ze środków budżetu państwa, przyznanych przez Ministra Nauki w ramach Programu Doskonała nauka II."



Ministry of Science and Higher Education
Republic of Poland



**Doskonała
Nauka II**

ORGANIZERS



POLITECHNIKA
LUBELSKA
LUBLIN UNIVERSITY
OF TECHNOLOGY



THE HENRYK NIEWODNICZAŃSKI
INSTITUTE OF NUCLEAR PHYSICS
POLISH ACADEMY OF SCIENCES



GDAŃSK UNIVERSITY
OF TECHNOLOGY

CO-ORGANIZER



AGH UNIVERSITY
OF KRAKOW

EXHIBITORS



LynXes

SPONSORS

Main sponsor:



Łukasiewicz
Institute of Microelectronics
and Photonics

Industrial sponsor:



Iron Analytics



WISSENSCHAFTLICHE ELEKTRONIK GMBH
Website: www.wissel.eu, www.wissel-instruments.de, www.wissel-gmbh.de

HONORARY PATRONAGE – MAYOR OF GDAŃSK



Patronat Honorowy
Prezydent
Miasta Gdańska